ISSN 2663-0419 (Online)
ISSN 2218-8754 (Print)

AZERBAIJAN NATIONAL ACADEMY OF SCIENCES

ANAS TRANSACTIONS

EARTH SCIENCES

www.journalesgia.com

2026
№1

Buraxılışına məsul: **Qabil Abıyev**

Dizayn/Qrafika: **Kərim Nəbiyev**
Xəlil Nəbiyev

Veb-redaktor: **Tofiq Rəşidov**

Jurnal Geologiya və Geofizika İnstitutunda yığılmış və səhifələnmişdir

* * *

Responsible for the issue: **Gabil Abiyev**

Design/Graphycs: **Karim Nabiyev**
Khalil Nabiyev

Web-editor: **Tofig Rashidov**

The journal has been compiled and paginated at the Geology and Geophysics Institute

* * *

Ответственный за выпуск: **Габил Абиев**

Дизайн/графика: **Керим Набиев**
Халил Набиев

Веб-редактор: **Тофиг Рашидов**

Журнал набран и сверстан в Институте геологии и геофизики

* * *

Ünvan: AZ1001, Bakı şəhəri, İstiqlaliyyət küçəsi 30, "ANAS Transactions, Earth Sciences"

Address: "ANAS Transactions, Earth Sciences" 30, Istiglaliyyat str., Baku, Azerbaijan, AZ1001

Адрес: AZ1001, г. Баку, Истиглалият, 30. Редакция "ANAS Transactions, Earth Sciences"

* * *

İcraçı redaktorlar: **A.A.İsrafilova, C.S.Qurbanova**
Executive Editors: **A.A.Israfilova, J.S.Gurbanova**
Исполнительные редакторы: **А.А.Исрафилова**
Дж.С.Курбанова

ELM
NƏŞRİYYATI

Formatı: 60x84$^{1/8}$. Həcmi: 16,25 ç.v.
Tirajı: 300 nüsxə

ANAS Transactions Earth Sciences 1 / 2026

http://www.journalesgia.com

IMPLEMENTATION OF DISRUPTIVE TECHNOLOGIES IN SEISMIC INTERPRETATION

Gorbunov A.A.[1], Lavrenova E.A.[1], Kerimov V.Yu.[1,2]*, Mustaev R.N.[1], Bunyatov A.A.[3]

[1]Russian State University for Geological Prospecting named after Sergo Ordzhonikidze, Russian Federation
23, Miklouho-Maclay str., Moscow, 117997
[2]Ministry of Science and Education of the Republic of Azerbaijan, Institute of Oil and Gas, Azerbaijan
9, F.Amirov str., Baku, AZ1000
[3]Middle East Technical University, Turkiye, Northern Cyprus Campus
99738, Güzelyurt
**Corresponding author: vagif.kerimov@mail.ru*

Keywords: *disruptive technologies, seismic interpretation, geological model, stratigraphy, hydrocarbons, stratigraphic traps, SAI-SVision technology*

Summary. The modern oil and gas industry is in urgent need of a radical increase in the efficiency of exploration activities to optimise project management. Traditional seismic interpretation technologies have reached their technological limits and are no longer capable of providing the required twofold reduction in desk study timelines while simultaneously improving the quality and detail of geological models. This paper examines an innovative development — SAI-SVision, a full-volume seismic interpretation technology designed to fundamentally transform the approach to organising and executing desk studies. The system's key advantage lies in its ability to rapidly create high-precision structural models. This enables reducing project timelines through the deep parallelisation of technological processes, enhancing the accuracy of integrating heterogeneous data based on a unified structural framework, and optimising decision-making under tight time constraints. The implementation of SAI-SVision delivers a substantial economic effect even at its current stage of development. Further prospects for the technology are linked to its integration directly into the seismic data processing stage, which will significantly improve the quality of depth-velocity models and the signal-to-noise ratio. The final stage of the system's evolution will be the launch of a specialised sedimentation module. This tool will provide the direct transformation of seismic data into a three-dimensional lithofacies grid, creating a reliable foundation for the detailed prediction of fluid saturation and geomechanical characteristics of the section. Thus, the technology elevates the geological modeling process to a qualitatively new, automated level.

Introduction

Conventional seismic interpretation technologies have reached their technological limits and can no longer deliver the efficiency levels required today. Specifically, to optimise project management and ensure timely decision-making, oil companies require a twofold reduction in office-based turnaround time. Simultaneously, this must be achieved alongside an increase in the quality of the resulting geological models. Meeting such demands through the modernisation of standard solutions is unfeasible. The only way forward is the deployment of disruptive innovations. However, even when such technologies are available, their adoption is hindered by several factors. The most formidable challenge is the complexity of integrating breakthrough technologies into production, as the quantum leap in efficiency they provide necessitates a new approach to achieve results: a shift in outdated paradigms and a fundamental modernisation of the entire production process (Fig. 1).

The paper introduces "SAI-SVision," an innovative full-volume seismic interpretation technology that delivers next-generation geological models and completely redefines the office-based interpretation paradigm.

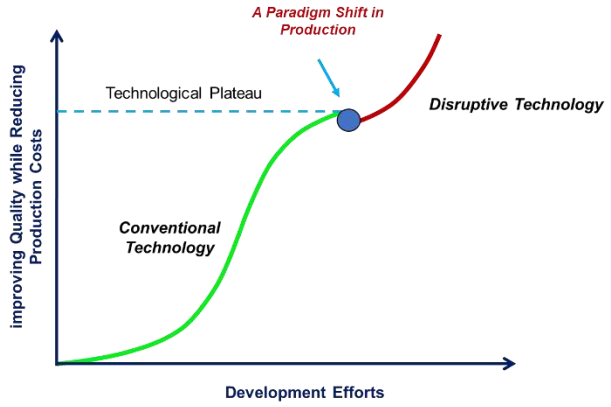

Fig. 1. Disruptive vs. Conventional Technology

Improving seismic interpretation performance via "SAI-SVision" technology

Conventional seismic interpretation is described as an exhausting, iterative sequential process that relies on expert-driven, manual, or semi-automatic tracking of selected horizons from seismic volume. This method is characterised by significant labor intensity, minimal data utilisation (less than 1%), a the high probability of missing prospective targets, substantial uncertainty, and generally low geological model quality, as multiple interpretations can be derived from the same dataset.

At the same time, automating the horizon tracking process fails to either reduce office-based turnaround time or improve the quality of the resulting geological models. This is because automation does not alter the fundamental approach based on analysing a few individual horizons, nor does it eliminate the drawbacks of data underutilisation and the cyclical, iterative nature of the interpretation process.

Full-volume interpretation ensures maximum utilisation of seismic data, which is transformed into a comprehensive model of the medium — the Stratigraphic Cube (SC). The SC is a three-dimensional grid where all nodes are linked by relative depositional ages. The level of detail in the Stratigraphic Cube matches the original seismic data, and its isosurfaces represent chronostratigraphic boundaries.

Analysis of the full-volume model is conducted using the "SVision" methodology. For this purpose, an animated model of sedimentary cover formation is created, typically incorporating several hundred of the most extensive chronostratigraphic boundaries. This model allows tracking changes in paleogeomorphological (in isochrons) and facies (in amplitudes) conditions within the study area, identifying prospective targets across all stratigraphic levels.

The full-volume interpretation approach resolves all the issues inherent in traditional methods, including project timelines, model ambiguity, missed targets, and horizon intersections. Turnaround times are reduced by an order of magnitude, and re-interpretation is no longer required, as the Stratigraphic Cube contains all possible surfaces that can be constructed. Furthermore, all surfaces are mutually consistent, which inherently eliminates intersections. Figure 2 presents examples of missed stratigraphic-type prospects from the standard approach, demonstrating the high efficiency of "SAI-SVision" technology in both marine and continental paleobasin environments.

In carbonate depositional environments, animated models enable the reconstruction of bioherm growth (Fig. 3). This allows for a detailed study of facies settings, including the identification of reef, debris flow (fore-reef), and back-reef lagoon facies.

A new paradigm for organising office-based interpretation workflows

As with any disruptive technology, "SAI-SVision" fundamentally transforms the very paradigm of the production workflow. Under the conventional approach, a sequence of procedures is performed with ambiguous results. This means that it is difficult to assess the economic impact before the work is completed, as the number of identified prospects, their resource potential, and the eventual development costs remain unknown (Kerimov et al., 2019).

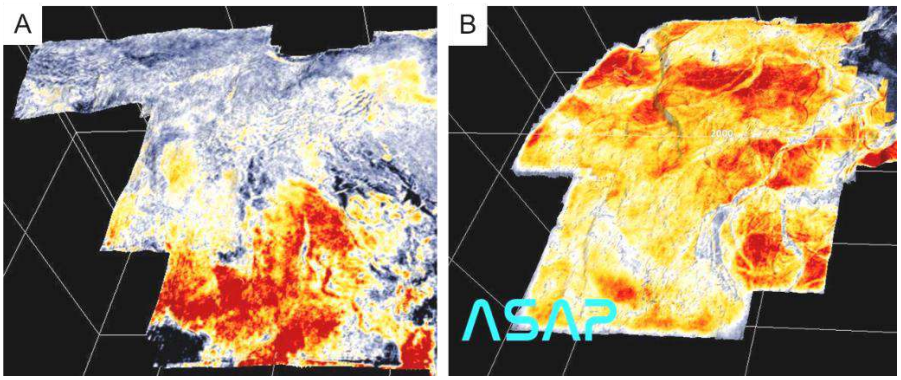

Fig. 2. Stratigraphic traps missed during conventional interpretation. Snapshots from "SVision" animated models: A – Western Siberia, Achimov formation; B – Western Siberia, continental Jurassic

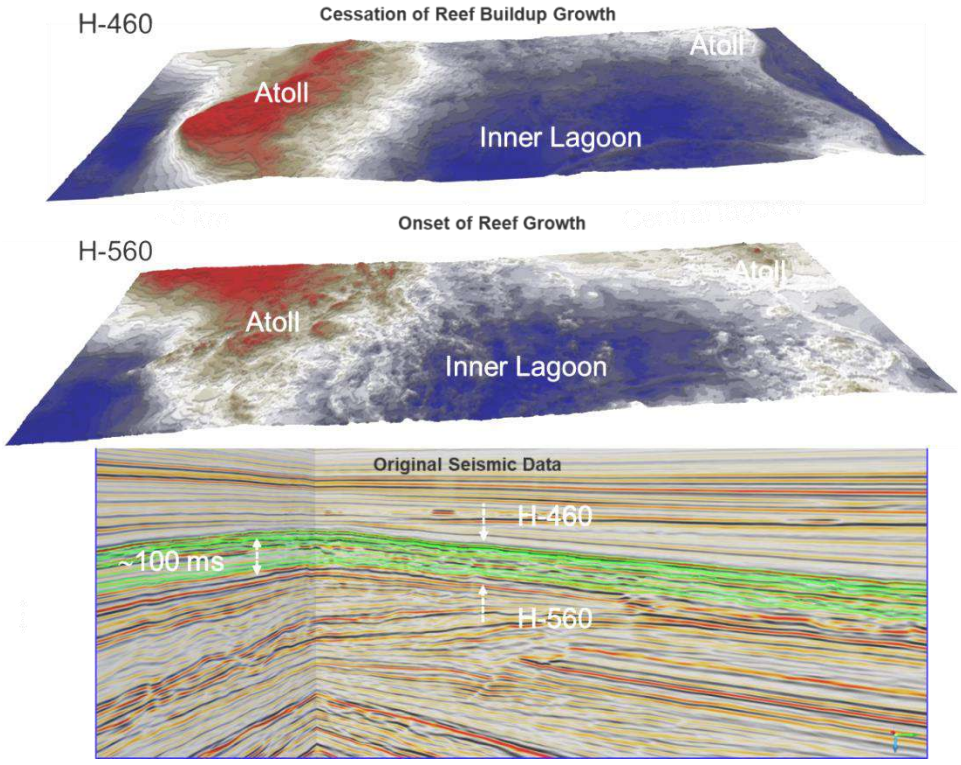

Fig. 3. Reconstruction of reef growth using "SAI-SVision" (North West Shelf, Australia)

In the case of full-volume interpretation, information regarding the presence and scale of all targets – both structural (anticlinal) and stratigraphic – is available within a few days of completing the data processing stage. Notably, one pilot project demonstrated that after eight months of office-based studies using conventional technology, an experienced service company failed to provide any additional geological data beyond what "SAI-SVision" had already delivered within just two days of starting the work (Gorbunov et al., 2021).

Leveraging these and other advantages of this disruptive technology requires a radical reorganisation of the production process at all levels: technical infrastructure, personnel, and regulatory frameworks.

First and foremost, current off-the-shelf interpretation software is fundamentally unsuitable for working with full-volume models (the Stratigraphic Cube), as these tools are designed for analysing individual horizons. Integrating hundreds or thousands of seismic surfaces into a standard analysis workflow is technically unfeasible. Therefore, beyond generating the full-volume model, the "SAI-SVision" technology also provides the capability for its rapid and efficient analysis through the creation of animated models (Guliev et al., 2018a).

On one hand, current technical tools are inapplicable within the framework of the new technology; on the other hand, their existing functionality becomes redundant. Specifically, there is no longer a need for conventional seismic attribute analysis, as detailed paleogeomorphological and lithofacies information is already captured on the Stratigraphic Cube isosurfaces and clearly visualised in "SVision" animated models. Figure 4 illustrates an example of identifying a deep-sea fan in clinoform deposits using "SAI-SVision" compared to the standard seismic attribute analysis methodology (Christensen, 1997, 2003).

Despite the large number of attributes and their combinations used, the maps show only blurred outlines of individual fan elements. Based on these results, it is impossible to assess the true scale of the object (Kerimov et al., 2017a). In contrast, the "SVision" animated model snapshot visualises the target with high resolution. It also clearly shows that a portion of the object extends beyond the study area (Kerimov et al., 2014; Kerimov et al., 2016a).

The implementation of this disruptive technology will also require specialists to significantly transform their professional skill sets. Some skills will become redundant (e.g., horizon correlation), while new ones must be acquired. The conventional geological modeling workflow is fragmented into separate disciplines: interpretation, well-to-seismic ties, inter-well correlation, attribute analysis, petrophysics, etc. (Kerimov et al., 2018). In this siloed approach, each specialist starts working with their own data type, which drastically reduces overall team efficiency; significant time is lost on subsequent coordination and the alignment of individual results, leading to the previously mentioned cyclical and iterative nature of the process (Kerimov et al., 2017b; Guliev et al., 2018b).

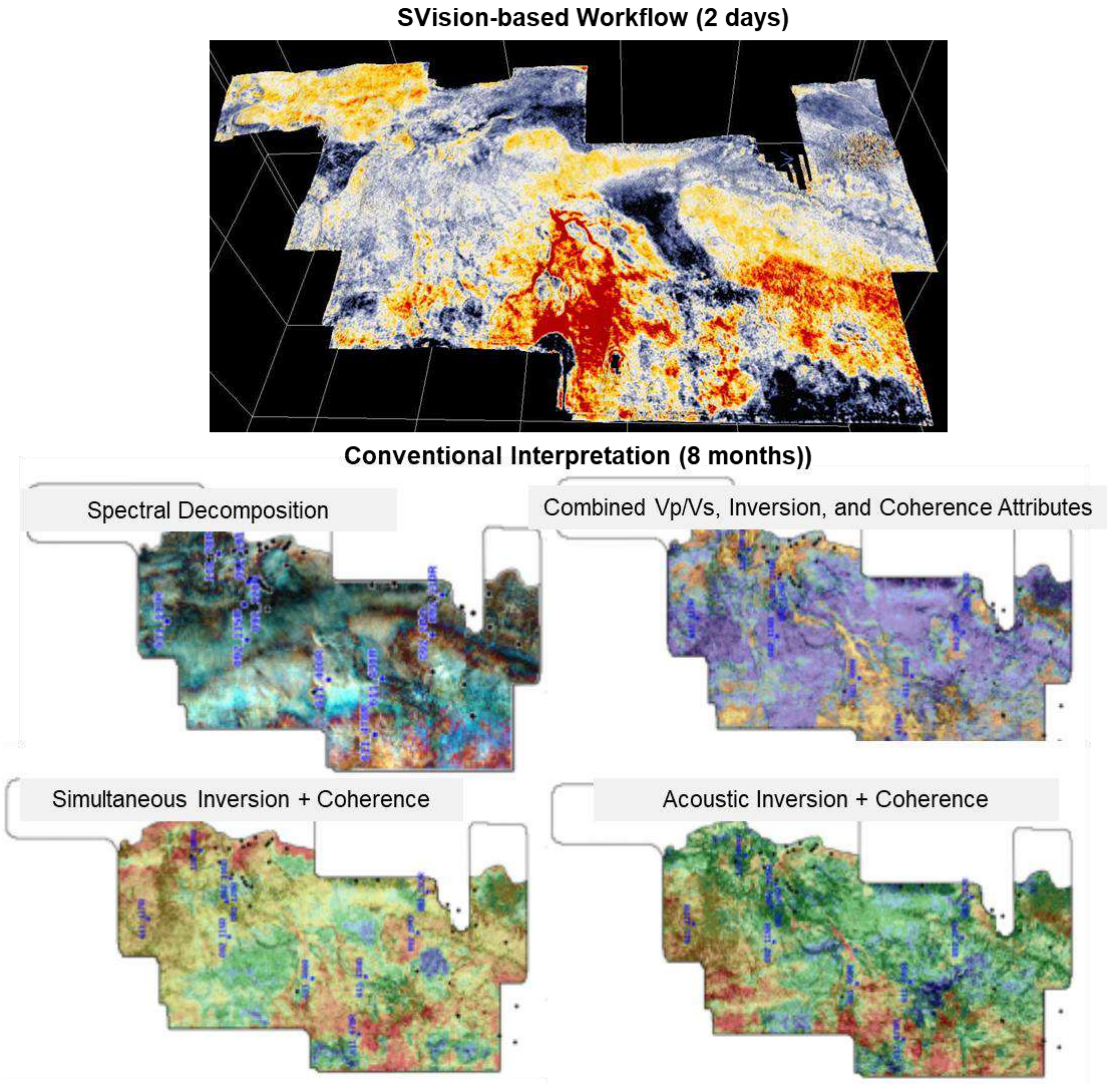

Fig. 4. Comparison of stratigraphic trap identification: "SAI-SVision" vs. conventional seismic attribute analysis

Under the new technology, team collaboration is organised more efficiently (Fig. 5). This is achieved because, once the Stratigraphic Cube is generated and the "SVision" animated models are collectively analysed, all specialists work simultaneously on a unified geological model concept, each within their own discipline.

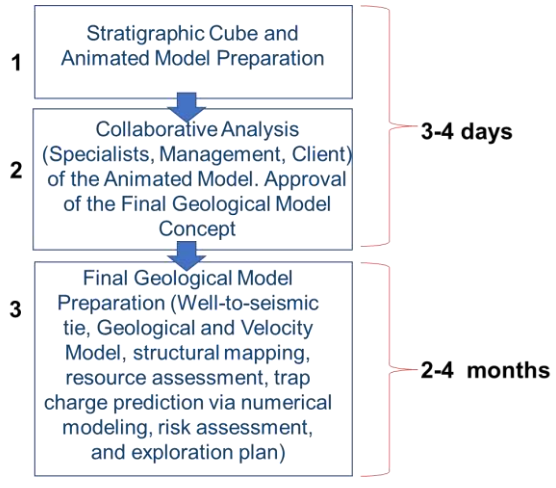

Fig. 5. Key stages of the "SAI-SVision" technology workflow

This approach offers an additional advantage by facilitating management involvement in the geological modeling process at the early stages of the project. This allows project optimisation based on animated model analysis, resource reallocation, and overall more effective project management (Gorbunov, Lavrenova, 2018). For instance, in current practice, the technical assignment (Scope of Work) for office-based studies is formulated before the work even begins. This is inefficient, as the geological features of the target remain unknown, making it generally impossible to select an optimal set of analytical methods. Consequently, some methods prescribed in the SOW prove ineffective, and the set objectives are not met (Lapidus et al., 2018), leading to additional work, budget overruns, and project delays. With "SVision" technology, the optimal list of methods is determined

based on the results of animated model analysis (Rachinsky, Kerimov, 2015; Kerimov et al., 2015a).

The ability to parallelise the interpretation process once, the structural framework (the Stratigraphic Cube) is established which allows the integration of multiple independent methods without increasing office-based turnaround time (Kerimov, Gorbunov et al., 2015; Kerimov et al., 2015b; 2015c). This results in more informative geological models. For example, by incorporating numerical modeling, it is possible to produce a fluid saturation map upon completion of the office-based studies, rather than a conventional reservoir map (Fig. 6).

Current realities are such that the existing regulatory framework – including standard technical assignment (SOW) practices, strictly regulated requirements for contractor personnel, mandated software and hardware, and procurement procedures – effectively prevents companies from adopting new technologies and increasing their operational efficiency. Consequently, a transformation of this sector of production activity is also essential (Kerimov et al., 2020; Kerimov et al., 2016b; Kerimov et al., 2015d).

Conclusions

By reorganising existing production processes, a substantial economic impact from "SAI-SVision" technology can be achieved even at its current stage of development. Rapid structural model generation reduces turnaround times through workflow parallelisation, enables the integration of a wider range of multidisciplinary methods, and increases overall interpretation efficiency by utilising a unified structural framework.

Further development of the technology toward its application during the seismic data processing stage will improve the quality of the depth-velocity model and the signal-to-noise ratio, ensuring even greater reductions in office-based turnaround time.

The subsequent development and integration of the "SAI-SVision" sedimentation module will allow the direct transformation of seismic data into a 3D lithofacies grid. This will provide the foundation for high-resolution fluid saturation prediction, geomechanical characterisation of the section, and advanced reservoir modeling.

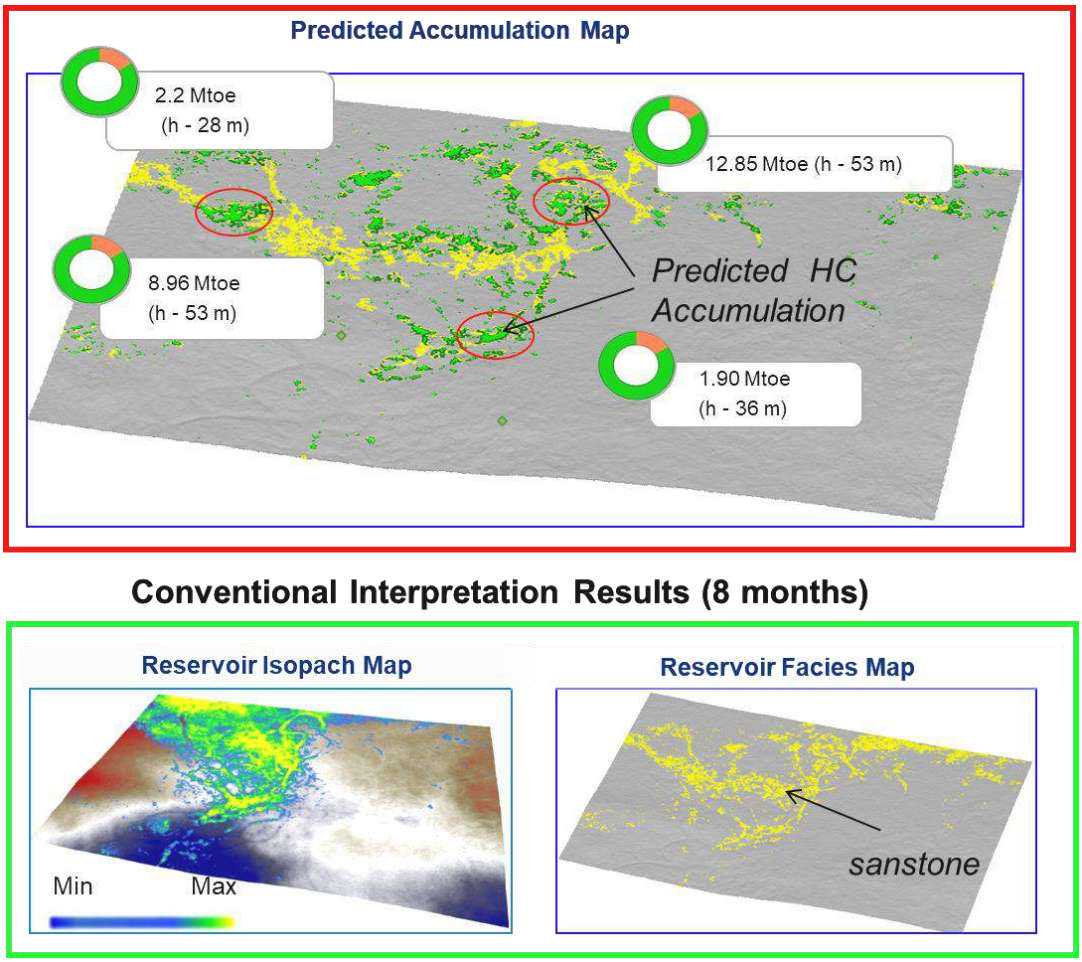

Fig. 6. Enhancement of geological model quality using "SAI-SVision" through interpretation workflow parallelisation and integration of numerical modeling. Project survey data (Shelf, Australia): survey area – 600 sq. km; record length – 5 s; number of wells – 4. Objective: Assessment of hydrocarbon potential in channel-fill deposits

REFERENCES

Christensen CM (1997) The Innovator's Dilemma: When new technologies cause great firms to fail. Harvard Business School Press, Boston, MA, p 225

Christensen CM (2003) The Innovator's Solution: Creating and Sustaining Successful Growth. Harvard Business School Press, Boston, p 320

Gorbunov A, Lavrenova E (2018) SAI - advanced solution to geologic objectives. Preprint. https://doi.org/10.13140/RG.2.2.30054.47689

Gorbunov AA, Murzin RR, Lavrenova EA et al (2021) Analysis of the results of full-volume seismic interpretation by the Svision method (technology "SAI"). Oil and Gas International Exploration Conference "ProGRRess 21. Geological exploration as a business", Sochi, Russia, 1-3 November (in Russian)

Guliev IS, Mustaev RN, Kerimov VY, Yudin MN (2018a) Degassing of the earth: Scale and implications. Gornyi Zhurnal 11:38–42. https://doi.org/10.17580/gzh.2018.11.06 (in Russian)

Guliev IS, Kerimov VY, Mustaev RN, Bondarev AV (2018b) The Estimation of the generation potential of the low permeable shale strata of the Maikop Caucasian series. SOCAR Proceedings 1:4–20. https://doi.org/10.5510/OGP20180100335 (in Russian)

Kerimov V, Kosyanov V, Lavrenova E, Gorbunov A (2019) Strategic innovation in hydrocarbon exploration. ProGREss 2019: Exploration as a Business – Oil and Gas International Exploration Conference: Exploration as a Business, 05–08 November, Sochi, Russia

Kerimov V, Rachinsky M, Mustaev R, Serikova U (2018) Geothermal conditions of hydrocarbon formation in the South Caspian basin. Iranian Journal of Earth Sciences 10:78–89

Kerimov VY, Bondarev AV, Mustaev RN, Khoshtaria VN (2017a) Estimation of geological risks in searching and exploration of hydrocarbon deposits. Oil Industry 8:36–41 (in Russian)

Kerimov VY, Bondarev AV, Osipov AV, Serov SG (2015a) Evolution of petroleum systems in the territory of Baikit anticlise and Kureiskaya syneclise (Eastern Siberia). Oil Industry 5:39–42 (in Russian)

Kerimov VY, Lavrenova EV, Kosyanov VV et al (2020) Implementation of disruptive innovations in exploration – problems and possible ways of their overcoming. 9th International Geological and Geophysical Conference, St. Petersburg, November 16-19, Geosciences: Transforming knowledge into resources, p 18 (in Russian)

Kerimov VY, Osipov AV, Mustaev RN, Monakova AS (2014) Modeling of petroleum systems in regions with complex geological structure. GEOMODEL 2014 –16th Science and Applied Research Conference on Oil and Gas Geological Exploration and Development. https://doi.org/10.3997/2214-4609.20142245

Kerimov VY, Shilov GYa, Mustaev RN, Dmitrievskiy SS (2016a) Thermobaric conditions of hydrocarbons accumulations formation in the low-permeability oil reservoirs of Khadum suite of the Pre-Caucasus. Oil industry 2:8–11 (in Russian)

Kerimov VYu, Gorbunov AA, Lavrenova EA, Osipov AV (2015b) Models of hydrocarbon systems in the Russian Platform-Ural junction zone. Lithology and Mineral Resources 50(5):394–406. https://doi.org/10.1134/S002449021505003X

Kerimov VYu, Mustaev RN, Bondarev AV (2016b) Evaluation of the organic carbon content in the low-permeability shale formations (as in the case of the Khadum Suite in the Ciscaucasia region). Oriental Journal of Chemistry 32(6):3235–3241

Kerimov VYu, Mustaev RN, Dmitrievsky SS et al (2015c) The shale hydrocarbons prospects in the low permeability Khadum formation of the Pre-Caucasus. Oil industry 10(50–53) (in Russian)

Kerimov VYu, Mustaev RN, Serikova US et al (2015d) Hydrocarbon generation accumulative system on the territory of Crimea Peninsula and adjacent Azov and Black Seas. Oil Industry 3:56–60 (in Russian)

Kerimov VYu, Mustaev RN, Yandarbiev NSh, Movsumzade EM (2017b) Environment for the formation of shale oil and gas accumulations in low-permeability sequences of the Maikop Series, Fore-Caucasus. Oriental Journal of Chemistry 33(2):879–892

Lapidus AL, Kerimov VY, Mustaev RN et al (2018) Natural bitumens: Physicochemical properties and production technologies. Solid fuel chemistry 52(6):344–355

Rachinsky MZ, Kerimov VY (Ed b Gorfunkel MV) (2015) Fluid dynamics of oil and gas reservoirs Scrivener Publ – Wiley, NY, USA, p 622

ВНЕДРЕНИЕ ИННОВАЦИОННЫХ ТЕХНОЛОГИЙ В СЕЙСМИЧЕСКОЙ ИНТЕРПРЕТАЦИИ

Горбунов А.А. [1], Лавренова Е.А.[1], Керимов В.Ю.[1,2]*, Мустаев Р.Н.[1], Буньятов А.А.[3]

[1]Российский государственный геологоразведочный университет им. Серго Орджоникидзе, Российская Федерация
117997, Москва, ул. Миклухо-Маклая, д.23

[2]Министерство науки и образования Азербайджанской Республики, Институт нефти и газа, Азербайджан
AZ1000, Баку, ул. Ф. Амирова, 9

[3]Кампус Ближневосточного технического университета на Северном Кипре, Турция
99738, Гюзельюрт

**Автор, отвечающий за переписку: vagif.kerimov@mail.ru*

Резюме. Современная нефтегазовая отрасль остро нуждается в радикальном повышении эффективности разведочных работ для оптимизации управления проектами. Традиционные технологии сейсмической интерпретации достигли своих технологических пределов и больше не способны обеспечить необходимое двукратное сокращение сроков кабинетных исследований при одновременном улучшении качества и детализации геологических моделей. Решение этой масштабной задачи невозможно путем частичной модернизации стандартных инструментов; требуется стратегический переход к инновационным, прорывным технологиям и полная замена устаревших производственных парадигм. В данной статье рассматривается инновационная разработка — технология полнообъемной сейсмической интерпретации «SAI-SVision», призванная фундаментально изменить подход к организации и выполнению камеральных работ. Ключевое преимущество системы заключается в возможности оперативного создания высокоточных структурных моделей. Это позволяет сокращать

сроки проектирования за счет глубокого распараллеливания технологических процессов, повышать точность комплексирования разнородных данных на базе единой структурной основы и оптимизировать принятие решений в условиях жестких временных ограничений. Внедрение «SAI-SVision» обеспечивает существенный экономический эффект уже на текущем уровне её развития. Дальнейшие перспективы технологии связаны с её интеграцией непосредственно в процесс обработки сейсмических данных, что позволит значительно улучшить качество глубинно-скоростных моделей и соотношение «сигнал-шум». Финальным этапом эволюции системы станет запуск специализированного седиментационного модуля. Данный инструмент обеспечит прямую трансформацию сейсмических данных в трехмерный грид литофаций, создавая надежный фундамент для детального прогнозирования флюидонасыщения и геомеханических характеристик разреза. Таким образом, технология переводит процесс геологического моделирования на качественно новый, автоматизированный уровень.

Ключевые слова: *прорывные технологии, сейсмическая интерпретация, геологическая модель, стратиграфия, углеводороды, стратиграфические ловушки, технология SAI-SVision*

SEYSMİK İNTERPRETASİYA SAHƏSİNDƏ İNNOVATİV TEXNOLOGİYALARIN TƏTBİQİ

Qorbunov A.A.[1], Lavrenova Y.A.[1,], Kərimov V.Y.[1,2]*, Mustayev R.N.[1], Bunyatov A.A[3]
[1]Serqo Orconikidze adına Rusiya Dövlət Geoloji Kəşfiyyat Universiteti, Rusiya Federasiyası
117997, Moskva, Mikluho-Maklay küç., 23,
[2]Azərbaycan Respublikası Elm və Təhsil Nazirliyi, Neft və Qaz İnstitutu, Azərbaycan
AZ1000, Bakı, F. Əmirov küç, 9
[3]Orta Doğu Teknik Üniversitesi, Şimali Kipr Kampusu,
99738, Güzelyurt, ŞKTC
**Yazışmalara məsul: vagif.kerimov@mail.ru*

Xülasə. Müasir neft və qaz sənayesi layihə idarəetməsini optimallaşdırmaq üçün kəşfiyyat əməliyyatlarının səmərəliliyini kökündən artırmalıdır. Ənənəvi seysmik şərh texnologiyaları texnoloji hədlərinə çatıb və artıq masaüstü tədqiqatların tələb olunan yarıya endirilməsini təmin etməklə yanaşı, geoloji modellərin keyfiyyətini və detallarını da yaxşılaşdıra bilmir. Bu iddialı vəzifə standart alətlərin qismən modernləşdirilməsi yolu ilə həll edilə bilməz; innovativ, irəliləyişli texnologiyalara strateji keçid və köhnəlmiş istehsal paradiqmalarının tamamilə dəyişdirilməsi tələb olunur. Bu məqalədə innovativ bir inkişaf — masaüstü işlərin təşkili və yerinə yetirilməsinə yanaşmanı kökündən dəyişdirmək üçün hazırlanmış tammiqyaslı seysmik şərh texnologiyası olan SAI-SVision müzakirə olunur. Sistemin əsas üstünlüyü yüksək dəqiqlikli struktur modelləri tez bir zamanda yaratmaq qabiliyyətidir. Bu, texnoloji proseslərin geniş paralelləşdirilməsi yolu ilə dizayn müddətini azaldır, fərqli məlumatların vahid struktur əsasda inteqrasiyasının dəqiqliyini artırır və sıx vaxt məhdudiyyətləri altında qərar qəbuletməni optimallaşdırır. SAI-SVision-ın tətbiqi hətta hazırkı inkişaf səviyyəsində belə əhəmiyyətli iqtisadi fayda təmin edir. Texnologiyanın gələcək perspektivləri onun dərinlik-sürət modellərinin keyfiyyətini və siqnal-səs-küy nisbətini əhəmiyyətli dərəcədə yaxşılaşdıracaq seysmik məlumatların emalına birbaşa inteqrasiyasındadır. Sistemin təkamülünün son mərhələsi ixtisaslaşmış çöküntü modulunun işə salınması olacaq. Bu alət seysmik məlumatların birbaşa 3D litofasiya şəbəkəsinə çevrilməsinə imkan verəcək və maye doymasının və yeraltının geomekanik xüsusiyyətlərinin ətraflı proqnozlaşdırılması üçün etibarlı bir təməl yaradacaq. Beləliklə, texnologiya geoloji modelləşdirməni keyfiyyətcə yeni, avtomatlaşdırılmış səviyyəyə qaldırır.

Açar sözlər: *qabaqcıl texnologiyalar, seysmik interpretasiya, geoloji model, stratiqrafiya, karbohidrogenlər, stratiqrafik tələlər, SAI-SVision texnologiyası*

ANAS Transactions Earth Sciences 1 / 2026

http://www.journalesgia.com

MODELING OF STRONG GROUND MOTION PARAMETERS AND ARTIFICIAL INTELLIGENCE ALGORITHMS FOR DESCRIBING SEISMIC PROCESSES

Bayramov A.A.[1]*, Yetirmishli G.J.[1], Babayev G.R.[2]*,
Hajiyev N.E.[2], Abusalimov N.G.[2], Aliyev M.M.[2]

[1] *Republican Seismic Survey Center, Azerbaijan National Academy of Sciences, Azerbaijan*
25, Nigar Rafibeyli str., Baku, AZ1001
[2] *Ministry of Science and Education of the Republic of Azerbaijan,*
Institute of Geology and Geophysics, Azerbaijan
119, H.Javid Ave., Baku, AZ1073
**Corresponding authors: babayev74@gmail.com, azad.bayramov@yahoo.com*

Keywords: *earthquake, strong ground motion, peak ground acceleration, mathematical modeling, median models, stochastic modeling, artificial intelligence*

Summary. A systematic analysis of mathematical and geophysical principles applied to the modeling of strong ground motion parameters under seismic loading conditions has been performed. The focus of the study is on one of the key characteristics of the seismic process — the peak ground acceleration (PGA), which represents a fundamental indicator of earthquake intensity. The methodological framework of the research is based on the analysis of median ground motion models that formalise the dependence of seismic impact parameters on the source characteristics, hypocentral distance, and geophysical conditions of the medium. Models of aleatory uncertainty are examined, reflecting the natural variability of ground motion parameters and ensuring the statistical correctness of model parameterisation. Particular attention is given to stochastic modeling, which allows reproducing the probabilistic distribution of strong ground motion scenarios. The application of stochastic algorithms enables the inclusion of both typical and rare extreme events, which is crucial for seismic hazard assessment. The aim of the study is to develop recommendations for the selection and application of mathematically and geophysically justified models, artificial intelligence (AI) algorithms that meet the criteria of accuracy, reliability, and reproducibility. A comparative analysis of different approaches has revealed their respective strengths and limitations, as well as identified the optimal areas of practical application. The practical significance of the research lies in the fact that properly selected and geophysical validated models improve the accuracy of ground motion prediction and enhance the efficiency of engineering calculations during the design of buildings and structures.

1. Introduction

Azerbaijan is located within the central part of the Mediterranean mobile belt and is characterised by high geological activity associated with the interaction of the Arabian and Eurasian lithospheric plates. The region is characterised by high seismicity, modern manifestations of magmatism and mud volcanism, intense landslide processes, and contrasting vertical and horizontal crustal movements (Babayev G. et al., 2020). These processes are clearly manifested in various geostructural zones of the country: in the Azerbaijani part of the Greater and Lesser Caucasus, the Kur Depression, the Gusar-Shabran region, the South Caspian Basin, and the Talysh fold zone. Previous studies have demonstrated that strong earthquakes in the Caspian region can dynamically trigger mud volcano activity, highlighting the complex interaction between seismic waves and near-surface geological systems (Babayev G. et al., 2019).

In recent decades, particularly between 2000 and 2025, seismic and tectonic activity has increased in the country and adjacent regions. Both earthquake sources within Azerbaijan and sources in neighboring countries have intensified, influencing the country's seismic hazard (Babayev T. et al., 2025a). Particular attention is being paid to the northern part of the country –the Greater Caucasus Thrust Zone – where regular observations are conducted using modern seismological equipment.

Under these conditions, developing and improving regional models for predicting strong ground

motion parameters is crucial for seismic hazard assessment and the adaptation of building codes. Azerbaijan's modernised seismic system currently allows the calculation of peak ground acceleration (PGA), peak ground velocity (PGV), and peak ground displacement (PGD), taking into account regional characteristics. The development and updating of such models will improve the accuracy of calculations used in engineering seismology and the development of detailed seismic zoning maps.

This study presents a comprehensive analysis of mathematical and geophysical approaches used in modeling strong ground motion parameters, including median prediction models, aleatory variability assessment, and stochastic modeling methods. From a geophysical perspective, the interpretation of the obtained relationships is based on taking into account the physical properties of earthquake foci, the structure of the lithosphere, and the propagation characteristics of seismic waves in various tectonic and geostructural zones. Given the multifactorial nature of the models under consideration (Bayramov et al., 2024), the results of the analysis provide a solid foundation for the development of physically based and regionally adapted ground motion models. The findings can contribute to improved seismic hazard assessment and the selection of reliable, geophysically correct models applicable to the specific seismotectonic conditions of Azerbaijan.

2. Ground motion models

The paper (Chernov et al., 2019) examines the development of effective models for strong ground motions during potentially hazardous earthquakes in the Alania region (Vladikavkaz, Russia). Models of individual ground motion characteristics are considered: peak ground accelerations PGA, periods of acceleration with maximum amplitude *Ta*, durations of the main phase of oscillations (τ), and macroseismic intensity of shaking (*I*). The earthquake intensity I at a given point is approximately proportional to the logarithm of the peak acceleration (1):

$$log_2 A_{max} \approx 0{,}1 \cdot 2(I - 7) \qquad (1)$$

here A_{max} is the peak acceleration in fractions of the acceleration of gravity *g*, *I* is the intensity of the earthquake at a given point.

The models are presented as probability distribution functions for the values of ground shaking parameters and magnitudes for various earthquake magnitudes (*M*) and distances to the source (*D*). First, the average statistical functions *PGA* (*M*, *D*), *Ta* (*M*, *D*), τ (*M*, *D*), and *I* (*M*, *D*) are determined. Then these functions are approximated to the conditions of the study area introducing corrections into these dependencies. The corrections are determined based on an analysis of the general seismotectonic conditions of the area, the characteristics of the seismic disturbance propagation environment, focal mechanisms, and other characteristics of the study region (Fig. 1). The authors of the article claim that the data they obtained contribute to increasing the accuracy and reliability of probabilistic assessments of seismic hazard and can be used for detailed seismic zoning.

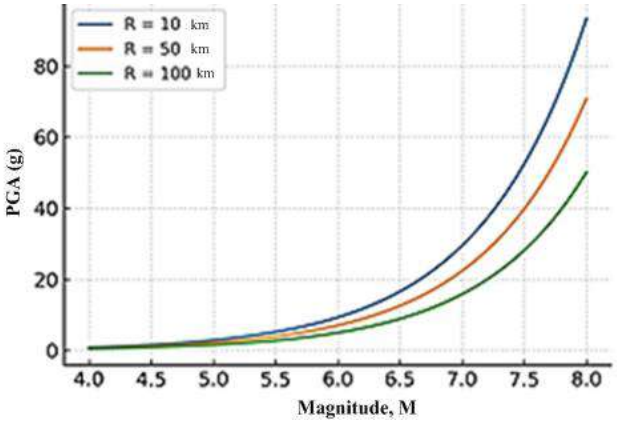

Fig. 1. Illustration of the relationship between PGA and magnitude for different source-to-site distances

In the works (Babayev G. et al., 2010; Babayev G. and Telesca, 2014), using macroseismic data from November 25, 2000 earthquake, an integrated analysis of seismicity, engineering geology, geomorphology, topography, and the impact of soil conditions was carried out in order to model one of the parameters of strong movements, maximum ground acceleration, and an assessment of the distribution dynamics over the area of the Absheron peninsula and the city of Baku. The authors found that most of the peninsula corresponds to an intensity of VIII–IX.

Figure 2 is a bar chart showing the importance of factors in predicting ground motion parameters.

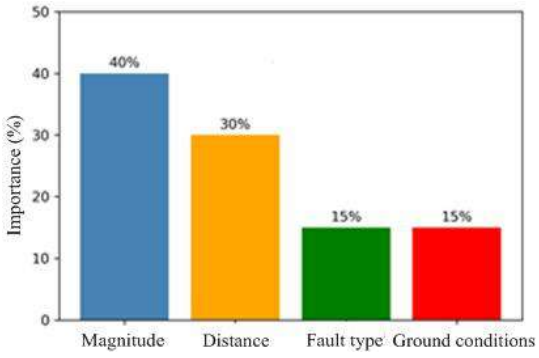

Fig. 2. Chart illustrating the contribution of different parameters to PGA prediction

The diagram shows that earthquake magnitude has the greatest influence on ground motion parameters, followed by distance to the epicenter. The contribution of fault type and soil conditions is significantly smaller, but they are also necessary for accurate forecasts.

3. Local geological conditions in modeling of strong ground motion parameters

Accounting for local geological conditions largely determine the nature and intensity of seismic effects at the surface. Even with identical earthquake source parameters (magnitude, depth, epicentral distance), significant variations in peak ground acceleration (PGA) values are observed due to differences in the engineering-geological properties of the medium. The key parameters influencing soil behavior under dynamic loading include density, elastic modulus, Poisson's ratio, as well as the velocities of compressional (Vp) and shear (Vs) waves. The shear wave velocity (Vs) is considered the most informative indicator and is widely used for classifying soils according to their seismic properties. Soils with low Vs values (loose, water-saturated deposits) tend to amplify seismic waves, whereas rock and dense soils are characterised by lower response amplitudes. In the initial problem formulation, the influence of local conditions was taken into account through the categorical parameter "soil type," used as one of the inputs to the neural network. However, to improve the accuracy and physical validity of the model, it is proposed to extend this approach by incorporating quantitative engineering-geological characteristics. In particular, the use of parameters such as Vs30, thickness of unconsolidated deposits, as well as damping and nonlinear soil behavior indicators is considered.

In addition to soil and lithological properties, specific geological features such as mud volcano systems may also respond dynamically to seismic excitation. Studies indicate that seismic waves can trigger mud volcanic activity in Azerbaijan, emphasizing the importance of accounting for such coupled geological processes in seismic hazard assessment (Babayev G. et al., 2019).

A significant role is played by the effect of local amplification associated with contrasts in the elastic properties of layers, as well as resonance phenomena that occur when the natural frequencies of the soil column coincide with the dominant frequencies of the seismic signal. Under such conditions, a substantial increase in motion amplitudes may be observed, directly affecting PGA values. Accounting for these effects is especially important while assessing seismic hazard in areas with complex geological structures. From the perspective of artificial intelligence algorithms, the incorporation of local conditions is achieved by expanding the input parameter vector and training the model on a more representative dataset reflecting the diversity of geological environments. The integration of additional parameters enables the neural network to capture more complex nonlinear relationships between medium characteristics and seismic response parameters. In the future, hybrid approaches combining machine learning methods with numerical modeling of seismic wave propagation may also be employed.

Thus, detailed consideration of local geological conditions is a necessary prerequisite for improving the accuracy of modeling strong ground motion parameters. Expanding the set of input parameters and conducting a deeper analysis of engineering-geological characteristics significantly enhances the predictive capability of the proposed model and ensures a more reliable assessment of seismic effects.

4. Median ground motion model

The study by Campbell and Bozognia (2008) introduced an empirical model describing median ground motion, enabling the estimation of PGA, PGV, PGD, as well as 5% damped linear elastic response spectra over a period range of 0.01 to 10 seconds. The model was developed using data from the PEER NGA database, which includes records of mainshock earthquakes occurring in active tectonic regions. Records deemed inappropriate for evaluating shallow ground motion were excluded from the dataset (Ancheta et al., 2013). The authors established relationships for the standard deviation of the horizontal geometric mean of ground motion. These relationships were applied to earthquakes with magnitudes between 4.0 and approximately 7.5–8.5 (depending on the faulting mechanism) and for source-to-site distances ranging from 0 to 200 km. The model incorporates several influencing factors, including magnitude saturation effects, attenuation with distance, faulting style, rupture depth, hanging-wall effects, both linear and non-linear site conditions, three-dimensional soil behavior, and both inter-event and intra-event variability.

To estimate the median ground motion, the authors proposed equation (2)

$$Ln\hat{Y} = f_{mag} + f_{dis} + f_{flt} + f_{hng} + f_{site} + f_{sed} \quad (2)$$

Here: Y is the median estimate of the geometric mean of the horizontal component, f_{mag} is the magnitude function, f_{dis} is the distance function, f_{flt} is the function describing the fault mechanism, f_{hng} is the function describing the hanging block (layer) of the fault, f_{site} is the response function of the soil section, f_{sed} is the response function of the synclinal fold (recall that this is a type of folded bending of the layers of the Earth's crust characterised by a concave shape,

an inclination of the layers to the axis and the occurrence of younger layers in the axial part and older ones on the wings.

5. Aleatory uncertainty model

Soil non-linearity (inhomogeneity) causes the standard deviation within an event to depend on the PGA amplitude of the supporting rock rather than on the magnitude, resulting in reduced aleatory uncertainty at high ground shaking levels (Liou and Abrahamson, 2025). Recall that aleatory uncertainty, or statistical uncertainty, is associated with the inherent randomness and variability of a system or process and arises from the stochastic nature of the environment, material inhomogeneity, temporal fluctuations, and spatial variations.

According to the random effects' regression analysis used to obtain the median ground motion model, the aleatory uncertainty model is given by equation (3):

$$LnY_{ij} = Ln\hat{Y}_{ij} + \eta_i + \varepsilon_{ij} \quad (3)$$

Here: η_i is the parameter characterizing the between-event residual for event i; $\hat{Y}_{ij}$, Y_{ij}, and ε_{ij} are the predicted value, observed value, and within-event residual, respectively, for record j of event i. Independent normally distributed variables η_i and ε_{ij} have zero means and estimated between-event and within-event standard deviations τ and σ, given by equations (4), (5), (6)

$$\tau = \tau_{lnY} \quad (4)$$

$$\sigma = \sqrt{\sigma^2_{lnY_B} + \sigma^2_{lnAF} + \alpha^2\sigma^2_{lnA_B} + 2\alpha\rho\sigma_{lnY_B}\sigma_{lnA_B}} \quad (5)$$

where the overall standard deviation equals

$$\sigma_T = \sqrt{\sigma^2 + \tau^2} \quad (6)$$

The authors believe that the proposed model is suitable for estimating PGA, PGV, PGD, and for the linear-elastic response spectra T = (0.01–10) s for weak continental earthquakes occurring in western North America and in other regimes of similar active tectonics (Campbell, Bozorgnia 2006; Stafford et al., 2008). The model is considered the most reliable for evaluation for 4.0 < M < 8.5 for ground slip, M < 8.0 for back thrusts, and M < 7.5 for normal faults; for tremor depths of 0–200 km; and seismic wave velocities of 150–1500 m/s.

6. Stochastic modeling

The work (Pavlenko V. and Pavlenko O., 2023) carried out studies of the parameters of vibrations of the Earth's surface during possible strong earthquakes in the future: peak accelerations and velocities, intensity, response spectra, duration, prevailing periods of vibrations and others in the Baikal rift zone. These parameters need to be assessed for the specific conditions of construction sites. The equation for predicting peak accelerations and velocities on rocky soil, depending on the magnitude of the earthquake and the distance from the source (Pavlenko V., Pavlenko O., 2023) based on records of local earthquakes, can be used in problems of assessing seismic hazard in the Baikal rift zone.

In the matter of choosing the functional form of the ground motion prediction equation (GMPE), the author adopted the equation (Boore and Atkinson, 2008), which made it possible to obtain the desired effects. The equation looks like (7):

$$ln(Y) = F_M(M) + F_D(R, M) + \varepsilon\sigma \quad (7)$$

Here: Y is a value of peak ground acceleration (PGA) in fractions of g or peak ground velocity (PGV) in cm/s; functions F_M and F_D describe the functional dependence on magnitude and distance, i.e. focal and pathway effects; M is an earthquake magnitude; R is an epicentral distance, or Joyner-Boer distance (the shortest distance from the observation point to the projection of the rupture plane onto the Earth's surface); ε is a residual of the regression model, reflecting the spread of observed values relative to the estimates of the regression model; σ is a standard deviation of the residual distribution.

To determine the values of the parameters of equation (6), the author used a two-stage regression method (Boore and Atkinson, 2008), which allows separating the determination of coefficients in the F_D and F_M functions. The resulting prediction equation for ground motion is applicable for $M = 4 \div 8$ and $R = 1 \div 200$ km. At the same time, observational data show a noticeable anisotropy of the medium, i.e. differences, at least, in the attenuation characteristics of seismic waves in different directions.

The work (Khalid and Razbin, 2024) presented a ground motion prediction model (GMPM) using Artificial Intelligence (AI) technology (Suleymanov et al., 2025), in particular, an artificial neural network (ANN) for shallow earthquakes, aimed at improving earthquake safety assessment. The proposed model uses the main input variables such as magnitude, fault type, epicentral distance and soil type, and the output variable is peak ground acceleration (PGA) at 5% attenuation.

To develop this model, 885 pairs of data were obtained from the Pacific Engineering Research Center, providing a robust data set for machine learning and algorithm testing. The ANN architecture includes 4 neural network nodes in the input

layer, two hidden layers each containing 25 neural network nodes, and an output layer with one node, resulting in 750 unknown weights and biases that the model must optimise (Dhanya et.al., 2019). After evaluating the model, the genetic algorithm was integrated with the artificial neural network model to improve its predictive capabilities. This integration aims to predict 20 potential earthquake scenarios, an important step in validating the model's performance. Figure 3 illustrates a flowchart derived from an analysis of this methodology (Dhanya et.al., 2019).

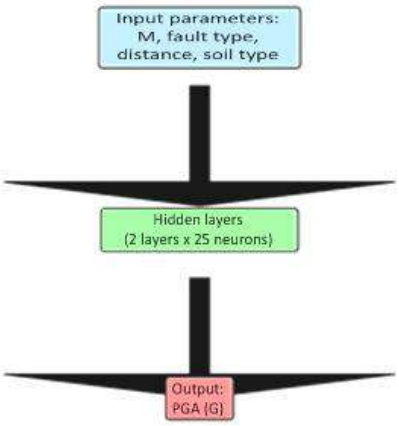

Fig. 3. Schematic structure of the artificial neural network for PGA prediction

The results (Dhanya et.al., 2019) were promising as the proposed model successfully predicted earthquakes in 15 out of 20 scenarios. These results highlight the high potential of the model in accurately predicting seismic events.

The summary analysis by the authors in the current study showed that ANN provided more accurate predictions. This highlights the need to update forecast models on the region (Babayev T. et.al., 2025b).

Analysis of the dependence of PGA on the hypocentral distance for various magnitudes (Fig. 4) shows a regular attenuation of seismic vibrations with increasing distance to the source. At the same time, earthquakes of greater magnitude are characterised by significantly higher PGA values and a longer radius of influence. This result confirms that magnitude and distance to the source are key factors determining the intensity of ground motion. The construction of this graph made it possible not only to visualise the physical nature of the attenuation, but also to justify the choice of these parameters as input nodes of the artificial neural network.

The graph plotted in this study serves as a starting point for developing and training an ANN model: it shows the range of values within which the neural network should capture patterns.

7. Conclusion

During the study, a comprehensive analysis of existing mathematical and geophysical models for predicting the parameters of strong ground motions was performed, taking into account median characteristics, aleatory uncertainty and stochastic modeling approaches. The geophysical aspect of the analysis is based on taking into account the seismotectonic conditions of the region, the structure of the lithosphere, the heterogeneity of velocity sections of the Earth's crust and local features of soil massifs that affect the amplitude-frequency parameters of vibrations. The models considered make it possible to assess seismic hazard in various tectonic zones and geological environments, however, each of them has its own limitations associated with the initial data, the range of applicability in magnitude and distance, as well as the type of soil foundation. The main input parameters are magnitude, fault type, epicentral distance, and soil type, while the output parameter is peak ground acceleration (PGA) at 5% damping. The structure of the neural network used consists of 4 nodes in the input layer, two hidden layers each containing 25 nodes, and an output layer with a single node, resulting in 750 unknown weights and biases that the model must optimise. After model evaluation, a genetic algorithm was integrated with the artificial neural network to improve its predictive capabilities. A total of 20 potential earthquake scenarios were predicted, which is an important step in validating the model's effectiveness. The proposed model successfully predicted earthquakes in 15 out of 20 scenarios, corresponding to a prediction accuracy of 75%. These results highlight the high potential of the model for accurate forecasting of seismic events in Azerbaijan.

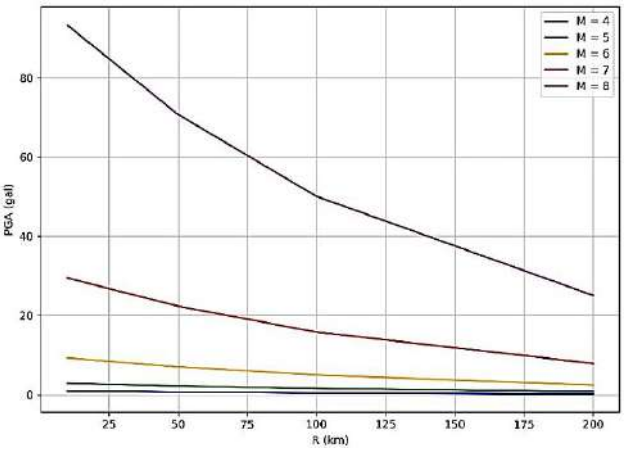

Fig. 4. Graph of the dependence of the hypocentral distance (R) on the PGA for different magnitudes (M)

Particular attention is paid to the integration of modern artificial intelligence technologies, in particular, artificial neural networks, which demonstrate high

predictive ability and allow considering complex nonlinear relationships between earthquake parameters and ground motion characteristics. A geophysical based combination of traditional physical models and machine learning algorithms opens up the possibility of creating a new generation of hybrid models, where physical and mathematical equations describe seismic processes, and neural network methods clarify nonlinear dependencies and regional effects.

Prospects for further research include next:

- development of regionally adapted equations for predicting ground movements for the territory of Azerbaijan, taking into account its seismotectonic structure and fault systems;
- expansion of the database through local and international seismological records and the inclusion of geophysical observation data;
- integration of GIS technologies for spatial modeling of zones of potential strong shaking using seismic geological parameters;
- application of hybrid models (physical + AI) to improve the accuracy of forecasts and ensure physical interpretability of results.

The implementation of these areas will improve the reliability of seismic hazard mapping, optimise the design of earthquake-resistant structures and reduce potential risks for the population and infrastructure.

REFERENCES

Ancheta TD et al (2013) PEER NGA-West2 Database, PEER Report 2013-03. Pacific Earthquake Engineering Research Center, University of California, Berkeley, CA

Babayev G, Ismail-Zadeh A, Le Mouel J –L (2010) Scenario-based earthquake hazard and risk assessment for Baku (Azerbaijan). Nat. Hazards Earth Systems Science 10(12):2697–2712. https://doi.org/10.5194/nhess-10-2697-2010

Babayev G and Telesca L (2014) Strong motion scenario of 25th November 2000 earthquake for Absheron peninsula (Azerbaijan). Journal of Natural Hazards 73:1647–1661, Springer Natural Link. https://doi.org/10.1007/s11069-014-1159-7

Babayev G, Kadirov F, Tibaldi A, Bonali F, Aliyev Y (2019) Dynamic triggering of mud volcanos in Azerbaijan by Caspian earthquakes. ANAS Transactions, Earth Sciences 2:47–53. https://doi.org/10.33677/ggianas20190200031

Babayev G, Telesca L, Agayeva S, Ismail-zade T, Muradi I, Aliyev Y, Aliyev M. (2020) Seismic hazard analysis for southern slope of the Greater Caucasus (Azerbaijan). Pure and Applied Geophysics 177(8):3747–3760. Springer Natural Link. https://doi.org/10.1007/s00024-020-02478-0

Babayev T, Babayev G, Irawan S, Bayramov E (2025b) Development of ANN-based data-driven ground motion model for Azerbaijan using temporal earthquake records of 2022–2024. Front Earth Si 13:1571640. https://doi.org/10.3389/feart.2025.1571640

Babayev TH and Aliyev YN, Babayev GR (2025a) Clustering analysis of 100-year international seismic catalogue for Azerbaijan. Geology and Geophysics of Russian South 15(1):105–118. https://doi.org/10.46698/VNC.2025.99.31.009

Bayramov AA, Abdullayev FN, Suleymanov SS, Karimova RD, Safarov HN, Rzayev EA (2024) Multifactor model for seismological research. Seismoprognosis observations in the territory of Azerbaijan 26(2):28–33. https://doi.org/10.59849/2219-6641.2024.2.28

Boore DM and Atkinson GM (2008) Ground-motion prediction equations for the average horizontal component of PGA, PGV, and 5%-damped PSA at spectral periods between 0.01 s and 10.0 s. Earthquake Spectra 24(1):99–138. https://doi.org/10.1193/1.2830434

Campbell KW and Bozorgnia Y (2006) Next generation attenuation (NGA) empirical ground motion models: can they be used in Europe? Proceedings of the First European Conference on Earthquake Engineering and Seismology 458:01–10. Geneva, Switzerland

Campbell KW and Bozorgnia YN (2008) NGA Ground motion model for the geometric mean horizontal component of PGA, PGV, PGD and 5% damped linear elastic response spectra for periods ranging from 0.01 to 10 s. Earthquake Spectra 24(1):139–171. https://doi.org/ 10.1193/1.2857546

Chernov YuK, Chernov AYu, Chitishvili MI (2019) Models of strong ground motions for probabilistic detailed seismic zoning of the territory of North Ossetia-Alania. Part I. Geology and Geophysics of the South of Russia 9(2):95–108. https://doi.org/10.23671/VNC.2019.2.31980

Dhanya, J, Sagar D, Raghukanth STG (2019) Predictive models for ground motion parameters using artificial neural network. In: Rao A, Ramanjaneyulu K (eds) Recent Advances in Structural Engineering, vol. 2. Series: Lecture notes in civil engineering, vol 12. Springer, Singapore. https://doi.org/10.1007/978-981-13-0365-4_8

Khalid F and Razbin M (2024) Modeling peak ground acceleration for earthquake hazard safety evaluation. Scientific Reports 14(31032). https://doi.org/10.1038/s41598-024-82171-7

Liou IY and Abrahamson N (2025) Framework for aleatory variability and epistemic uncertainty for the Ground-Motion characterization based on the level of simplification. Bulletin of the Seismological Society of America 115(1):296–314. https://doi.org/10.1785/ 0120240141

Pavlenko VA and Pavlenko OV (2023) Stochastic modeling and development of an equation for predicting ground movements in the Baikal rift zone. Physics of the Earth 1:54–66. https://doi.org/10.31857/S0002333723010039 (in Russian)

Stafford PJ, Strasser FO, Bommer JJ (2008) An evaluation of the applicability of the NGA models to ground-motion prediction in the Euro-Mediterranean region. Bull. Earthquake Eng. 6(2):149–177.

Suleymanov S, Bayramov AA, Abdullayev FN (2025) Studing of seismic processes using AI technology. Current directions of development of information and communication technologies and control tools. Proceedings of 15-th International Scientific and Technical Conference 1(1):47, April 24–25 2025, Kharkiv. https://doi.org/10.32620/ICT.25.tl

МОДЕЛИРОВАНИЕ ПАРАМЕТРОВ СИЛЬНЫХ КОЛЕБАНИЙ ГРУНТА И АЛГОРИТМЫ ИСКУССТВЕННОГО ИНТЕЛЛЕКТА ДЛЯ ОПИСАНИЯ СЕЙСМИЧЕСКИХ ПРОЦЕССОВ

Байрамов А.А.[1]*, Етирмишли Г.Д.[1], Бабаев Г.Р.[2]*, Гаджиев Н.Э.[2], Абусалимов Н.Г.[2], Алиев М.М.[2]
[1]Республиканский Центр Сейсмологической Службы,
Национальная Академия наук Азербайджана, Азербайджан
AZ1001, Баку, ул. Н.Рафибейли, 25
[2] Министерство науки и образования Республики Азербайджан, Институт геологии и геофизики, Азербайджан
AZ1073, Баку, просп. Г.Джавида 119
***Авторы, отвечающие за переписку: babayev74@gmail.com, azad.bayramov@yahoo.com*

Резюме. Выполнен системный анализ математических и геофизических принципов, применяемых при моделировании параметров сильных движений грунта в условиях сейсмических воздействий. В центре внимания находится одна из ключевых характеристик сейсмического процесса — максимальное ускорение грунта, являющееся важнейшим индикатором интенсивности землетрясений. Методологическая основа исследования опирается на анализ медианных моделей движения грунта, позволяющих формализовать зависимость параметров сейсмического воздействия от исходных характеристик очага, гипоцентрального расстояния и геофизических условий среды. Рассматриваются модели алеаторной неопределённости, отражающие природную изменчивость параметров движения, что обеспечивает корректность параметризации и возможность учёта статистического разброса данных наблюдений. Особое внимание уделено стохастическому моделированию, позволяющему воспроизводить вероятностное распределение сценариев сильных движений. Применение стохастических алгоритмов обеспечивает охват как типовых, так и редких экстремальных событий, что имеет принципиальное значение для оценки сейсмической опасности. Цель исследования — разработка рекомендаций по выбору и применению математических и геофизически обоснованных моделей, алгоритмов ИИ, удовлетворяющих критериям достоверности, надёжности и воспроизводимости результатов. Сравнительный анализ различных подходов позволил выявить их сильные и слабые стороны, а также определить оптимальные области практического использования. Практическая значимость заключается в том, что корректно выбранные и геофизически обоснованные модели обеспечивают повышение точности прогнозирования параметров сейсмических воздействий и оптимизацию инженерных расчётов при проектировании зданий и сооружений.

Ключевые слова: *землетрясение, сильные движения грунта, максимальное ускорение грунта, математическое моделирование, срединные модели, стохастическое моделирование, искусственный интеллект*

SEYSMİK PROSESLƏRİN TƏSVİRİ ÜÇÜN GÜCLÜ YER HƏRƏKƏTİ PARAMETRLƏRİNİN MODELLƏŞDİRİLMƏSİ VƏ SÜNİ İNTELLEKT ALQORİTMLƏRİ

Bayramov A.A.[1]*, Yetirmişli Q.C.[1], Babayev Q.R.[2]*, Hacıyev N.E.[2], Abusəlimov N.G.[2], Əliyev M.M.[2]
[1]Respublika Seysmoloji Xidmət Mərkəzi, Azərbaycan Milli Elmlər Akademiyası, Azərbaycan
AZ1001, Bakı, N.Rəfibəyli küç., 25
[2]Azərbaycan Respublikasının Elm və Təhsil Nazirliyi, Geologiya və Geofizika İnstitutu, Azərbaycan
AZ1073, Bakı, H. Cavid prosp., 119
[*]Yazışmalara məsul: babayev74@gmail.com, azad.bayramov@yahoo.com

Xülasə. Seysmik təsirlər altında güclü yer hərəkətlərinin parametrlərinin modelləşdirilməsində istifadə olunan riyazi və geofiziki prinsiplərin sistemli təhlili aparılmışdır. Diqqət seysmik prosesin əsas xüsusiyyətlərindən biri üzərindədir: zəlzələ intensivliyinin ən mühüm göstəricisi olan maksimum yer sürətlənməsi. Tədqiqatın metodoloji əsası seysmik təsir parametrlərinin mənbənin ilkin xüsusiyyətlərindən, hiposentral məsafədən və ətraf mühitin geofiziki şərtlərindən asılılığını rəsmiləşdirməyə imkan verən yer hərəkətinin median modellərinin təhlilinə əsaslanır. Tədqiqatın geofiziki konteksti litosferin strukturunu, yer qabığının sürət bölmələrinin heterojenliyini, seysmik dalğaların yayılmasının xüsusiyyətlərini və yerli geoloji şəraitin rəqslərin amplituda-tezlik xüsusiyyətlərinə təsirini əhatə edir. Bu amillər proqnoz tənliklərinin formasını və yer hərəkətinin təhlilində istifadə olunan modellərin parametrlərini müəyyən edir. Hərəkət parametrlərinin təbii dəyişkənliyini əks etdirən aleator qeyri-müəyyənlik modelləri nəzərdən keçirilir ki, bu da parametrləşdirmənin düzgünlüyünü və müşahidə məlumatlarının statistik səpələnməsini nəzərə almaq imkanını təmin edir. Güclü hərəkət ssenarilərinin ehtimal paylanmasının təkrar istehsalına imkan verən stoxastik modelləşdirməyə xüsusi diqqət yetirilir. Stokastik alqoritmlərin istifadəsi həm tipik, həm də nadir ekstremal hadisələrin əhatə olunmasını təmin edir ki, bu da seysmik təhlükənin qiymətləndirilməsi üçün əsasdır. Tədqiqatın məqsədi nəticələrin etibarlılıq, etibarlılıq və təkrar istehsal meyarlarına cavab verən riyazi və geofiziki cəhətdən təsdiqlənmiş modellərin və süni intellekt alqoritmlərinin seçilməsi və tətbiqi üçün tövsiyələr hazırlamaq idi. Müxtəlif yanaşmaların müqayisəli təhlili bizə onların güclü və zəif tərəflərini müəyyən etməyə, həmçinin praktiki tətbiq üçün optimal sahələri müəyyən etməyə imkan verdi. Praktiki əhəmiyyəti ondan ibarətdir ki, düzgün seçilmiş və geofiziki cəhətdən əsaslandırılmış modellər seysmik təsir parametrlərinin proqnozlaşdırılmasında artan dəqiqliyi və bina və tikililərin layihələndirilməsində mühəndis hesablamalarının optimallaşdırılmasını təmin edir.

Açar sözlər: *zəlzələ, güclü yer hərəkəti, maksimum yer sürəti, riyazi modelləşdirmə, orta modellər, stokastik modelləşdirmə, süni intellekt*

ANAS Transactions Earth Sciences 1 / 2026

http://www.journalesgia.com

AQUIFER POTENTIAL IN ALLUVIUM LITOLOGY USING THE HORIZONTAL-TO-VERTICAL SPECTRAL RATIO (HVSR) METHOD, CASE STUDY: COASTAL DEMAK, INDONESIA

Nurwidyanto M.I.*, Harmoko U., Gernowo R., Fernando G.A.

Department of Physics, Faculty of Science and Mathematics, Diponegoro University, Indonesia
Semarang 50275, Indonesia
**Corresponding author: irhammn@gmail.com*

Keywords: *Microtremor, HVSR, Aquifer, the Poisson*'s *ratio, v_s, the Coastal Demak, groundwater*

Summary. The coastal area of Demak is composed of alluvial plains influenced by the presence of coastal deposits. The alluvial area has materials such as silt clay, grained clay, medium sand, silty sand, silt, clay, and sediment. Knowledge of soil structure and modulus of elasticity in the coastal area of the Demak Regency is essential to determine the potential of aquifers in an area. Research using the HVSR (horizontal to vertical spectral ratio) microtremor method was conducted to determine the potential for aquifers beneath the ground surface in the Demak Coastal area. Data collection was carried out at 89 points for 10 minutes using a 3-component TDS type 303S seismograph and a sampling rate of 20 Hz. Microtremor data were processed using Excel, Geopsy, and Dinver software to obtain the v_s and Poisson ratio parameters. The difference between aquicludes can be determined by combining the v_s value with the Poisson's ratio. The value of $v_s < 350$ m can describe the presence of soft clay, stiff clay and silt structures, while the Poisson's ratio describes the saturation of the material. Aquifers can be found with a combination of values ranging from $350 < v_s < 1500$ m and the Poisson's ratio > 0.3. Potential aquifers with saturated clay aquicludes are found at stations 5, 57 and 73, while unsaturated clay aquicludes are found at station 61. Potential aquifers with silt aquicludes are found at stations 14, 60, 71, 38 and 34.

Introduction

Demak is a regency in the Central Java Province located at coordinates 6°43'26" – 7°09'43" South Latitude and 110°27'58" – 110°48'47" East Longitude (BPS Demak Regency, 2020). It borders the Jepara Regency and the Java Sea to the north, Kudus and Grobogan Regencies to the east, Grobogan and Semarang Regencies to the south, and Semarang City to the west. Historically, the Demak Regency was originally a swampy area, resulting in unstable soil structure, particularly on the north coast. Flooding is common during the rainy season, and cracks in the soil are due to muddy structure during the dry season (Rahmawan et al., 2016).

Geologically, the coastal area of Demak consists of alluvial plains influenced by coastal and river sediments (Thanden et al., 1996). Alluvium and coastal deposits will form an unconfined aquifer (Santosa et al., 2021). Geoelectric data in the Demak area indicate the presence of an unconfined aquifer around this research area (Trihatmoko et al., 2020). According to Nurwidianto et al., (2024), most of the Demak area has low dominant frequency, indicating the presence of a very thick alluvium layer (> 30 m). Soil structure and elastic modulus are important parameters in interpreting aquifer potential. Therefore, to determine the soil structure and elastic modulus in the coastal area of the Demak Regency, geophysical methods are needed, one of which is the HVSR method. This method compares the spectrum of the horizontal component with the vertical component of microwaves by assuming that most microwaves are shear waves and ignoring surface waves (Rayleigh and Love waves).

The HVSR method is similar to the transfer function between sediment wave oscillations and bedrock. According to Nakamura (1989), this method is an analytical method based on observations of shear wave propagation for various geological conditions and can be used to determine the value of the amplification factor and the dominant period value in an area that can be estimated from the peak period of the H/V ratio of microtremors (Nakamura, 2000). Through inversion, a v_s value will be produced that can represent the presence of rock structures below the ground surface, as well as the S-wave velocity value (v_s) and the Poisson's ratio that can represent

rock structures and the potential presence of groundwater below the ground surface.

Theory And Geology Research Area

The Demak Regency located on the north coast of Central Java has a significant potential for tidal flooding due to the relatively flat terrain and annual sea level rise. This impacts several villages in the Sayung District, such as Sriwulan, Tambakroto, Gemulak, Bedono, Tugu, Surodadi, Banjarsari, Sidorejo, and others. The coastal area of Demak consists of alluvial plains influenced by coastal and river sediments (Mulyono, 1996). Based on lithology, the area contains silt clay, grained clay, medium sand, silt sand, silt, clay, and so on. The excavated rocks in the area are sedimentary.

In general, the HVSR method is a passive seismic method that uses three components in its measurements: two horizontal components (East-West and North-South), and one vertical component. This method has been widely used to identify the fundamental frequency resonance of buildings and subsurface structures. Natural frequency and amplification are two important parameters resulting from the HVSR method, and its inversion can be used to determine the characteristics and structure of the subsurface, namely the v_s value and the Poisson's ratio related to the physical parameters of subsurface rocks (Herak, 2008). Equation 1 can be interpreted as the longitudinal wave equation. Based on this wave equation, the longitudinal seismic wave velocity or P-wave velocity (v_p) is obtained as:

$$v_p = \frac{(\lambda' + 2\mu)^{\frac{1}{2}}}{\rho} \quad (1)$$

The velocity of transverse waves (S waves) is a wave that comes after the primary wave (P wave) with transverse shear vibrations in a plane perpendicular to the direction of propagation, with a velocity of 60% of the P wave (Telford et al., 1990). The value of v_s in equation 2 can represent the rock structure and is written as follows:

$$v_S = \left(\frac{\mu}{\rho}\right)^{\frac{1}{2}} \quad (2)$$

where v_s is the S-wave velocity (m/s), λ' is Lame's constant, μ is the shear modulus (N/m^2), and ρ is the density (kg/m^3). S-waves can only propagate through solids, so they cannot penetrate liquids (Arintalofa et al., 2020). The v_s value can represent the rock structure.

The Poisson's ratio is the ratio of transverse contraction to longitudinal elongation when the rod is stretched. The Poisson's ratio can be used in the analysis of the presence of water in the soil by utilising transverse contraction to longitudinal strain or elongation as a result of changes in normal stress due to compression or dilation (Das Braja, 1993). In the form of the ratio of the longitudinal wave velocity v_p to the shear wave v_s, the Poisson's ratio can be written as equation 3 (Lay and Wallace, 1995), and classification is in Table 1:

$$\sigma = \frac{v_p^2 - 2v_s^2}{2(v_p^2 - v_s^2)} \quad (3)$$

Table 1

Classification of Poisson Ratio

Value Range	Classification
0.15 – 0.3	Unsaturated clay, sand and gravel
0.3 – 0.35	Silt
0.35 – 0.45	Saturated Clay

Research methods

This research was conducted using a quantitative descriptive method by collecting data in the form of microtremor signal measurements in the form of time-domain seismic signals. Primary data measurement began with the creation of a microtremor measurement survey design of 89 points (Fig. 1) using Google Earth Pro software with a distance between measurement points of 1000-3000 m.

Fig. 1. Map of the location of data collection points in UTM coordinates

Microtremor signal measurements were carried out using a Triaxial Geophone VHL PS 2B and recorded with a GL 240 type data logger (Yulianto and Yuliyanto, 2023a). Seismograph installation requires a geological compass to indicate the north direction, and data collection for each point is carried out for 10 minutes with a sampling rate of 20 Hz (Yuliyanto et al., 2017 and Irham et al., 2021).

The obtained microtremor data was converted to .dat format using Notepad++ software and then converted to .txt format (Yuliyanto and Yulianto, 2023b). Once the data were in .txt format, it could be processed using Geopsy software to obtain the H/V curve (Yuliyanto et al., 2017; Nurwidyanto et al., 2023). Figure 2 shows the microtremor signals captured during the measurements and is the initial data. Then, inversion was performed using Dinver software to obtain the density, v_p and v_s values, and depth through the resulting H/V curve (Figure 3) (Yulianto, Yuliyanto 2023).

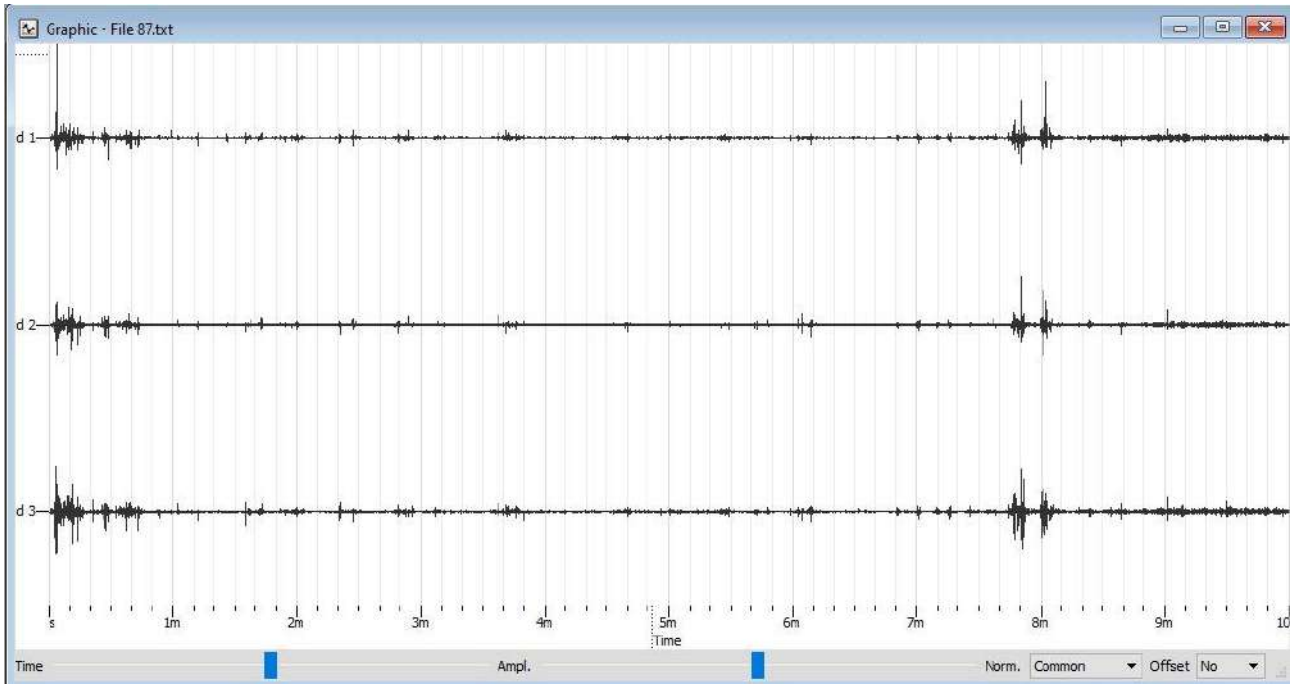

Fig. 2. Microtremor signal at station 87

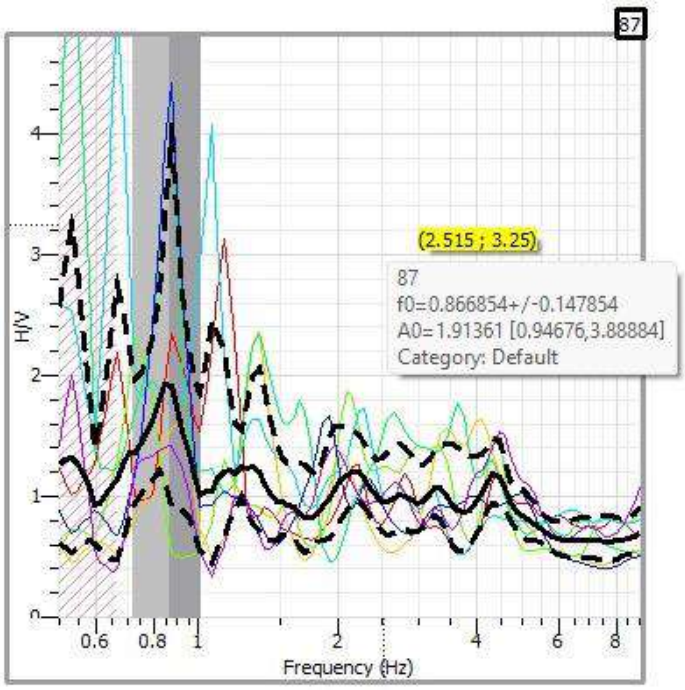

Fig. 3. HV curve at station 87

The results of the inversion have density, v_p, and v_s values at each specific depth according to the characteristics of each area (Yuliyanto et al., 2025). The Poisson's ratio value is obtained using the equation 3. The data is then sorted based on certain depths, namely 0, 10, 20, 30, 40, 50, 60, and 70 m. The selection of these depths is to make it easier to find out specific changes in soil structure within a range of 10 m. Data modeling was performed using ArcGIS software, a spatial analysis tool used in the interpolation process. Interpolation is used to create 2D patterns to estimate values at locations where data is unavailable or unmeasured based on the values of known sample points in the surrounding data.

Results and Discussion

Groundwater aquifers can be identified by observing the v_s value and Poisson's ratio. The v_s value can be used to determine the rock structure in an area. Based on the ASCE 7-16 classification regarding the v_s value, the v_s value can be classified into 5 sections. The first section is the classification of soft soils less than 175 m/s. The second section is the classification of medium soils with v_s values of 175 to 350 m/s. The third section is the classification of hard, very dense soils and soft rocks with v_s values of 350-750 m/s. The fourth section is the classification of bedrock with v_s 750-1500 m/s (Keçeli, 2012). The fifth section is the classification of hard rocks with v_s values of more than 1500 m/s. The Poisson's ratio can explain the fluid content contained in a rock.

Aquifers are located beneath impermeable layers. In this case, the impermeable layer is saturated with water but cannot transmit large amounts of water, or is impermeable (aquiclude). Aquifers in alluvial areas are usually found in gravel and sand, while aquicludes are found in silt and clay. Based on this, they can be classified into areas that are aquicludes/aquifugs and those that are aquifers. Figure 4 explains the v_s values at depths of (a) 0 m, (b) 10 m, (c) 20 m and (d) 30 m. Figure 5 explains the v_s values at depths of (a) 40 m, (b) 50 m, (c) 60 m, (d) 70 m. Figure 6 shows the Poisson's ratio values at depths of (a) 0 m, (b) 10 m, (c) 20 m and (d) 30 m. Figure 7 shows the Poisson's ratio values at depths of (a) 40 m, (b) 50 m, (c) 60 m and (d) 70 m.

Potential aquifers are found in several locations in the study area, with three types of aquicludes: saturated clay, unsaturated clay and silt. The differences between aquicludes can be identified by combining the v_s value <350 and the Poisson's ratio range in Table 1. A v_s value <350 (with soft and medium soil structures according to ASCE 7-16) can indicate the presence of soft clay, stiff clay, and silt structures, while the Poisson ratio reflects the saturation of the material. Aquifers can be found by the presence of a combination of values ranging from $350 < v_s < 1500$ and the Poisson's ratio > 0.3 (in alluvial areas) (Yuliyanto, Nurwidyanto, 2021).

The potential for aquifers with saturated clay aquicludes is found at stations 5, 57, and 73, while unsaturated clay aquicludes are found at station 61. Station 5 shows the presence of a 50 m thick aquiclude (0-50m) with saturated clay and sand as an aquifer at a depth of more than 60 m. Station 57 has an aquiclude at a depth of 0-30 m and an aquifer at a depth of 40-60 m. At a depth of 70 m there is no potential aquifer. Station 73 has a 30 m thick aquiclude with a depth of 0-30 m, and an aquifer was found at a depth of 40 m with a thickness of more than 30 m. Station 61 has an unsaturated clay aquiclude with a thickness of 40 m (0-40 m), and sand was found as an aquifer at a depth of 50 m with a thickness of more than 20 m.

The potential of aquifer with silt aquiclude is found at stations 14, 60, 71, 38 and 34. Station 14 shows the presence of a 40 m thick aquiclude (0-40 m) with silt and sand types as aquifers at depths of more than 50 m. Station 60 has an aquiclude at a depth of 30-40 m and an aquifer at a depth of 50 m with a thickness of more than 20 m. Stations 71 and 38 have a 60 m thick aquiclude with a depth of 0-60 m, and an aquifer was found at a depth of 70 m. Station 34 has an unsaturated clay aquiclude with a thickness of 10 m (40-50 m), and sand was found as an aquifer at a depth of 60 m with a thickness of more than 10 m.

Stations 1, 2, and 51 are areas with sand lithology, as evidenced by the presence of v_s values ranging from $350 < v_s < 1500$ and the Poisson's ratio < 3. Previous research by Trihatmoko et al. (2020) showed a similar interpretation using the geoelectric method. The results of the geoelectric (GL-04) from that study showed a resistivity value of 2.38 at a depth of 10 m, which can be classified as sand saturated with seawater. Depths of 20-60 m indicate a classification of a sand layer with clay inserts. This justifies the use of this microtremor method in determining subsurface potential.

Conclusion

The difference between aquicludes can be identified by combining the v_s value with the Poisson's ratio. A v_s value < 350 m can indicate the presence of soft clay, stiff clay, and silt structures, while the Poisson's ratio indicates the material's saturation. Aquifers can be identified by a combination of a range of $350 < v_s < 1500$ m and the Poisson's ratio >0.3. Potential aquifers with saturated clay aquicludes are found at stations 5, 57, and 73, while unsaturated clay aquicludes are found at station 61. Potential aquifers with silt aquicludes are found at stations 14, 60, 71, 38, and 34.

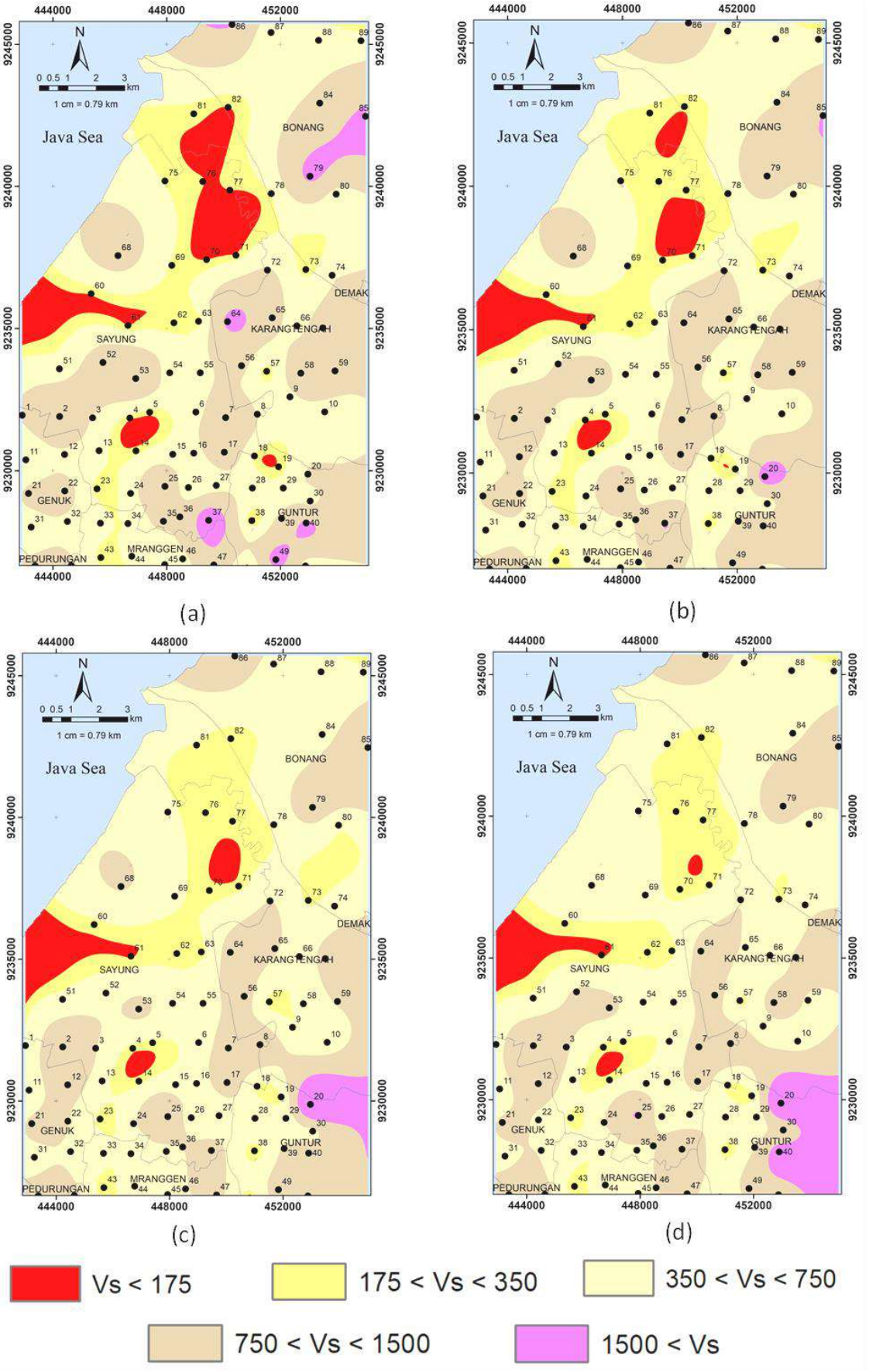

Fig. 4. Modeling v_s at depth (a) 0 m (b), 10 m (c), 20 m (d), 30 m

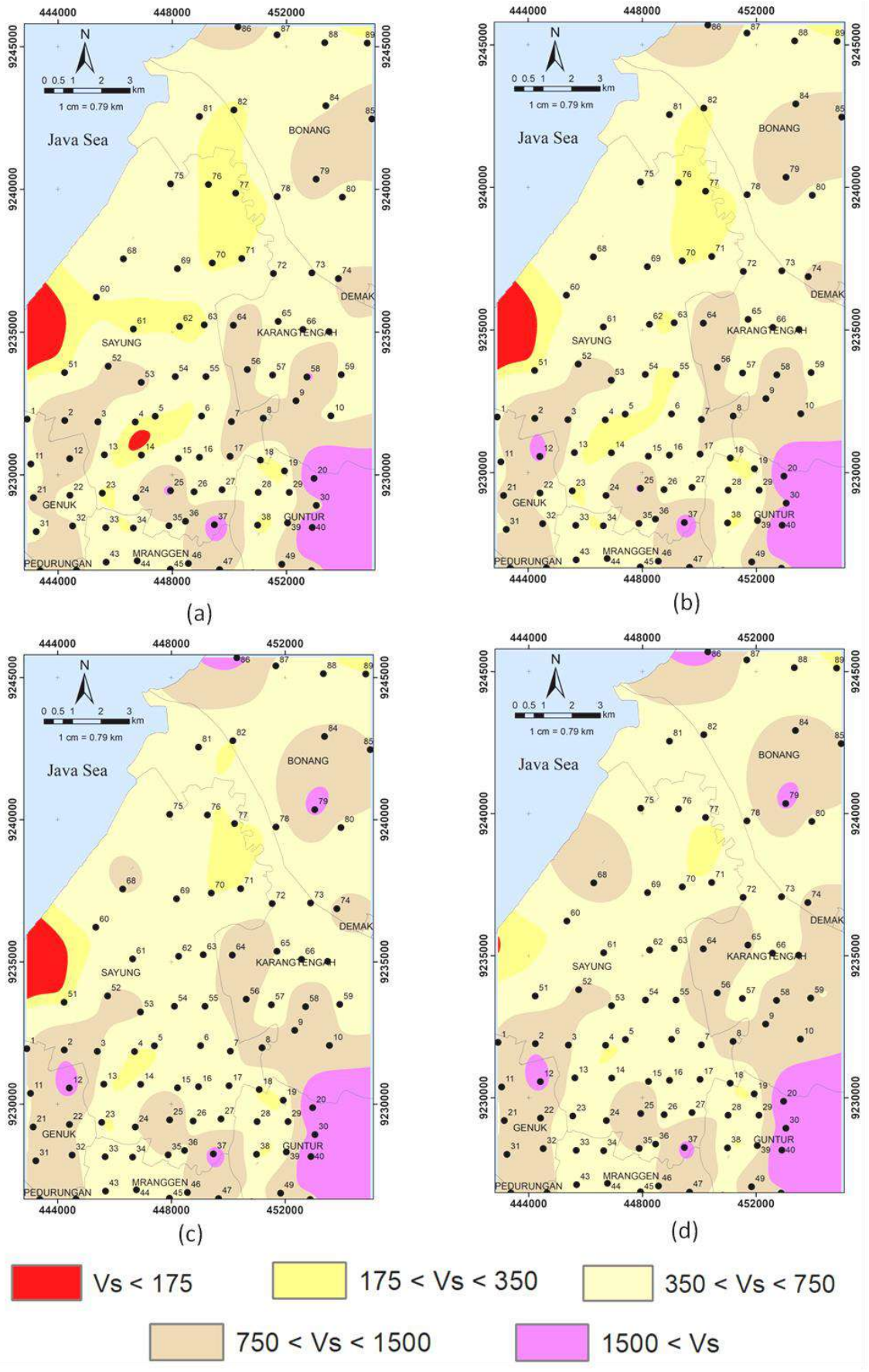

Fig. 5. Modeling v_s at depth (a) 40 m, (b) 50 m, (c) 60 m, (d) 70 m

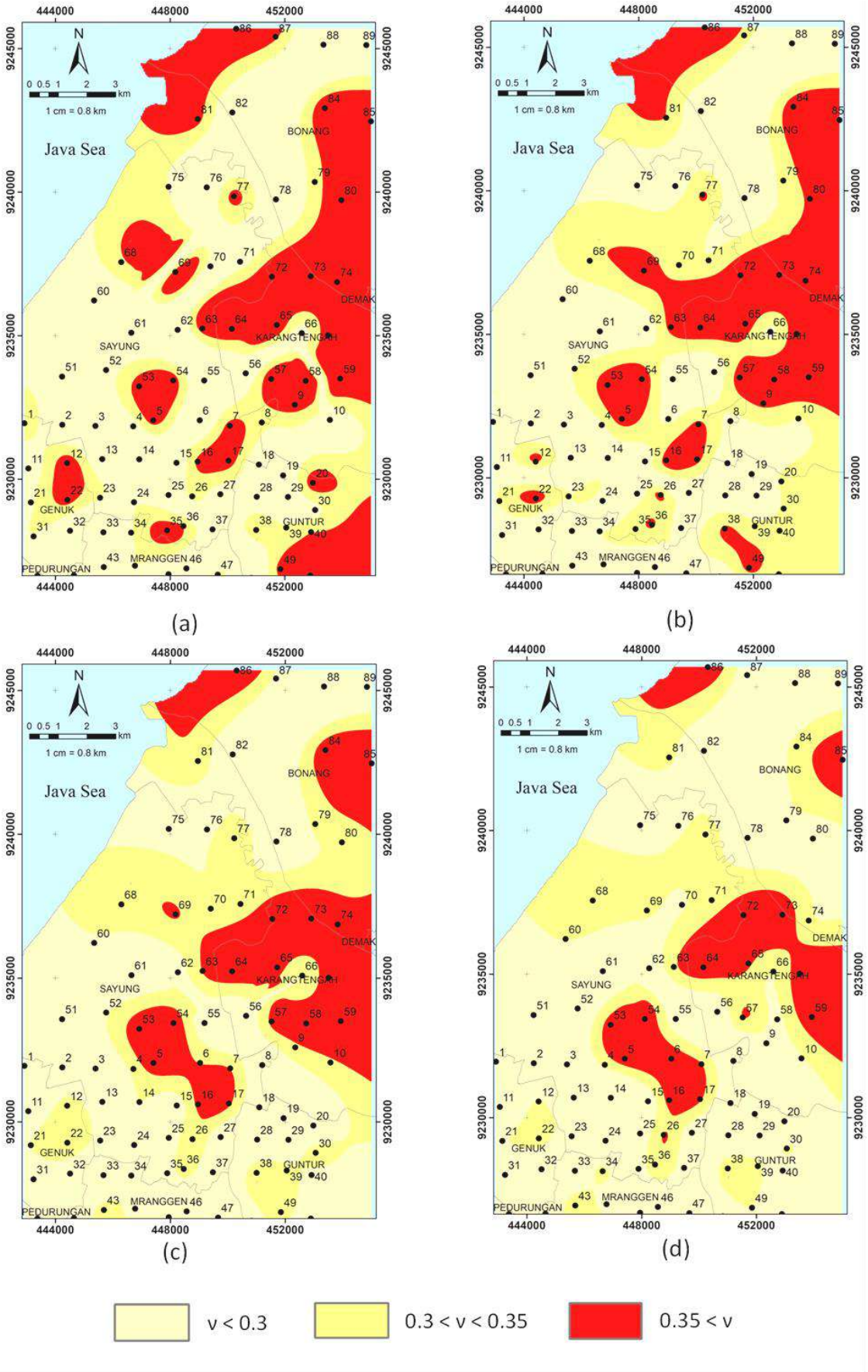

Fig. 6. The Poisson's ratio modeling at depth (a) 0 m, (b) 10 m, (c) 20 m, (d) 30 m

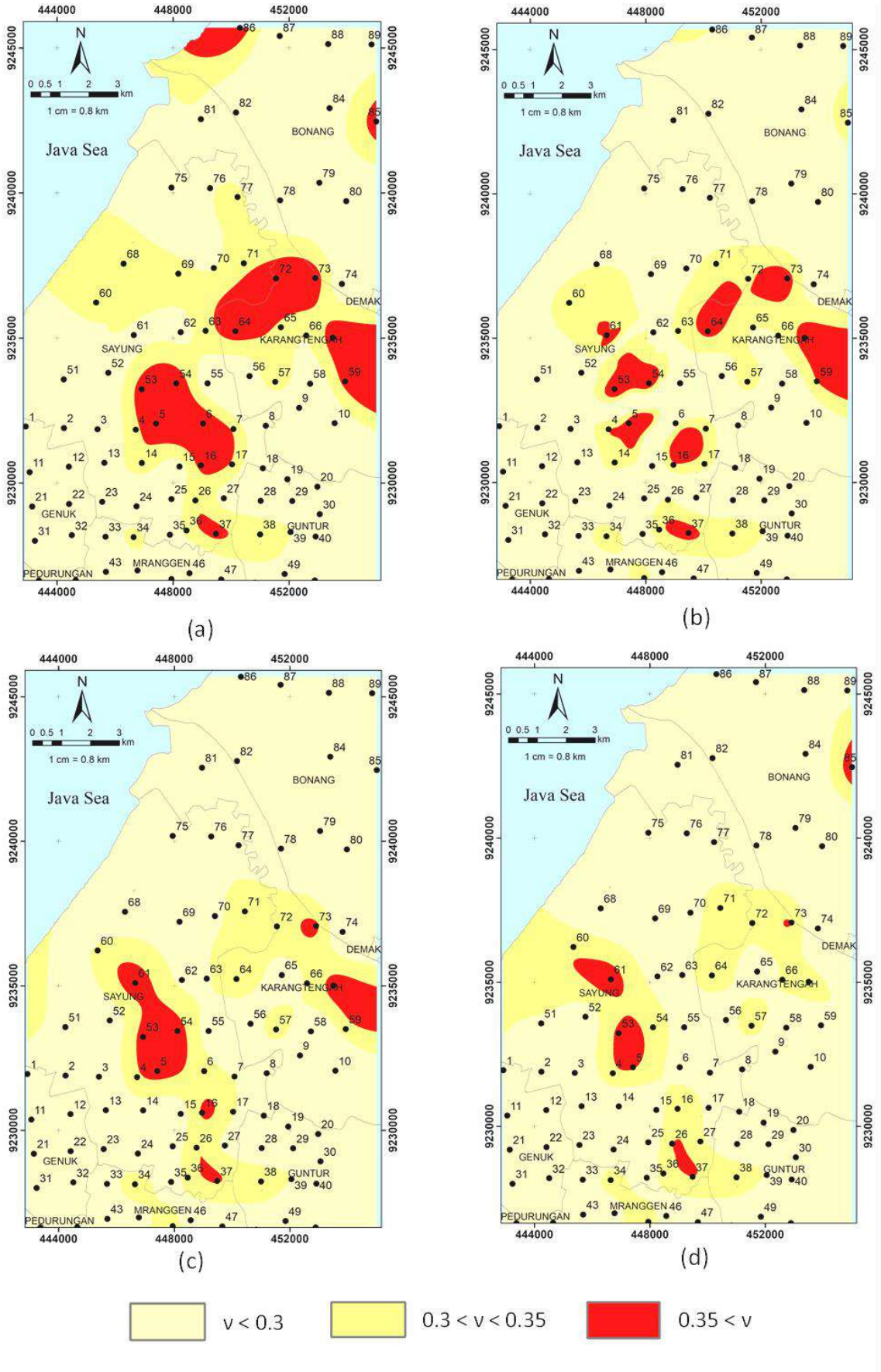

Fig. 7. Poisson ratio modeling at depth (a) 40 m, (b) 50 m, (c) 60 m, (d) 70 m

REFERENCES

American Society of Civil Engineers (2017) Minimum design loads and associated criteria for buildings and other structures (ASCE/SEI 7–16), ASCE. http://doi.org/10.1061/9780784414248

Arintalofa V, Yuliyanto G, Harmoko U (2020) Subsurface characterization of Diwak Derekan geothermal field by HVSR analysis method based on microtremor data. AIP Conference Proceedings, 2296(1). https://doi.org/10.1063/5.0030356

BPS Demak Regency (2020) Demak Regency in figures. BPS Demak Regency. Demak

Das BM (1993) Principles of geotechnical engineering. 3rd edn. PWS Publishing Company, Boston

Herak M (2008) Model HVSR-A matlabs tool to model horizontal to vertical spectral ratio of ambient noise. Journal Computer and Geosciences 34(11): 1514–1526. https://doi.org/10.1016/j.cageo.2007.07.009

Irham MN, Zainuri M, Yuliyanto G, Wirasatriya A (2021) Measurement of ground response of Semarang coastal region risk of earthquakes by Horizontal to Vertical Spectral Ratio (HVSR) microtremor method. IOP Publishing Journal of Physics: Conference Series, 1943(1):012033. http://doi.org/10.1088/1742-6596/1943/1/012033

Keçeli A (2012) Soil parameters which can be determined with seismik velocities. Jeofizik 16:17–29

Lay T, Wallace TC (1995) Modern global seismology. Academic Press, USA, p 521

Mulyono P (1996) Quaternary geological map of the Demak Plate, Java, Bandung. Center for Geological Research and Development

Nakamura Y (1989) a method for dynamic characteristics estimation of subsurface using mikrotremor on ground surface. Q. Rep. RTRI Railw Tech Res Inst 30(1):25-33

Nakamura Y (2000) Clear identification of fundamental idea of Nakamura's technique and its applications. The 12th World Conference on Earthquake Engineering, Auckland, New Zealand, 30 January-4 February 2000, p 2656

Nurwidyanto MN, Harmoko U, Gernowo R et al (2024) Analysis of earthquake vulnerability of the Demak coastal area based on the HVSR (horizontal to vertical spectral ratio) method. Indonesian Journal of Applied Physics 14(2). https://doi.org/10.13057/ijap.v14i2.90703

Nurwidyanto MN, Zainuri M, Wirasatriya A, Yuliyanto G (2023) Microzonation for earthquake hazards with HVSR microtremor method in the coastal areas of Semarang, Indonesia. Geographia Technica 18(1):177–188. http://doi.org/10.21163/GT_2023.181.13

Rahmawan LE, Yuwono BD, Awaluddin M (2016) Monitoring survey of land surface deformation in coastal areas using GPS measurement method in Demak Regency in 2016. Jurnal Geodesi Undip 5(4):44–55 (in Indonesian)

Santosa DPP, Hadian MSD, Zakaria Z (2021) Hydrostratigraphy and aquifer geometry in Palu Groundwater Basin, Central Sulawesi Province after earthquake. Jurnal Sumber Daya Air 17(1):25–38. https://doi.org/10.32679/jsda.v17i.695 (in Indonesian)

Telford WM, Telford WM, Geldart LP (1990) Applied Geophysics. Cambridge University Press, Cambridge, p 792. https://doi.org/10.1017/CBO9781139167932

Thanden RE, Sumadiredja H, Richards PW et al (1996) Geological map of the Magelang and Semarang Sheets, Jawa. Geological Research and Development Centre. Bandung, Indonesia

Trihatmoko E, Wiguna HS, SanjotoTB et al (2020) Preliminary research on seawater intrusion in Sriwulan Village, Demak, Indonesia. Indonesian Journal of Oceanography 2(4):396-402. https://doi.org/10.14710/ijoce.v2i4.9304 (in Indonesian)

Yulianto T, Yuliyanto G (2023a) Microtremor data and HVSR method in the kaligarang fault zone Semarang, Indonesia. Data In Brief 49(109428). https://doi.org/10.1016/j.dib.2023.109428

Yuliyanto G, Yulianto T (2023b) Microtremor data and HVSR method of geothermal manifestation of Mt. Telomoyo, Central Java, Indonesia. Data In Brief 51:109721. https://doi.org/10.1016/j.dib.2023.109721

Yuliyanto G, Harmoko U, Widada S (2017) Identify the slip surface of land slide in Wirogomo Banyubiru Semarang Regency using HVSR method. Int J Appl Environ Sci 12:2069–2078

Yuliyanto G, Nurwidyanto MI (2021) Integrated survey to identify potential groundwater aquifers in Jabungan Semarang using geoelectric and microtremor methods. IOP Publishing Journal of Physics: Conference Series 1943(012026). http://doi.org/10.1088/1742-6596/1943/1/012026

Yuliyanto G, Nurwidyanto MIN, Harmoko U et al (2025) Aquifer zone delineation using correlation between microtremor methods and geoelectricity, ANAS Transactions 1:79–88. https://doi.org/10.33677/ggianas20250100143

ОПРЕДЕЛЕНИЕ ПОТЕНЦИАЛА ВОДОНОСНОГО СЛОЯ АЛЛЮВИАЛЬНЫХ ОТЛОЖЕНИЙ С ИСПОЛЬЗОВАНИЕМ МЕТОДА ГОРИЗОНТАЛЬНОГО И ВЕРТИКАЛЬНОГО СПЕКТРАЛЬНЫХ ОТНОШЕНИЙ (HVSR) НА ПРИМЕРЕ ПРИБРЕЖНОЙ ЗОНЫ ДЕМАКА, ИНДОНЕЗИЯ

Нурвидьянто М.И.*, Хармоко У., Герново Р., Фернандо Г.А.

Факультет физики, факультет естественных наук и математики, Университет Дипонегоро, Индонезия
Семаранг 50275, Индонезия
**Автор, отвечающий за переписку: irhammn@gmail.com*

Резюме. Прибрежная зона Демак состоит из аллювиальных равнин, на которые повлияло наличие прибрежных отложений. Аллювиальная зона содержит такие материалы, как иловая глина, зернистая глина, средний песок, илистый песок, ил, глина и осадок. Знание структуры почвы и модуля упругости в прибрежной зоне округа Демак необходимо для определения потенциала водоносных горизонтов в этом районе. Исследования с использованием метода микросейсм HVSR (горизонтально-вертикальное спектральное отношение) были проведены для определения потенциала водоносных горизонтов под поверхностью земли в прибрежной зоне Демак. Сбор данных проводился в 89 точках в течение 10 минут с использованием 3-компонентного сейсмографа TDS типа 303S и частотой дискретизации 20 Гц. Данные микросейсм обрабатывались с помощью программного обеспечения Excel, Geopsy и Dinver для получения параметров v_s и коэффициента Пуассона. Разницу между водоупорами можно определить, объединив значение v_s с коэффициентом Пуассона. Значение $v_s < 350$ м может характеризовать наличие мягких глинистых, плотных глинистых и иловых структур, в то время как коэффициент Пуассона характеризует водонасыщенность материала. Водоносные горизонты могут быть обнаружены при сочетании значений от $350 < v_s < 1500$ м и коэффициенте Пуассона > 0.3. Потенциальные водоносные горизонты с насыщенными глинистыми водо-

упорами обнаружены на станциях 5, 57 и 73, в то время как ненасыщенные глинистые водоупоры – на станции 61. Потенциальные водоносные горизонты с иловыми водоупорами обнаружены на станциях 14, 60, 71, 38 и 34.

Ключевые слова: *микротремор, HVSR, водоносный слой, коэффициент Пуассона, v_s, прибрежная зона Демак, грунтовые воды*

İNDONEZİYANIN DEMAK SAHİL ZONASI NÜMUNƏSİNDƏ ÜFÜQİ ŞAQULİ SPEKTRAL ƏLAQƏLƏR (HVSR) METODUNDAN İSTİFADƏ EDƏRƏK ALLÜVİAL ÇÖKÜNTÜLƏRİN SULU QATININ POTENSİALININ TƏYİNİ

Nurvidyanto M.I.*, Harmoko U., Gernovo R., Fernando G.A.

Fizika fakültəsi, təbiət elmləri və riyaziyyat fakültəsi, Diponeqoro Universiteti, İndoneziya Semarang 50275, İndoneziya

**Yazışmalara cavabdeh olan müəllif: irhammn@gmail.com*

Xülasə. Demak sahil zonası. Sahil çöküntülərinin təsirinə məruz qalmış allüvial düzənliklərdən ibarətdir. Allüvial zonada lil, gil, dənəvər gil, orta qum, lilli qum, lil, gil və çöküntü kimi materiallar var. Demak sahil bölgəsindəki torpağın strukturu və elastiklik modulu haqqında məlumat bölgədəki sulu təbəqələrin potensialını təyin etmək üçün lazımdır. Demak sahil zonasında Yer səthinin altındakı sulu təbəqələrin potensialını təyin etmək üçün HVSR mikroseysm metodundan (üfüqi şaquli spektral nisbət) istifadə edərək tədqiqatlar aparılmışdır. Məlumatların toplanması 89 nöqtədə 10 dəqiqə ərzində 3 komponentli TDS tipli 303S seysmoqraf və 20 Hz nümunə dərəcəsi ilə aparılmışdır. Mikroseism məlumatları vs parametrləri və Poisson əmsalı əldə etmək üçün Excel, Geopsy və Dinver proqramı ilə işlənmişdir. Su müqaviməti arasındakı fərqi vs dəyərini Poisson əmsalı ilə birləşdirərək müəyyən edilə bilər. Vs dəyəri < 350 m yumşaq gil, sıx gil və lil quruluşlarının mövcudluğunu xarakterizə edə bilər, Poisson əmsalı isə materialın Su doymasını xarakterizə edir. Akiferlər 350 < vs < 1500 m və Poisson əmsalı > 0.3 arasındakı dəyərlərin birləşməsi ilə aşkar edilə bilər. Doymuş gil su keçirməyən potensial sulu təbəqələr 5, 57 və 73 stansiyalarında, doymamış gil su keçiriciləri isə 61-ci stansiyada tapılır. 14, 60, 71, 38 və 34-cü stansiyalarda lil su keçirməyən potensial sulu təbəqələr aşkar edilmişdir.

Açar sözlər: *mikrotremor, HVSR, sulu təbəqə, Poisson əmsalı, vs, Demak sahil zonası, yeraltı sular*

ANAS Transactions Earth Sciences 1 / 2026

http://www.journalesgia.com

HIGH-RESOLUTION REMOTE SENSING UNMASKS QANATS IN GOBUSTAN

Khabarova O.V.[1]*, Eppelbaum L.V.[2,3]

[1]Interdisciplinary Centre for Security, Reliability and Trust, University of Luxembourg
29, Avenue J.F.Kennedy, Luxembourg, L-1855
[2]Department of Geophysics, Tel Aviv University, Israel
Ramat Aviv 6997801, Tel Aviv
[3]Azerbaijan State Oil and Industry University, Azerbaijan
20, Azadlig Ave., Baku, AZ1010
**Corresponding author: olga.khabarova@uni.lu*

Keywords: *remote sensing, Gobustan, qanats, combined geophysical analysis, informational approach*

Summary. Recent studies demonstrate the effectiveness of integrated archaeo-geophysical tools in addressing a wide range of geological and environmental challenges. This approach combines geophysical methods with archaeological fieldwork or remote sensing to support the preliminary survey and analysis of archaeological sites, potentially enhanced by machine learning techniques to estimate the shapes and characteristics of subsurface objects. The present study emphasises the value of informational and probabilistic approaches as optimal tools for assessing and integrating critical data for archaeological research. We employ remote sensing to locate archaeological objects in the Gobustan region of Azerbaijan, which was inscribed on the UNESCO World Heritage List in 2007, and we demonstrate the substantial potential of combined archaeo-geophysical analyses to identify different categories of historical features in this area. For the analysis of freely accessible remote sensing data from different years and missions, advanced interpretation methodologies were applied. We have identified a sophisticated irrigation system characteristic of the Achaemenid Empire period extending beyond the Gobustan National Reserve, comprising interconnected canals, artificial lakes, and ponds, and associated with nearby settlements. The ancient qanats (kehrizes) easily recognisable in satellite images are among the most compelling discoveries, which have not previously been documented in this area. The next stage of this investigation will involve applying surface (or low-altitude) magnetic field analyses, including qualitative and quantitative interpretations of anomalies and three-dimensional modeling. At this stage, reliable physical-archaeological models (PAM) will be developed. The final stage of the research will consist of direct archaeological excavations guided by the established PAM.

1. INTRODUCTION

In 1966, Gobustan was declared a state reserve in Azerbaijan, and in 2007, it was inscribed on the UNESCO World Heritage List. The Gobustan area is well known worldwide for its extensive distribution of mud volcanoes (e.g., Aliyev et al., 2015) and rock paintings (e.g., Rustamov, 2003; Farajova, 2018). Meanwhile, given the centuries-long history of human presence in this area, it is likely to contain a wealth of historical information, including a greater number of yet undiscovered cultural objects, beyond the two phenomena mentioned above. The Israeli and international experiences suggest that a variety of geophysical methods can be effectively applied to locate different types of buried archaeological objects. These methods include magnetic prospecting (Eppelbaum, 2011, 2015), the very low frequency method (Eppelbaum, 2021), the self-potential method (Eppelbaum, 2020), near-surface temperature surveys (Eppelbaum, 2009), and microgravity (Eppelbaum, 2025). Given the complex and variable geological conditions in the area, these geophysical methods will be applied to the zones identified through satellite imagery analyses.

Our preliminary remote sensing (RS) analysis of satellite imagery in the region indicates the presence of various archaeological objects, presumably dating to different epochs, that have neither been documented nor mentioned in existing literature. This suggests that non-invasive remote sensing methods can serve as an initial step in the investigation, after which the most promising targets can be examined using LiDAR and surface geophysical methods. Such an approach is particularly relevant because the archaeological objects in this area may contain subsurface layers extending several meters deep.

Based on numerous innovative technologies, remote sensing is a powerful tool for detecting a variety of previously unknown targets (e.g., Eppelbaum et al., 2024; Khabarova et al., 2024; Birkenfeld et al., 2026). The most illustrative archaeological objects identified through remote sensing are qanats, underground aqueducts constructed using ancient techniques developed over thousands of years. The key idea is to connect the uphill water source to settlements and fields downhill, where there are no rivers, lakes, or groundwater lenses, so gravity works in humans' favor. The underground channels enabled avoiding water contamination, evaporation, and heating. The extension of qanats may reach tens of kilometers.

Qanats were first invented in the ancient Persian Empire and were later adopted by Greek, Roman, and Muslim civilisations. From an aerial perspective, the qanats mainly built during the Achaemenid Empire period can be recognised by a series of evenly spaced vertical shafts used during the construction of the underground water channels (Buławka et al., 2024). In modern Iran, many qanats that are thousands of years old remain functional, although the shaft openings are sometimes only detectable from above through variations in soil color or vegetation patterns. Therefore, identified qanats could be used to access underground water resources. The concept is frequently discussed in the literature (e.g., Endreny and Gokcekus, 2009; Nasiri and Mafakheri, 2015; Abedi et al., 2023; Mohajerani et al., 2024). Although thousands of qanats are known in Azerbaijan, for the first time our study reports the presence of numerous qanat shafts in the Gobustan area.

2. METHOD AND DATA

This study forms part of a larger research initiative exploring the use of remote sensing in archaeological investigations. Within this framework, the focus lies on the archaeological landscape of Gobustan, employing an integrated methodology that combines high-resolution satellite imagery, geophysical modeling, and comparative spatial analysis (Eppelbaum et al., 2024; Khabarova et al., 2024). The study relied on imagery from multiple satellite platforms, including Google Earth Pro (Maxar Technologies), CNES/Airbus, and the Pleiades constellation, with spatial resolutions ranging from 2 meters in multispectral bands to 0.5 meters in the panchromatic band. A key aspect of the approach was temporal layering: images captured in different seasons and across multiple years were overlaid to highlight subtle landscape features shaped by variations in shadow, vegetation, and seasonal soil moisture. This combination of spatial and temporal data enabled the detection of features that might otherwise remain invisible, forming the foundation for subsequent geophysical surveys and comparative spatial analysis.

Unlike many other archaeological features, whose origins and functions often remain uncertain when analysed using remote sensing techniques, qanats exhibit relatively straightforward morphological characteristics, forming linear alignments of vertical shafts that are discernible in aerial or satellite imagery. At ground level, these structures are often unrecognisable, as individual shafts are spaced several meters apart and may be detectable only through subtle variations in soil color or vegetation patterns. Systematic analysis of high-resolution satellite and aerial imagery enables the identification and mapping of these features, providing a reliable non-invasive method for documenting their spatial distribution.

3. INFORMATIONAL APPROACH

It is well known that most inverse problem solutions in geophysics are ill-posed. It means, according to Hadamard (1902), that the solution does not exist, is not unique, or is not a continuous function of the observed geophysical data (so that a small perturbation in the observations can cause an arbitrary error in the solution). This fact calls for the broad application of informational and probabilistic methodologies in applied geophysics.

Estimating the information value of geophysical and other means can be formalised based on the following criteria (revised after Eppelbaum et al., 2003) (Figure 1): (1) Informativeness of the application (informational criterion Γ); (2) Cost of implementing the method (cost criterion C); (3) Time required to carry out the method (time criterion T).

Criteria C and T are easy to calculate directly, but criterion Γ is a non-trivial research problem. A simplified algorithm can be written as:

$$\Omega = \Gamma \cup C \cup T, \tag{1}$$

where $\cup$ is the symbol of the unification.

All the available archaeological/geological information can be represented as the classic three-level model (Figure 1): (a) syntactic – quantity of information, (b) semantic – content of information, and (c) pragmatic – value of information. The logical-heuristic model for describing environmental information thus takes the following form (Eppelbaum et al., 2003):

$$\Gamma = I \cup R \cup V, \tag{2}$$

where I is the quantitative estimation of information, R is the estimation of informational reliability corresponding to the semantic criterion, and V is the estimation of informational value in terms of feasibility according to the pragmatic criterion.

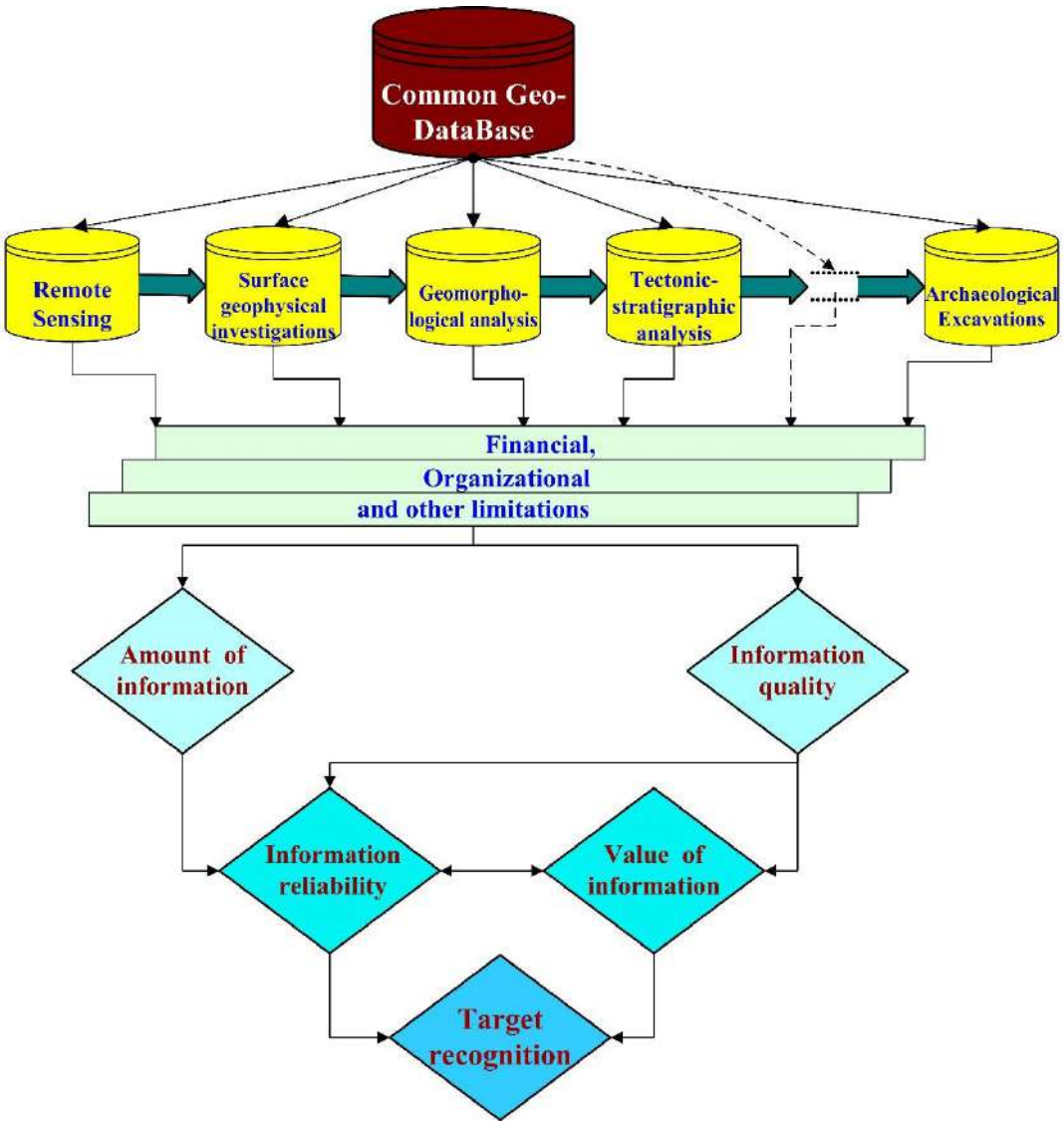

Fig. 1. General scheme for accumulating and processing geospatial information

Algorithm (2) is based on the fundamental terms of information theory and is combined with the structural (hierarchical) approach. This approach defines each indicator as a structure that reflects a set of typical situations and then uses the information measure to calculate the value of each estimator. Parameters V and R should be estimated archaeologically, but this is beyond the scope of this paper. Here, parameters V and R will be neglected, and it is assumed that $\Gamma = I$.

4. EXAMPLES OF REMOTE SENSING DATA ANALYSIS IN GOBUSTAN

RS multidisciplinary analysis has been recognised as a powerful tool for discovering subsurface archaeological targets (Kadhim and Abed, 2023; Tiwari et al., 2023; Eppelbaum et al., 2024; Khabarova et al., 2024). Machine learning techniques can be used to make integrated studies more effective. Applied to archaeology, machine learning (or computer vision methods) has significantly transformed RS data analysis by enabling advanced algorithms to process vast quantities of imagery from satellites and aerial platforms (Davis, 2019). Examples are given in Figures 2 and 3.

The complex physical-geological conditions of the Gobustan region complicate the application of surface geophysical methods. In contrast, satellite imagery provides extensive spatial coverage, including high-resolution images of most terrestrial landscapes. Freely accessible imagery often achieves a spatial resolution of approximately 0.5 meters, sufficient to detect archaeological features at the surface, even when the objects are located several meters below it. This resolution enables the identification of a wide range of environmental and industrial archaeological structures. Among the most significant features found in this study are qanats, as illustrated in Figures 2 and 3. Both figures show qanats approximately 10 km in length, which we identified through

the analysis of multi-year satellite imagery. The yellow dashed lines indicating their locations are intentionally offset to avoid overlapping with the underlying patterns. Although linear sequences of shafts may be obscured in areas affected by sediment deposition or anthropogenic disturbances, numerous qanats connecting former river courses with settlements or agricultural fields at lower elevations were identified, with three traceable over several kilometers.

Fig. 2. Preliminary results of the qanat (kehriz) discovery in the Gobustan area (I). The yellow-dashed line follows the qanat shaft line, which may be traced up to several kilometers from the inlet. Satellite images are taken in May 2009 (main image) and October 2023 (enlarged area). The distance between shafts is 4-5 m

Determining the chronological age of these structures is currently not possible, and on-site investigations are required for accurate dating. However, dating qanats is inherently challenging, as accessing the underground channels is both technically difficult and potentially hazardous. Furthermore, qanats may contain limited stratigraphic information or incorporate artifacts from multiple periods, as flowing water can erode surrounding deposits and transport older materials into the channel, complicating the interpretation of their temporal context. As the next step, the RS analysis must be combined with geophysical and geochemical methods.

Fig. 3. Preliminary results of the qanats (kehriz) discovery in the Gobustan area (II). The yellow-dashed lines crossing the river highlight the qanat location. The yellow arrow indicates the irrigation canal

5. DISCUSSION AND CONCLUSIONS

Qanats, underground water systems, have been in continuous use since their invention in the Persian Empire approximately 3,000 years ago and remain functional in many regions today. These structures are widely distributed across the South Caucasus, Central Asia, and the Near and Middle East. In this study, we report the discovery of qanats in Gobustan, located approximately 70 km southwest of Baku, Azerbaijan, using remote sensing techniques. The presence of qanats in Gobustan has not been documented in previous reviews or reference works (e.g., Guliyev, 2021). Their distinct linear arrangement and repeated patterns clearly exclude natural or geological processes as a plausible explanation for these features.

It should be emphasised that the identified qanats represent only one category of the detected ancient features. Other archaeological objects observed in the area include: (1) the ruins of a columned structure, possibly a temple, tentatively at-

tributed to the ancient Roman period; (2) elongated polished stone slabs on mountaintops, measuring 200–300 meters in length, whose alignment and surface treatment are unlikely to be natural; (3) traces of artificial ponds, some tens of meters in diameter, some of which were probably used for extracting chemicals from the volcano mud. Humans could have utilised mud deposits primarily for clay, plaster, and pigments derived from iron and manganese oxides abundant in the area (e.g., Hajiyeva et al., 2025); (4) wide channels (presumably, irrigation canals) and narrow channels associated with the ponds, running parallel over several kilometers; and (5) remains of multiple settlements located both in the valleys and on the slopes of mud volcanoes.

The solution to this "four colors" mathematical problem (Eppelbaum, 2014) shows that two independent geophysical methods are sufficient to characterise archaeological potential. We propose to apply two independent geophysical methods together: Remote Sensing and high-precision magnetic prospecting (Figure 4).

A unique interpretation system has been developed for analyzing magnetic fields in complex physical-geological environments: oblique magnetisation, rugged terrain relief, and the superposition of magnetic fields of various ranks (Eppelbaum et al., 2001; Eppelbaum, 2011, 2015).

The integrated analysis of RS and magnetic survey datasets can be performed by calculating threshold pixels using color classification or by evaluating the magnitude and directional coherence of vector fields (Eppelbaum et al., 2025). In the most promising areas identified, supplementary investigations using low-altitude LiDAR surveys at 30–40 meters may be required to refine the detection of subtle surface and subsurface features. The combined application of these two independent geophysical methods, high-resolution RS and detailed magnetic surveys, will facilitate the construction of robust physical-archaeological models. These models can subsequently guide targeted, direct archaeological excavations, maximising the efficiency and accuracy of field investigations.

Acknowledgements

We express our sincere gratitude to the rector of Baku State University, Prof. Elchin Babayev, for his assistance in implementing this project.

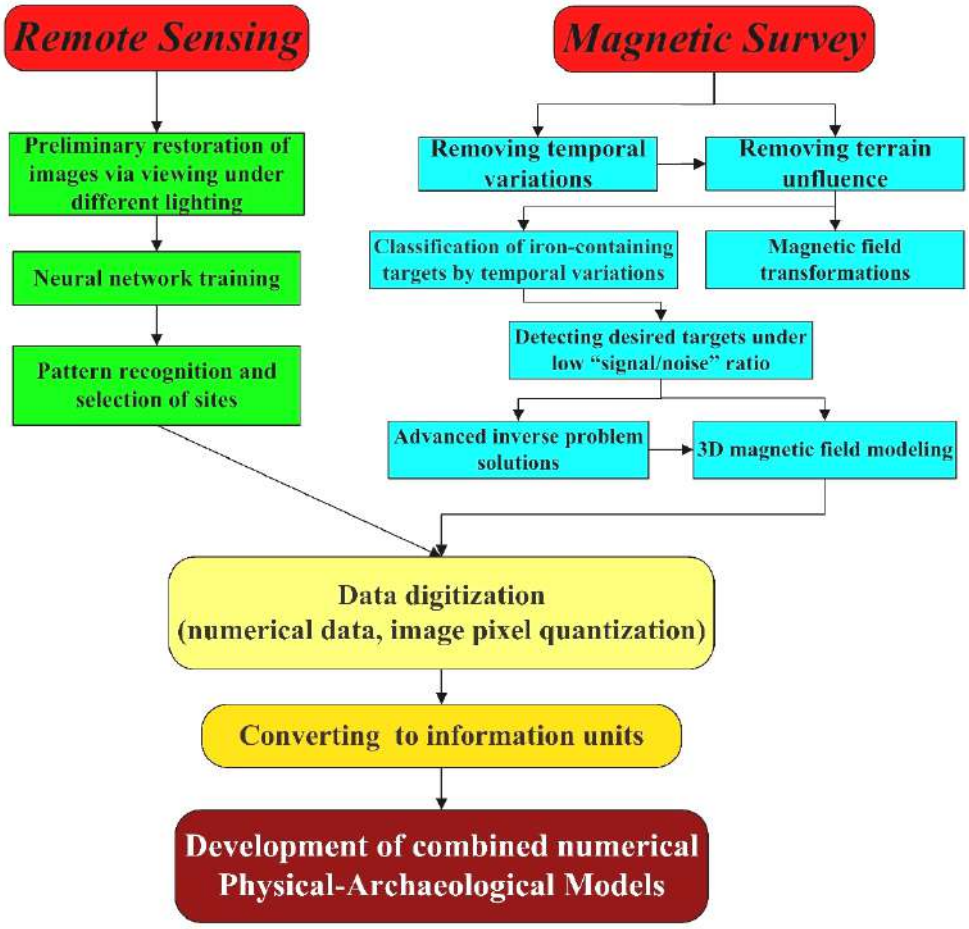

Fig. 4. A generalised flow-chart of combined Remote Sensing and magnetic investigations

REFERENCES

Abedi S et al (2023) Comprehensive classification and categorization of Qanat features: an interdisciplinary exploration using landscape infrastructure concept and semi-systematic review. Environ Systems Research 12**(**35). https://doi.org/10.1186/s40068-023-00318-3

Aliyev AdA, Guliyev IS, Dadashov FH et al (2015) Atlas of the World: Mud Volcanoes. Nafta Press, Baku, p 321

Birkenfeld M, Khabarova O, Eppelbaum L and Berger U (2026) Reassessing Rujm el-Hiri: Aerial imagery and stone circles in the proto-historic Southern Levant. PLOS One 21(3):1–19. https://doi.org/10.1371/journal.pone.0339952

Buławka N, Orengo HA, Berganzo-Besga I (2024) Deep learning-based detection of qanat underground water distribution systems using HEXAGON spy satellite imagery. Journal of Archaeological Science 171:106053. https://doi.org/10.1016/j.jas.2024.106053

Davis D (2019) Object-based image analysis: a review of developments and future directions of automated feature detection in landscape archaeology. Archaeological Prospecting 26:155–163. https://doi.org/10.1002/arp.1730

Eppelbaum LV (2009) Near-surface temperature survey: An independent tool for buried archaeological targets delineation. Jour of Cultural Heritage 10(1):e93–e103. https://doi.org/10.1016/j.culher.2009.08.001

Eppelbaum LV (2011) Study of magnetic anomalies over archaeological targets in urban conditions. Physics and Chemistry of the Earth 36(16):1318–1330. https://doi.org/10.1016/j.pce.2011.02.005

Eppelbaum LV (2014) Four color theorem and applied geophysics. Applied Mathematics 5(4): 658–666. https://doi.org/10.4236/am.2014.54062

Eppelbaum LV (2015) Quantitative interpretation of magnetic anomalies from thick bed, horizontal plate, and intermediate models under complex physical-geological environments in archaeological prospection. Archaeological Prospection 23(2):255–268. https://doi.org/10.1002/arp.1511

Eppelbaum LV (2020) Quantitative analysis of self-potential anomalies in archaeological sites of Israel: an overview. Environmental Earth Sciences 79(377):1–15. https://doi.org/10.1007/s12665-020-09117-w

Eppelbaum LV (2021) VLF-method of geophysical prospecting: A non-conventional system of processing and interpretation (implementation in the Caucasian ore deposits). ANAS Transactions, Earth Sciences 2:16–38. https://doi.org/10.33677/ggianas20210200060

Eppelbaum LV (2025) Microgravity employment in archaeology – available experience and future perspectives. Ig Min Res 3(8):296–314. https://doi.org/10.61927/igmin311

Eppelbaum LV, Eppelbaum VM, Ben-Avraham Z (2003) Formalization and estimation of integrated geological investigations: an informational approach. Geoinformatics 14(3):233–240. https://doi.org/10.3997/2214-4609-pdb.191.P15

Eppelbaum LV, Khabarova O, Birkenfeld M (2024) Advancing archaeo-geophysics through integrated informational-probabilistic techniques and remote sensing. Journal of Applied Geophysics 227(105437):1–12. https://doi.org/10.1016/j.jappgeo.2024.105437

Eppelbaum LV, Khesin BE, Itkis SE (2001) Prompt magnetic investigations of archaeological remains in areas of infrastructure development: Israeli experience. Archaeological Prospection 8(3):163–185. https://doi.org/10.1002/arp.167

Endreny TA and Gokcekus H (2009) Ancient eco-technology of qanats for engineering a sustainable water supply in the Mediterranean Island of Cyprus. Environ Geology 57 (Special Issue):249–257. https://doi.org/10.1007/s00254-008-1274-4

Farajova M (2018) About specifics of rock art of Gobustan and some innovative approaches to its interpretation ("Firuz 2" shelter). Quaternary Intern 491:78–98

Guliyev A (2021) Azerbaijan Qanats. Elm, Baku, p 256

Hadamard J (1902) On partial differential equations and their physical significance. Princeton University Bull 13:49–52 (in French)

Hajiyeva S, Aliyeva T, Shakhnazarova N, Jafarova N (2025) Chemical and ecological characterization of mud volcanoes in the southern part of Gobustan. Universum**:** Chemistry and Biology 9(135):4–8. https://doi.org/10.32743/UniChem.2025.135.9.20744

Kadhim I and Abed FM (2023) A critical review of remote sensing approaches and deep learning techniques in archaeology. Sensors 23(6):2918. https://doi.org/10.3390/s23062918

Khabarova O, Birkenfeld M, Eppelbaum L (2024) Discussion points of the remote sensing study and integrated analysis of the archaeological landscape of Rujm el-Hiri. Remote Sensing 16(22):4239. https://doi.org/10.3390/rs16224239

Mohajerani M, Dokhanian F, Estaji H et al (2024) Geospatial distribution of qanats in Middle Eastern countries: Potential for sustainable groundwater systems. Jour of Arid Environ 222(105170). https://doi.org/10.1016/j.jaridenv.2024.105170

Nasiri F and Mafakheri MS (2015) Qanat water supply systems: a revisit of sustainability perspectives. Environ. Systems Research 4(13). https://doi.org/10.1186/s40068-015-0039-9

Rustamov J (2003) Petroglyphs of Gobustan. Kooperatsiya, Baku, p 103 (in Russian)

Tiwari A, Silver M, Karnieli A (2023) A deep learning approach for automatic identification of ancient agricultural water harvesting systems. Int Jour of Appl Earth Observation and Geoinformation 118(103270):1–13. https://doi.org/10.1016/j.jag.2023.103270

ОБНАРУЖЕНИЕ КЯРИЗОВ В ГОБУСТАНЕ ПО ДАННЫМ ДИСТАНЦИОННОГО ЗОНДИРОВАНИЯ ВЫСОКОГО РАЗРЕШЕНИЯ

Хабарова О.В.[1]* and Эппельбаум Л.В.[2,3]

[1]Междисциплинарный центр безопасности, надежности и уверенности, Люксембургский университет, Люксембург
L-1855, Люксембург, просп. Кеннеди, 29
[2]Кафедра геофизики, Факультет точных наук, Тель-Авивский университет, Израиль
Рамат Авив 6997801, Тель-Авив
[3]Азербайджанский Государственный Университет Нефти и Промышленности, Азербайджан
AZ1010, Баку, просп. Азадлыг, 20
**Автор, отвечающий за переписку: olga.khabarova@uni.lu*

Резюме. Недавние исследования демонстрируют эффективность интегрированных археогеофизических инструментов в решении широкого спектра геологических и экологических задач. Этот подход сочетает геофизические методы с археологическими полевыми работами или дистанционным зондированием для поддержки предварительного обследования и анализа археологических объектов, потенциально дополненного методами машинного обучения для оценки форм и характеристик подземных объектов. Настоящее исследование подчеркивает ценность информационных и вероятностных подходов как оптимальных инструментов для оценки и интеграции критически важных данных для археологических исследований. Мы использовали дистанционное зондирование для обнаружения археологических объектов в Гобустанском регионе Азербайджана, который был внесен в Список всемирного наследия ЮНЕСКО в 2007 году, и продемонстрировали существенный потенциал комбинированного археогеофизического анализа для выявления различных древних исторических объектов в этом районе. Для анализа свободно доступных данных дистанционного зондирования за разные годы и миссии были применены передовые методы интерпретации. Мы выявили сложную ирригационную систему, характерную для периода империи Ахеменидов, простирающуюся за пределы Гобустанского национального заповедника и включающую взаимосвязанные каналы, искусственные озера и пруды, ассоциирующиеся с близлежащими поселениями. Древние кяризы, легко идентифицируемые на спутниковых снимках, относятся к числу наиболее убедительных находок, ранее не документированных в этой области. Следующий этап исследования будет включать применение анализа магнитного поля на поверхности (или на малой высоте), в том числе качественную и количественную интерпретацию аномалий и трехмерное моделирование. На этом этапе будут разработаны надежные физико-археологические модели (ФАМ). Заключительный этап исследования будет состоять из непосредственных археологических раскопок, проводимых в соответствии с разработанными ФАМ.

Ключевые слова: *Дистанционное зондирование, Гобустан, кяризы, комбинированный геофизический анализ, информационный подход*

QOBUSTANDA KƏHRİZLƏRİN YÜKSƏK DƏQİQLİKLİ UZAQDAN ZONDLAMA MƏLUMATLARI ƏSASINDA MÜƏYYƏNLƏŞDİRİLMƏSİ

Xabarova O.V.[1]* və Eppelbaum L.V.[2,3]

[1]Təhlükəsizlik, Etibarlılıq və Etibar üzrə Fənlərarası Mərkəz, Lüksemburq Universiteti, Lüksemburq
[2]Geofizika kafedrası, Dəqiq Elmlər Fakültəsi, Tel-Əviv Universiteti, İsrail
Ramat-Əviv 6997801, Tel-Əviv
[3]Azərbaycan Dövlət Neft və Sənaye Universiteti, Azərbaycan
Azadlıq prospekti, 20, Bakı, AZ1010
**Yazışmalara cavabdeh olan müəllif: olga.khabarova@uni.lu*

Xülasə. Son tədqiqatlar göstərir ki, inteqrasiya olunmuş arxeo-geofiziki alətlər geniş spektrli geoloji və ekoloji problemlərin həllində yüksək effektivliyə malikdir. Bu yanaşma arxeoloji sahə işləri və ya uzaqdan zondlama ilə geofiziki metodların birləşdirilməsinə əsaslanır və arxeoloji obyektlərin ilkin tədqiqi və təhlilini dəstəkləyir; həmçinin yeraltı obyektlərin forma və xüsusiyyətlərini qiymətləndirmək üçün maşın öyrənməsi texnikaları ilə gücləndirilə bilər. Təqdim olunan tədqiqat arxeoloji araşdırmalar üçün mühüm məlumatların qiymətləndirilməsi və inteqrasiyası baxımından informasiya və ehtimal yanaşmalarının optimal alətlər kimi əhəmiyyətini vurğulayır. Biz Qobustan regionunda arxeoloji obyektlərin müəyyənləşdirilməsi üçün uzaqdan zondlama metodlarından istifadə edirik; bu ərazi 2007-ci ildə UNESCO World Heritage List-nə daxil edilmişdir. Tədqiqat bu ərazidə müxtəlif kateqoriyalara aid tarixi strukturların aşkar edilməsində kombinə olunmuş arxeo-geofiziki analizlərin böyük potensialını nümayiş etdirir. Müxtəlif illərə və missiyalara aid sərbəst əldə edilə bilən uzaqdan zondlama məlumatlarının təhlili üçün qabaqcıl interpretasiya metodologiyaları tətbiq edilmişdir. Biz Əhəmənilər dövrünə xas olan, Qobustan Milli Qoruğunun hüdudlarından kənara çıxan və bir-biri ilə əlaqəli kanalları, süni gölləri və gölməçələri əhatə edən, yaxınlıqdakı yaşayış məntəqələri ilə birləşdirilən mürəkkəb suvarma sistemini müəyyən etdik. Peyk görüntülərində asanlıqla müəyyən edilə bilən qədim kəhrizlər bu ərazidə əvvəllər sənədləşdirilməmiş ən cəlbedici tapıntılar sırasındadır. Tədqiqatın növbəti mərhələsində səthi (və ya aşağı hündürlüklü) maqnit sahəsi analizləri, o cümlədən anomaliyaların keyfiyyət və kəmiyyət baxımından şərhi və üçölçülü modelləşdirmə həyata keçiriləcəkdir. Bu mərhələdə etibarlı fiziki-arxeoloji modellər (PAM) hazırlanacaqdır. Araşdırmanın yekun mərhələsi isə formalaşdırılmış PAM əsasında istiqamətləndirilən birbaşa arxeoloji qazıntılardan ibarət olacaqdır.

Açar sözlər*: Məsafədən zondlama, Qobustan, kəhriz, kombinə edilmiş geofiziki analiz, informasiya yanaşması*

ANAS Transactions Earth Sciences 1 / 2026

http://www.journalesgia.com

ELECTRICAL RESISTIVITY SURVEY AND THE NEAR-SURFACE STRUCTURE EXPLORATION OF THE SHIKHZAHIRLI MUD VOLCANO (AZERBAIJAN)

Kadirov F.A.[1,2,3], Salamov A.M.[1], Safarov R.T.[1,2]*, Najafov O.F.[1], Samadli P.M.[2], Mammadov S.G.[1], Zamanova A.H.[1,2]

[1]Ministry of Science and Education of the Republic of Azerbaijan, Institute of Geology and Geophysics, Azerbaijan
119 H. Javid Ave., Baku, AZ1073
[2]Ministry of Science and Education of the Republic of Azerbaijan, Institute of Oil and Gas, Azerbaijan
9, F.Amirov str., Baku, AZ1000
[3]Faculty of Geology, Baku State University, Azerbaijan
33, Acad. Zahid Khalilov str., Baku AZ 1148
**Corresponding author: rafiqsafarov@gmail.com*

Keywords: *mud volcano, eruption, vertical electrical sounding, resistivity, geoelectrical section, Shikhzahirli, fault*

Summary. Mud volcanism is widespread in Azerbaijan, with over 300 land- and offshore mud volcanoes. These volcanoes are associated with oil and gas fields, and many of them are currently active. The Shikhzahirli mud volcano is located west-northwest of Baku, in the Shamakhi-Gobustan region, and is one of the world's active mud volcanoes. From 1844 to 2025, there were approximately 25 major eruptions. The last volcano eruption occurred on January 9, 2021 in three phases. The longest was the third phase, which lasted 7 minutes. Geoelectrical measurements, consisting of the vertical electrical sounding (VES) method, were performed for the first time in the Shikhzahirli mud volcano occurrence, aiming to evaluate the near-surface mud chambers, as well as to track the feeder channel. The VES measurements indicate that within the first 50 m below ground surface, no shallow-depth accumulation chambers occurred. The eruption triggered by gas accumulation appears to branch in the near-surface region; in one location, the upward migration path is almost vertical, whereas in others it is slanted. As a result of investigations, it was found that the volcano most likely has two vents located at the hinge of an anticline. The rocks in the geological section of the study area have been found to have relatively high moisture content. The probable thickness of the volcanic breccia is estimated to be consistent with the depth of the bedrock surface, which ranges from 135 to 150 m. Proposed multidirectional faults, presumably formed because of a mud volcano eruption, were identified.

Introduction

Mud volcanism is widespread in Azerbaijan: there are over 300 mud volcanoes (Aliyev et al., 2015; Yakubov et al., 1971) on land and offshore. These volcanoes are associated with oil and gas fields, and most of them are currently active. The Shikhzahirli mud volcano located in the Shamakhi-Gobustan region is one of the most active volcanoes in the world (Aliyev, Bayramov, 1999, 2000; Alizadeh et al., 2016; Kokh et al., 2017). From 1844 to 2025, there were approximately 25 major eruptions. The location map of the Shikhzahirli mud volcano and effusion of volcanic breccia are shown in Fig. 1 and Fig. 2, respectively.

Mud volcanoes observed in Azerbaijan pose serious problems due to the negative consequences they cause, but since they are unstable and unpredictable phenomena, it is highly desirable to better understand their activity to prevent possible casualties: large mud flows and flames that can sometimes accompany an eruption.

Since the Shikhzahirli mud volcano is one of the active volcanoes and is unique in terms of the large volume of erupted mud flow and the composition of emitted gases, it is necessary to study its area in detail using deep geophysical measurements.

The aim of this study is to investigate the electrical properties and trace the feeder channel of the Shikhzahirli mud volcano using geoelectrical survey (vertical electrical sounding, VES) (Fig.1).

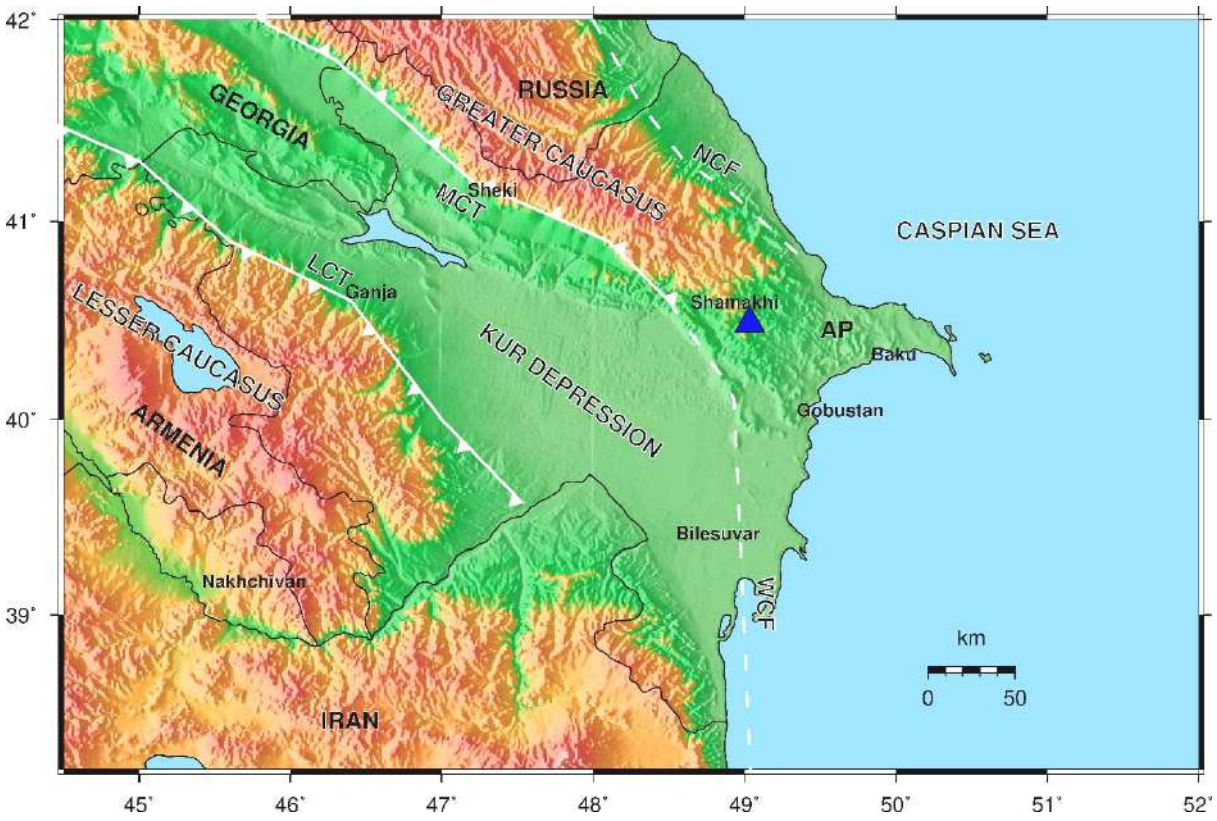

Fig. 1. The location of the Shikhzahirli mud volcano (blue triangle).
AP – The Absheron peninsula, NCF – The North Caspian Fault, MCT – The Main Caucasus Thrust, LCT – The Lesser Caucasus Thrust, WCF – The West Caspian Fault

Fig. 2. The Shikhzahirli mud volcano. Effusion of volcanic breccia (Aliyev, Yetirmishli, 2021)

Geological and geodynamic background

The Shikhzahirli mud volcano is located in the Shamakhi-Gobustan depression zone of Azerbaijan. The deepest eastern part of the Shamakhi-Gobustan depression, filled with shallow-water Pliocene sediments, merges with an area of the same sediments on the Absheron Peninsula and, together with the latter, forms the Absheron-Gobustan periclinal depression, which forms the northwestern rim of the vast and deep South Caspian Basin (Khain, 1984).

In Gobustan, it is distinguished by the development of the Paleogene and Miocene deposits at the

surface and by the almost strictly latitudinal orientation of its folds with isoclinal and even imbricated structures. The Absheron deposits are widespread in the Shamakhi-Gobustan region. They contribute to the construction of structural units of various shapes and are dislocated with varying degrees of intensity.

Most mud volcanoes are concentrated in areas that experienced prolonged subsidence not only during the Quaternary but also during previous geological periods: the Lower Kur Depression, the Absheron Pericline and Shamakhi-Gobustan Foredeep, and the South Caspian Basin. Mud volcanoes are widespread in all these depression zones, indicating strong manifestations of oscillatory, folding, and faulting movements during the Anthropogenic period (Kadirov, Mukhtarov, 2004). The primary cause of mud volcanism was negative oscillatory movements combined with folding and faulting movements (Ali-Zade, 1987; Kadirov et al., 2005). A geological map of the Shikhzahirli mud volcano area is shown in Fig. 3.

Figure 4 illustrates the velocity data for global positioning system (GPS) sites within the area encompassing the western and southern shores of the South Caspian Sea along with the distribution of mud volcanoes (Kadirov et al., 2008; Kadirov, Safarov, 2013; Kadirov et al., 2014, 2024).

On a large scale, the GPS velocity field shows the northeastward motion of the Caucasus region and its neighboring areas relative to Eurasia, south of the Main Caucasus Thrust Fault (MCT). It is noteworthy that significant reductions in site velocities and clockwise rotation are observed between sites west of the West Caspian Fault (WCF) in the Kur Depression and Talish region, and sites located to the east of the WCF within the Absheron Peninsula. The observed decrease and disparity in GPS vector directions indicate elevated strain accumulation rates of approximately 6 millimeters per year in the southern direction towards the Absheron Peninsula. Furthermore, GPS-derived motions on the northern slope of the Greater Caucasus and along the Caspian coast in Azerbaijan north of the Absheron Peninsula suggest the presence of south-dipping thrust faulting along the North Caucasus. This thrust faulting is characterised by a southward inclination within the Absheron Peninsula and continues inland from the Caspian coast, traversing the peninsula in a westerly direction before terminating at the Caspian Sea.

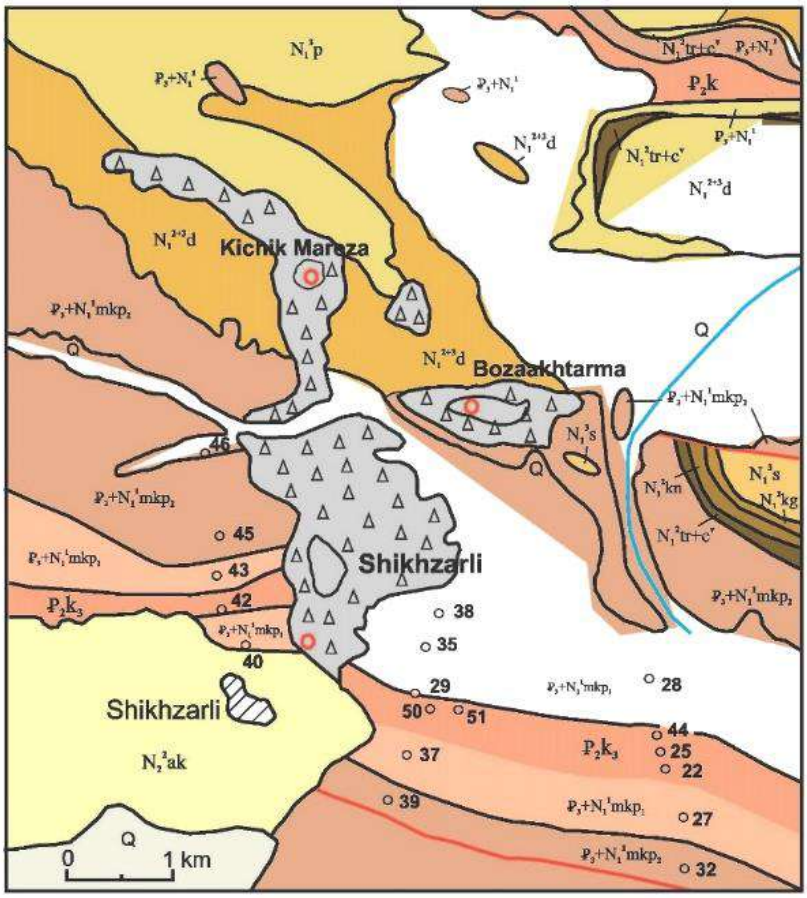

Fig. 3. Geological map of Shikhzahirli mud volcano location area (Aliyev et al., 2015)

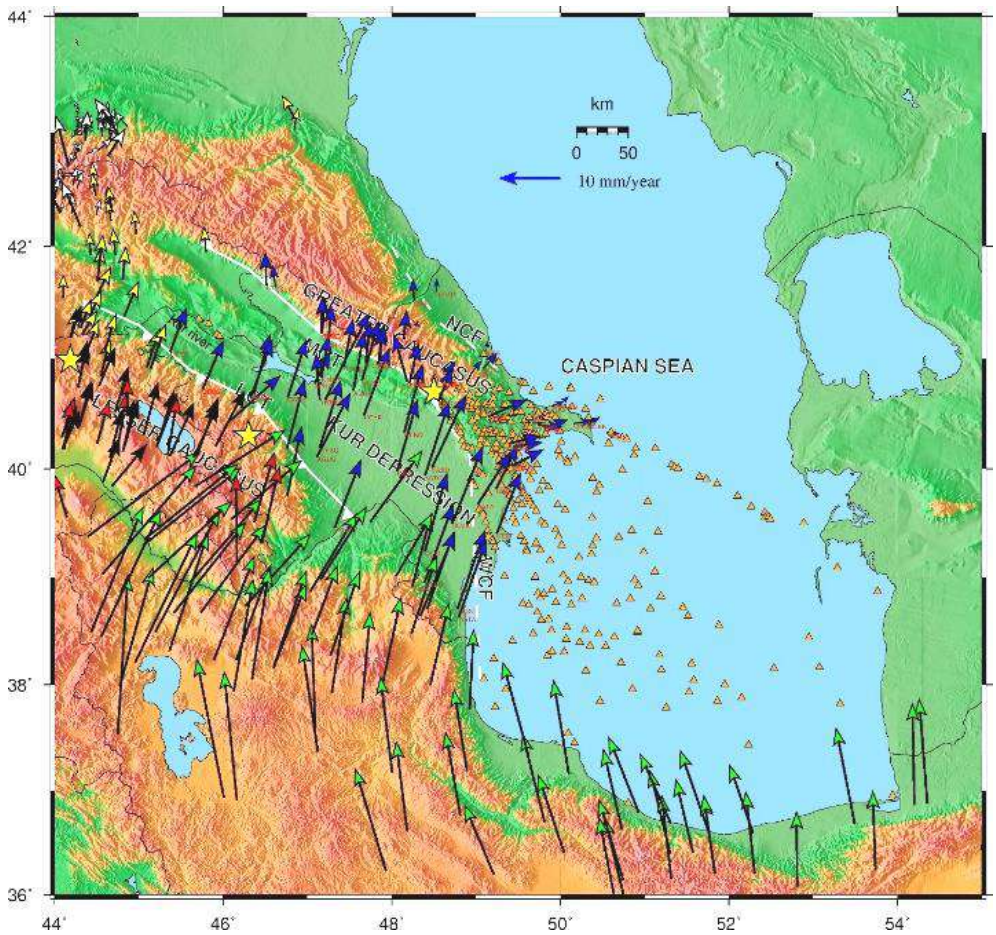

Fig. 4. GPS velocities with respect to Eurasia for the eastern AR-EU collision zone. Yellow stars show 1139, M7.3 Ganja; 1902, M6.9 Shamakhi; 1988, M6.8 Spitak and 1991, M7.0 Racha earthquake epicenters. Blue arrows indicate Azerbaijan GPS sites (Kadirov et al., 2024), green arrows stand for the Iranian GPS sites (Raeesi et al., 2017), Red arrows show the Armenian GPS sites (Karakhanyan et al., 2013), Yellow arrows demonstrate Georgian GPS sites (Sokhadze et al., 2018), White arrows display the Russian GPS sites (Milyukov et al., 2015), Black arrows are velocities from Reilinger et al., (2006). Orange triangles show the mud volcanoes.

Furthermore, the GPS vectors in the region, specifically in the Absheron Peninsula and along the western Caspian coast, exhibit a pronounced eastward motion. This eastward shift is interpreted as the result of a left-lateral strike-slip mechanism acting within this segment of the fault.

Contractions are observed in the Greater Caucasus, Gobustan, the Kur Depression, the Nakhchivan Autonomous Republic, and the areas bordering Iran. The contraction axes show that crustal shortening in the Greater Caucasus region occurs in a northeasterly direction, with the shortening in the Shamakhi region (MEDR) being nearly submeridional. The deformation rate between the KURD (Kurdemir) and MEDR (Madrasa) GPS points is ~16 x 10^{-8}/yr.

Geophysical surveys. Methodology and interpretation of field work

As noted above, comprehensive field geophysical surveys were conducted along five profiles by the electrical prospecting method using a four-electrode symmetrical AMNB array.

It should be noted that electrical prospecting using the vertical electrical sounding (VES) method was conducted in this area for the first time.

As it is well known, the modern VES theory is based on the Schlumberger mathematical model. It allows calculating the apparent electrical resistivity (ρ_a) of a multilayer medium with horizontal interfaces, depending on the specific electrical resistivity (ρ_s), the thickness of the individual layers, and the size of the VES survey setup. However, using this model precludes the possibility of a definitive solution to the inverse problem – determining the depth of horizontal interfaces and the specific electrical resistivity of individual layers from a set of ρ_a values obtained during measurements with different setups (Lowrıe, 2007; Griffiths, King, 1981; Keller, Frischknecht, 1966).

This goal can be mostly achieved by constructing a new model based on the following simplifying assumptions on the characteristics of the current distribution in a flat-layered medium when placing electrodes on the daylight surface:

– the measured ρ_a value characterises the geological section to a certain depth H, which is entirely determined by the ratio between the dimensions of potential (MN) and the feeder (AB) lines, and when MN<<AB the value of H is AB/2 (in practice, MN should be no more than 0.1 AB);

– the ρ_a value is determined only by the vertical component of the current density, i.e., it represents a certain averaged electrical characteristic of the medium in the vertical direction, depending on the specific electrical resistances ρ_{si} of each layer, and the "contribution" to the value of ρ_a of each ρ_{si} depends on the thickness of the given layer h_i.

The adopted assumptions allow constructing the following simple formula, which establishes a correspondence between the set of values (ρ_{si}, h_i) of the n-layer section and the value of ρ_a:

$$\rho_a = \frac{\rho_1 h_1 + \rho_2 h_2 + \cdots + \rho_{si} h_i}{h_1 + h_2 + \cdots h_i} = \frac{\sum_{i=1}^{n} \rho_{si} h_i}{\sum_{i=1}^{n} h_i} \quad (1)$$

where, $\sum_{i=1}^{n} h_i$, $m=h_i$, m is the depth of the n-th layer base.

Since, according to the accepted assumption, the value of h_i is completely determined by the relationship between MN and AB, and therefore, formula (1) can be used to solve the inverse problem of determining the parameters of a geoelectric section from a set of ρ_a values obtained with different sizes of the survey setup. Indeed, given a series of successive ρ_{ai} values and h_i (i = 1, 2, ... n), one can sequentially determine h_i and ρ_{si}, i.e., the thickness and specific resistivity of each layer.

This means that for any i-th layer $h_i = h_i - h_{i-1}$ or $h_i = (AB/2)_i - (AB/2)_{i-1}$ (2)

To calculate the apparent electrical resistivity ρ_a, the formula

$$\rho_a = K_{VES} * \Delta U_{mV} / I_{mA} \quad (3)$$

was used (Yakubovski, Renard, 1991).

And to determine the specific electrical resistivity of individual layers, formula (4) is used, when $\rho_{ai} > \rho_{ai-1}$. (Popov et al., 1990; Galin, 1989)

$$\rho_{si} = \left[\rho_{ai} * \left(\frac{AB}{2}\right)_i - \rho_{ai-1} * \left(\frac{AB}{2}\right)_{i-1}\right] / \left[\left(\frac{AB}{2}\right)_i - \left(\frac{AB}{2}\right)_{i-1}\right] \quad (4)$$

and in the case $\rho_{ai-1} > \rho_{ai}$ the formula

$$\rho_{si} = \left\{\left[\left(\frac{AB}{2}\right)_i - \left(\frac{AB}{2}\right)_{i-1}\right] * \rho_{ai-1} * \rho_{ai}\right\} / \left[\rho_{ai-1} * \left(\frac{AB}{2}\right)_i - \rho_{ai} * \left(\frac{AB}{2}\right)_{i-1}\right] \quad (5)$$

(Salamov et al., 2015) is used.

Expressions (2), (3), and (4) are the main calculation formulas in the proposed method for determining the parameters of the geoelectric section based on VES data for installations with MN<<AB.

As follows from formulas (2), (4), and (5), the proposed model enables determination of the thickness and specific electrical resistivity of any layer, regardless of the parameters of the overlying layer.

Taking into account the above, for the purpose of detailed dissection of the geological section and more accurate depth determination of the individual lithological varieties, as a result of experimental measurements carried out using the VES method, the sizes of the feeder line AB/2 and the receiver line MN/2 were adopted, respectively: AB/2 =1; 2; 3; 4; 5; 6; 7; 8; 9; 10,10; 12,12; 14; 16; 18; 20; 22; 24,24; 26,26; 28; 30; 32; 34; 36,36; 38,38; 40,40; 42; 44; 46; 48; 50,50; 52; 54; 56; 58; 60; 63; 66; 69; 72,72; 75,75; 78; 81; 84; 87; 90,90; 93,93; 96; 99; 102; 105; 108; 111; 114; 117; 120; 125,125; 130,130; 135, 140; 145; 150; 155; 160; 165; 170; 175; 180; 185; 190; 195; 200 and MN/2=0,3; 0,3; 0,3; 0,3; 0,3; 0,3; 0,3; 0,3; 0,3; 0,3; 0,3; 0,3; 1; 0,3; 1; 1; 1; 1; 1,2; 1,2; 2, 2, 2, 2; 2,3; 2,3; 2,3; 3; 3; 3; 3; 3,5; 3,5; 5; 5; 5; 5; 5; 5; 5; 5,7; 5,7; 7; 7; 7; 7; 7,9; 7,9; 9; 9; 9; 9; 9; 9; 9; 9; 9; 9,12; 9,12; 12; 12; 12; 12; 12; 12; 12; 12; 12; 12; 12; 12; 12; 12; 12; 12; 12,15 (Salamov et al., 2025).

Increasing the number of measurements at a single observation point made it possible to identify thin layers in the geological section of the study area (Popov et al., 1990; Galin, 1989; Salamov et al., 2015, 2023, 2025).

The profile directions were northeast, southwest, and east-west (Fig. 5).

For field measurements, ERA-MAX electrical prospecting equipment operating at 4.88 Hz was used.

Results and Discussion

Geophysical field surveys using the VES method were conducted in the Shikhzahirli mud volcano area. These measurements determined the apparent electrical resistivity of rocks within the geological section across the area and to a depth of 200 meters. The resulting apparent electrical resistivity values were interpreted, and the specific electrical resistivity of rocks was determined (Fig. 6).

Based on the apparent and specific electrical resistivity values, corresponding sections were constructed along 5 profiles (I-I, II-II, III-III, IV-IV, V-V). These are the vertical sections based on apparent electrical resistivity values, and the supposed lithological-geophysical sections based on specific electrical resistivity values.

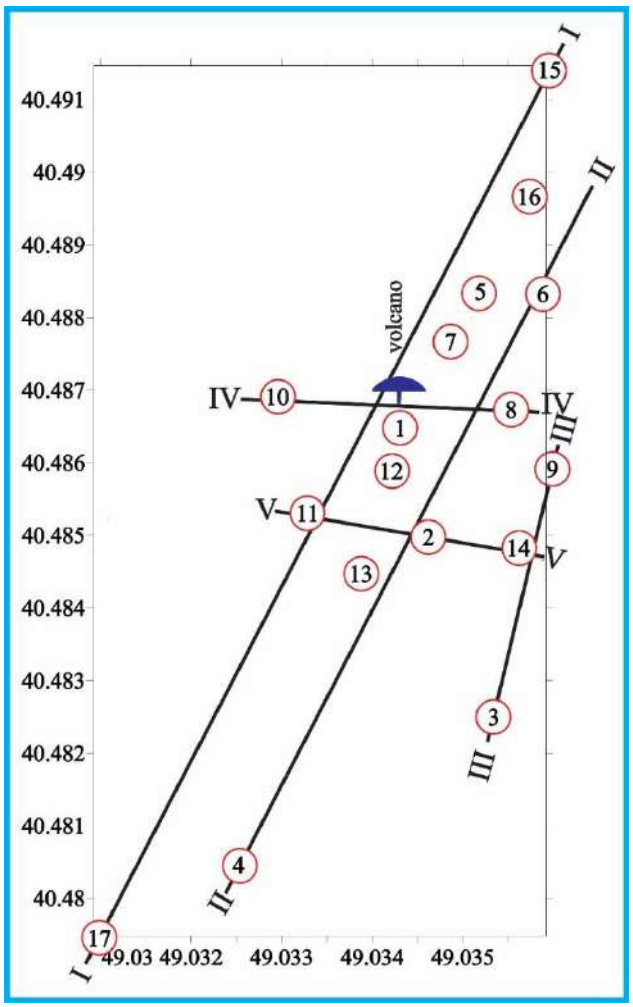

Fig. 5. Layout of geophysical profiles

1 – geophysical profile lines; 2 – VES points

According to the profile I-I section constructed, it is evident that, up to a depth of 200 m, the apparent electrical resistivity (ρa) of rocks varies between 1 and 18, while the specific electrical resistivity (ρs) changes from 0.5 to 14 Ohm-m (Fig. 6).

Approximately eight layers of varying thicknesses, approximately 15–20 m, are traced to the studied depth, indicating the duration of the eruption. The specific electrical resistivity ρ_s of these layers varies between 4 and 14 Ω · m.

In the section the thickness of identified layers is almost similar and has a relatively plain bedding and are placatively deformed. This suggests that these layers formed during a prolonged mud volcano eruption in a marine environment. The catalog indicates that the Shikhzahirli mud volcano has erupted 24 times, excluding marine eruptions. However, the data obtained from geophysical surveys refute this information. In general, it is necessary to clarify what a volcanic eruption is and can minor volcanic activity be called an eruption?

The top of the bedrock layers was identified at a depth of approximately 135-150 m, and their ρ_s values range from 12 to 14 Ohm-m.

The bedrock layers are intersected by faults in different directions.

The mud volcano vent is believed to lie within the interval of the VES №1–11 survey points, in the hinge part of the anticline. The centerline of this structure has an arcuate outline. In the area of VES №13–16 survey points, eruption material (slurry) with ρ_s of 0.5–3.0 Ohm-m is accumulated, forming a mushroom-shaped vent, which is typical of mud volcanoes.

To trace the areal and depth distribution of rocks using the averaged values of ρ_a and ρ_s, corresponding maps were constructed (Fig. 7).

On the ρ_a map, from north to south, rocks with different types are observed. In the northern part of the area, ρ_a values change between 4.5-6.0 Ohm-m, while in the central part of the study area, a lineage of rocks in a northeast-southwest direction with low ρ_a values of 3.3-4.5 Ohm-m is observed. Finally, in the southern part, rocks with relatively high ρ_a values (4.5–9.0 Ohm m) are observed.

The volcanic vent area is characterised by very low ρ_a values, which are associated with the liquid material of the mud volcano.

On the ρ_s map, two distinct areas are distinguished based on specific electrical resistivity: a relatively high-resistivity area, where rock resistivity varies between 5 and 14 Ohm-m, developed in the northern and western parts of the area; and a low-resistivity area, encompassing the southeastern part of the area, where sediment resistivity varies between 0.3 and 4.8 Ohm-m (Fig. 7).

Analysis of the given maps suggests that the mud volcano area stands out from the rest of the area by having low electrical resistivity, which is natural.

Based on the average values of natural moisture content (W_r) and moisture content of rocks underwater (W_{rw}), corresponding maps were constructed (Fig. 8).

The purpose of compiling these maps was to thoroughly examine the areal and depth distributions of the supposed natural moisture content and the moisture content of underwater rocks.

The mud volcano area is conventionally divided into three parts based on natural moisture content. The northern part of the area is characterised by low natural moisture content W_r, varying between 22% - 28%, both in depth and area. In the central part, these indicators range from W_r = 28% to 34% (Fig. 8). In the southern part of the study area, natural moisture content increases significantly, reaching 50% and higher.

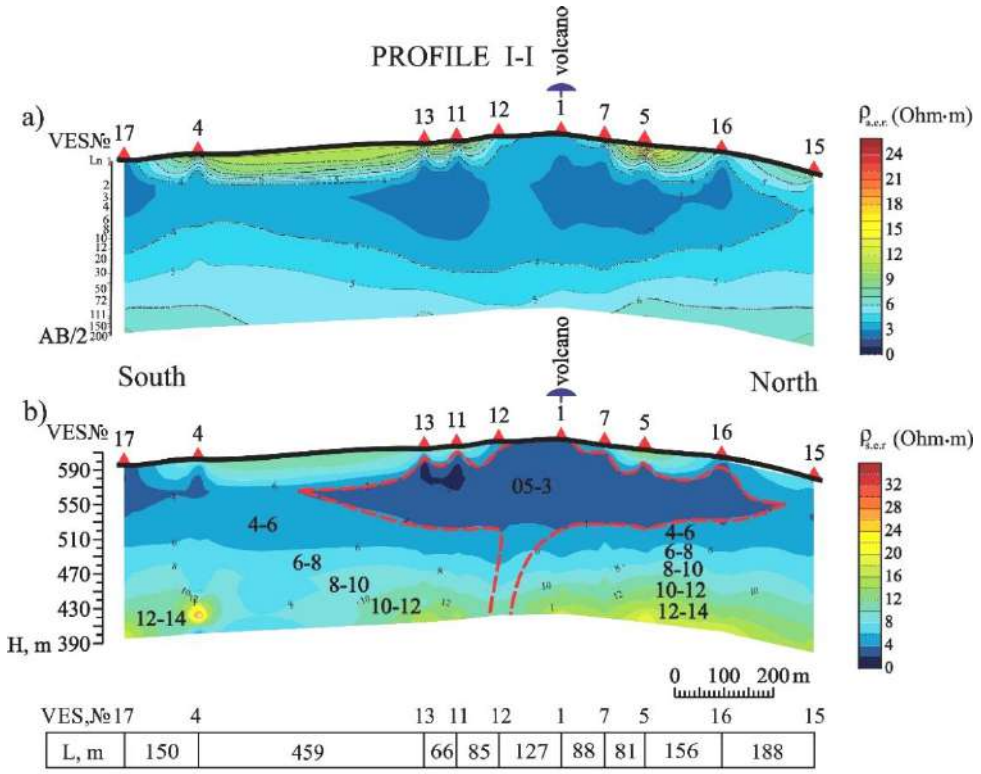

Fig. 6. Sections along profile I-I based on VES data: a – vertical section based on apparent electrical resistivity values of rocks; b – supposed lithological-geophysical section based on specific electrical resistivity values

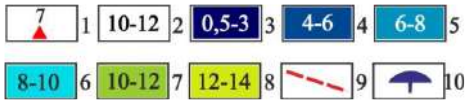

1 – VES points and their numbers; 2 – values of specific electrical resistivity of rocks; 3-8 – resistivity intervals; 9 – supposed faults identified by VES data; 10 – mud volcano crater

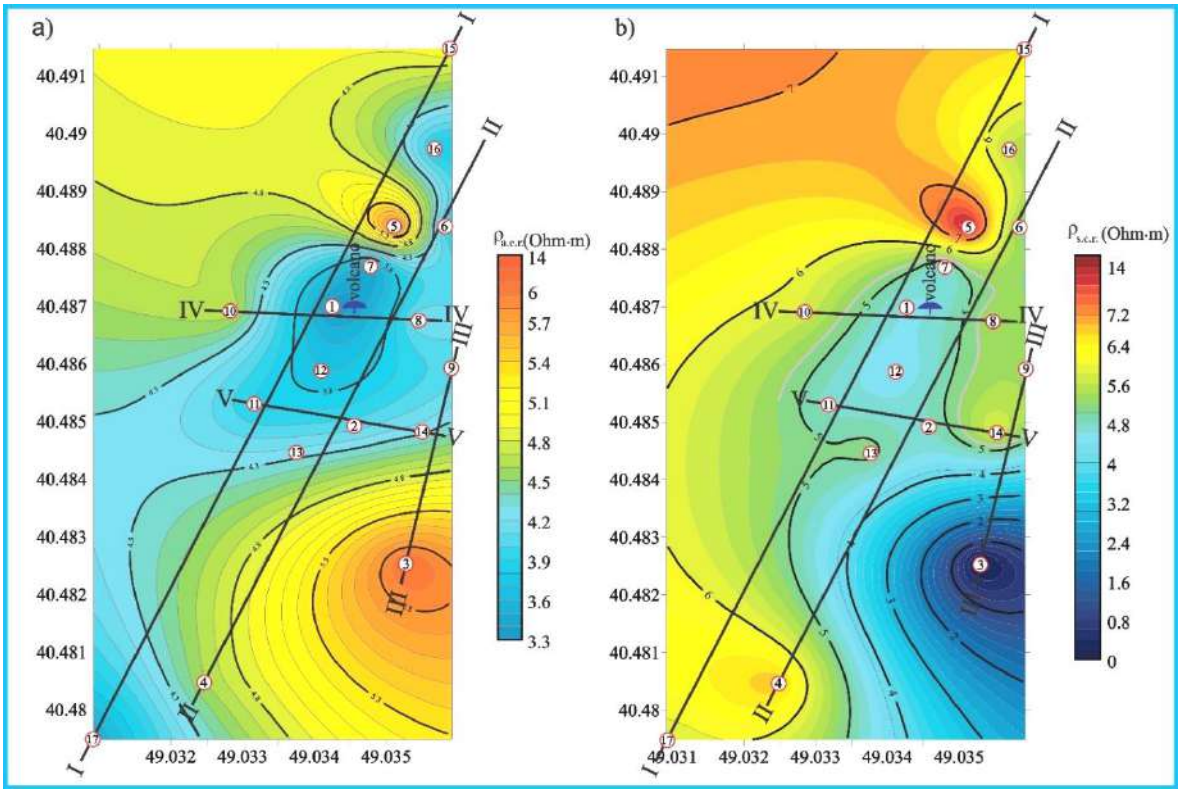

Fig. 7. Maps of ρ_a and ρ_s constructed based on VES data

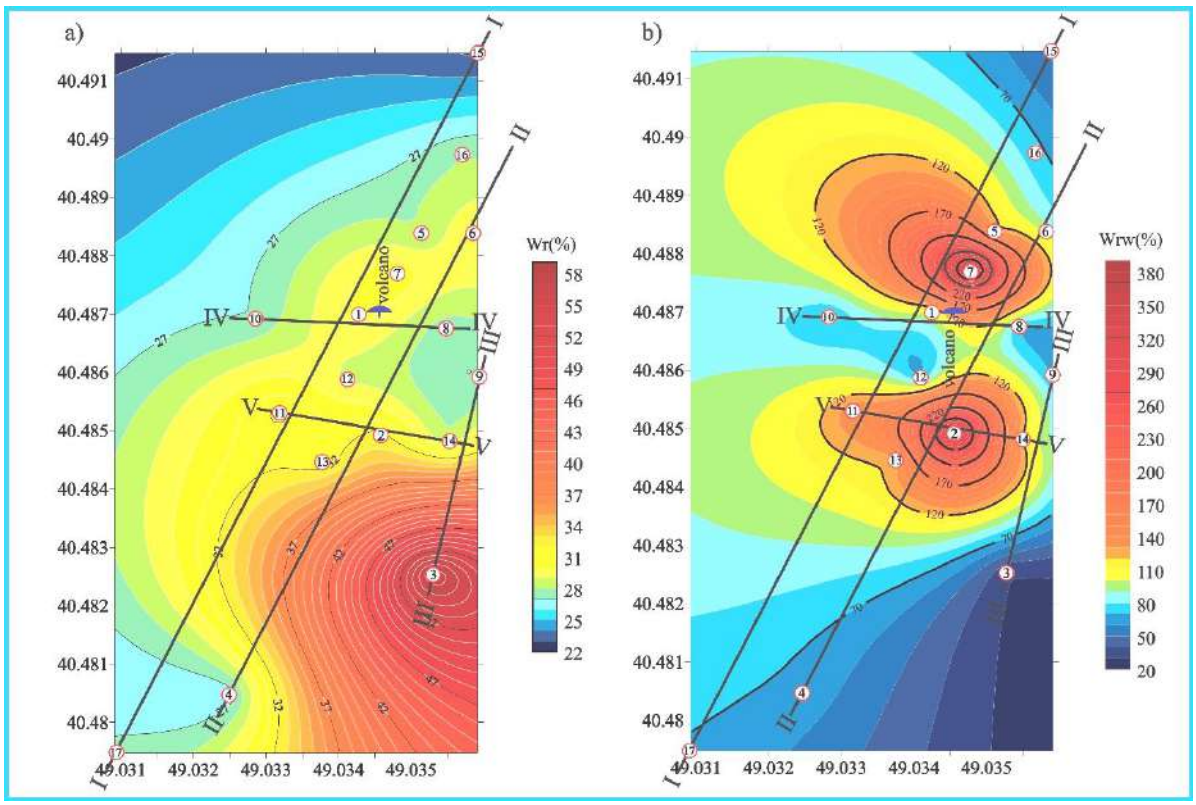

Fig. 8. W_r (a) and W_{rw} (b) maps constructed based on VES data

A moisture content map of the underwater rock revealed that the mud volcano presumably has two vents – one near VES №7 and the other near VES №2, which is a new finding.

In these areas, the data suggest that the rocks composing the geological section are in a substrate (slurry) state.

Based on VES geophysical survey data, rock densities were determined for the geological cross-section of the study area. As a result, maps of the supposed rock densities (a) and underwater rock densities (b) were constructed.

The purpose of these maps was to more precisely determine the area of the future mud volcano crater (Fig. 9).

According to the map of the supposed rock density V_r (Figure 9a), the study area is divided into three parts from south-east to north-west.

In the south-eastern part of the area, the rock density changes between 0.9-1.38 t/m^3, in the middle part of the area, rock densities along the stripe in north-east south-west direction varies in the range of 1.4-1.78 t/m^3, and finally, in the north-western part, these indicators vary within the range of 1.78-1.86 t/m^3.

The map of underwater rock densities also identifies three areas of varying rock density in the geological section.

In the southeastern part of the study area, underwater rocks have a specific weight of 0.89-0.96 t/m^3. In the central part of the area, a section with a low specific weight of 0.81-0.88 t/m^3 is identified.

It is assumed that the area with a low specific weight of underwater rocks is associated with both the liquid products of the mud volcano and atmospheric precipitation.

Based on the compiled map of underwater rock density, it can be assumed that the future crater of the mud volcano will be approximately bound by a line with a value of 0.88 t/m^3. It should be noted that the area of the future crater, at least, cannot be smaller than the outlined one.

Based on the average seismic acceleration, a section with low seismic acceleration is identified in the central part of the study area, coinciding with the vents of the mud volcano (Fig. 10a). The lowest seismic acceleration values are observed around VES №2, 11, and 13, which may be related to the second vent of the mud volcano.

The data obtained indicate that the mud volcano area is highly seismically active.

Faults in various directions were identified in the volcano crater. In other words, there is no correlation between fault directions. This suggests that these faults formed due to a mud volcano eruption (Fig. 10 b).

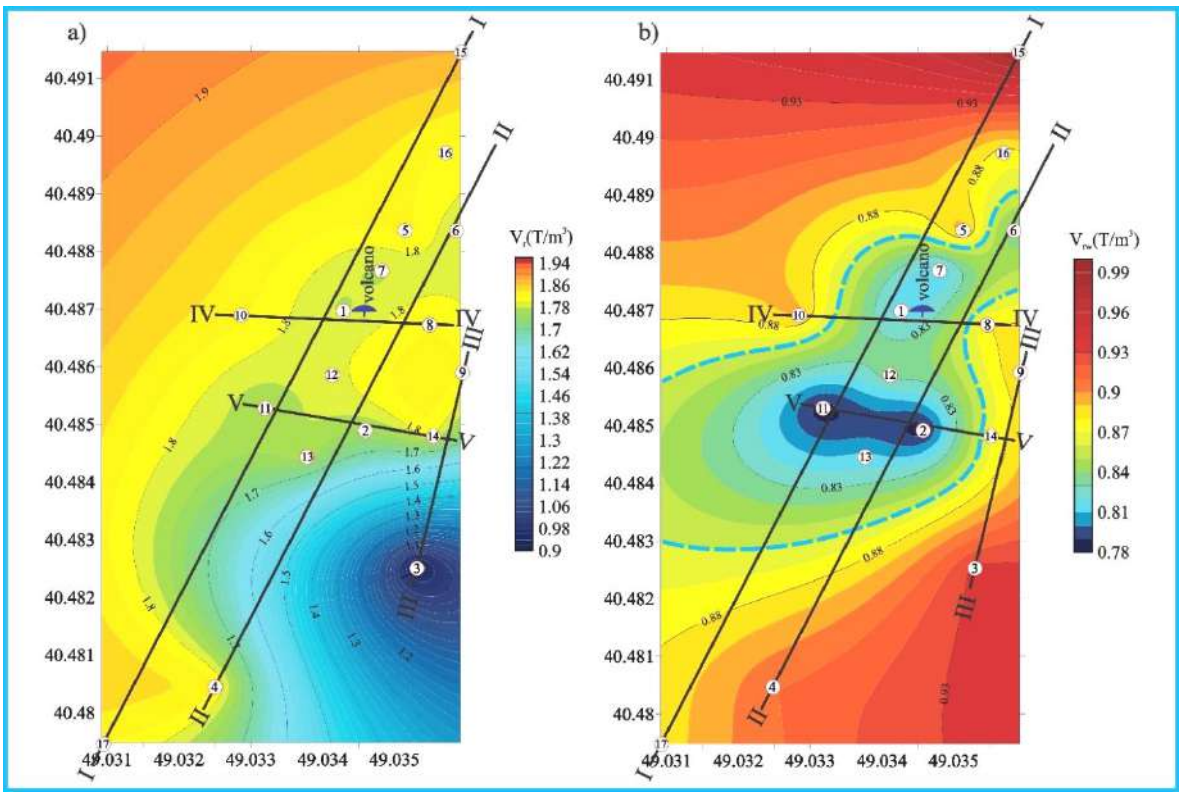

Fig. 9. Maps of the rock densities V_r (a) and V_{rw} (b) compiled using VES data

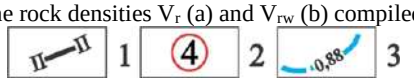

1 – geophysical profiles; 2 – VES points; 3 – 0.88 t/m^3 line

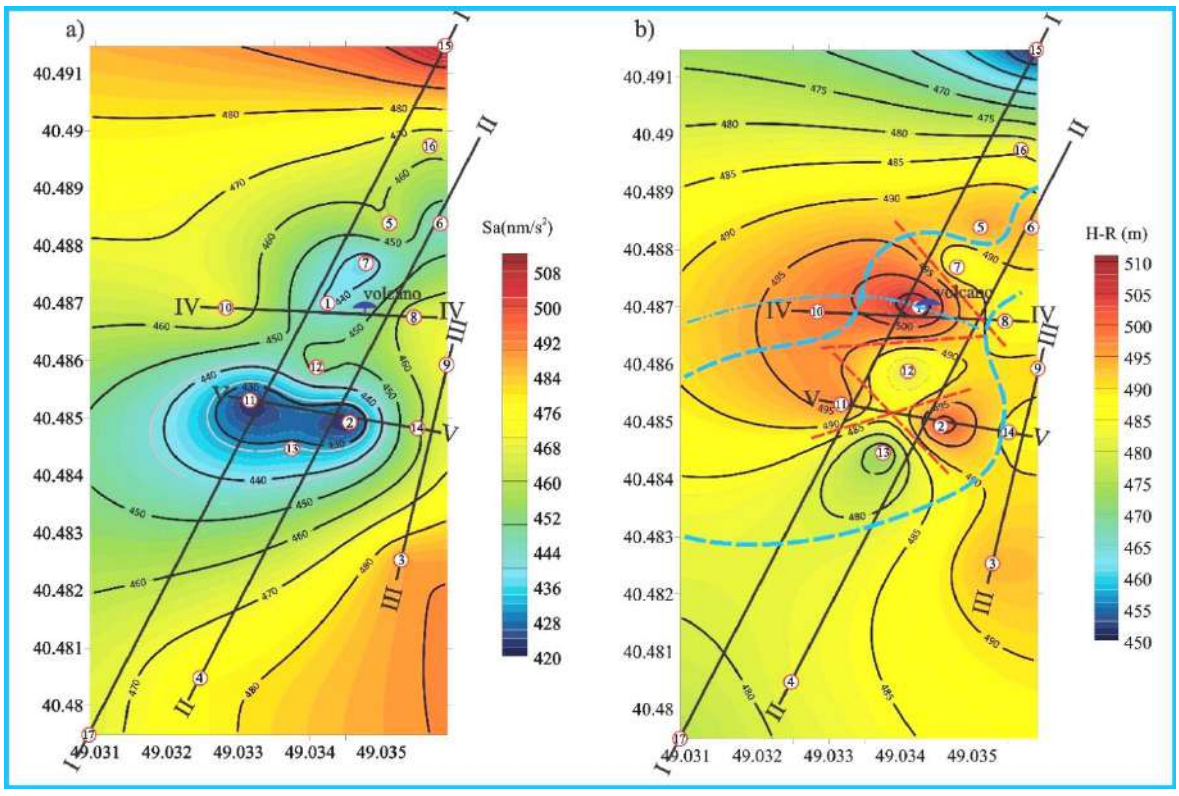

Fig. 10. The maps of seismic acceleration (a) and geophysical survey results (b)

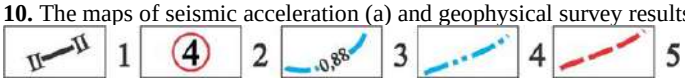

1 – geophysical profile lines; 2 – VES points; 3 – 0.88 t/m^3 lines; 4 – axis of the anti-cline; 5 – supposed faults identified based on the geophysical survey results

Conclusions

Key results of the geophysical survey:

– Detailed dissections of the geological section to a depth of 200 m were conducted;

– Supposed multidirectional faults were identified, presumably formed because of the mud volcano eruption;

– The mud volcano's vent is assumed to dip northeast;

– It was established that the volcano's vent is located in the hinge of an anticline structure;

– It is assumed that the mud volcano is most likely has two vents;

– The main eruption is assumed to have occurred in a marine environment;

– The probable thickness of the volcanic breccia is estimated to be compatible with the depth of the bedrock top, which ranges between 135 and 150 m;

The rocks in the geological section of this area have been found to have relatively high moisture content;

– The density of the rocks in the geological section varies within narrow limits.

It should be noted that the objectives of the geophysical survey were successfully achieved and can be applied to similar problems due to the applied fieldwork methodology.

This work was done by the support of the Oil and Gas Institute, Ministry of Science and Education of the Republic of Azerbaijan.

REFERENCES

Aliyev AdA, Bayramov AA (1999) Some aspects of the tectonics of mud volcanic zones of Gobustan. Proceedings of Azerbaijan Academy of Sciences. The sciences of Earth 1:129–131(in Russian)

Aliyev AdA, Bayramov AA (2000) New data on the features of mud volcanism in the Shamakhi-Gobustan region. Proceedings of geology institute, Azerbaijan Academy of Sciences 28:5–17 (in Russian)

Aliyev AdA, Guliyev IS, Dadashev FG, Rahmanov RR (2015) Atlas of the world mud volcanoes. Publishing house Nafta-Press, Sandro Teti Editore, p 321

Aliyev AdA, Yetirmishli GD (2021) New data on eruptions of mud volcanoes in Azerbaijan. Geology and Geophysics of Russian South 11(2):22–35 (in Russian)

Ali-Zade SA (1987) Anthropocene of Azerbaijan. Elm, Baku, p 244 (in Russian)

Alizadeh AA, Guliyev IS, Kadirov FA, Eppelbaum LV (2016) Geosciences in Azerbaijan, vol 1. Geology. Springer, Heidelberg – N.Y., p 239

Galin DL (1989) Interpretation of engineering geophysics data. Nedra, Moscow, p 114 (in Russian)

Griffiths DH, King RF (1981) Applied geophysics for geologists and engineers: the elements of geophysical prospecting. 2nd edn, Pergamon Press, p 201

Kadirov F, Lerche I, Guliyev I et al (2005) Deep structure model and dynamics of mud volcanoes, Southwest Absheron Peninsula (Azerbaijan). Energy Explor Exploit 23(5):307–332. https://doi.org/10.1260/014459805775992717

Kadirov F, Mammadov S, Reilinger R, McClusky S (2008) Some new data on modern tectonic deformation and active faulting in Azerbaijan (according to Global Positioning System measurements). Proceedings of Azerbaijan Academy of Sciences. The sciences of Earth 1:82–88

Kadirov F, Yetirmishli G, Safarov R et al (2024) Results from 25 years (1998–2022) of crustal deformation monitoring in Azerbaijan and adjacent territory using GPS. ANAS Transaction. Earth Sciences 1:28–43. https://doi.org/10.33677/ggianas20240100107

Kadirov FA, Guliyev IS, Feyzullayev AA et al (2014) GPS-based crustal deformations in Azerbaijan and their influence on seismicity and mud volcanism. Izvestiya, Physics of the Solid Earth, 50:814–823. 6 https://doi.org/10.1134/S1069351314060020

Kadirov FA, Mukhtarov ASh (2004) Geophysical fields, deep structure and dynamics of the Lokbatan Mud Volcano. Izvestiya, Physics of the Solid Earth 40(4):327–333 (in Russian)

Kadirov FA, Safarov RT (2013) Deformation of the Earth's crust of Azerbaijan and adjacent territories based on GPS measurements. Proceedings of Azerbaijan National Academy of Sciences, The Sciences of Earth 1:47–55 (in Russian)

Karakhanyan A, Vernant P, Doerflinger E et al (2013) GPS constraints on continental deformation in the Armenian region and Lesser Caucasus. Tectonophysics 592:39–45. https://doi.org/10.1016/j.tecto.2013.02.002

Keller GV, Frischknecht FC (1966) Electrical methods in Geophysical Prospecting. Pergamon press, New York, reprinted edn, Chapt 3, p 89–180

Khain VE (1984) Regional geotectonics. Alpine Mediterranian belt. Nedra, Moscow, p 344 (in Russian)

Kokh SN, Sokol EV, Dekterev AA et al (2017) The 2011 strong fire eruption of Shikhzarli mud volcano, Azerbaijan: a case study with implications for methane flux estimation. Environ Earth Sci 76(701). https://doi.org/10.1007/s12665-017-7043-5

Lowrıe W (2007) Fundamentals of geophysics. 2nd edn, Cambridge University Press, Swiss Federal Institute of Technology, Zürich, p 381

Milyukov VK, Mironov AP, Rogozhin EA et al (2015) Velocities of contemporary movements of the Northern Caucasus estimated from GPS observations. Geotecton 49:210–218. https://doi.org/10.1134/S0016852115030036

Popov EA, Ten KM, Funtikov GN et al (1990) Guidelines for the use of VES for the detailed dissection of the section in solving geological and engineering-geological problems. Rotaprint, Moscow, p 52 (in Russian)

Raeesi M, Zarifi Z, Nilfouroushan F et al (2017) Quantitative analysis of seismicity in Iran. Pure Appl Geophys 174:793–833. https://doi.org/10.1007/s00024-016-1435-4

Reilinger R, McClusky S, Vernant P et al (2006) GPS constraints on continental deformation in the Africa-Arabia-Eurasia continental collision zone and implications for the dynamics of plate interactions. J Geophys Res 111(BO5411). https://doi.org/10.1029/2005JB004051

Salamov AM, Kadirov AG, Salamov FA, Pashayev TR (2015) Investigation of the landslide in the Khizi region of Azerbaijan by the method of Vertical Electrical Sounding. Inzhenerniye izyskaniya (Engineering survey) 5-6:50–56 (in Russian)

Salamov AM, Mammadov VA, Rashidov TM et al (2023) Electrical resistivity tomography of Lokbatan mud volcano: inner structure and formation mechanism. ANAS Transactions, Earth Sciences 1:49–59. https://doi.org/10.33677/ggianas20230100093

Salamov AM, Safarov RT, Zamanova AH et al (2025) Assessment of exogenıc geologıcal process dynamıcs in the Yanardag area of Absheron peninsula (Azerbaijan) based on Vertıcal Electrıcal Soundıng data, ANAS Transactions. Earth Sciences 2:106–113. https://doi.org/10.33677/ggianas20250200158

Sokhadze G, Floyd M, Godoladze T et al (2018) Active convergence between the Lesser and Greater Caucasus in Georgia: Constraints on the tectonic evolution of the Lesser–Greater Caucasus continental collision. Earth and Planetary Science Letters 481:154–161. https://doi.org/10.1016/j.epsl.2017.10.007

Yakubov AA, Alizade AA, Zeynalov MM (1971) Mud volcanoes of the Azerbaijan SSR. Publishing House of the Academy of Sciences of the Azerbaijan SSR, Baku, p 255 (in Russian)

Yakubovski YuV, Renard IV (1991) Electrical prospecting. Nedra, Moscow, p 347 (in Russian)

ИССЛЕДОВАНИЯ МЕТОДОМ ЭЛЕКТРИЧЕСКОГО СОПРОТИВЛЕНИЯ И ИЗУЧЕНИЕ ПРИПОВЕРХНОСТНОЙ СТРУКТУРЫ ГРЯЗЕВОГО ВУЛКАНА ШЫХЗАХЫРЛИ (АЗЕРБАЙДЖАН)

Кадиров Ф.А.[1,2,3], Саламов А.М.[1], Сафаров Р.Т.[1,2]*, Наджафов О.Ф.[1], Самедли П.М.[2], Мамедов С.Г.[1], Заманова А.Г.[1,2]

[1]Министерство науки и образования Республики Азербайджан, Институт геологии и геофизики, Азербайджан AZ1073, Баку, просп. Г.Джавида, 119

[2]Министерство науки и образования Республики Азербайджан, Институт нефти и газа, Азербайджан AZ1000, Баку, ул. Ф.Амирова, 9

[3]Геологический факультет, Бакинский государственный университет, Азербайджан AZ1148, г. Баку, ул. акад. Захида Халилова, 33

**Автор, отвечающий за переписку: rafiqsafarov@gmail.com*

Резюме. Грязевой вулканизм широко распространен в Азербайджане, на суше и на море насчитывается более 300 грязевых вулканов. Эти вулканы связаны с месторождениями нефти и газа, и многие из них в настоящее время активны. Грязевой вулкан Шыхзахырлы расположен к западу-северо-западу от Баку, в Шамахы-Гобустанской области и является одним из активно действующих грязевых вулканов. С 1844 года по 2025 год произошло около 25 сильных извержений. Последнее извержение вулкана произошло 9 января 2021 года и состояло из трех фаз. Самым продолжительным извержением была третья фаза, длившаяся 7 минут. С целью оценки приповерхностных грязевых камер, а также отслеживания питающего канала в районе грязевого вулкана Шыхзахырлы впервые были проведены геоэлектрические измерения, выполненные методом вертикального электрического зондирования (ВЭЗ). Измерения ВЭЗ показали, что на глубине первых 50 м от поверхности земли не обнаружено неглубоких камер накопления. Извержение, вызванное накоплением газа, в приповерхностном слое, по-видимому, носит разветвленный характер: в одном месте восходящий путь миграции имеет почти вертикальное направление, в других – наклонное. В результате проведенных исследований было установлено, что вулкан, скорее всего, имеет два жерла, расположенных в шарнире антиклинальной структуры. Породы в геологическом разрезе исследуемой области характеризуются относительно высоким содержанием влаги. Предполагаемая толщина вулканической брекчии оценивается как соответствующая глубине залегания верхнего слоя коренных пород, которая колеблется в пределах 135–150 м. Были выявлены предполагаемые системы разломов разного направления, предположительно образовавшиеся в результате извержения грязевого вулкана.

Ключевые слова: *грязевой вулкан, извержение, вертикальное электрическое зондирование, сопротивление, геоэлектрический разрез, Шыхзахырлы, разлом*

ELEKTRİK MÜQAVİMƏTİ MÜŞAHİDƏLƏRİ VƏ ŞIXZAHIRLI PALÇIQ VULKANINDA KİÇİK DƏRİNLİKLƏRDƏ MÖVCUD OLAN STRUKTURLARIN TƏDQİQİ (AZƏRBAYCAN)

Qədirov F.Ə.[1,2,3], Salamov Ə.M.[1], Səfərov R.T.[1,2*], Nəcəfov O.F.[1], Səmədli P.M.[2], Məmmədov S.Q.[1], Zamanova A.H.[1,2]

[1]Azərbaycan Respublikasının Elm və Təhsil Nazirliyi, Geologiya və Geofizika İnstitutu, Azərbaycan AZ1073, Bakı, H.Cavid prosp., 119

[2]Azərbaycan Respublikasının Elm və Təhsil Nazirliyi, Neft və Qaz İnstitutu, Azərbaycan AZ1000, Bakı, F.Əmirov küç., 9

[3]Geologiya Fakültəsi, Bakı Dövlət Universiteti, Azərbaycan AZ1148, Bakı, akad. Zahid Xəlilov küç., 33

**Yazışmalara məsul: rafiqsafarov@gmail.com*

Xülasə. Palçıq vulkanizmi Azərbaycanda geniş yayılmışdır, quruda və dənizdə 300-dən çox palçıq vulkanı mövcuddur. Bu vulkanlar neft və qaz yataqları ilə əlaqəlidir və bir çoxu hazırda aktivdir. Şıxzahırlı palçıq vulkanı Bakının qərb şimal-qərb hissəsində, Şamaxı-Qobustan rayonunda yerləşir və dünyanın aktiv palçıq vulkanlarından biridir. 1844-cü ildən 2025-ci ilə qədər təxminən 25 böyük püskürmə baş vermişdir. Vulkanın son püskürməsi 9 yanvar 2021-ci ildə baş vermiş və üç fazadan ibarət olmuşdur. Ən uzun püskürmə üçüncü fazada baş vermiş və 7 dəqiqə davam etmişdir. Şıxzahırlı palçıq vulkanı ərazisində ilk dəfə olaraq səthə yaxın palçıq kameralarının qiymətləndirilməsi, eləcə də qidalandırıcı kanalın izlənməsi məqsədilə şaquli elektrik zondlama üsulundan (ŞEZ) ibarət geoelektrik ölçmələri aparılmışdır. ŞEZ ölçmələri yer səthindən 50 m altda, kiçik dərinlikdə yığılma kameralarının mövcud olmadığını göstərmişdir. Qaz yığılması ilə tətiklənən püskürmə səthə yaxın bölgədə şaxələnir, bir yerdə yuxarıya doğru miqrasiya yolu demək olar ki, şaquli istiqamətdə olsa da, digər yerlərdə mailidir. Tədqiqatlar nəticəsində müəyyən olunmuşdur ki, vulkanın antiklinal strukturun şarnirində yerləşən çox güman ki, iki boğazı mövcuddur. Tədqiqat sahəsinin geoloji kəsilişindəki süxurların nisbətən yüksək nəmliliyə malik olduğu aşkar edilmişdir. Vulkanik brekçiyanın ehtimal olunan qalınlığının 135-150 m arasında dəyişməklə ana süxurların tavanının dərinliyi ilə uyğun olduğu təxmin edilir. Çox güman ki, palçıq vulkanının püskürməsi nəticəsində əmələ gəlmiş müxtəlif istiqamətli qırılmalar sistemi müəyyən edilmişdir.

Açar sözlər: *palçıq vulkanı, püskürmə, şaquli elektrik zondlama, müqavimət, geoelektrik kəsiliş, Şıxzahırlı, qırılma*

ANAS Transactions Earth Sciences 1 / 2026

http://www.journalesgia.com

PETROLOGY, ALTERATION AND MINERALISATION OF MULTIPHASE INTRUSION ROCKS IN THE BABAK RIVER AND SIGUNTU RIVER, PALOPO, SOUTH SULAWESI, INDONESIA

Sudirman[1]*, Maulana A.[2], Umar H.[2]

[1]Geology Master Study Program, Department of Geological Engineering, Hasanuddin University, Gowa, Indonesia

Jl. Perintis Kemerdekaan Km.10 Tamalanrea, Makassar, Sulawesi, Selatan Indonesia, 92119

[2] Department of Geological Engineering, Faculty of Engineering, Hasanuddin University, Gowa, Indonesia

Jl. Perintis Kemerdekaan Km.10 Tamalanrea, Makassar, Sulawesi, Selatan Indonesia, 92119

Corresponding author: sudirmantg@gmailcom

Keywords: *petrogenesis, alteration, mineralisation, hydrothermal, granitoid, Siguntu River, Babak River*

Summary. The research was conducted along the Siguntu River and Babak River in the Latuppa area, Palopo, South Sulawesi. This study aims to investigate the petrogenesis of granitoid rocks and their implications for hydrothermal mineralisation processes. Methods included detailed field observations combined with microscopic laboratory analyses, comprising petrography, mineragraphy and X-ray fluorescence geochemistry of major rock oxides. The study area is dominated by plutonic rocks classified as granitoids, including quartz diorite, granodiorite, and porphyry quartz monzonite, as well as sub-volcanic rocks represented by porphyry andesite. Geochemical data from hydrothermally altered granitoids, particularly granodiorite and porphyry quartz monzonite, indicate derivation from acidic magmas with granodiorite to granite compositions. These rocks are classified as I-type granitoids with high-K calc-alkaline affinity, metaluminous to weakly peraluminous character, and magnesian composition. The presence of three granitoid types suggests multiphase intrusive activity within the study area. This activity generated potassic alteration assemblages characterised by secondary biotite, secondary K-feldspar, anhydrite, and magnetite; inner propylitic alteration with actinolite, epidote and diaspore; and phyllic alteration composed of sericite, quartz, chlorite and pyrite. Associated mineralisation of bornite, chalcopyrite and covellite is typical of porphyry-type deposits. In contrast, sub-volcanic intrusions produced adularia alteration assemblages consisting of adularia, sericite, quartz and pyrite, accompanied by sphalerite and chalcopyrite mineralisation characteristic of epithermal deposits. Overall, hydrothermal alteration and mineralisation indicate an overprinting of porphyry systems by epithermal systems formed in a syn-collisional setting evolving toward crustal extension, associated with granitoid exhumation to shallow crustal levels.

1. Introduction

The presence of mineral deposits is related to a geological complex. One location that has geological complexity and proven mineral deposits is Sulawesi Island. Sulawesi with its distinctive K-shaped pattern is located between the Eurasian Plate, the Indian-Australian Plate, and the Pacific Plate which interact and collide (Katili, 1978) (Figure 1). The implications of these interactions resulted in Sulawesi with four arms of the mega-tectonic province, including the west-north arm which consists of volcanic magmatic product rocks (Sukamto, 1975; Katili, 1978; Hall, 2002; Satyana et al., 2011). Magmatic products in Sulawesi are partly distributed in the south arm (Priadi et al., 1994; Polve et al., 1997; Surono and Hartono, 2013). The series of magmatic products in the form of granitoid rocks are associated with ore deposits, in the form of epithermal Au-Cu deposits, base metal mineralisation, and Cu-Au-Mo porphyry (Maulana et al., 2013).

The Palopo granitoid covers an area of about 30 km^2 and intrudes the Eocene-Oligocene age Toraja Formation and Lamasi Complex (Bergman et al., 1996; White et al., 2017). Historical exploration activities have been conducted by several parties to find mineralisation prospects in the Palopo Region (Van Leeuwen and Peters, 2011). The research will be undertaken in Babak River and Siguntu River as

part of the mineral deposit exploration process to analyse the relationship of granitoid rock petrogenesis to the presence of hydrothermal mineralisation in Latuppa Area, Palopo (Figure 2).

2. Regional Geology

The Palopo granitoids are located within a belt of calc-alkaline granitoids of the Miocene-Pliocene age (Polvé et al., 1997). Some samples from the Palopo Granite show the presence of milonites that developed after the crystallisation of the granite. This is confirmed by the microstructure, e.g. brittle-fracturing and mechanically induced grain size reduction of recrystallised feldspar and quartz. U-Pb zircon ages of 6.3 Ma were obtained from deformed granodiorite and 5.0 Ma from undeformed granodiorite indicating mylonitisation times between 6.3 Ma and 5.0 Ma (White et al., 2017).

The distribution of granitoid rock types in the form of granodiorite units in the Latuppa Area are characterised by consisting of holocrystalline crystallinity texture, faneritic granularity, euhedral-subhedral fabric shape, and equigranular relations. The mineral composition comprises quartz, plagioclase, biotite, and hornblend (Salang, 2022).

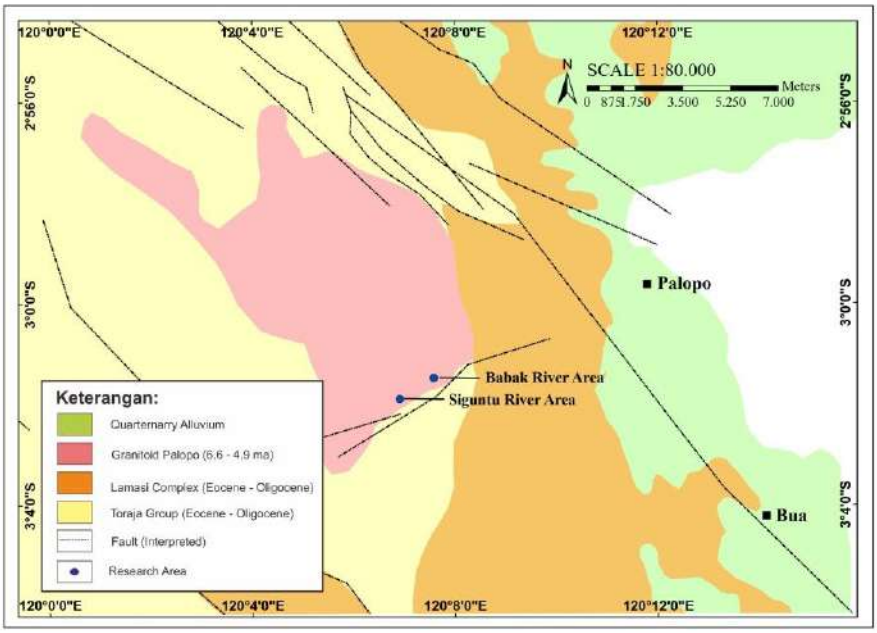

Fig. 1. Regional geology of the study area (White et al., 2017)

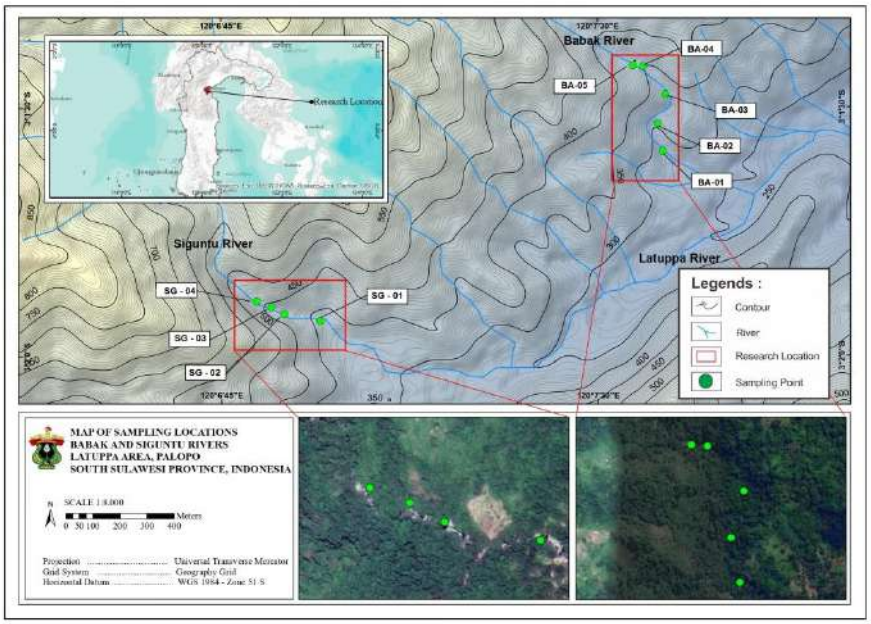

Fig. 2. Research location and sampling points

3. Data and Method

Field data collection stages through direct surveys in the field using geological mapping. Field identification is based on the presence of traces of hydrothermal solution activity in the form of the presence of altered, mineralised rocks and vein zones as well as in areas that have not undergone alteration to see the relationship. The study locations include the Babak River and Siguntu River in the Latuppa Area. Observation of outcrops and rock sampling were carried out in a representative in the research area. A total of nine samples were collected, consisting of five samples from the Babak River (BA-01, BA-02, BA-03, BA-04, and BA-05) and four samples from the Siguntu River (SG-01, SG-02, SG-03, and SG-04). The characteristics of the outcrops encountered show a massive rock structure, so the sampling method is chip sampling and at the outcrops with vein features, the direction and dimensions of the vein are measured.

Microscopic analysis through petrography is used to observe primary minerals and alteration minerals and their characteristics through rock samples (fresh rock and alteration) in the form of thin sections, with an incision thickness of 0.3 mm, and observed under a polarising microscope. Microscopic analysis through mineragraphy is used to determine the type of ore mineral, texture, and its relationship with other ore minerals through observation of rock samples prepared in the form of polished sections and observed under a refraction microscope. Geochemical analysis through XRF (X-Ray Fluorescence Spectrometry) was used to determine the major element content values (SiO_2, TiO_2, Al_2O_3, Fe_2O_3, FeO, MnO, MgO, CaO, Na_2O, K_2O, and P_2O_5) through x-ray fluorescence emitted by atoms in the sample when exposed to x-rays performed on fresh rock samples.

4. Results

4.1. Lithology

Quartz diorite is found in the Babak River which shows intrusive contact with metagranodiorite. The rock shows a massive and slightly foliated structure. Petrographic analysis shows a faneritic texture, consisting of quartz (22%), plagioclase (30%), orthoclase (6%), biotite (8%), muscovite (6%), hornblende (10%), pyroxene (17%), and chlorite (1%) (Figure 4).

Granodiorite is found in the undeformed and mostly deformed form in the Babak River (Figure 3). There are parallel quartz veins, intersecting quartz veins, single quartz veins, pyrite and chalcopyrite, and diorite enclaves. Petrographic analysis shows a faneritic texture, consisting of quartz (21-25%), plagioclase (20-23%), orthoclase (10-18%), biotite (12-15%), muscovite (8-12%), hornblende (2-5%), pyroxene (5-8%), opaque (1-3%), titanite (1%), zircon (1%), sericite (3-6%), epidote (1%), actinolite (1-2%), chlorite (2%), and diaspore (1-2%) (Figure 4). Deformation traces showing ductile deformation observed under a microscope show characteristics of low-grade mylonitic such as the formation of fish texture in mica, porphyroclast from feldspar minerals, undulose extinction quartz texture, bulging texture, and lobate contacts.

Fig. 3. Outcrop and rock appearance of the study area a) Contact of granodiorite intrusion to quartz diorite, b) Contact of andesite intrusion to quartz monzonite, c) Sample of granodiorite with diorite enclave, d) Sample of quartz diorite, e) Sample of andesit and quartz monzonite, f) Sample of quartz monzonite with diorite enclave

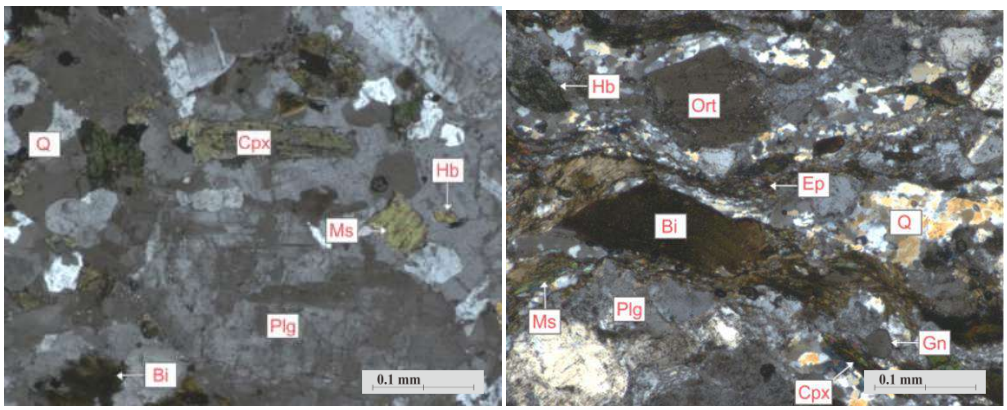

Fig. 4. The Petrographic appearance of rocks a) Granodiorite, b) Deformed granodiorite. Abbreviations: Q – quartz, Cpx – Clinopyroxene, Bi – biotite, Ms – muscovite, Plg – plagioclase, Hb – hornblende, Ort – orthoclase, Ep – epidote, Gn – garnet

The porphyry quartz monzonite encountered at Siguntu River contains parallel quartz veins, intersecting quartz veins, single quartz veins, pyrite and chalcopyrite, and diorite enclaves (Figure 3). Petrographic analysis shows a faneroporphyritic texture, consisting of quartz (14-15%), plagioclase (23-25%), orthoclase (20-22%), biotite (10-12%), muscovite (9-12%), hornblende (2-3%), pyroxene (2-3%), opaq (1-3%), garnet (1%), titanite (0.5%), zircon (1%), sericite (2-8%), adularia (1%), epidote (1-2%), actinolite (1%), diaspore (1-2%), and anhydrite (1%) (Figure 5).

Porphyry andesite is found in Siguntu River which shows intrusive contact with porphyry quartz monzonite rocks (Figure 3). Petrographic analysis shows a porphyroafanitic texture, consisting of quartz (8%), plagioclase (30%), orthoclase (6%), biotite (9%), hornblende (10%), pyroxene (16%), groundmass (12%), opaque (3%), sericite (2%), adularia (1%), and epidote (1%) (Figure 5).

4.2. Alteration

Petrographic analysis can show changes in the mineralogy of rock constituents, to identify changes in primary minerals from magma crystallisation to alteration minerals formed later due to reactions with hydrothermal solutions. Lawless et al. (1997) classify the level of alteration and the results of petrographic observations show the level of rock alteration with a value of 5% to 13% is included in the weakly altered category with a standard value of <25%. The results of petrographic analysis (Table 1) and (Figure 6) show an overprint of alteration zones between potassic-inner propylitic, phyllic, and adularia. The potassic alteration type is characterised by the presence of secondary biotite and secondary K-feldspar minerals associated with anhydrite minerals, while the association of actinolite and epidote reflects the inner propylitic alteration type. The potassic and inner propylitic alteration zones are overprinted with phyllic alteration characterised by the presence of sericite and quartz, and overprinted with adularia alteration characterised by the presence of adularia, quartz, and sericite. It is estimated that the alteration process has occurred in the temperature range of 280-350^{o}C with three alteration episodes.

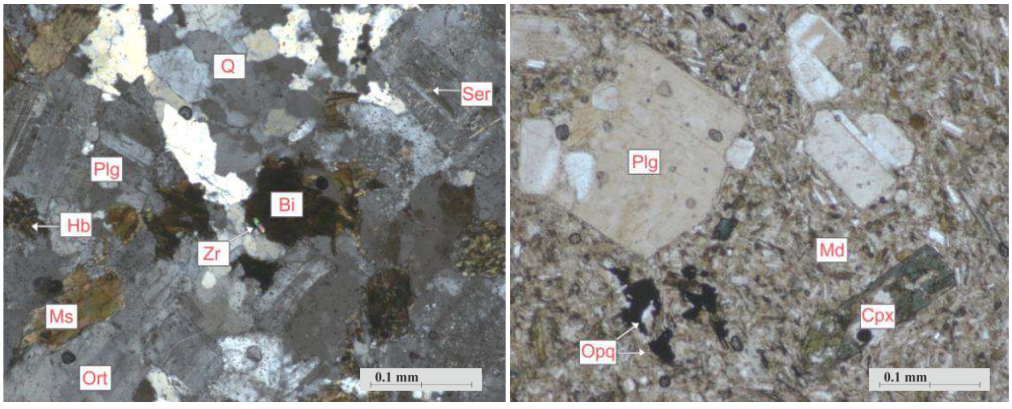

Fig. 5. The Petrographic appearance of rocks a) Porphyry quartz monzonite, b) Porphyry andesite. Abbreviations: Q – quartz, Plg – plagioclase, Bi – biotite, Ms – muscovite, Ort – orthoclase, Hb – hornblende, Ser – sericite, Zr – zircon, Cpx – clinopyroxene, Opq – opaque mineral, Md – groundmass

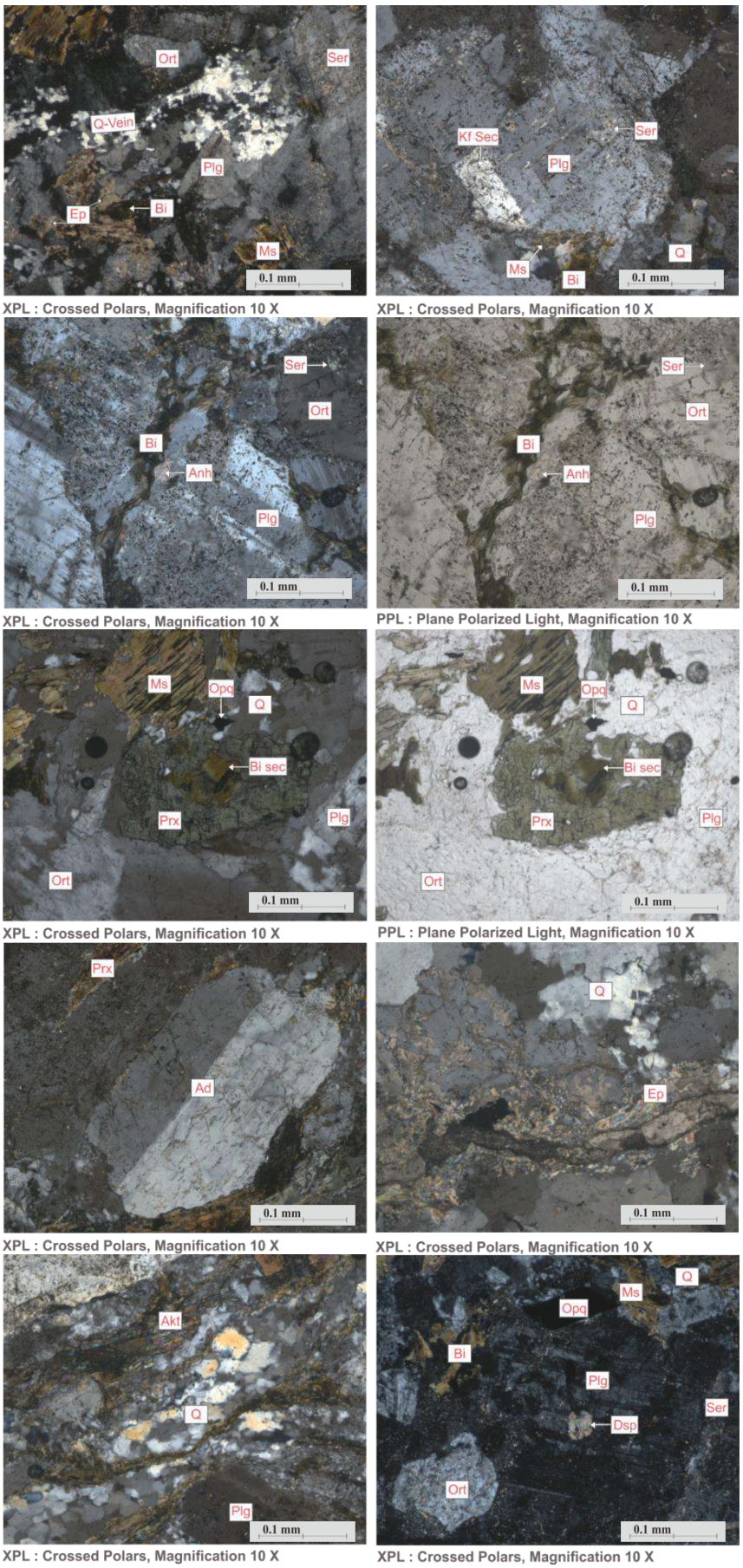

Fig. 6. The appearance of alteration minerals in the petrographic results consists of quartz veins (Q-Vein), secondary K-feldspar (Kf sec), secondary biotite (Bi sec), sericite (Ser), anhydrite (Anh), adularia (Ad), epidote (Ep), actinolite (Akt), and diaspore (Dsp)

Table 1

Temperature range of formation of potassic - inner propylitic, phyllic, and adularia overprint alteration minerals (*White, Hedenquist, 1995; *Thompson, Thompson, 1996; *Corbett, Leach 1998)

Alteration Type	Alteration Minearls	Temperature (celcius degrees) 0 100 200 300
Overprint potasik, inner propilitik, phyllic, adularia	Sec Biotite*	
	Sec K-feldspar*	
	Quartz**	
	Anhydrite**	
	Actinolite**	
	Epidote**	
	Diaspore*	
	Sericite*	
	Adularia*	

4.3. Mineralisation

The ore minerals found are formed under certain physiochemical conditions, so the mineralisation process has a sequence of mineral formation in this case paragenesis. Some minerals are formed primarily from the crystallisation of magma, some are carried by hydrothermal solutions and precipitated during the cooling process, and some are due to oxide-hydroxide process due to interaction with meteoric water-dominant conditions.

The stages of ore mineral formation can be identified through observation of the texture of each mineral (Table 2) and (Figure 7). It is estimated that magnetite minerals are formed at the beginning of mineralisation related to magmatic-hydrothermal conditions. Under transfer conditions, hydrothermal solutions that carry sulfides, oxides, and metal elements, then interact with magnetite, so that it will undergo a replacement process by pyrite, arsenopyrite, bornite, and hematite minerals characterised by partial replacement of the rim of magnetite. The ongoing hydrothermal transfer process results in the replacement of pyrite and bornite by chalcopyrite and covellite, and chalcopyrite and covellite minerals infilling with quartz veins and disseminated in the rock. The same process takes place in magnetite-hematite which is replaced by the oxide-hydroxide mineral goethite under meteoric water dominant conditions. The formation of sphalerite is attributed to hydrothermal solutions brought by the intrusion of porphyry andesite under epithermal conditions that intruded porphyry quartz monzonite. Sphalerite then undergoes replacement by pyrite minerals, further pyrite minerals will undergo replacement by chalcopyrite.

4.4 Geochemistry

Rock geochemical analysis in the form of main oxide elements was carried out on granitoid rock types associated with the presence of hydrothermal solution activity results in the form of quartz veins, alteration minerals, and ore minerals. This aims to analyse the geochemical characteristics of granitoid rocks that carry hydrothermal mineralisation (Table 3).

Table 2

Paragenesis of ore minerals in the Siguntu River and Babak River

Mineralization	Stage I	Stage II	Stage III
	Magmatic-Hydrothermal	Hydrothermal	Hydrothermal
Pyrite			
Chalcopiryte			
Covellite			
Bornite			
Arsenopyrite			
Sphalerite			
Magnetite			
Hematite			
Goetite			

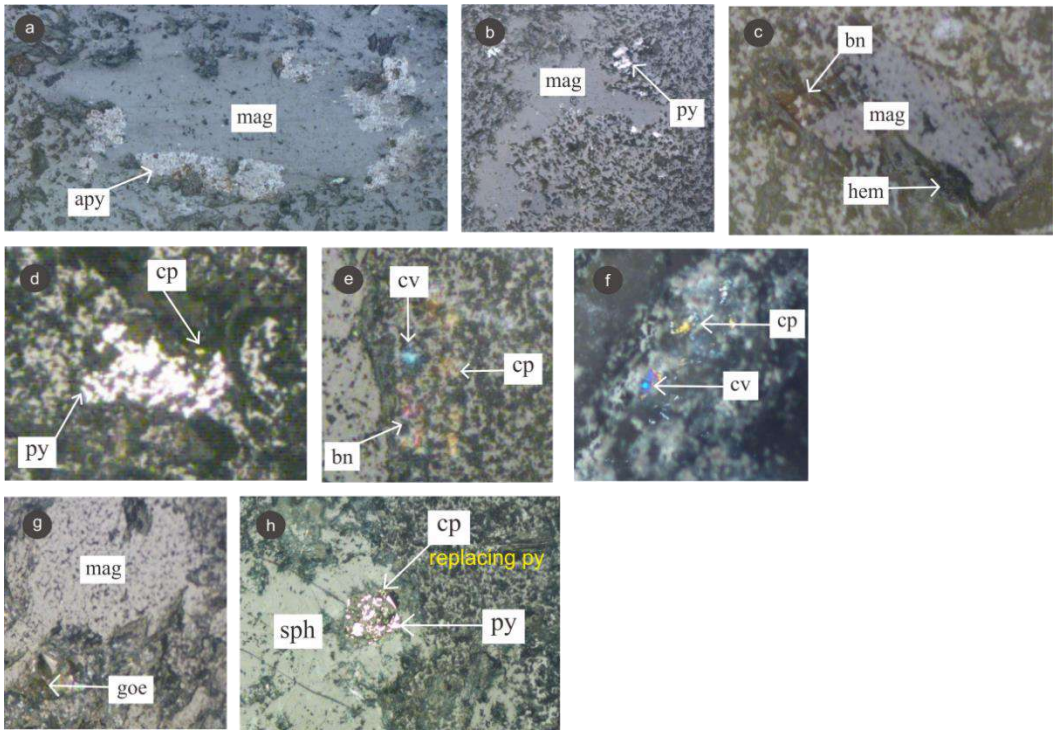

Fig. 7. Microscopic appearance of ore mineral texture a) Replacement of magnetite by arsenopyrite, b) Replacement of magnetite by pyrite, c) Replacement of magnetite by bornite and hematite, d) Replacement of pyrite by chalcopyrite, e) Replacement of bornite by chalcopyrite and covellite, f) Infilling of chalcopyrite and covellite in quartz veins, g) Replacement of magnetite-hematite by goethite, h) Replacement of sphalerite by pyrite and replacement of pyrite by chalcopyrite

Table 3

Major oxide content of the granitoid rock samples of the study area

Mayor Elements	**Id Sample**		
	BA-01A (wt%)	**BA-04 (wt%)**	**SG-04 (wt%)**
SiO_2	65,02	64,31	67,37
Al_2O_3	16,43	16,71	15,92
Fe_2O_3	3,61	4,25	3,07
CaO	3,96	4,63	3,02
Na_2O	3,65	3,58	3,47
K2O	3,61	2,83	3,93
MgO	2,57	2,42	1,81
MnO	0,05	0,07	0,04
P_2O_5	0,17	0,174	0,15
Cr_2O_3	0,06	0,07	0,06
TiO_2	0,48	0,53	0,42
LOI	0,39	0,43	0,74
Total	**100**	**100**	**100**

The major oxides in rocks can be applied in determining rock characteristics such as magma type and affinity, determining rock names, alumina variations, and rock formation environments.

The basis for classification the rocks refers to the TAS classification according to Cox et al. (1979), based on the ratio between silica value (SiO_2) and alkali value ($Na_2O + K_2O$). Samples BA-01A and BA-04 are classified as granodiorite and sample SG-04 is classified as granite (Figure 8a). Determination of magma affinity type refers to the classification according to Paccerillo and Taylor (1976), with a comparison between silica (SiO_2) and alkali potassium (K_2O). Based on the ratio of silica and alkali potassium values, the three samples belong to the high-K calc-alkaline series (Figure 8b). Based on the comparison of A/CNK and A/NK values according to Shand (1943), it is known that samples BA-01A and BA-04 with A/CNK < 1 or A/NK > 1 are metaluminous and sample SG-04 with

A/CNK > 1 or A/NK > 1 is peraluminous (Figure 8c). The results of the analysis of the aluminous level of rocks show a metaluminous level in granodiorite rocks and a weak peraluminous level in granite. According to Frost et al., (2001) granitoid rocks with metaluminous to weak peraluminous levels with silica content of 56-77 wt% are included in I-type granitoids. Based on the comparison of silica and ferro-magnesian values based on Chappel and White (1974), the three samples belong to the magnesian type (Figure 8d). The results of determining the tectonic environment based on Batchelor and Bowden (1985), the formation of granitoid rocks in the R1 and R2 multication diagrams indicate a pre-plate collision environment towards syn-collision (Figure 8e).

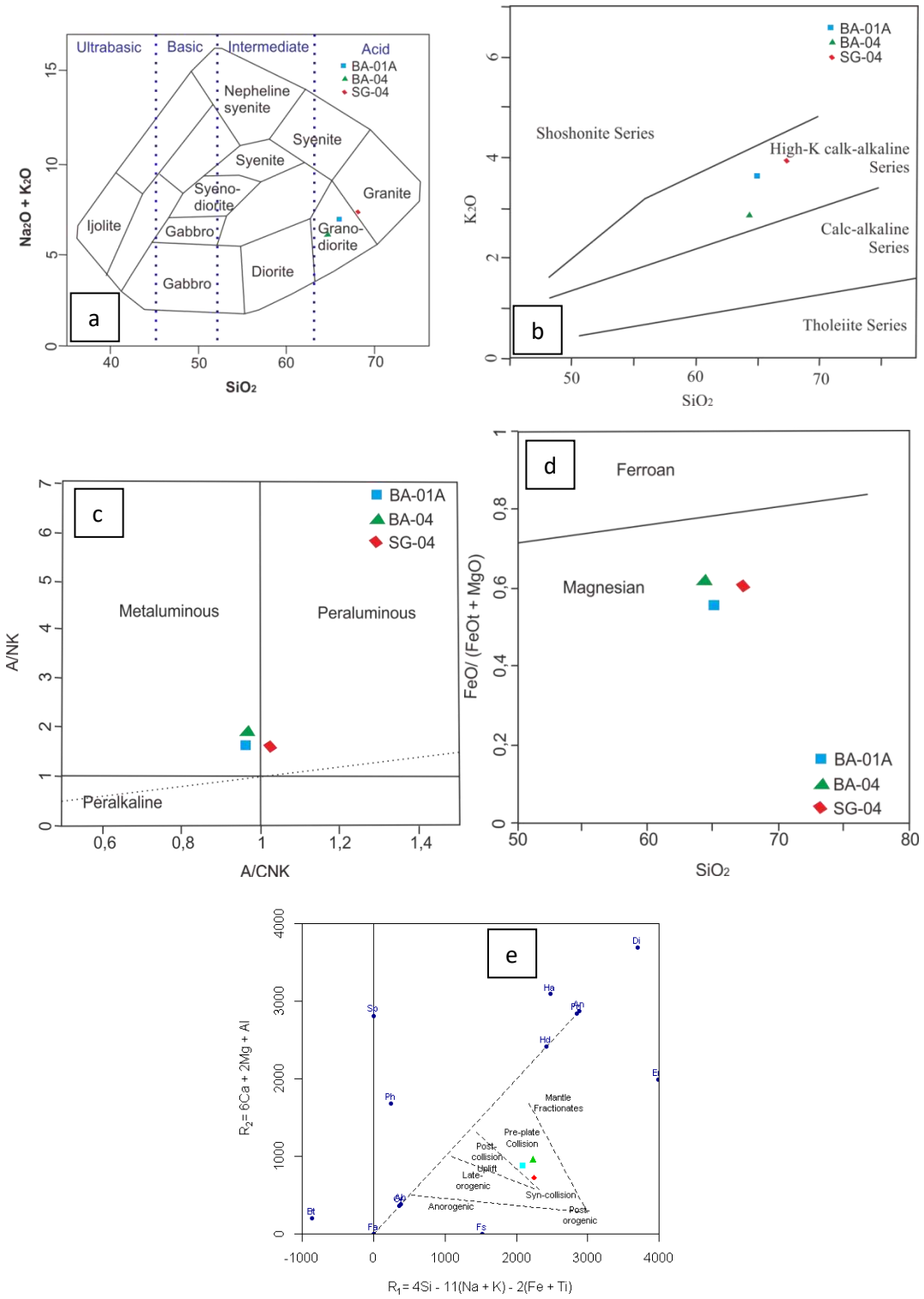

Fig. 8. Results of geochemical characteristics determination a) Rock name determination, b) Magma affinity, c) Alumina variation, d) Ferro-magnesian, e) Tectonic environment

5. Discussion

Based on petrological and geochemical data, the granitoid of the study area was formed at the transition of the tectonic process from pre-plate collision to syn-collision in the compression setting between the West Sulawesi Microcontinent and the Sula-Spur Microcontinent to late-collision in the extension setting due to the Banda Sea plate roll back (Figure 9). Based on the age of the oldest granitoid rock, the quartz diorite, which is 6.4 Ma (Zhang et al., 2020), the granitoid magma formation process occurred before 6.4 Ma, which is interpreted as Middle Miocene to Late Miocene.

The initial pre-plate collision tectonic process was associated with the subduction of the Indo-Australian Plate beneath the West Sulawesi Microcontinent which resulted in partial melting of the mafic rock component and mantle component to produce mafic magma. Hildreth and Moorbath 1988; Richards, 2003, explained that hydrous mafic magma from the mantle wadge will be transferred to the mash zone (melting, assimilation, storage, homogenisation) at the base of the continental crust, followed by the rise of magma to shallower levels to form granitoid rocks. The mafic magma undergoes differentiation to form plagioclase, pyroxene, magnetite, and other non-hydrous minerals that increase the H_2O content in solution and will undergo assimilation with lower crustal components to form more intermediate magmas which are thought to be related to the formation of quartz diorite. Geochemical analyses comparing SiO_2 and other oxide content indicate fractionated crystallisation at the beginning to form plagioclase, hornblende, and pyroxene minerals while K_2O-containing minerals will crystallise at the end to form orthoclase, biotite, and muscovite. During syn-collision, intermediate magmas undergo further differentiation and assimilation with potassium-rich crustal components such as metasediments to produce acidic magmas that move up to the middle crust where magmas mingling with quartz diorites to eventually form granodiorites containing biotite and muscovite. The syn-collision process associated with compression forces caused some of the granodiorite to deform in the ductile zone. Meanwhile, the late-collision process associated with the extension force produces asthenospheric upwelling and delamination of the lower crust so that there is assimilation between the potassium-rich lower crustal components and the mantle which is the source of porphyry quartz monzonite or granite.

Hydrothermal fluid activity in the Latuppa area occurs at mesozonal depth (Musri et al., 2011). The rock intrusion process of the study area consists of early intrusive forming quartz diorite, inter-intrusive forming early porphyry from granodiorite, late-intrusive forming late- mineral porphyry from porphyry quartz monzonite, and intrusive post porphyry forming porphyry andesite which is tectonically associated with the process of exhumation due to crustal extension resulting in stages of hydrothermal fluid penetration and environmental changes to become shallower resulting in alteration overprints and ore mineral replacement (Figure 10).

The alteration process shows an overprint between potassic-phyllic-adularia, inner propylitic-phyllic-adularia, also shown replacement of magnetite ore minerals by pyrite, bornite, arsenopyrite, replacement of pyrite by chalcopyrite, and replacement of sphalerite by pyrite followed by replacement of pyrite by chalcopyrite. Maulana et al., (2019) estimated the exhumation of Granitoids related to the Palopo Granitoids in Mamasa and Masamba at a rate of 0.37 and 1.6 mm/year.

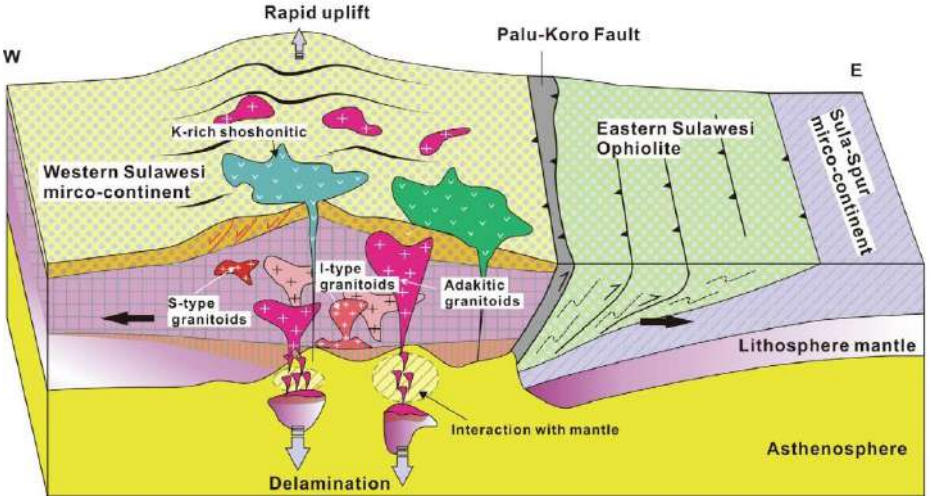

Fig. 9. Illustration of the tectonic evolution of Miocene-Pliocene pre-plate collision, syn-collision, and late-collision (extension) related to granitoid magma formation in the West Sulawesi Microcontinent (Liu et al., 2020)

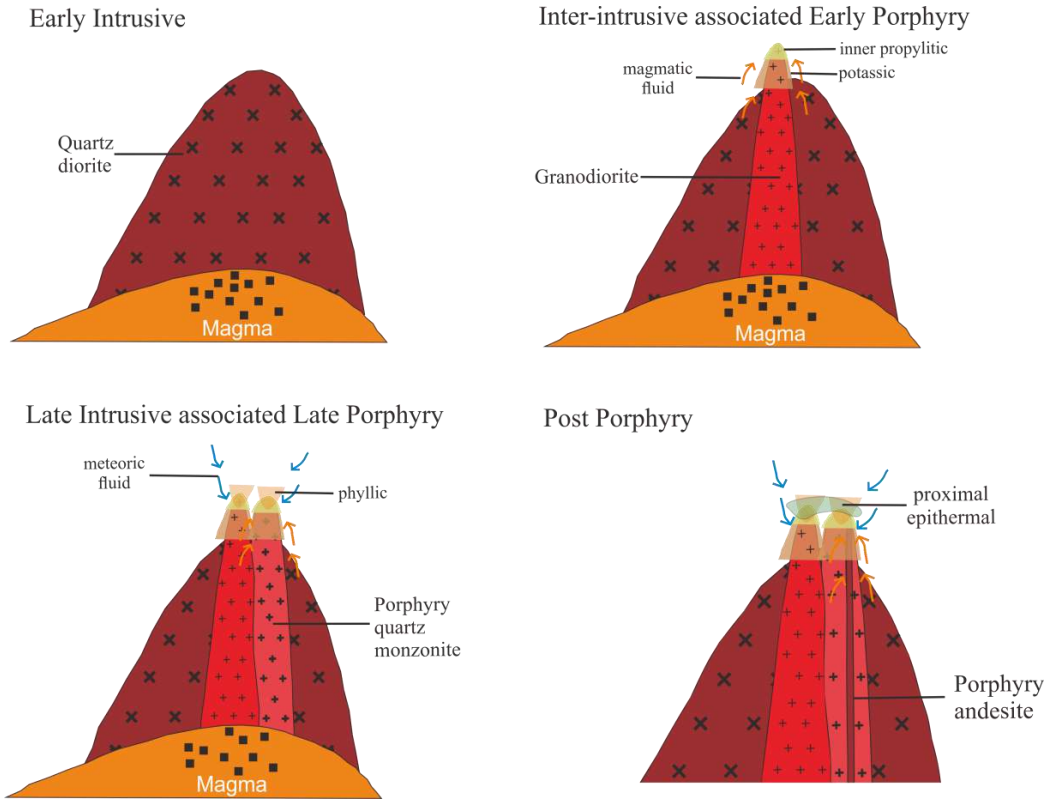

Fig. 10. Illustration of the genetic model of alteration and mineralisation stages of the study area (Illustration adapted from Sillitoe (2010); Musri et al. (2011))

The types of deposits formed are associated with potassic, inner propylitic and phyllic alteration and mineralisation of bornite, chalcopyrite and covellite belonging to the porphyry deposit type. The porphyry deposit type is associated with magmatism of granodiorite and porphyry quartz monzonite I-type granitoids containing high-K calc-alkaline with metaluminous to weak peraluminous. The exhumation process places the granitoids associated with porphyry deposits into shallower crustal levels which are then overprinted by deposit types associated with adularia alteration and sphalerite-chalcopyrite mineralisation characteristic of epithermal deposit types in proximal environments associated with late magmatism in the form of porphyry andesite subvolcanic intrusions. Shallower conditions led to the formation of hydrothermal fluids from the epithermal system flowing through the zone of alteration and porphyry mineralisation. These fluids added new alteration minerals and mineralisation, creating a complex combination of minerals from both systems.

6. Conclusions

From the compilation of field data and laboratory analysis, it was concluded:

1. The lithology of the study area consists of granitoid-type plutonic rocks in the form of quartz diorite and granodiorite in Sungai Babak and granitoid-type plutonic rocks in the form of porphyry quartz monzonite and sub-volcanic rocks in the form of porphyry andesite in Sungai Babak.

2. The geochemistry of granitoid rocks associated with hydrothermal mineralisation in the form of granodiorites and granites which are I-type granitoid, high-K calc-alkaline, metaluminous to weakly peraluminous, formed in pre-plate collision to syn-collision, and late collision environments associated with compression to extension forces that produce acidic magmas from the melting of mafic rocks that undergo differentiation and assimilation with the lower crust.

3. The study area experienced multiphase intrusion associated with mineralisation in the inter-intrusive (granodiorite) to late-intrusive (porphyry quartz monzonite/granite) forming overprints of potassic alteration, inner propylitic, phyllic, and bornite-chalcopyrite- covellite mineralisation belonging to the porphyry deposit type, and post porphyry intrusive forming adularia alteration and sphalerite-chalcopyrite mineralisation belonging to the epithermal deposit type. The porphyry deposit type is overprinted by epithermal deposits.

Acknowledgements

The authors would like to thank the Latuppa Regional Government for permission to conduct the research and thank you for support in using the laboratory of the Department of Geology, Hasanuddin University.

REFERENCES

Batchelor RA, Bowden P (1985) Petrogenetic interpretation of granitoid rock series using multicationic parameters. Chemical Geology 48:43–55

Bergman SC, Coffield DQ, Talbot JP et al (1996) Tertiary tectonic and magmatic evolution of Western Sulawesi and the Makassar Strait, Indonesia: evidence for a Miocene continent-continent collision. In: Hall R, Blundell DJ (eds) Tectonic Evolution of SE Asia. Geological Society of London Special Publication 106(1):391-429. https://doi.org/10.1144/gsl.sp.1996.106.01.25

Chappell BW, White AJR (1974) Two contrasting granite types. Pacific Geology 8:173–174.

Corbett GJ, Leach TM (1998) Southwest Pacific rim gold-copper systems: structure, alteration and mineralization. Special publications of the society of economic geologists 6:238. https://doi.org/10.5382/SP.06

Cox KG, Bell JD, Pankhurst RJ (1979) The interpretation of igneous rocks. G Allen and Unwin, London. http://dx.doi.org/10.1007/978-94-017-3373-1

Frost BR, Barnes CG, Collins WJ et al (2001) A geochemical classification for granitic rocks. Journal of Petrology 42(11):2033–2048

Hall R (2002) Cenosoic geological and plate tectonic evolution of SE Asia and the SW Pacific: computer-based reconstruction, model and animations. Journal of Asian Earth Science 20(4):353–431. https://doi.org/10.1016/S1367-9120(01)00069-4

Hildreth WS, Moorbath S (1988) Crustal contribution to arc magmatism in the Andes of Central Chile. Contributions to Mineralogy and Petrology 98:455–489

Katili JA (1978) Past and present geotectonic position of Sulawesi, Indonesia. Tectonophysics 45(4):289–322. https://doi.org/10.1016/ 0040-1951(78)90166-X

Lawless JV, White PJ, Bogie I (1997) Important hydrothermal minerals and their significance. Geothermal and Mineral Services Division, Kingston-Morrison Ltd, p 63

Liu J, Zhang J, Hsia J et al (2020) Late Miocene to Pliocene crustal extension and lithospheric delamination revealed from the ~5 Ma Palopo granodioritic intrusion in Western Sulawesi, Indonesia. Journal of Asian Earth Sciences 201(104506). https://doi.org/10.1016/j.jseaes.2020.104506

Maulana A, Van Leeuwen T, Watanabe K et al (2019) Exhumation and tectonomagmatic processes of the granitoid rocks from Sulawesi, Indonesia: Constrain from petrochemistry and geothermobarometry study. Indonesian Journal on Geoscience 6(2):153–174. DOI:10.17014/ijog.6.2.153-174

Maulana A, Yonezu K, Watanabe K, Imai A (2013) Granitic magmatism and related ore deposit in Sulawesi, Indonesia. Paper presented at International Symposium on Earth Science and Technology in Fukuoka, Japan, 3-4 December

Musri M, Suparka E, Tambun B (2011) Model geologi alterasi dan mineralisasi hidrotermal Daerah Latuppa, Palopo, Sulawesi Selatan. The 36th HAGI and 40th IAGI Annual Convention and Exhibition Makassar, 26 – 29 September, Proceeding JCM

Paccerillo A, Taylor SR (1976) Geochemistry of Eocene calc-alkaline volcanic rocks from the Kastomumu area northern Turkey. Contributions to Mineralogy and petrology 58:63 – 81

Polve M, Maury R, Bellon H, Rangin C et al (1997) Magmatic evolution of Sulawesi (Indonesia): constraints on the Cenozoic geodynamic history of Sundaland active margin. Tectonophysics, 272(1):69–92. https://doi.org/10.1016/S0040-1951(96)00276-4

Priadi B, Polve M, Maury RC et al (1994) Tertiary and Quaternary magmatism in Central Sulawesi: chronological and petrological constraints. Journal of Southeast Asian Earth Sci. 9(1-2):81–93. https://doi.org/10.1016/0743-9547(94)90067-1

Richards JP (2003) Tectono-magmatic precursors for porphyry Cu-(Mo Au) deposit formation. Econ Geol 98:1515–1533. https://doi.org/10.2113/gsecongeo.98.8.1515

Surono S, Hartono U (2013) Geologi Sulawesi (Geology of Sulawesi). LIPI Press, Pusat Survei Geologi, Badan Geologi KESDM, Jakarta

Salang NI (2022) Geologi dan geokimia batuan granodiorit Daerah Latupa, Kecamatan Mungkajang, Kota Palopo, Provinsi Sulawesi Selatan (Geology and geochemistry of graniodiorite rocks in Latuppa Area, Mungkajang Sub-district, Palopo City, South Sulawesi Province). Thesis, Hasanuddin University, Unpublished (in Indonesian)

Satyana AH, Faulin T, Mulyati SN (2011) Tectonic evolution of Sulawesi Area: Implications for proven and prospective petroleum plays. Proceedings JCM Makassar 2011, The 36th HAGI and 40th IAGI Annual Convention and Exhibition

Shand SJ (1943) Eruptive Rocks: Their genesis, composition, classification, and their relation to ore deposits with a chapter on meteorites. John Wiley and Sons, New York

Sillitoe RH (2010) Porphyry copper systems. Society of Economic Geologists, Inc. Economic Geology 105(1):3–41. http://dx.doi.org/10.2113/gsecongeo.105.1.3

Sukamto R (1975) The structure of Sulawesi in the light of plate tectonics. Proceedings of the Regional Conference on the Geology and Mineral Resources of Southeast Asia, Jakarta, August 4-7

Thompson AJB, Thompson JFH (1996) Atlas of alteration. Geological Association of Canada, Mineral Deposits Division

Van Leeuwen TM, Peters PE (2011) Mineral deposits of Sulawesi. Proceedings of the Sulawesi Mineral Resources, Seminar MGEI-IAGI, 28-29 November, Manado, North Sulawesi, Indonesia. https://doi.org/10.13140/2.1.3843.2322

White LT, Hall R, Armstrong AR et al (2017) The geological history of the Latimojong Region of Western Sulawesi. Journal Asian Earth Science 138:72–91. https://doi.org/10.1016/j.jseaes.2017.02.005

White NC, Hedenquist JW (1995) Epithermal gold deposits: styles, characteristics and exploration. SEG Newsletter 23(1):9–13

Zhang X, Tien C.Y, Chung SL et al (2020) A Late Miocene magmatic flare-up in West Sulawesi triggered by Banda slab rollback. GSA Buletin 132:(11-12)

ПЕТРОЛОГИЯ, ИЗМЕНЕНИЯ И МИНЕРАЛИЗАЦИЯ МНОГОФАЗНЫХ ИНТРУЗИВНЫХ ПОРОД В РАЙОНАХ РЕК БАБАК И СИГУНТУ, ПАЛОПО, ЮЖНЫЙ СУЛАВЕСИ, ИНДОНЕЗИЯ

Судирман[1]*, Маулана А.[2], Умар Х.[2]
[1]Магистерская программа по геологии, Факультет геологической инженерии, Университет Хасануддин, Гова, Индонезия
92119, Южный Сулавеси, Макассар, Тамаланреа, Jl. Перинтис Кемердекаан km. 10
[2]Факультет геологической инженерии, Университет Хасануддин, Гова, Индонезия
92119, Южный Сулавеси, Макассар, Тамаланреа, Jl. Перинтис Кемердекаан km. 10
**Ответственный за переписку: sudirmantg@gmailcom*

Резюме. Исследование было проведено вдоль рек Сигунту и Бабак в районе Латуппа, город Палопо, Южный Сулавеси. Целью данного исследования является изучение петрогенезиса гранитоидных пород и их влияния на процессы гидротермальной минерализации. В работе использовались методы детальных полевых наблюдений в сочетании с микроскопическими лабораторными исследованиями, включающими петрографический и минераграфический анализы, а также геохимический анализ основных оксидов пород методом рентгенофлуоресцентной спектроскопии (XRF). Район исследований преимущественно сложен плутоническими породами, классифицируемыми как гранитоиды, включая кварцевый диорит, гранодиорит и порфировый кварцевый монцонит, а также субвулканические породы, представленные порфировым андезитом. Геохимические данные по гранитоидным породам, подвергшимся гидротермальной переработке, в частности по гранодиориту и порфировому кварцевому монциниту, свидетельствуют об их образовании из кислых магм с составом от гранодиорита до гранита. Данные породы относятся к гранитоидам I-типа, характеризуются высококалиевой кальций-щелочной серией, мета-алюминиевым до слабо пералюминиевого составом и магнезиальной природой. Наличие трех типов гранитоидов указывает на многофазную интрузивную деятельность в пределах исследуемой территории. В результате этой деятельности сформировались калиевые ассоциации гидротермального изменения, характеризующиеся вторичным биотитом, вторичным калиевым полевым шпатом, ангидритом и магнетитом; внутренняя пропилитовая ассоциация с актинолитом, эпидотом и диаспором; а также филлитовая ассоциация, представленная серицитом, кварцем, хлоритом и пиритом. Ассоциированная минерализация борнита, халькопирита и ковеллина характерна для месторождений порфирового типа. В отличие от этого, субвулканические интрузии обусловили развитие адулярных измененных ассоциаций, включающих адуляр, серицит, кварц и пирит, сопровождаемых минерализацией сфалерита и халькопирита, типичной для эпитермальных месторождений. В целом, гидротермальные изменения и минерализация указывают на наложение эпитермальных систем на более ранние порфировые системы, сформированные в синколлизионной тектонической обстановке, которая эволюционировала в сторону растяжения земной коры и сопровождалась эксгумацией гранитоидных пород к приповерхностным уровням коры.

Ключевые слова: *петрогенез, альтерация, минерализация, гидротермальный гранитоид, р. Сигунту, р. Бабак*

İNDONEZİYADA CƏNUBİ SULAVESİNİN PALOPO ƏYALƏTİNDƏ BABAK VƏ SİQUNTU ÇAYLARINDA ÇOXFAZALI İNTRUZİV SÜXURLARIN PETROLOGİYASI, DƏYİŞDİRİLMƏSİ VƏ MİNERALLAŞMASI

Sudirman[1]*, Maulana A.[2], Ömər H.[2]
[1]Geologiya üzrə magistr proqramı, Geoloji Mühəndislik Fakültəsi, Həsənuddin Universiteti, Qova, İndoneziya
92119, Cənubi Sulavesi, Makassar, Tamalanrea, Jl. Perintis Kemerdekaan km. 10
[2]Geoloji mühəndislik fakültəsi, Həsənuddin Universiteti, Qova, İndoneziya
92119, Cənubi Sulavesi, Makassar, Tamalanrea, Jl. Perintis Kemerdekaan km. 10
**Yazışmalara məsul: sudirmantg@gmailcom*

Xülasə. Tədqiqat Cənubi Sulavesinin Palopo şəhərinin Latuppa bölgəsindəki Siguntu və Babak çayları boyunca aparılmışdır. Bu tədqiqatın məqsədi qranit süxurların petrogenezini və onların hidrotermal minerallaşma proseslərinə təsirini öyrənməkdir. Əsərdə petroqrafik və mineraloqrafik analizlər, həmçinin rentgen flüoresan spektroskopiya (XRF) üsulu ilə süxurların əsas oksidlərinin geokimyəvi analizi daxil olmaqla mikroskopik Laboratoriya tədqiqatları ilə birlikdə ətraflı mədən müşahidələri metodlarından istifadə edilmişdir. Tədqiqat sahəsi əsasən kvars diorit, qranodiorit və porfir kvars monsonit və porfir andezit ilə təmsil olunan subvulkanik süxurlar da daxil olmaqla qranitoidlər kimi təsnif edilən plutonik süxurlardan ibarətdir. Hidrotermal emaldan keçmiş qranitoid süxurları, xüsusən qranodiorit və porfir kvars monsoniti üçün geokimyəvi məlumatlar, qranodioritdən qranitə qədər olan tərkibi olan turşu magmalardan əmələ gəldiyini göstərir. Bu süxurlar I tip qranitoidlərə aiddir, yüksək kalium kalsium-qələvi seriyası, meta-alüminiumdan bir qədər peralumin tərkibinə və maqneziya təbiətinə malikdir. Üç növ qranitoidin olması tədqiq olunan ərazidə çox fazalı müdaxilə fəaliyyətini göstərir. Bu fəaliyyət nəticəsində ikincil biotit, ikincil kalium feldispat, anhidrit və maqnetit ilə xarakterizə olunan hidrotermal dəyişikliyin kalium birləşmələri meydana gəldi; aktinolit, epidot və Diasporla daxili propilit əlaqəsi; serisit, kvars, xlorit və pirit ilə təmsil olunan fillit Dərnəyi. Bornit, xalkopirit və kovellinin əlaqəli minerallaşması porfir tipli yataqlar üçün xarakterikdir. Bunun əksinə olaraq, subvulkanik müdaxilələr epitermal yataqlara xas olan sfalerit və xalkopiritin minerallaşması ilə müşayiət olunan adulyar, serisit, kvars və pirit daxil olmaqla adulyar dəyişdirilmiş birləşmələrin inkişafına səbəb oldu. Ümumiyyətlə, hidrotermal dəyişikliklər və minerallaşma, yer qabığının uzanmasına doğru inkişaf etmiş və qranitoid süxurların qabığın səthə yaxın səviyyələrinə eksqumasiyası ilə müşayiət olunan sinkollizasiya tektonik şəraitdə əmələ gələn əvvəlki porfir sistemlərində epitermal sistemlərin üst-üstə düşməsini göstərir.

Açar sözlər*: petrogenez, alterasiya, minerallaşma, hidrotermal qranitoid, River Siquntu, River Babak*

ANAS Transactions Earth Sciences 1 / 2026

http://www.journalesgia.com

MAGMATIC-HYDROTHERMAL EVOLUTION AND ORE POTENTIAL OF THE BEKTAKARI-BNELIKHEVI KNOT, BOLNISI ORE DISTRICT, LESSER CAUCASUS

Mindiashvili G.[1]*, Bluashvili D.[2], Lipartia T.[2], Iobidze G.[2], Makadze M.[1], Jafaridze N.[2], Benashvili K.[2], Khetsuriani G.[2], Bluashvili V.[2]

[1]Ivane Javakhishvili Tbilisi State University, Georgia
1, Ilia Chavchavadze Ave., Tbilisi, 0179
[2]Georgian Technical University, Georgia
77, Kostava Str., Tbilisi, 0175
**Corresponding author: giorgim1994@gmail.com*

Keywords: *hydrothermal alteration, geochemistry, mineralisation, magmatism*

Summary. This study investigates the petrological, geochemical, and geodynamic characteristics of intrusive and sub volcanic rocks within the Bektakari–Bnelikhevi ore knot, situated in the southern segment of the Lesser Caucasus. The research integrates detailed mineragraphic observations with whole-rock geochemical data obtained from 17 samples collected from eight drill cores. Major and trace element compositions were determined using X-ray fluorescence (XRF) spectrometry, providing a robust dataset for evaluating magma evolution and hydrothermal alteration processes. Petrographic examination reveals significant variability in mineral assemblages, textures, and alteration patterns, reflecting complex magmatic differentiation and subsequent hydrothermal overprinting. The intrusive rocks display systematic compositional trends consistent with a calc-alkaline magmatic series generated in a subduction-related tectonic environment and influenced by mantle-derived melts interacting with crustal components. Geochemical discrimination diagrams show pronounced enrichment in large-ion lithophile elements (LILE) together with depletion in high-field-strength elements (HFSE), supporting formation in a convergent margin setting associated with arc magmatism. Mineragraphic observations of sulfide assemblages, including pyrite, chalcopyrite, sphalerite, and galena, indicate multiple stages of hydrothermal mineralisation linked to evolving magmatic fluids and structural pathways for fluid migration. These features collectively suggest the presence of a long-lived magmatic–hydrothermal system capable of generating metal-enriched fluids and favourable conditions for ore deposition. The results highlight the metallogenic significance of the Bektakari–Bnelikhevi ore knot and contribute to a broader understanding of arc-related mineralisation processes within the Lesser Caucasus sector of the Tethyan metallogenic belt.

Introduction

The Bektakari-Bnelikhevi region, located in the Lesser Caucasus of southern Georgia, occupies a structurally complex segment of the Arabia-Eurasia convergence zone, shaped by long-lived subduction, back-arc extension, and subsequent collisional events (Adamia et al., 2010). This tectonic setting has played a critical role in magma generation, emplacement, and associated hydrothermal activity, thereby creating favorable conditions for ore-forming systems in arc-related plutonic complexes.

The regional geology is defined by a thick Upper Cretaceous volcano-sedimentary sequence, comprising Campanian and Senonian carbonate–terrigenous units (Gasandami and Mashavera suites), which are intruded by Cenomanian–Turonian dioritic and quartz dioritic plutonic bodies (k1, k2 units). These plutons are spatially and genetically associated with rhyodacitic and basaltic subvolcanic rocks (K2 units), emplaced along major fault systems and structurally prepared conduits. The intrusive and subvolcanic rocks are characterised by widespread hydrothermal alteration zones, often accompanied by disseminated and vein-hosted sulfide mineralisation. These features suggest prolonged magmatic-hydrothermal evolution in a tectonically permeable upper crust.

The geological map of the Bektakari-Bnelikhevi region (Fig.1) highlights the spatial association between dioritic intrusions, subvolcanic rocks, and mapped mineralised zones. Notably, alteration halos

and drillholes concentrate near intrusive contacts and along fault-controlled zones, indicating the influence of syn- and post-magmatic structural controls on fluid migration and metal deposition. Recent remote sensing-based studies further emphasise the role of structural lineaments and alteration patterns in delineating prospective zones within the Bektakari–Bnelikhevi ore knot (Mindiashvili et al., 2024a). This structural magmatic interplay is typical of subduction-related metallogenic belts worldwide (Richards, 2003; Sillitoe, 2010), where magmatic arcs interact with deep-seated trans-crustal faults to localise ore systems.

Despite clear mineral potential of the region, recent studies have demonstrated the value of integrating geochemical datasets with advanced analytical approaches, including machine learning, to better constrain hydrothermal system architecture and ore-forming processes within the Bektakari–Bnelikhevi ore knot and the Bolnisi ore district (Mindiashvili et al., 2024b). Nevertheless, the petrological and metallogenic framework of the Bektakari-Bnelikhevi intrusive system remains undercharacterised. Accordingly, the objective of this study is to investigate the petrogenesis of the intrusive and subvolcanic rocks using mineragraphic and geochemical data, to reconstruct their formation conditions, and to assess the geodynamic and metallogenic processes that influenced ore localisation. By linking the mineralogical and geochemical features to the regional tectonic context, this research contributes to a broader understanding of arc-related ore-forming systems in the Lesser Caucasus and adjacent segments of the Tethyan metallogenic belt.

Method of study

This study integrates mineralographic and geochemical analyses to investigate the petrogenesis and metallogenic potential of intrusive and subvolcanic rocks in the Bektakari–Bnelikhevi ore knot. 17 representative rock samples were collected from 8 drill cores targeting geologically distinct intrusive bodies and hydrothermally altered zones. Sampling was based on lithological variation, visible mineralisation, and stratigraphic position.

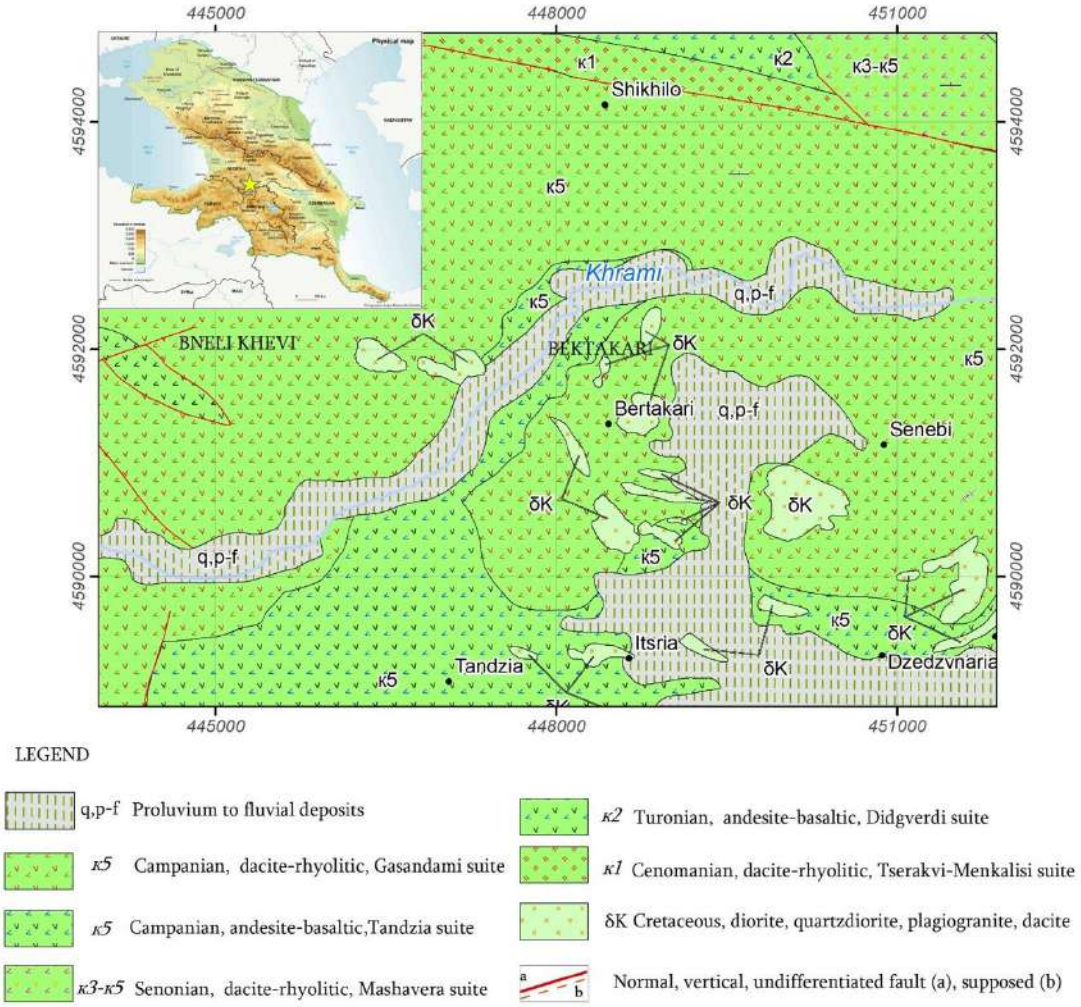

Fig. 1. Geological map of the Bektakari–Bnelikhevi region (modified after Adamia et al., 2020), showing Upper Cretaceous volcano-sedimentary units, intrusive complexes, and mapped fault systems. The spatial distribution of units highlights tectonomagmatic controls on ore-forming processes

Mineralographic investigations were conducted on polished thin sections using reflected light microscopy. The objective was to identify ore minerals, describe their textural associations, and interpret the paragenesis of the mineralising system. Particular focus was placed on the morphology, mutual relationships, and replacement textures of pyrite, chalcopyrite, sphalerite, galena, and associated quartz minerals. These observations followed standard practices outlined by Craig and Vaughan (1994) and were supplemented with high-resolution photomicrography.

Geochemical analyses were carried out using X-ray fluorescence (XRF) spectrometry to determine the concentrations of major and trace elements. Sample preparation followed conventional protocols, including crushing, pulverizing, and pelletizing. The obtained elemental data were used for petrological classification, magmatic trend analysis, and tectonomagmatic interpretation.

Interpretation of the geochemical data employed a range of classification and discrimination diagrams. The Total Alkali–Silica (TAS) diagrams proposed by Cox et al. (1979) and refined by Middlemost (1994) were applied for basic rock classification. Additional classification followed the Enrique and Esteve (2019) scheme on plutonic rocks, which integrates alkali-lime index, silica saturation, and aluminium saturation indicators. Chemical variation was further explored using the R1–R2 diagram of De la Roche et al. (1980), and magmatic affinity was assessed with the AFM ternary plot after Irvine and Baragar (1971).

To evaluate the alumina saturation state, the Alumina Saturation Index (ASI) was calculated following the method outlined by Maniar and Piccoli (1989). Tectonic setting discrimination was based on the Ti–V (Shervais, 1982), Ti–Zr (Pearce and Cann, 1973), and Ti–Zr–Sr diagrams. Trace element behavior and geochemical signatures were visualised using multi-element spider diagrams normalised to primitive mantle values (Sun and McDonough, 1989; Taylor and McLennan, 1985).

Data visualisation and statistical processing were performed using GCDkit (Janoušek et al., 2006) and IgPet software. All geochemical interpretations were conducted by established international standards for igneous petrology and ore geology.

Results

The petrochemical and mineragraphical composition of the intrusive rocks from the Bektakari–Bnelikhevi ore knot reflects a coherent magmatic and hydrothermal evolution shaped by a convergent tectonic regime. The data reveal compositional convergence around intermediate to post-mafic magmas, evolving through subduction-modified petrogenetic processes and culminating in structurally controlled ore formation.

The polished section observations demonstrate diverse sulfide assemblages reflecting successive mineralisation pulses (Fig. 2).

Pyrite is ubiquitously present as both early and late-stage phases, forming euhedral crystals as well as anhedral overgrowths and fine-grained dissemination. Its associations with chalcopyrite, sphalerite, galena, and quartz vary in space and texture across sampled intervals. In several specimens, sphalerite appears to be partially replaced by chalcopyrite, implying an evolving sulfur and metal activity within the ore fluids. Intergrowth textures between chalcopyrite and galena, and their inclusion in quartz vein fragments, suggest cyclic fluid influxes and overprinting episodes, commonly seen in arc-related polymetallic systems (Hedenquist and Lowenstern, 1994; Sillitoe, 2010).

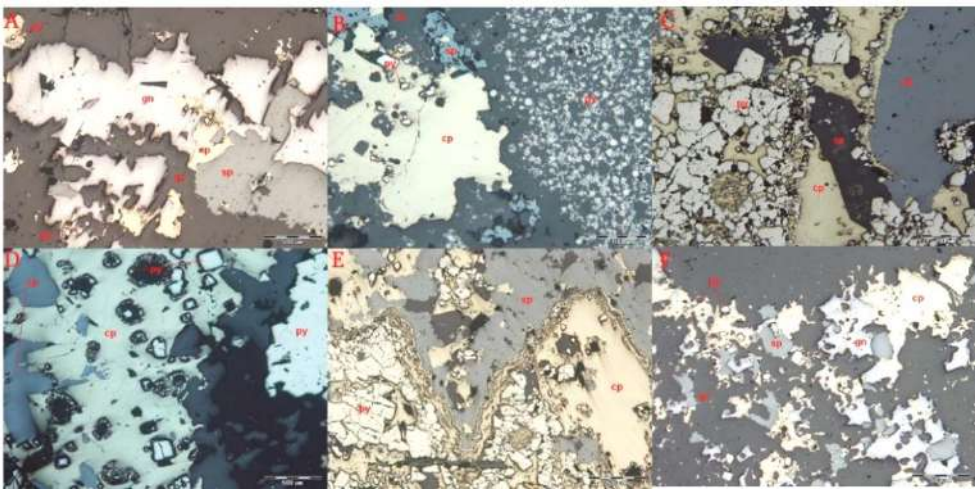

Fig. 2. Reflected light photomicrographs of representative ore textures. (A) Intergrowth of sphalerite (sp), galena (gn), and pyrite (py) with minor quartz (qz) and epidote (ep) in a sulfide-rich veinlet. (B) Chalcopyrite (cp) surrounded by fine-grained disseminated pyrite and sphalerite; quartz is present along vein boundaries. (C) Zoned sulfide texture with chalcopyrite (cp) and pyrite (py) embedded in sphalerite (sp) matrix; quartz vein (qz) crosscutting sulfides. (D) Large chalcopyrite grains with disseminated pyrite and sphalerite in a vein-parallel setting. (E) Pyrite overgrowth on earlier chalcopyrite cores, forming reaction rims within a sphalerite-rich matrix. (F) Disseminated pyrite within a sphalerite-galena-chalcopyrite assemblage, associated with quartz veins (qv); evidence of replacement and co-precipitation

Geochemical classification reveals a compositional spread dominantly within syenodioritic to quartz-dioritic fields, with additional representation of gabbroic varieties. This is evident in the TAS and R1–R2 classification schemes, which underscore a calc-alkaline lineage (Fig. 3).

The AFM ternary diagram (Fig. 4) further delineates a dual trend toward both tholeiitic and calc-alkaline magmatism, implying the influence of varying degrees of mantle melting and potential crustal assimilation during magmatic ascent. The consistency of metaluminous to weakly peraluminous signatures across the studied samples observed through alumina saturation indices corresponds with typical subduction-related intrusives. Such values point to source magmas derived from an enriched lithosphe-ric mantle wedge, occasionally modified by recycled crustal inputs (Maniar and Piccoli, 1989; Barbarin, 1999).

The trace element distribution patterns show significant deviation from mid-ocean ridge or within-plate settings (Fig. 5). HFSE depletions (notably Nb, Ta, Ti) coupled with LILE enrichments (Cs, Rb, Ba) form a geochemical fingerprint characteristic of arc magmas, where slab-derived fluids contribute incompatible elements to the mantle source (Sun, McDonough, 1989).

The clear negative Nb–Ta anomalies support the hypothesis of a subducting slab's involvement, consistent with models of fluid-mobile element transport during subduction metasomatism (Pearce and Peate, 1995). This interpretation is reinforced by tectonomagmatic discrimination diagrams (Fig. 6) Ti–V, Ti–Zr, and Ti–Zr–Sr plots consistently position the samples within fields associated with island arc tholeiites and calc-alkaline basalts. The concentration of data in these fields underscores a magmatic origin rooted in arc-related tectonics, consistent with the geodynamic evolution of the Lesser Caucasus region during the Late Cretaceous (Adamia et al., 2010).

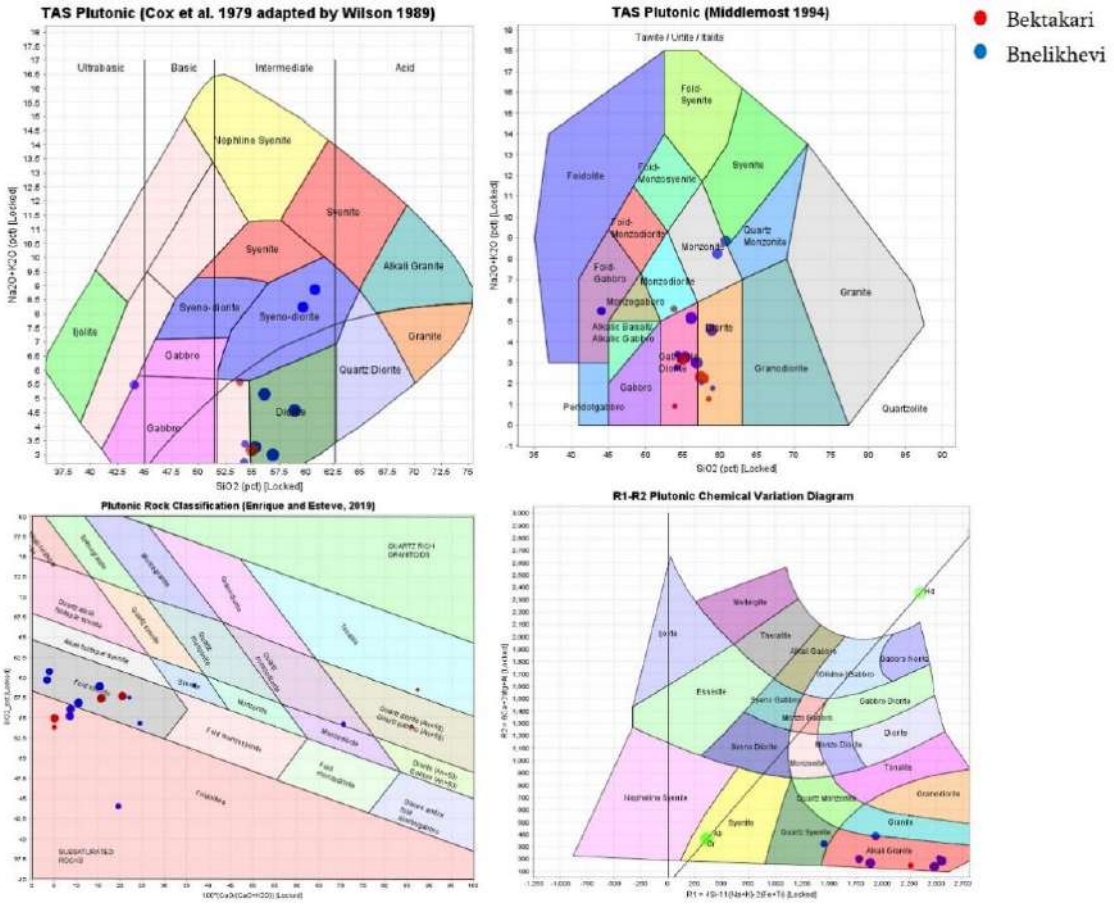

Fig. 3. Geochemical classification diagrams of intrusive rocks from the Bektakari–Bnelikhevi region. (Top left) Total Alkali–Silica (TAS) diagram after Cox et al. (1979) as modified by Wilson (1989), showing that most samples plot in the syeno-diorite to quartz diorite fields, consistent with intermediate plutonic compositions. (Top right) TAS classification scheme from Middlemost (1994), confirming the calc-alkaline nature of the samples and their distribution across quartz diorite, monzodiorite, and gabbro fields. (Bottom left) multi-parameter plutonic rock classification diagram integrating CaO–Na_2O–K_2O ratios and silica content, indicating a dominant cluster in the metaluminous, arc-related field. (Bottom right) R1–R2 classification diagram after De la Roche et al. (1980), further constraining the samples within the monzonitic to dioritic compositional range

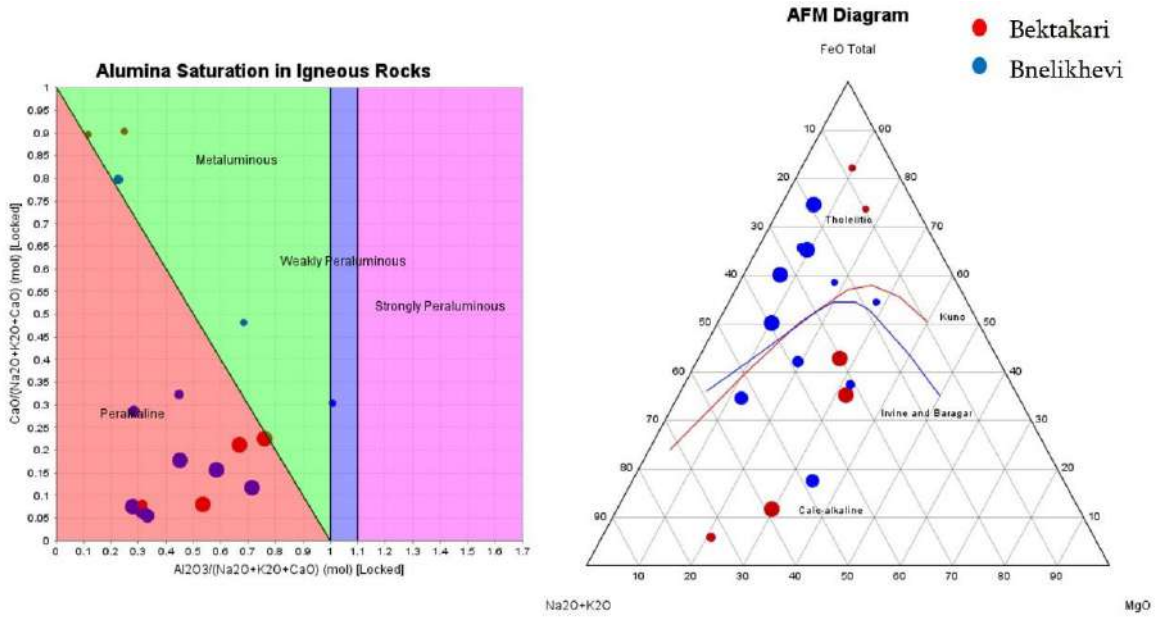

Fig. 4. Geochemical indicators of magmatic affinity and alumina saturation in intrusive rocks from the Bektakari–Bnelikhevi region. (Left) Alumina Saturation Index (ASI) diagram after Maniar and Piccoli (1989), plotting molar $Al_2O_3/(Na_2O + K_2O + CaO)$ versus $CaO/(Na_2O + K_2O + CaO)$, shows that the samples are predominantly metaluminous to weakly peraluminous, with minor peralkaline signatures. These characteristics are typical of arc-related calc-alkaline intrusions and suggest magma generation from a hydrated mantle wedge, variably influenced by crustal assimilation. (Right) AFM (FeO^*–MgO–$(Na_2O + K_2O)$) ternary diagram modified after Irvine and Baragar (1971), indicating dual magmatic trends spanning both tholeiitic and calc-alkaline fields. This suggests varying degrees of partial melting and magmatic differentiation, consistent with subduction-modified arc environments.

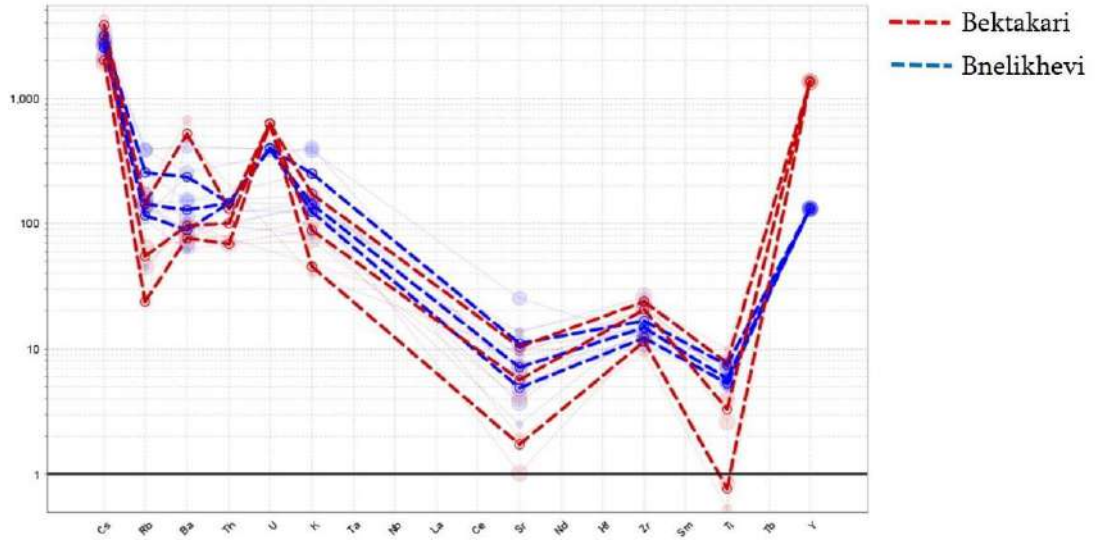

Fig. 5. Primitive mantle-normalised multi-element spider diagram of representative intrusive samples from the Bektakari–Bnelikhevi ore knot**,** showing trace element patterns for Bektakari (red dashed lines) and Bnelikhevi (blue dashed lines). Normalisation values are after Taylor and McLennan (1985)

The integration of mineralogical textural relationships and geochemical data suggests that mineralisation was genetically linked to the magmatic evolution of the host intrusions. The observed replacement textures and sulfide zoning are indicative of dynamic ore-forming processes driven by volatile exsolution and fluid phase separation from crystallising melts. These processes are typical of porphyry-style systems where magmatic fluids ascend and precipitate metals in structurally favorable zones (Richards, 2003). Notably, the temporal overlap between intrusive emplacement and ore mineral precipitation supports a synchronous magmatic-hydrothermal system. The presence of high-temperature minerals (pyrite, chalcopyrite) alongside secondary alteration products implies a downward temperature gradient, compatible with late-stage fluid evolution in an open hydrothermal system.

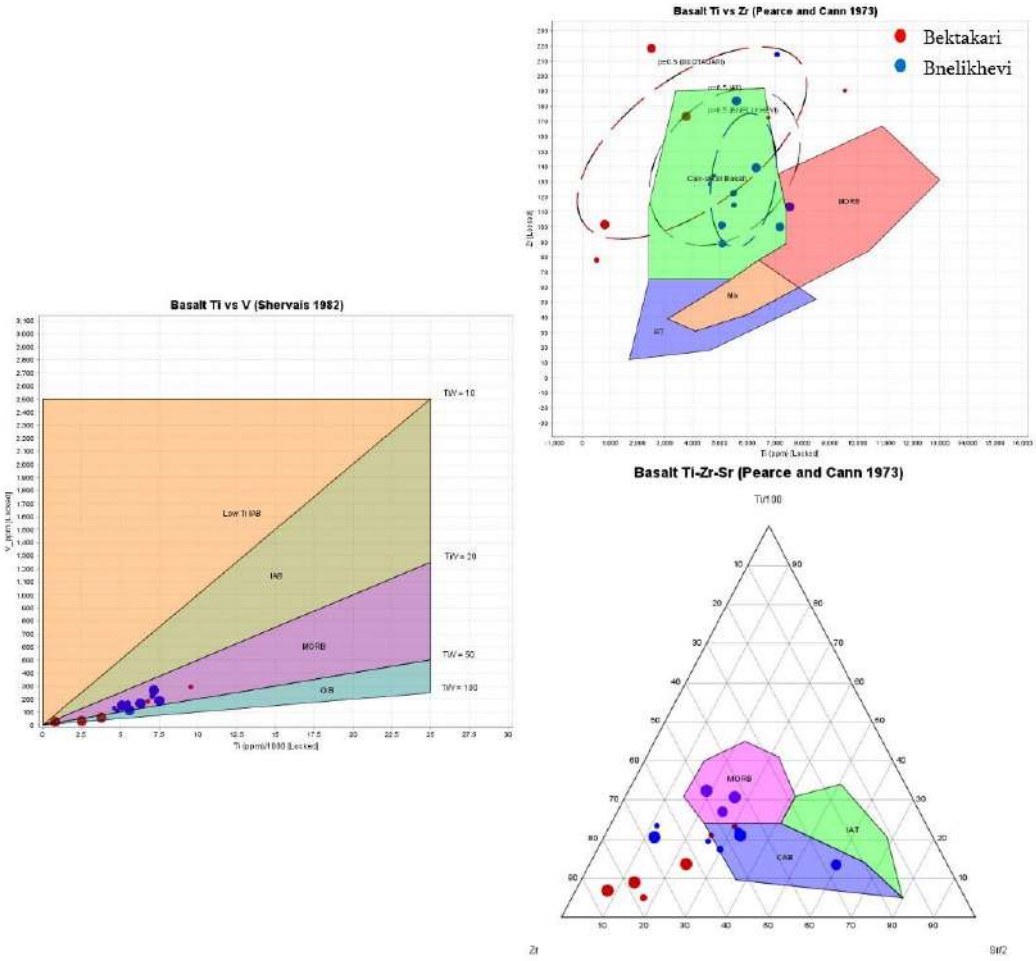

Fig. 6. Tectonic discrimination diagrams on intrusive and subvolcanic rocks from the Bektakari–Bnelikhevi region. (Top right) Ti vs Zr plot (Pearce and Cann, 1973) shows that most samples plot within the calc-alkaline basalt (CAB) and island arc tholeiite (IAT) fields, suggesting derivation from a subduction-modified mantle source typical of volcanic arc settings. (Top left) Ti vs V diagram (Shervais, 1982) further supports an island arc basalt affinity with most samples falling within the IAB field and exhibiting low Ti/V ratios, characteristic of fluid-fluxed mantle wedge magmatism. (Bottom right) Ti-Zr-Sr ternary plot (Pearce and Cann, 1973) demonstrates compositional clustering within the arc-related fields (CAB, IAT), reinforcing a tectonomagmatic environment influenced by subduction zone dynamics. These results collectively indicate that the Bektakari and Bnelikhevi magmatic systems are products of arc-related geodynamic processes

Discussion

The integrated mineralographic and geochemical data from the Bektakari–Bnelikhevi intrusive complex provide a coherent framework to understand the magmatic evolution, tectonic setting, and metallogenic significance of this ore-bearing system. The magmatism of the region reflects hallmark characteristics of subduction-related processes with implications for the broader metallogenic architecture of the Lesser Caucasus, a segment of the Tethyan Metallogenic Belt.

The compositional and tectonomagmatic characteristics of the studied rocks point toward a calc-alkaline suite formed in a convergent margin setting. This is evidenced by systematic enrichment in large ion lithophile elements (LILE: Rb, Ba, K, Th) and depletion in high field-strength elements (HFSE: Nb, Ta, Ti), which are geochemical hallmarks of arc magmatism (Sun and McDonough, 1989). The negative anomalies in Nb–Ta and Ti, paired with high Th/U ratios, are indicative of slab-derived fluids influencing the mantle wedge, resulting in the generation of hydrous, oxidised, and metal-fertile melts (Macpherson et al., 2006).

The AFM and R1-R2 trends, showing coexistence of tholeiitic and calc-alkaline characteristics, reflect a magmatic evolution pathway driven by varying degrees of partial melting, fractional crystallisation, and possible magma mixing. Such duality is typical in arc-front to back-arc transitions, where both fertile mantle sources and crustal assimilation exert control on magma chemistry (Dilek and Altunkaynak, 2009). The metaluminous to weakly peraluminous nature of the intrusive bodies, as suggested by the ASI plot, also aligns with arc-type granitoid series (Barbarin, 1999).

The mineral associations observed, primarily pyrite, chalcopyrite, sphalerite, and galena, display clear evidence of multiple hydrothermal pulses. Textural features such as replacement rims, intergrowths, and fine-grained dissemination indicate dynamic redox conditions during mineral deposition. These textures are consistent with

ore-forming systems where metal precipitation occurs via sulfidation, boiling, and fluid mixing (Hedenquist and Lowenstern, 1994; Sillitoe, 2010).

Moreover, the close spatial and temporal relationship between the intrusive host rocks and mineralisation, as evidenced by replacement textures and ore distribution, suggests a genetic link to synmagmatic fluid release. This model aligns with globally recognised porphyry and epithermal systems, where metal transport and deposition are primarily driven by magmatic-hydrothermal fluids exsolved during magma crystallisation (Richards, 2003). The observed mineralogical zoning, from chalcopyrite-rich to sphalerite- and galena-dominated zones, likely reflects cooling gradients and progressive fluid-rock interaction.

The geochemical and mineralogical characteristics of the Bektakari–Bnelikhevi system are in strong agreement with other ore-bearing magmatic complexes within the Lesser Caucasus and East Anatolian Accretionary Complex. This region has been shaped by the long-lived subduction of the Neotethyan oceanic lithosphere and subsequent collisional events during the Late Cretaceous to Cenozoic (Adamia et al., 2010). Similar geodynamic processes are known to control porphyry and epithermal Cu-Au-Mo mineralisation throughout the Tethyan Belt, including in the Zangezur (Armenia), Çöpler (Turkey), and Bor-Madjanpek (Serbia) districts (Janković, 1997).

The tectonic discrimination diagrams (Ti–V, Ti–Zr–Sr) firmly place the Bektakari–Bnelikhevi rocks within the arc-related field, further supporting the regional-scale subduction imprint. The metallogenic evolution of this region thus reflects a classic model of arc magmatism, fluid-melt separation, and ore formation in an active continental margin, with Bektakari–Bnelikhevi representing a prospective segment within this system.

The identified mineral assemblages, fluid evolution textures, and magmatic geochemistry point to a metallogenically fertile magmatic system capable of concentrating Cu–Pb–Zn–Au metals. Given the compositional similarity to arc-related porphyry systems and the presence of ore-controlling structures, the Bektakari–Bnelikhevi zone holds significant potential for porphyry and epithermal-style mineralisation.

The identification of calc-alkaline, hydrous, and oxidised intrusions favorable for metal transport and precipitation supports exploration models that prioritise intrusive centers associated with LILE-enriched, HFSE-depleted geochemical signatures. Furthermore, the vertical mineralogical zoning observed suggests differences in mineralisation processes, where early magmatic-hydrothermal mineralisation is overprinted by lower-temperature, fluid-dominated alteration phases.

Conclusion

The Bektakari–Bnelikhevi intrusive system emerges from this study not simply as a site of mineral accumulation but as a complex and evolving geochemical environment, where magmatic and hydrothermal processes are intricately interwoven with the structural architecture of the upper crust. The system reveals internal coherence in its magmatic chemistry and external variability in its ore mineralogy, suggesting that metal deposition was governed less by single-event fluid pulses and more by protracted geodynamic conditions that preserved thermal and compositional gradients over time. This complexity does not imply chaos, but rather a subtle equilibrium between melt evolution, volatile segregation, and permeability structure, each contributing to metallogenic expression of the system.

While the available data shed light on the spatial and compositional patterns of the intrusive bodies and their associated mineralisation, they also underscore the limitations of a solely petrochemical and mineralographic perspective. The absence of temporal constraints inhibits a precise reconstruction of the mineralisation chronology. Moreover, the lack of direct fluid composition data leaves opens the question of the origin, temperature, and redox state of the hydrothermal solutions responsible for metal transport and deposition. These unresolved dimensions prevent full integration of the Bektakari–Bnelikhevi system into regional metallogenic models, particularly those concerning the diachronic evolution of arc-related porphyry systems in the Lesser Caucasus. To address these gaps, future investigations should move beyond static observations and embrace temporally and chemically resolved methods. Isotopic analyses of rocks and minerals would clarify the sources of magmas and fluids, while micro thermometric and stable isotope techniques could refine the conditions of ore precipitation. Establishing the timing of intrusive phases and mineralisation events would critically strengthen genetic interpretations and may even reveal episodic metal enrichment related to tectonic pulses. Additionally, integrating geophysical models with structural mapping and drill core analysis could illuminate the deeper architecture of the magmatic plumbing system, enhancing our understanding of how fluids migrated, pooled, and mineralised.

Acknowledgment

The authors express their sincere gratitude to Rich Metals Group (RMG) for providing access to geological and geochemical data, which served as a foundational resource for the completion of this research. The authors also acknowledge Caucasian Mining Group (CMG) for geological mapping materials and the geological map of the Bolnisi ore district used in this study.

REFERENCES

Adamia Sh, Bukia A, Zakaraia D, Zakariadze G, Migineishvili R, Sadradze N, Gavtadze T, Shavishvili I, Chkhotua T (2020) Geological map of the Bolnisi ore district (scale 1:50,000) and explanatory note. Caucasian Mining Group (CMG), Tbilisi

Adamia S, Chabukiani A, Zakariadze G and Sadradze N (2010) Geodynamic evolution of the Eastern Black Sea–Transcaucasus region. In: Sosson M, Kaymakci N, Stephenson RA, Bergerat F, Starostenko VI (eds) Sedimentary basin tectonics from the Black Sea and Caucasus to the Arabian Platform. Geological Society, London, Special Publications 340:261–280. https://doi.org/10.1144/SP340.12

Barbarin B (1999) A review of the relationships between granitoid types, their origins and their geodynamic environments. Lithos 46(3):605–626. https://doi.org/10.1016/S0024-4937(98)00085-1

Craig JR and Vaughan DJ (2nd ed) (1994) Ore microscopy and ore petrography. Wiley, New York, p 434

Cox KG, Bell JD, Pankhurst RJ (1979). The interpretation of igneous rocks. George Allen and Unwin, London, p 459

De la Roche H, Leterrier J, Grandclaude P, Marchal M (1980) A classification of volcanic and plutonic rocks using R1-R2 diagrams and major element analyses. Chemical Geology 29(1–4):183–210. https://doi.org/10.1016/0009-2541(80)90020-0

Dilek Y and Altunkaynak S (2009) Geochemical and temporal evolution of Cenozoic magmatism in western Turkey: mantle response to collision, slab break-off, and lithospheric tearing in an orogenic belt. Geological Society, London, Special Publications 311:213–233. https://doi.org/10.1144/SP311.8

Enrique P and Esteve S (2019) Comparative study of the classification of plutonic and volcanic rocks using the normative Q′(F′)-ANOR and chemical SiO_2–100CaO/(CaO+K_2O) diagrams. Geogaceta 66: 95–98

Hedenquist JW and Lowenstern JB (1994) The role of magmas in the formation of hydrothermal ore deposits. Nature 370(6490):519–527. https://doi.org/10.1038/370519a0

Irvine TN and Baragar WRA (1971) A guide to the chemical classification of the common volcanic rocks. Canadian Journal of Earth Sciences 8(5):523–548. https://doi.org/10.1139/e71-055

Janoušek V, Farrow CM, Erban V (2006) Interpretation of whole-rock geochemical data in igneous geochemistry: Introducing Geochemical Data Toolkit (GCDkit). Journal of Petrology 47(6):1255–1259. https://doi.org/10.1093/petrology/egl013

Janković S (1997) The Carpatho–Balkanides and adjacent areas: A sector of the Tethyan Eurasian metallogenic belt. Mineralium Deposita 32(5):426–433. https://doi.org/10.1007/s001260050110

Macpherson CG, Dreher ST, Thirlwall MF (2006) Adakites without slab melting: High pressure differentiation of island arc magma, Mindanao, Philippines. Earth and Planetary Science Letters 243(3–4):581–593. https://doi.org/10.1016/j.epsl.2005.12.034

Maniar PD and Piccoli PM (1989) Tectonic discrimination of granitoids. Geological Society of America Bulletin 101(5):635–643. https://doi.org/10.1130/0016-7606(1989)101<0635:TDOG>2.3.CO;2

Middlemost EAK (1994) Naming materials in the magma/igneous rock system. Earth-Science Reviews 37(3–4):215–224. https://doi.org/10.1016/0012-8252(94)90029-9

Mindiashvili G, Bluashvili D, Iobidze G et al (2024a) Application of machine learning to hydrothermal system analysis: geochemical insights from the Bektakari–Bneli Khevi Ore Knot, Southern Georgia. Bulletin of the Mineral Research and Exploration (Bull Min Res Exp). https://doi.org/10.19111.bulletinofmre.1768420

Mindiashvili G, Iobidze G, Lipartia T et al (2024b) Identification of the data obtained by the remote sensing method within the Bektakari–Bnelikhevi Ore Knot. Mining Journal 1(47):48–62. https://doi.org/10.36073/1512-407X/2024-48-62

Pearce JA and Cann JR (1973) Tectonic setting of basic volcanic rocks determined using trace element analyses. Earth and Planetary Science Letters 19(2):290–300. https://doi.org/10.1016/0012-821X(73)90129-5

Pearce JA and Peate DW (1995) Tectonic implications of the composition of volcanic arc magmas. Annual Review of Earth and Planetary Sciences 23(1):251–285. https://doi.org/10.1146/annurev.ea.23.050195.001343

Richards JP (2003) Tectono-magmatic precursors for porphyry Cu-(Mo-Au) deposit formation. Economic Geology 98(8):1515–1533. https://doi.org/10.2113/gsecongeo.98.8.1515

Shervais JW (1982) Ti–V plots and the petrogenesis of modern and ophiolitic lavas. Earth and Planetary Science Letters 59(1):101–118. https://doi.org/10.1016/0012-821X(82)90120-0

Sillitoe RH (2010) Porphyry copper systems. Economic Geology 105(1):3–41. https://doi.org/10.2113/gsecongeo.105.1.3

Sun SS and McDonough WF (1989) Chemical and isotopic systematics of oceanic basalts: Implications for mantle composition and processes. In: Saunders AD, Norry MJ (Eds) Magmatism in the Ocean Basins Geological Society, London, Special Publications 42:313–345. https://doi.org/10.1144/GSL.SP.1989.042.01.19

Taylor SR and McLennan SM (1985) The continental crust: its composition and evolution. Blackwell, Oxford, p 312

Wilson M (1989) Igneous petrogenesis: A global tectonic approach. Springer, Dordrecht. https://doi.org/10.1007/978-1-4020-6788-4

МАГМАТОГЕННО-ГИДРОТЕРМАЛЬНАЯ ЭВОЛЮЦИЯ И РУДНЫЙ ПОТЕНЦИАЛ КОМПЛЕКСА БЕКТАКАРИ-БНЕЛИХЕВИ, БОЛНИССКИЙ РУДНЫЙ РАЙОН, МАЛЫЙ КАВКАЗ

Миндиашвили Г.[1]*, Блуашвили Д.[2], Липартия Т.[2], Иобидзе Г.[2], Макадзе М.[1], Джафаридзе Н.[2], Бенашвили К.[2], Хецуриани Г.[2], Блуашвили В.[2]

[1]Тбилисский государственный университет имени Иване Джавахишвили, Грузия
0179, Тбилиси, просп. Илии Чавчавадзе,1
[2]Грузинский технический университет, Грузия
0175, Тбилиси, ул. Костава, 77
**Автор, отвечающий за переписку: giorgim1994@gmail.com*

Резюме. В данной работе рассматриваются петрологические, геохимические и геодинамические особенности интрузивных и субвулканических пород рудного узла Бектакари–Бнелихеви, расположенного в южной части Малого Кавказа. Исследование основано на детальном минераграфическом анализе 17 образцов горных пород, отобранных из 8 буровых скважин, а также на данных валового химического состава, полученных методом рентгенофлуоресцентной спектрометрии (XRF). Комплексное использование минераграфических наблюдений и геохимических данных позволило выявить особен-

ности магматической эволюции интрузивных тел и связанных с ними процессов гидротермальной минерализации. Интрузивные породы характеризуются значительным текстурно-композиционным разнообразием и формируют кальциево-щелочную магматическую серию, связанную с субдукционно-модифицированным мантийным источником и взаимодействием мантийных расплавов с континентальной корой. Геохимические дискриминационные диаграммы демонстрируют обогащение крупноионными литофильными элементами (LILE) и обеднение высокозарядными элементами (HFSE), что характерно для магматических систем, формирующихся в условиях конвергентных окраин и островных дуг. Минералогические и текстурные особенности сульфидной минерализации, представленной пиритом, халькопиритом, сфалеритом и галенитом, свидетельствуют о многостадийной гидротермальной активности, тесно связанной с процессами кристаллизации магмы и последующей циркуляцией рудоносных флюидов. Установленные текстуры замещения и зональности минералов отражают динамические изменения физико-химических параметров рудоотложения. Полученные результаты подтверждают существование длительно функционировавшей магмато-гидротермальной системы, контролируемой структурными и термическими факторами. Рудный узел Бектакари–Бнелихеви рассматривается как перспективный участок в пределах тетисского металлогенического пояса и в контексте дуговых рудообразующих систем Малого Кавказа, что подчеркивает его металлогенический потенциал и значение для дальнейших геологоразведочных исследований.

Ключевые слова: *гидротермальное изменение, геохимия, минерализация, магматизм*

BEKTAKARİ-BNELIHEVİ KOMPLEKSİNİN MAQMATOGEN-HİDROTERMAL TƏKAMÜLÜ VƏ FİLİZ POTENSİALI, BOLNİSİ FİLİZ RAYONU, KİÇİK QAFQAZ

Mindiaşvili G.[1]*, Bluaşvili D.[2], Lipartiya T.[2], İobidze G.[2], Makadze M.[1], Cəfəridze N.[2], Benaşvili K.[2], Xetsuriani G.[2], Bluaşvili V.[2]

[1]İvane Cavaxişvili adına Tbilisi Dövlət Universiteti, Gürcüstan
0179, Tbilisi, İliya Çavçavadze prospekti, 1
[2]Gürcüstan Texniki Universiteti, Gürcüstan
0175, Tbilisi, Kostava küç., 77
**Yazışmalara məsul: giorgim1994@gmail.com*

Xülasə. Təqdim olunan məqalədə Kiçik Qafqazın cənub hissəsində yerləşən Bektakari–Bnelihevi filiz düyününün intruziv və subvulkanik süxurlarının petroloji, geokimyəvi və geodinamik xüsusiyyətləri araşdırılmışdır. Tədqiqat 8 qazma quyusundan götürülmüş 17 süxur nümunəsinin mineraloqrafik təhlili və rentgen-flüoresans spektrometriyası (XRF) vasitəsilə əldə edilmiş ümumi kimyəvi məlumatlarına əsaslanır. Mineraloqrafik müşahidələr və geokimyəvi analizlərin birgə tətbiqi intruziv süxurların maqmatik təkamül xüsusiyyətlərini və onlarla əlaqəli hidrotermal minerallaşma proseslərini daha dəqiq müəyyən etməyə imkan vermişdir. İntruziv süxurlar tekstur və tərkib baxımından müxtəliflıyi etdirir və subduksiya ilə modifikasiya olunmuş mantiya mənbəyi ilə əlaqəli kalsium-qələvi maqmatik sıra əmələ gətirir. Geokimyəvi diskriminasiya diaqramları iri ionlu litofil elementlərin (LILE) zənginləşməsini və yüksək yüklü sahə güclü elementlərin (HFSE) azalmasını nümayiş etdirir ki, bu da konvergent kənar və qövs tipli maqmatik mühit üçün səciyyəvidir. Pirit, xalkopirit, sfalerit və qalenitdən ibarət sulfid minerallaşmasının tekstur və paragenetik xüsusiyyətləri çoxmərhələli hidrotermal fəaliyyətin mövcudluğunu göstərir və maqmatik təkamüllə sıx bağlıdır. Əvəzlənmə teksturaları və mineral zonallığı filizəmələgəlmə proseslərinin fiziki-kimyəvi şəraitinin zamanla dəyişdiyini göstərir. Alınmış nəticələr uzunmüddətli fəaliyyət göstərmiş maqmatik-hidrotermal sistemin mövcudluğunu və onun struktur, tektonik və istilik amilləri ilə idarə olunduğunu təsdiqləyir. Bektakari–Bnelihevi filiz düyünü Tethys metallogenik qurşağı və Kiçik Qafqazın qövs tipli filiz sistemləri çərçivəsində perspektivli sahə kimi qiymətləndirilir və regionun metallogenik potensialının öyrənilməsi baxımından mühüm əhəmiyyət kəsb edir.

Açar sözlər: *hidrotermal dəyişiklik, geokimya, minerallaşma, maqmatizm*

ANAS Transactions Earth Sciences 1 / 2026

http://www.journalesgia.com

FEATURES OF HEAVY METAL MIGRATION IN TECHNOGENIC ZONES OF THE ABSHERON PENINSULA

Aliyev Ch.S.[1], Kazimova L.A.[2]*

[1]Ministry of Science and Education of the Republic of Azerbaijan,
Institute of Geology and Geophysics, Azerbaijan
119, H.Javid ave., Baku, AZ1143
[2]Department of Industrial Safety and Labor Protection,
Azerbaijan State Oil and Industry University, Azerbaijan
34, Azadlig ave., Baku, AZ1010
**Corresponding author: Latifa.ismaylova@gmail.com*

Keywords: *soil samples, technophilicity, Clarke values, geochemical characteristics, migration*

Summary. One of the principal indicators characterising the intensity of extraction and utilisation of chemical elements is technophilicity, defined as the ratio between the annual extraction or production of an element (tons per year) and its Clarke concentration in the lithosphere. Numerous chemically analogous elements, despite substantial differences in both Clarke values and production volumes, demonstrate similar or comparable degrees of technophilicity. Technophilicity is a highly dynamic parameter that evolves in response to anthropogenic activity. For example, the continuous increase in oil and gas extraction has contributed to the progressive growth of carbon technophilicity. Likewise, the large-scale production of phosphate fertilizers, dolomite, and magnesite has led to a marked increase in the technophilicity of phosphorus and magnesium. The present study involved comprehensive multi-aspect investigations aimed at assessing the distribution patterns of heavy metals across different environmental media. The Absheron Peninsula was selected as the study area, and numerous samples were collected from various oil-contaminated sites throughout the region. The results obtained from the field investigations and subsequent laboratory analyses revealed the accumulation of a wide spectrum of heavy metals in the soils, including Pb, As, Cr, Cu, Zn, Se, Al, Fe, and Mn. Significant correlations identified between soil pH, organic matter content, and the exchangeable and reducible fractions of most heavy metals indicate that the migration behaviour and mobility patterns of these elements can be reliably predicted in advance.

1. Introduction

The Absheron Peninsula, located in the southwestern part of the Caspian Sea, is characterised by its unique geological and geomorphological structure as well as its complex landscape differentiation features. The formation of the relief of the peninsula has been primarily influenced by complex tectonic processes, its geographical position, and volcanic activity.

The earliest geological data concerning the southeastern slope of the Greater Caucasus within the Azerbaijani territory (up to 1917) was obtained by V.H.Abikh, K.I.Bogdanovich and S.Simonovich's studies. Subsequent investigations conducted between 1917 and 1956 by K.N.Paffenholz, D.V.Drobyshev, V.V.Weber, A.N.Solovkin, A.Ch.Sultanov, M.M.Aliyev, I.V.Mushketov, N.S.Shatsky, V.Y.Khain, A.Ahmadov, F.Sh.Shikhaliyev, I.Valiyev, H.Hasanov, A.Alizadeh, I.Guliyev and H.Aliyev further enriched the geological understanding of the region.

Based on the findings and references from these researchers, it can be stated that the area is predominantly composed of Tertiary (Neogene) and Quaternary (Anthropogenic) deposits.

Study Area. The lithological composition of the rocks within the Absheron Peninsula primarily consists of carbonate-terrigenous, clayey, and argillaceous flysch formations; coarse-grained continental marine formations; sandy-clayey formations; sandy-shale subformations; fine-grained molasse formations; folded continental marine red formations; sandy clays; limestones; clayey-gravel and pebble deposits; silts and clays; clayey-sandy mixtures; shell-bearing sands (including dune sands); and breccias of mud volcanoes (Aliyev, 1978; Milanovsky, Khain, 1963).

According to M.V.Abramovich, M.M.Aliyev and V.Y.Khain (1952), it is appropriate to distinguish eight geomorphological regions within the territory of the Greater Caucasus: the Main Caucasus Range encompassing the high mountainous zone; the southwestern part of the Main Caucasus Range; the southern slope of the Greater Caucasus; the southeastern termination of the Greater Caucasus (including the Shahdagh zone, Dubrar, Western Absheron–Gobustan, and Eastern Absheron); the piedmont Neogene zone; the Alazani–Ayrichay valley; the Qusar inclined plain; and the Caspian coastal lowlands (Abramovich et al., 1952).

It should be noted that the Absheron Peninsula represents a continuation of the folded structures of the Greater Caucasus extending southeastward. Due to the region's exposure to active tectonic movements during various geological periods, numerous anticlinal uplifts and fault lines are present across the territory.

Based on the conducted studies, it can be stated that the Gobustan and western Absheron areas are underlain by the Cretaceous deposits belonging to the southeastern termination of the Greater Caucasus. Within the Absheron Peninsula, the eastern part is conventionally separated by the Fatmai–Zigh anticlinal structure (Milanovsky, Khain, 1963). It is known that the northern part of the peninsula is characterised by a complex tectonic framework. One of the main reasons for this structural complexity is that the anticlinal uplifts are primarily composed of the Upper Cretaceous deposits, while the younger Paleogene sediments of the Tertiary period overlie the synclinal zones.

It is also well established that Absheron is one of the regions with the highest density of mud volcanoes in the world. The cones and craters formed by their eruptions shape the peninsula's unique geomorphological landscape and contribute to the complex migration patterns of geochemical elements within its terrestrial environments.

The gravimagnetic field of the Absheron Peninsula is characterised by negative anomalies. Deeper minima are mainly observed in the marine areas located to the northeast and southeast of the peninsula. On land, a broad regional minimum is partially manifested in the eastern part of the peninsula within the area of the Kel fold. From this zone, the anticlinal structure rises toward the south, southwest, and west extending to the southern and southeastern "slopes" of the Dibrar gravitational maximum, which corresponds to the axial part of the southeastern termination of the Greater Caucasus. This constitutes the main regional principle of the gravity field. The field is complicated by a number of local anomalies whose number, complexity, and intensity increase westward, which is associated with both the intensification of tectonic complexity and the proximity of denser deep-seated rocks to the surface.

The primary objective of this study is to identify the transformation processes occurring in technogenic landscapes under natural and anthropogenic geochemical anomalies within the Absheron Peninsula – an area characterised by complex geological and geomorphological conditions. The study also aims to determine the migration and accumulation patterns of pollutants that drive landscape transformations in such technogenic environments.

2. Research methods

The present study is based on the analysis of research materials collected over a period of 10 – 20 years. Comparative analyses were carried out using data and findings from previous investigations conducted by researchers such as B.A.Budagov, A.H.Ahmadov, Q.I.Rustamov, A.I.Gahramanov, E.K.Alizadeh, E.C.Karimova, and others. In selecting appropriate geochemical analytical methods and approaches, we relied on the scientific works of prominent scholars including B.B.Polynov, A.I.Perelman, M.A.Glazovskaya, V.V.Alekseyenko, S.G.Batulin, E.N.Borisenko, Y.Y.Sayet, M.A.Ivanova, B.F.Mitskevich, L.N.Shevchenko, A.N.Gulahmadov and B.G.Shakuri. In addition to these classical sources, contemporary international research has also been thoroughly examined, including B.J.Alloway, M.K.Andersen, K.I.Raulund-Rasmussen, B.W.Strobel, D.L.Sparks, A.O.Splodytel, H.Alphan and other's works.

Considering the significant scientific and practical importance of studying the geochemical characteristics of landscapes contaminated by oil extraction activities in the traditional oil-producing region of the Absheron Peninsula, particular attention in this research was devoted to the eco-geochemical investigation of the most polluted areas – specifically the Balakhani, Sabunchu, and Ramana sites.

The landscapes of these territories are mainly characterised by sandy-gray and sandy gray-brown soils formed under *Artemisia-Alhagi* (wormwood–camelthorn) and *Artemisia*-ephemeral vegetation types.

The first stage of this research involved the collection of more than 130 samples of various origins from different sites, including rock specimens, followed by the determination of their geochemical composition. During soil sampling, factors such as weather conditions and sampling time (preferably morning hours) were taken into consideration. Pits with a depth of 100 cm were excavated, and samples were collected at 10 cm intervals along the soil profile. Sampling along the vertical soil profile is essen-

tial for assessing the penetration depth and migration patterns of chemical elements.

After collection, the soil samples were air-dried and prepared for subsequent laboratory analyses. Geochemical analyses were conducted using advanced analytical instruments, including an X-ray fluorescence spectrometer (RFA, S8 Tiger), an X-ray diffractometer, and an inductively coupled plasma mass spectrometer (ICP-MS 7700e), along with other complementary laboratory equipment (Aliyev, Kazimova, 2024).

According to the results of spectral analyses, the carbonate–terrigenous, clayey, and argillaceous flysch formations of the area are enriched in B, Mo, Cu, Mn, Zn, and V. The coarse-grained continental–marine formations contain elevated concentrations of Mo, As, Mn, Co, V and Ag; the sandy clays are enriched in B, Ni, Mo, Co, Ag and As; while the limestones, clay–gravel mixtures, silts, and clays are rich in B, Mo, Cu, Sn, Zn, V, Pb, Ni and Cr.

It is well known that landscapes and their components are formed on the Earth's surface, and therefore, when determining and comparing the concentrations of elements distributed within landscapes, it is appropriate to employ *Clarke values* as reference baselines (Yaroshevsky, 2006).

Table 1 presents the concentration coefficients (Clarke ratios) obtained by comparing the concentrations of chemical elements identified in rock samples collected from various locations across the Absheron Peninsula with the average abundances of those elements in the Earth's crust.

Based on the results presented in the table, the chemical elements contained within these rocks can be classified into three groups.

The **first group** includes elements such as Sr, Ba, F, and Ag, whose average concentrations approximately correspond to their respective Clarke values. If the mean contents of these elements reflect the typical geochemical characteristics of equivalent rock types in the Earth's crust, then the elements belonging to the other two groups represent specific geochemical features unique to the rocks of the Absheron Peninsula.

The **second group** comprises elements whose average concentrations in the studied rocks are significantly higher than the Clarke values (enrichment coefficient, KK>1K_K > 1KK>1). These include Sc (KK=151–322K_K = 151–322KK =151–322), Ca (KK=5.0–8.3K_K = 5.0–8.3KK =5.0–8.3), and Cl (KK=95.6–708.2K_K = 95.6–708.2KK=95.6–708.2).

The **third group** consists of microelements whose concentrations in the rocks are lower than the Clarke values (KK<1K_K < 1KK<1), such as Mn (KK=0.1–0.3K_K = 0.1–0.3KK=0.1–0.3), Fe (KK=0.1–0.2K_K = 0.1–0.2KK=0.1–0.2), V (KK=0.1–0.2K_K = 0.1–0.2KK=0.1–0.2) and Zr (KK=0.1–0.2K_K = 0.1–0.2KK=0.1–0.2) among others.

The composition of the rocks forming the lithological foundation of landscapes is also reflected in the composition of other landscape components (soils, waters, and vegetation) within the studied area.

The pronounced differentiation of the natural background levels of heavy metals complicates the development of strict threshold criteria for their concentrations in landscapes. For example, in acidic and alkaline soils, the MPCs of cadmium and lead may differ by nearly an order of magnitude. Therefore, MPCs must be established for major soil–geochemical regions and for geochemical soil associations with similar acid–alkaline and redox conditions, which exhibit comparable levels of resistance to pollutants (Yao et al., 2025). As an approximate reference indicator, the Clarke values of elements in the lithosphere and soils can be used (Ahnstrom, Parker, 2001; Khalid et al., 2017; Rustamov, Ismaylova, 2022)

3. Results and analysis

Landscape-Geochemical Analysis of the Study Area and Patterns of Pollutant (Heavy Metal) Accumulation

The relief of the Absheron Peninsula and the degree of its dissection create favorable conditions for the high chemical activity of waters and for an intensive water exchange between both soil-forming and underlying bedrock layers. As a result, the water, soil, and vegetation of the area–indeed, all components of the landscape–become enriched with chemical elements characteristic of the region. Therefore, the composition and concentration of chemical elements within the landscape components of the study area largely depend on the composition of the parent rocks (Abramovich et al., 1952).

It is essential to consider the physico-chemical parameters of the soil along the humus horizon while conducting a landscape-geochemical analysis. Parameters such as pH, humus content, and moisture should be analysed (Avessalomova, Ivanov, 2019).

Spectral analyses revealed the presence of a number of microelements in the sandy gray and sandy gray-brown soils of the study area. The analysis of the concentration clark values for these microelements (as exemplified in Table 7 on the Balakhani area) indicates a notable accumulation of chlorine, boron, molybdenum, lead, cadmium, indium, bromine, antimony, palladium, silver and tin. Among these, several elements—particularly chlorine, cadmium, indium, palladium, and antimony—stand out for their especially high concentration clark values (Aliyev, Kazimova, 2024).

Table 1

Microelement composition of rock samples collected from the territories of the Absheron Peninsula
A–107 Balakhani. Oil-contaminated area

No.	Elements		Average content, %		Clarke concentration
	Atomic number	Chemical symbol	In the composition of the rock	Clarke value in the Earth's crust	
1	20	Ca	21.36	2.96	7.2
	21	Sc	0.26	0.001	260
	25	Mn	0.0087	0.1	0.087
	26	Fe	0.21	4.65	0.04
	33	As	0.0012	0.00017	7.06
	35	Br	0.00045	0.00021	2.14
	37	Rb	0.00034	0.015	0.02
	38	Sr	0.08	0.034	2.35
	39	Y	0.00023	0.0029	0.079
	40	Zr	0.0033	0.017	0.19
	47	Ag	0.00064	0.000007	91.43
	20	Ca	9.67	2.96	3.266
	25	Mn	0.015	0.1	0.15
	26	Fe	0.62	4.65	0.612
	33	As	000075	0.0017	0.44
	37	Rb	0.00082	0.015	0.05
	38	Sr	0.06	0.034	1.764
	39	Y	0.00024	0.0029	0.08
	40	Zr	0.0060	0.017	0.35
	49	In	0.0015	0.000025	60

Table 2

A-108, Balakhani area

No.	Elements		Average content, %		Clarke concentra-tion
	Atomic number	Chemical symbol	In the composition of the rock	Clarke value in the Earth's crust	
1	20	Ca	7.24	2.96	2.45
	25	Mn	0.0098	0.1	0.098
	26	Fe	0.51	4.65	0.11
	37	Rb	0.00083	0.015	0.05
	38	Sr	0.015	0.034	0.44
	39	Y	0.00048	0.0029	0.17
	40	Zr	0.0073	0.017	0.43

Table 3

A–109 Ramana area

№	Elements		Average content, %		Clarke concentra-tion
	Atomic number	Chemical symbol	In the composition of the rock	Clarke value in the Earth's crust	
1	20	Ca	26.97	2.96	9.11
	21	Sc	0.36	0.001	360
	25	Mn	0.01	0.1	0.1
	26	Fe	0.29	4.65	0.062
	35	Br	0.00068	0.00021	3.24
	37	Rb	0.00034	0.015	0.02
	38	Sr	0.09	0.034	2.65
	39	Y	0.00015	0.0029	0.05
	40	Zr	0.0021	0.017	0.12

Table 4

A-110 Sabunchu. Lake Area

№	Elements		Average content. %		Clarke concen-tration
	Atomic number	**Chemical symbol**	**In the composition of the rock**	**Clarke value in the Earth's crust**	
1	20	Ca	19.28	2.96	6.51
	21	Sc	0.16	0.001	160
	30	Zn	0.0031	0.0083	0.37
	33	As	0.00092	0.0017	0.54
	37	Rb	0.00054	0.015	0.036
	38	Sr	0.12	0.034	3.53
	39	Y	0.00031	0.0029	0.11
	22	Ti	0.23	0.45	0.51
	25	Mn	0.09	0.1	0.9
	26	Fe	3.25	4.65	0.7
	39	Y	0.0013	0.0029	0.45
	40	Zr	0.0049	0.017	0.29

Table 5

A–111 Lokbatan

№	Elements		Average content, %		Clarke concentration
	Atomic number	**Chemical symbol**	**Atomic number**	**Chemical symbol**	
	25	Mn	0.08	0.1	0.8
	26	Fe	0.5	4.65	0.1
	37	Rb	0.0008	0.015	0.05
	38	Sr	0.01	0.034	0.29
	39	Y	0.0004	0.0029	0.14
	40	Zr	0.002	0.017	0.12
	50	Sn	0.001	0.00025	4
	51	Sb	0.001	0.00005	20
	20	Cd	11.11	2.96	3.75
	22	Ti	0.06	0.45	0.13
	25	Mn	0.09	0.1	0.9
	37	Rb	0.002	0.015	0.13
	39	Y	0.001	0.0029	0.34
	41	Nb	0.0002	0.002	0.1
	20	Ca	2.96	2.96	6.61
	21	Sc	0.001	0.001	130
	33	As	0.0010	0.0017	0.59

Table 6

Results of chemıcal analyses of soils ın the Absheron area

Profile No.	**Depth, cm**	**pH**	**humus, %**	**Hygroscopic Moisture, %**
1	**2**	**3**	**4**	**5**
K–107 Balakhani	0–10	8.4	3.90	0.73
	10–35	9.3	5.16	1.80
	35–60	9.0	5.00	2.07
K–108 Balakhani	0–10	8.4	7.41	0.82
	10–30	9.8	2.68	2.47
	30–60	10.4	2.50	0.63
K–109 Sabunchu	0–10	8.8	3.75	1.12
	10–35	8.9	3.48	0.80
	35–70	9.2	2.57	1.02

1	2	3	4	5
K–110 Ramana	0–20	8.4	5.17	1.93
	20–40	8.8	0.25	1.69
	40–100	8.9	0	1.11
K–111 Ramana	0–10	10.5	10.85	0.69
	10–30	9.2	5.80	0.60
	30–60	9.0	1.87	1.17
	60–100	9.2	2.34	0.99
K–112 Balakhani, “Tamiz shahar”	0–10	9.0	0.87	1.17
	10–30	9.0	0.87	1.86
	30–60	9.2	2.63	2.30
K–113 Zabrat I	0–10	9.0	0.88	1.62
	10–60	9.8	6.85	1.28
	60–100	9.0	12.44	1.71
K–114 Ramana	0–10	9.8	4.64	1.46
	10–35	9.6	4.66	1.47
	35–70	9.2	11.17	1.06
K–115 Sabunchu	0–10	8.9	14.51	1.03
	10–35	8.9	5.53	0.90
	35–70	9.5	3.44	1.23
K–116 Sabunchu, Duzlu lake	0–10	9.2	5.32	0.62
	10–35	9.0	3.49	0.44
	35–70	8.6	2.96	1.34
K–117 Haci Zeynalabdin	0–10	8.1	0.25	0
	10–30	8.1	0.46	0
	30–60	8.5	0.20	0
	60–100	8.0	0.51	0
K–118 Yeni Yashma	0–10	7.8	0.27	4.45
	10–30	7.9	0.80	4.50
	30–60	7.8	0.91	4.45
K–119 Shurabad	0–10	8.3	2.11	2.71
	10–20	8.4	1.07	4.27
	20–60	8.1	0.80	4.28
K–120 Khirdalan, Bozdag, Guzdak	0–10	7.9	0.27	4.22
	10–30	7.8	0.27	5.13
	30–70	8.0	0.37	3.94
K–121 Bayanata mountain. Guzdak	0–10	7.8	0.73	2.50
	10–30	8.1	0.64	4.45
	30–60	8.0	1.0	2.86
	60–100	8.0	0.73	3.03
K–122 Sungurdag	0–10	7.8	1.95	5.07
	10–30	7.7	0.60	7.34
	30–60	8.1	0.91	7.05
K–123 Lokbatan	60–100	8.0	1.0	7.33
	0–10	8.0	3.16	2.15
	10–30	7.9	1.27	3.32
	30–60	7.7	1.11	2.95
	60–100	8.0	1.84	2.82
K–124 Garadagh	0–10	7.9	3.69	1.45
	10–30	8.2	1.58	2.70
	30–60	7.9	1.04	1.50
	60–100	8.1	0.52	2.60
K–125 Sangachal	0–10	7.5	0.89	2.53
	10–30	7.4	1.58	1.52
	30–60	7.5	4.22	1.85
	60–100	7.7	3.92	1.92

1	2	3	4	5
K–126 Shixlar	0–10	7.8	1.29	0
	10–30	8.0	3.62	0
	30–60	7.9	0.62	0
	60–100	7.7	0.93	0
K–127 Gobustan	0–10	7.4	1.03	0
	10–30	7.7	1.70	0
	30–60	7.7	0.25	1.52
	60–100	7.8	3.16	2.76
K–128 Fatmai	0–10	7.8	3.10	0
	10–30	8.1	0.93	0
	30–60	8.3	0	0
	60–100	8.2	0.10	0
K–129 Dubandi	0–10	8.0	0.62	0
	10–30	7.8	0.25	0
	30–60	7.9	0.77	0
	60–100	7.8	1.29	0
K–130 Zira	0–10	8.0	0.78	1.41
	10–30	7.8	1.08	0
	30–60	7.9	1.70	0
	60–100	7.9	2.32	0

Table 7

Microelement composition of soil samples collected from the territories of the Absheron peninsula
K-107 Balakhani. Oil-contaminated area

Elements		**Average Amount, %**		**Clarke of concen-tration**
№-si	**Chemical symbol**	**In the soil composition**	**Clarke of the Earth's crust**	
(0–10 sm)				
17	Cl	2.6699	0.017	157.05
26	Fe	0.1166	4.65	0.03
37	Rb	0.00058	0.015	0.04
38	Sr	0.00289	0.034	0.09
39	Y	0.00017	0.0029	0.06
40	Zr	0.0020	0.017	0.12
(**10–35 sm**)				
26	Fe	0.1295	4.65	0.03
37	Rb	0.00066	0.015	0.04
38	Sr	0.00317	0.034	0.009
39	Y	0.00031	0.0029	
40	Zr	0.0030	0.017	0.10
(35–60 sm)				
26	Fe	0.1747	4.65	0.03
7	Rb	0.00068	0.015	0.04
38	Sr	0.0037	0.034	0.11
39	Y	0.00029	0.0029	0.1
40	Zr	0.0040	0.017	0.23

Soil samples collected from different sites vary in their microelement content. In the soil of the Balakhani area, the chlorine concentration fluctuates between 157.1 and 164.4, averaging 142.9. It should be noted, however, that in technogenically transformed landscapes, the distribution patterns of microelements differ sharply from those in natural landscapes. This divergence is not solely due to anthropogenic transformation but also depends on the presence of water bodies or river valleys within the area. In his research (Khalid et al., 2017) noting that the lowest metal concentrations are typically recorded in river valleys. Based on their migration capacity, metals can be categorised as follows: elements with moderate migration ability (iron and nickel), and those with high migration potential–zinc, manganese, lead and copper (Chen et al., 2017).

Before proceeding with the analysis of the table data, it is necessary to first consider the normative reference values and conduct comparisons accordingly. The relevant international standards are presented in Table 8 (Huixia Liu et al., 2025).

Based on the results of the conducted analyses and tests, we will refer to the classifications established by prior researchers to determine the level of contamination in the area.

Note: These standards are based on the "World Reference Base for Soil Resources" (2022) and the "FAO Guidelines for Soil Description" (1999) documents by the Food and Agriculture Organization (FAO).

Pollutants are classified according to their hazard levels (Cheng et al., 2020; Geng et al., 2024):

- **Class I (highly hazardous):** As, Cd, Hg, Se, Pb, Fe, benzo[a]pyrene, Zn;
- **Class II (moderately hazardous):** B, Co, Ni, Mo, Cu, Sb, Cr;
- **Class III (low hazard):** Ba, V, W, Mn, Sr and others.

In the practice of ecological–geochemical research, indicative hazard assessments of contamination in anomalous zones are commonly employed to evaluate environmental conditions. Each hazard level is associated with specific types of morbidity in the population, particularly among children:

- **Level I:** increased overall morbidity;
- **Level II:** higher incidence of chronic respiratory diseases and functional disorders.
- **Level III:** increased incidence of reproductive dysfunction, disorders of the immune system, and other long-term adverse effects.

Using the existing classification and the results of the obtained analytical data, it is possible to determine both the level of technogenic pollution and the specific pollutants present in the study area.

As shown in Table 1, in area A107, only a trace amount of arsenic (As, 0.0012%) was detected among the classified heavy metals, while no other heavy metals were found. Therefore, the A107 sampling site can be classified as a Level I pollution zone.

In area A108, manganese (Mn) and chromium (Cr) were detected, indicating that this site can be classified as a Level III pollution zone.

In area A109, no significant concentrations of the listed heavy metals were observed; hence, according to the classification, it does not belong to any pollution level.

In area A110, the presence of arsenic (As) and iron (Fe) was recorded, which allows this site to be classified as a Level I pollution zone.

In area A111, both arsenic (As) and cadmium (Cd)–which belong to the category of hazardous heavy metals–were detected, and therefore this area is also classified as a Level I pollution zone.

Based on the conducted analyses, it can be concluded that highly hazardous heavy metals occur in the soil of the study area only in very low concentrations.

Table 8

Comparative analysis of key indicators on semi-desert, gray, and gray-brown soil types with the corresponding parameters of the Absheron Peninsula

Soil Type	**Indicators**			
	Soil horizon	**Ph (WRB~FAO)**	**humus (WRB~FAO)**	**Absheron**
Semi-desert (Desert Soil)	Topsoil / A horizon (0–20 cm)	7.0–8.5	1-6%	0,3-1,5%
	Subsoil / B horizon (20–60 cm)	8.5–9.0	0,5-4%	0,1-0,3%
	Parent material / C horizon (60–100 cm)	8.5–9.0	0,2-3%	≤0,1%
(Brown Soil)	Topsoil / A horizon (0–20 cm)	pH 5.5–6.5	0,3-1%	0.4-1.0%
	Subsoil / B horizon (20–60 cm)	5.5–6.0	0.1-0.3%	0.1-0.3%
	Parent material / C horizon (60–100 cm)	6.0–7.0	≤,0.1	≤0.1%
(Chestnut soils)	Topsoil / A horizon (0–20 cm)	6.5–8.0	0.5-0.9%	0.8-1.5%
	Subsoil / B horizon (20–60 cm)	6.0–7.8	0.9-1.5%	0.3-0.6%
	Parent material / C horizon (60–100 cm)	6.0–7.5	1.0-1.5%	0.1-0.3

Excluding the sections located in Balakhani, Ramana, Zabrat, and Sabunchu, as well as Lokbatan, Garadagh, and Sangachal—areas that are more heavily contaminated with oil (sections K107–K116 and K123–K125)—the soil profiles of other sections show that the humus content varies between 0.20% and 3.62%, gradually and consistently decreasing from the upper horizons toward the lower layers.

In oil-free areas, the highest humus content was recorded in the Shykhlar area (section K126) within the 10–30 cm horizon, amounting to 3.62%, while the lowest value was observed in the Haji Zeynalabdin Taghiyev settlement (section K117) within the 30–60 cm horizon, where it was 0.20%.

The results indicate that the maximum levels of mineral compounds are found in areas that are relatively more contaminated with oil, whereas the minimum levels are characteristic of areas unaffected by oil pollution.

Tables 2–7 present the results of the chemical analyses of soil samples collected from the study area. These soils, which are predominantly characterised by alkaline to strongly alkaline conditions (pH = 8.4–10.5), exhibit humus contents reaching up to 10.15% and 14.51% in the upper layers of the sections located in Ramana village and the Sabunchu area, respectively. The humus content gradually decreases toward the lower soil horizons, ranging from 1.87% to 3.44%.

The unusually high humus content, which is not typical for the Absheron region should not be interpreted as an indicator of an abundance of humified organic compounds or decomposed materials characteristic of fertile topsoils. Rather, it should be viewed as a consequence of oil contamination. This interpretation is further supported by the unexpected discovery of “buried humus layers” in the deeper horizons (60–100 cm and 35–70 cm) of the soil profiles taken from the more heavily polluted Zabrat I and Ramana village areas.

As shown in Table 2, the humus content in Zabrat I increases with depth: 0.88% in the 0–10 cm layer, 6.85% in the 10–60 cm layer, and reaching 12.44% in the 60–100 cm layer. A similar trend is observed in the Ramana area, where the humus content, instead of decreasing with depth, shows an anomalous upward pattern—from 4.64% in the upper 0–10 cm layer to 11.17% in the 35–70 cm horizon (section 114).

This inverse distribution pattern clearly indicates that the downward migration of oil and petroleum products under the influence of gravity has led to the accumulation of hydrocarbons in the deeper soil layers, resulting in artificially elevated “humus” values at those depths.

4. Conclusion

Except for the areas that are more heavily contaminated with oil, the soils in all investigated sites are characterised by neutral to slightly alkaline conditions, with pH values ranging from 7.4 to 8.5. The leaching of carbonates from the upper soil layers contributes to the formation of a weakly alkaline environment (pH = 7.4–8.2) near the surface, while their accumulation in deeper horizons results in a more strongly alkaline environment (pH = 8.0–8.5).

Excluding the oil-contaminated sections K107–K116, as well as K123, K124, and K125 located in Balakhani, Ramana, Zabrat, Sabunchu, Lokbatan, Garadagh, and Sangachal, the humus content in the soil profiles of the remaining study areas varies between 0.20% and 3.62%, showing a regular and gradual decrease from the upper horizons toward the lower layers.

In non-contaminated areas, the highest humus content was recorded in the Shykhlar area (section K126) within the 10–30 cm horizon (3.62%), while the lowest value was observed in the Haji Zeynalabdin Taghiyev settlement (section K117) within the 30–60 cm horizon (0.20%).

The results indicate that the maximum levels of mineral compounds occur in areas relatively more contaminated with oil, whereas the minimum levels are observed in non-contaminated soils.

In the oil-contaminated areas, the upper soil horizons show a higher accumulation of microelements such as chlorine (Cl), palladium (Pd), antimony (Sb), terbium (Tb), cadmium (Cd), indium (In), and silver (Ag). Conversely, elements such as strontium (Sr), zirconium (Zr), vanadium (V), rubidium (Rb), and iron (Fe) are found in smaller quantities in the upper layers compared to the lower horizons. The concentration of other elements varies irregularly along the soil profile.

Based on the analytical data, three levels of contamination zones were identified within the study area:

Level I contamination zones – observed in sites A107, A110, and A111;

Level III contamination zone – identified in site A108, where manganese (Mn) and chromium (Cr) were detected;

No contamination level – assigned to site A109, where no heavy metals were observed according to the adopted classification.

Acknowledgement

The authors would like to thank ASOIU and Institute of Geology and Geophysics of Azerbaijan.

REFERENCES

Abramovich MV, Aliyev MM, Khain VY (1952) Geology of Azerbaijan. Geomorphology, Stratigraphy. Published by the Academy of Sciences of the Azerbaijan SSR. Baku, p 559 (in Russian)

Ahnstrom ZAS, Parker DR (2001) Cadmium reactivity in metal-contaminated soils using a coupled stable isotope dilution-sequential extraction procedure. Environ Sci Technol 35(1):121–126. https://doi.org/10.1021/es001350o

Aliyev ChS, Kazimova LA (2024) Assessment of a radioecological situation in Azerbaijan, based on spectral analyses of radionuclides. Journal of Environmental Engineering and Science 19 (3):200–205. https://doi.org/10.1680/jenes.23.00048

Aliyev GA (1978) Soils of the Greater Caucasus (within the Azerbaijan SSR). Part I. Elm, Baku, p 158 (in Russian)

Aliyev GA, Volobuev VR (1953) Soils of the Azerbaijan SSR. Azerbaijan SSR Baku, p 450 (in Russian)

Avessalomova IA, Ivanov AN (2019) Biogeochemistry of landscapes of the Matua Island (Central Kuril Islands). Vestnik Moskovskogo universiteta, Seriya 5 Geografiya (5):77–85 (in Russian)

Chen H, Koopal LK, Xiong J, Avena M, Tan W (2017) Mechanisms of soil humic acid adsorption onto montmorillonite and kaolinite. J Colloid Interf Sci 504:457–467. https://doi.org/10.1016/j.jcis.2017.05.078

Cheng W, Lei S, Bian Z, Zhao Y, Li Y, Gan Y (2020) Geographic distribution of heavy metals and identification of their sources in soils near large, open-pit coal mines using positive matrix factorization. J Hazard Mater 387:121–126. https://doi.org/10.1016/j.jhazmat.2019.121666

FAO–ISRIC (1999). Guidelines for profile description. 3rd edition, FAO, Rome, p 70

Geng N, Xia Y, Li D, Bai F, Xu C (2024) Migration and transformation of heavy metal and its fate in intertidal sediments: A Review. Processes 12(2):311–324. https://doi.org/10.3390/pr12020311

Huixia Liu, Bingjie Yu, Zongjiu Sun, Panxing He, Yiqiang Dong, Helong Yang (2025) Spatial variability and driving factors of soil pH in the desert grasslands of northern Xinjiang. Environmental Research 276(121489). https://doi.org/10.1016/j.envres.2025.121489

Khalid S, Shahid M, Niazi NK, Murtaza B, Bibi I, Dumat C (2017) A comparison of technologies for remediation of heavy metal contaminated soils. J Geochem Explor 182(B):247–268. https://doi.org/10.1016/j.gexplo.2016.11.021

Luo X, Wu C, Lin Y, Li W, Deng M, Tan J, Xue S. (2023) Soil heavy metal pollution from Pb/Zn smelting regions in China and the remediation potential of biomineralization. J Environ Sci 125:662-677. https://doi.org/10.1016/j.jes.2022.01.029

Milanovsky EE, Khain VE (1963) Essays on the regional geology of the USSR: The geological structure of the Caucasus. Moscow University Press, Moscow, p 378 (in Russian)

Rustamov G, İsmaylova L (2022) Geochemistry landscape classification: toxicity of chemical elements and their impact on human health. Environ Geochem Health 44:631–643. https://doi.org/10.1007/s10653-020-00747-4

World Reference Base for Soil Resources (2022). International soil classification system for naming soils and creating legends for soil maps, 4-th edition, 2022

Yao J, Qian J, Ji D (2025) Machine learning-based analysis of heavy metal migration under acid rain: Insights from the RF and SVM Algorithms. Minerals 15(6) 663. https://doi.org/10.3390/min15060663

Yaroshevsky AA (2006) Abundances of chemical elements in the Earth's crust. Geochem. Int. 44:48–55. https://doi.org/10.1134/S001670290601006X

ОСОБЕННОСТИ МИГРАЦИИ ТЯЖЁЛЫХ МЕТАЛЛОВ В ТЕХНОГЕННЫХ ЗОНАХ АБШЕРОНСКОГО ПОЛУОСТРОВА

Алиев Ч.С.[1], Казымова Л.А.[2]*

[1]Министерство науки и образования Республики Азербайджан, Институт геологии и геофизики, Азербайджан AZ1073, Баку, просп.Г.Джавида, 119

[2]Кафедра промышленной безопасности и охраны труда, Азербайджанский государственный университет нефти и промышленности, Азербайджан AZ1010, Баку, просп. Азадлыг, 34

**Автор, отвечающий за переписку: latifa.ismaylova@gmail.com*

Резюме. В представленной статье рассматриваются особенности миграции тяжёлых металлов в нефтезагрязнённых почвах, а также потенциальные угрозы для здоровья человека и окружающей среды в районах их накопления. Миграционные свойства тяжёлых металлов в почве зависят от множества различных факторов. В статье приведены результаты разносторонних исследований, направленных на изучение закономерностей распределения тяжёлых металлов в различных средах. В качестве района исследования был выбран Абшеронский полуостров, откуда были отобраны многочисленные пробы с различных участков, загрязнённых нефтью. В данном исследовании рассматриваются физико-химические и геохимические характеристики почв в нефтяных и незагрязненных районах. Результаты показывают, что большинство почв являются нейтральными или с увеличением щелочности в более глубоких горизонтах слегка щелочными из-за карбонатных процессов. Содержание гумуса значительно варьируется от более высоких значений в поверхностных слоях до их постепенного снижения по глубине в незагрязненных почвах. Нефтяное загрязнение меняет эту структуру и связано с повышением концентрации минеральных соединений. Полученные результаты исследований и лабораторных анализов показывают значительное накопление в почвах различных тяжёлых металлов, таких как Pb, As, Cr, Cu, Zn, Se, Al, Fe и Mn. В целом, результаты указывают на значительное влияние загрязнения нефтью на состав почвы, распределение элементов и качество окружающей среды. Значимая корреляция между pH почвы, содержанием органических веществ и обменными и восстановимыми фракциями большинства тяжёлых металлов подтверждает возможность предварительного прогнозирования закономерностей их миграции.

Ключевые слова: *образцы почв, технофильность, значения Кларка, геохимические характеристики, миграция*

ABŞERON YARIMADASININ TEXNOGEN DƏYIŞİLMİŞ ZONALARINDA AĞIR METALLARIN MİQRASİYA XÜSUSİYYƏTLƏRİ

Əliyev Ç.S.[1], Kazımova L.A.[2]*

[1]Azərbaycan Respublikası Elm və Təhsil Nazirliyi, Geologiya və Geofizika İnstitutu, Azərbaycan
AZ1073, Bakı, H.Javid prosp., 119
[2]Sənaye təhlükəsizliyi və əmək mühafizəsi kafedrası, Azərbaycan Dövlət Neft və Sənaye Universiteti, Azərbaycan
AZ1010, Bakı, Azadliq prosp., 34
**Yazışmalara məsul: latifa.ismaylova@gmail.com*

Xülasə. Təqdim olunan məqalədə Ağır metalların neftlə çirklənmiş torpaqlarda miqrasiya xüsusiyyətləri və bu metalların toplandığı ərazilərdə insan sağlamlığı və ətarf mühit üçün yarada biləcəyi təhlükələr şərh olunur. Ağır metalların torpaqda miqrasiya xüsusiyyətləri bir çox müxtəlif amillərdən asılıdır. Məqalədə müxtəlif aspektli tədqiqatlar aparılaraq ağır metalların fərqli mühitlərdə paylanma qanunauyğunluqları tədqiq olunmuşdur. Tədqiqat ərazisi olaraq. Abşeron yarımadası seçilmişdir və ərazidə fərqli neftlə çirklənmiş ərazilərdən çoxsaylı nümunələr götürülmüşdür. Təqdim olunan tədqiqat neftlə çirklənmiş və çirklənməmiş ərazilərdə torpaqların fiziki-kimyəvi və geokimyəvi xüsusiyyətlərinin tədqiqinə həsr olunmuşdur. Nəticələr göstərir ki. torpaqların əksəriyyəti karbonat prosesləri səbəbindən neytral və ya bir qədər qələvidir. daha dərin qatlarda isə qələvilik artır və humus tərkibi əhəmiyyətli dərəcədə dəyişir. səth təbəqələrində daha yüksək həddə çirklənməmiş qatlarda isə dərinlik artdıqca tədricən azalır. Tədqiqatlar və laboratoriya analizlərindən əldə edilən nəticələr torpaqlarda Pb. As. Cr. Cu. Zn. Se. Al. Fe və Mn müxtəlif ağır metalların əhəmiyyətli dərəcədə toplandığını göstərir. Ümumilikdə. nəticələr neft çirklənməsinin torpaq tərkibinə. element paylanmasına və ətraf mühitin keyfiyyətinə əhəmiyyətli təsirini göstərir. Torpaq pH. üzvi maddələrin tərkibi və əksər ağır metalların dəyişdirilə bilən və azaldıla bilən fraksiyaları arasında əhəmiyyətli bir korrelyasiya onların miqrasiya modellərinin ilkin proqnozlaşdırılmasının mümkünlüyünü təsdiqləyir. Aparılan təqdiqatlar və laborator analizlərin nəticələri göstərir ki. torpaqlarda kifayət qədər müxtəlif ağır metalların Pb. As. Cr. Cu. Zn. Se. Al. Fe. Mn toplanması müşahidə olunur. Torpaq pH-ı. üzvi maddələri və ağır metalların əksəriyyətinin mübadilə oluna bilən və reduksiya olunan fraksiyaları ilə əhəmiyyətli korrelyasiyası sübut edir ki. ağır metalların miqrasiyası qanunauyğnluqlarını öncədən proqnozlaşdırmaq mümkündür.

Açar sözlər: *torpaq nümunələri, texnofillik, Klark ədədi, geokimyəvi xüsusiyyətlər, miqrasiya*

ANAS Transactions Earth Sciences 1 / 2026

http://www.journalesgia.com

UPDATED HYDROCARBON RESOURCE ASSESSMENT OF THE MIDDLE KUR DEPRESSION, AZERBAIJAN

Tagiyev M.F.[1]*, Khuduzade A.I.[2], Akhundov Sh.Kh.[1], Akhundova Kh.R.[1]

[1]SOCAR, "OilGasScientificResearchProject" Institute, Azerbaijan

88a, H. Zardabi, Baku, AZ1122

[2]SOCAR, PU "AzNeft", Azerbaijan

73, Neftchiler, AZ1000, Baku

**Corresponding author: mushfiq.taghiyev@socar.az*

Keywords: *the Middle Kur Depression, oil and gas presence, prospective resources of hydrocarbons, C3 category of resources*

Summary. By the present time, the Middle Kur Depression territory has been subjected to dense and wide-ranging field geophysical, mainly seismic, investigations, resulting in a considerable clarification of the deep structure of the basin's sedimentary cover. Seismic sounding has made it possible to identify and delineate numerous structural highs, the areas of which vary from several to the first tens of square kilometers. While the existence of many previously recognised structures has been confirmed, a number of them were found to be considerably smaller in area compared with the results of earlier structural interpretations. In some cases, positive elements earlier interpreted as closed structures were found to be structural noses or were not confirmed. The areal characteristics of the identified structures together with the volumetric parameters such as thickness of the prospective reservoirs, their fluid storage capacity and predicted phase state of hydrocarbon accumulations allowed for calculation of prospective C3 resources. A forecast of the prospective oil and gas resources of the Paleogene and Cretaceous deposits in the Middle Kur Depression, which have proven industrial hydrocarbon potential, is presented. Estimates of C3 resources were presented for a number of prospective structures in the oil and gas bearing regions of Kur-Iori interfluve, Ganja and Muradkhanly, covering a total of 57 structures. The distribution of prospective resources across depth intervals reveals a clear distinction between the studied regions. The highest volumes of hydrocarbon resources are associated with depths of 3–4 km, while stratigraphically the largest resources are concentrated in the Eocene complex.

INTRODUCTION

The Kur intermountain depression occupies the easternmost and deepest part of the South Caucasus microplate. The depression is subdivided into the Middle Kur and Lower Kur segments within Azerbaijan (Huseynov, Shirinov, 1985).

The Middle Kur Depression is situated between the anticlinoria of the Greater and the Lesser Caucasus within the Kura intermountain depression, which represents a large synclinorium. It is bounded to the northwest by the Martkobi transverse structural saddle, to the southeast by the Araks deep fault, to the northeast by the Saatly–Mingachevir zone of buried uplifts, and to the southwest by the Fore-Lesser Caucasus deep fault (Khain, Alizadeh, 2005; Mamedov, 1977).

Deep seismic sounding data indicate that the surface of the pre-Alpine basement occurs at depths ranging from 2 to 16 km. Longitudinal and transverse deep faults define the configuration of major tectonic elements and influence the formation of both the basement surface, which is block-faulted and stepwise deepens toward the Caspian Sea, and the structure of the sedimentary cover (Nemčok et al., 2011).

Two major first-order tectonic troughs are distinguished within the Middle Kur Depression: the Iori–Ajinohur trough in the northwest and the Yevlakh–Aghjabedi trough in the southeast. These troughs are arranged in an en echelon pattern, articulate with one another, and represent separate petroliferous provinces. Within the territory of Azerbaijan, the Iori–Ajinohur trough includes the second-order Ajinohur, Alazani–Agrichay, and Jeyranchol troughs. The Yevlakh–Aghjabedi trough is represented by the Fore-Lesser Caucasus marginal monocline and the Goranboy–Muradkhanly second-order trough.

The pre-Jurassic basement undergoes stepwise subsidence from the margins toward the axial zone of

the depression, as well as along its strike from west to east, except within the Kurdamir–Saatly saddle.

Two structural complexes are distinguished within the Alpine sedimentary cover of the depression. The lower complex is represented by Mesozoic–Eocene carbonate–volcanogenic formations corresponding to the geosynclinal stage of development. These are overlain by an Oligocene–Anthropogene complex composed of orogenic molasse, which is subdivided into two subunits: the Lower Oligocene–Miocene (Maykop Fm.) subunit and the Upper Middle-Upper Miocene–Quaternary subunit.

The Mesozoic–Eocene complex is composed of a flysch formation and is characterised by gentle, stepwise bedding complicated by both small local uplifts and structural protrusions, as well as by longitudinal and transverse disjunctive faults.

The upper structural level formed as a result of oscillatory movements of varying intensity across different parts of the region is characterised by a gradual upward attenuation of folding within the stratigraphic section, where both horizontal and vertical structural zonation are observed.

GEOCHEMICAL REVIEW

According to Feyzullayev, Huseynov and Lerche (2016), most oils in the Middle Kur Basin originated from organic matter deposited in a saline lacustrine environment with a contribution of terrestrial material. Integration of biomarker evidence, Rock-Eval pyrolysis data, and paleo- and current thermal conditions indicates that the oils of the Middle Kur Basin were derived primarily from the middle-mature Tertiary source rocks with a possible contribution from the Cretaceous sediments.

Based on geochemical indicators, a source rock–oil correlation was established between the Upper Eocene–Maykop core samples and oils recovered from reservoirs ranging in age from Cretaceous to Lower Miocene (Klosterman et al., 1997). Although the investigated oils differ in density, bulk and hydrocarbon composition, and extent of biodegradation, the authors underscore their genetic unity within a single oil family. The petroleum fluids are interpreted to have been generated within Tertiary lithofacies complexes formed under essentially identical depositional environments.

In the Mesozoic-Cenozoic sediments of the Middle Kur Depression type II and III organic matter are dominant (Akhundov et al., 2021; Kocharli et al., 2019; Feyzullayev, 2025).

Seventeen core samples collected from wells drilled on structural highs were studied for organic maturity (13 of Eocene, 2 of Oligocene-Lower Miocene and 2 of Lower Cretaceous age). They spanned depth interval from 2000 to 4700 m. Based on %Ro measurements and pyrolysis parameters, the Middle and the Upper Eocene strata of the Yevlakh–Aghjabedi Depression remained thermally immature, as burial temperatures were insufficient to promote effective organic matter transformation (Akhundov et al., 2021). The depocentral parts of the depression are likely to have experienced a more advanced level of source rock catagenesis compared to the marginal areas.

OIL AND GAS PRESENCE

The study area is characterised by the widespread occurrence of oil, gas, and water shows of differing nature and intensity across a wide stratigraphic interval.

Reservoirs and seals of the Upper Cretaceous and the Eocene deposits of the Middle Kur Depression are characterised by diversity in composition and genesis, which causes sharp variations in well productivity in individual areas (Akhundov et al., 2022).

In the previously published work, we provided a brief description of the hydrocarbon accumulations identified in the Middle Kur Depression. In addition, highly prospective, prospective, and low-prospective zones were identified within the depression for further exploration and prospecting activities (Khuduzade et al., 2025).

Zones of extended longitudinal faults crossing possible hydrocarbon migration pathways indicate the presence of favorable structural-tectonic conditions for oil and gas accumulation in this area. The generalisation of factual data showed that the distribution of oil and gas accumulations is associated with faults that either divide structures into blocks and partially seal the discovered reservoirs, or act as lithological-fault or fault-stratigraphic seals.

The stratigraphic units of proven industrial hydrocarbon potential include the Upper Cretaceous volcanogenic and, to some extent, volcanogenic–carbonate deposits, the Eocene volcanogenic–sedimentary rocks, the Maykop sedimentary formations, as well as the Chokrak horizon (Alizadeh, 2008; Khuduzade et al., 2023).

Commercial oil deposits in the Upper Cretaceous volcanogenic formations have been discovered on the northeastern flank of the Yevlakh–Aghjabedi trough, in the Muradkhanly and Zardab areas (Guliyev, Guliyeva, 2012).

The Upper Cretaceous carbonate rocks are widely distributed but commercial oil accumulations have not been identified. In the Muradkhanly area, a local accumulation is noted within the carbonates, while in the Sovetler area, a flow of formation water with gas and oil has been encountered. On the Gazanbulag structural high, oil was encountered during testing of several wells. In the Terter area, strong oil–gas shows were observed culminating in a flow-

ing oil well. Minor oil inflows were noted only in the Dalimammadli, Naftalan, Gulluja, and Beylagan areas, and signs of hydrocarbon presence were identified in core samples from the Tarsdaller area.

The hydrocarbon potential of the Paleogene deposits has been established throughout the stratigraphic section in all oil and gas bearing regions of the Middle Kur Depression. Oil inflows and oil-gas shows have been recorded in individual wells, and signs of hydrocarbon presence from discrete intervals have been observed in the most of areas. Small oil accumulations have been identified as follows: in the Paleocene–Lower Eocene deposits, in the Gazanbulag, Naftalan, Dalimammadli, Duzdag–Godakboz, Ajidere, Sariyaldag, Aghjabedi, and Borsunlu–Kurekchay areas; in the Middle Eocene deposits, in the Dalimammadli, Gazanbulag, Naftalan, Borsunlu–Kurekchay, Terter, Duzdag–Godakboz, Muradkhanly, Zardab, Jafarli, Amirarkh, Tarsdaller, Gurzundag, and Damirtepe–Udabno areas; and in the Upper Eocene deposits, in the Dalimammadli, Gazanbulag, Godakboz and Zardab areas.

The Maykop deposits are the most extensively developed and studied. In the Ganja oil and gas bearing region, oil reserves were discovered in the Maykop deposits in the Naftalan, Gazanbulag, Ajidere, Terter, and Dalimammadli areas; oil inflows in individual wells were recorded in the Borsunlu, Aghjabedi, Beylagan, Shirvanly, and Gulluja areas; and signs of hydrocarbon presence were identified in the Sariyaldag, Aliushaghi and Bozyeri areas. The oil fields at Gazanbulag, Ajidere, Naftalan and Terter were in production until 1979.

In the Muradkhanly oil and gas bearing region, oil reserves have been established in the Muradkhanly and Zardab areas, while intense oil-gas shows in the Maykop formation were recorded in the Mil and Amirarkh areas.

The low level of data on the hydrocarbon presence of Maykop deposits in the oil and gas bearing region of the Kur-Iori interfluve is due to the fact that intervals where oil-gas shows were recorded during drilling were not tested.

Figure 1 presents a schematic map showing the distribution of oil fields and prospective structures within the Middle Kur Depression. Based on seismic data and the geological-geophysical characteristics of the structures, an assessment of prospective C3-category resources was carried out for these areas. A necessary condition was the presence of closed traps within structural highs. Figure 2 shows examples of structural maps for several areas of the Middle Kur Depression.

The concept of "oil and combustible gas resources" covers estimates of groups of identified and unidentified hydrocarbon accumulations that vary in their level of study and reliability. It covers a wide range of values from accumulated production, detailed explored (cat. A, B, C1) and preliminary estimated (cat. C2) reserves to prospective (cat. C3) and predicted resources (cat.D1 and D2) of liquid and gaseous hydrocarbons (Methodological guidelines…, 1983).

Forecast estimates of resources are necessary for planning the development of the oil industry in the long term, as well as for identification of priorities in exploration work.

The term “total resources” combines two groups that differ sharply from each other. The identified reserves of already discovered, explored and involved in development deposits are included in the first of them. Unidentified, not yet discovered resources, only assumed, predicted on the basis of geological and geophysical data and established ideas about the geological structure and oil and gas potential of the assessed regions are included in the second group. The establishment of commercial oil and gas potential (i.e. the discovery of a field) is the main boundary separating groups of identified and unidentified resources of a zone, region or area of oil and gas accumulation. In the traditional classification of reserves (accepted in the former USSR and still used today), such a boundary is drawn within categories C.

Preliminary estimated reserves of category C2 in already discovered fields, deposits and horizons exposed by drilling are separated from less reliable prospective resources of new horizons (category C3). The oil and gas potential of the latter has not yet been established by drilling in the fields of this oil and gas-bearing region.

Traps (objects) in these potentially oil-containing horizons should be prepared for exploratory drilling and outlined on the basis of study by geological and geophysical methods tested in this area. Based on this, estimates of prospective resources (cat. C3) should be classified as a group of undetected hydrocarbon volumes (Methodological guidelines, 1983).

According to the degree of reliability hydrocarbon resources of sedimentary basins are divided into three categories: C3, D1 and D2.

The quantitative assessment of predicted resources (D1, D2) is based on the analysis of geological criteria for the oil and gas potential of known areas and territories, and the application of specified reference characteristics to unknown objects. These objects may be located within known areas or in adjacent regions that have similar geological characteristics for the formation and accumulation of oil and gas.

The division between the D1 and D1 categories is somewhat speculative. Category D1 may include lithostratigraphic objects which oil and gas potential in the given large territory has not yet been proven, but their hydrocarbon productivity has been established in

the adjacent territories with comparable geological characteristics. Category D2 is related to resources of promising but poorly studied territories and lithological-stratigraphic complexes. Therefore, it is not possible to speak about the reliability or good justification of the quantitative estimates of categories D1 and D2.

Different approaches and reference parameters may be used when quantitatively assessing the oil and gas potential of individual regions. As a result, the predicted resources can demonstrate significant fluctuations (Khuduzade et al., 2020).

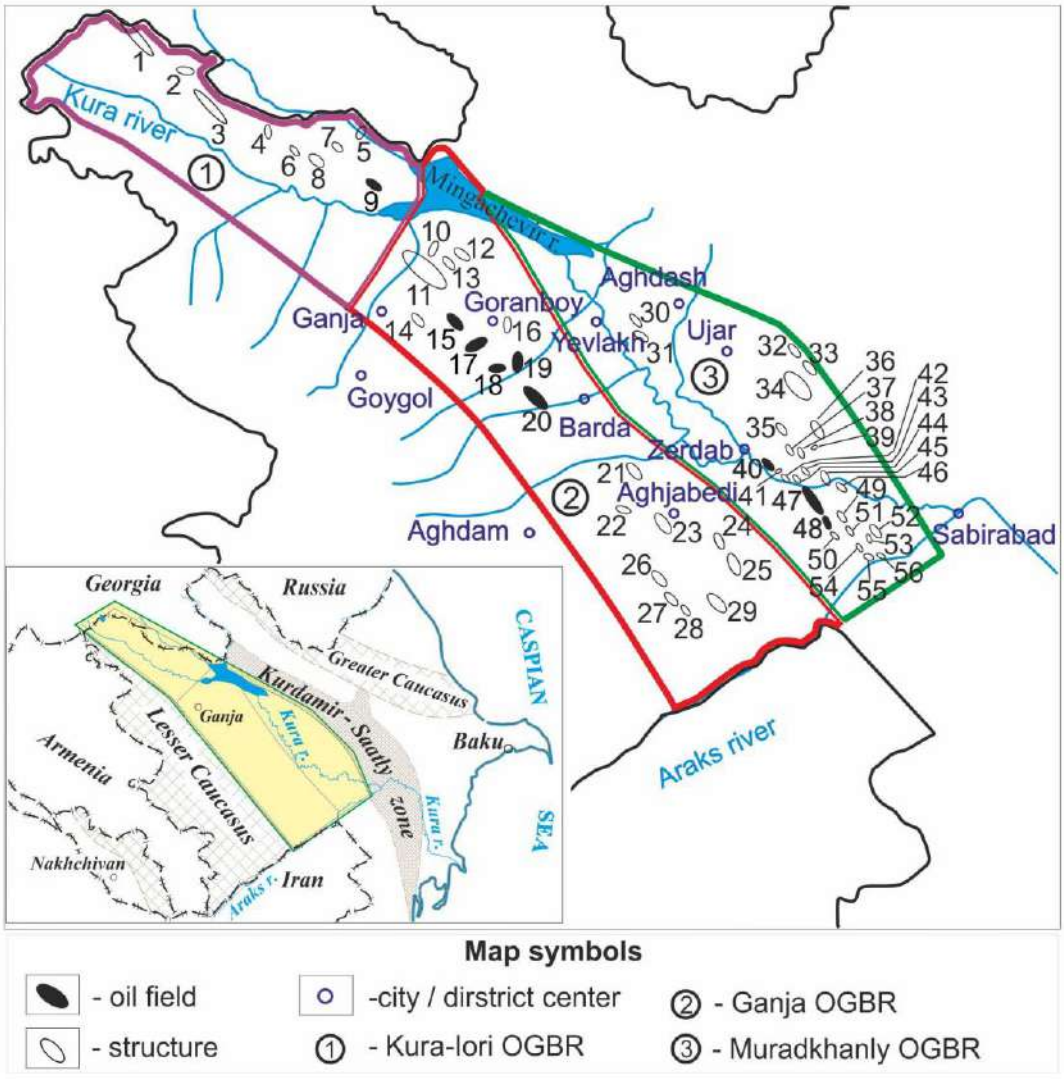

Kura-lori OGBR

1 - Damirtepe-Udabno
2 - Sazhdag
3 - Molladag
4 - Aghtepe
5 - Eldaroyughu
6 - Garbi Gurzundag
7 - Kollug
8 - Gurzundag
9 - Tarsdaller

Ganja OGBR

10 - Soyugkhanly
11 - Dalimammadli
12 - Bozyeri
13 - Fakhrali
14 - Ziyadkhan
15 - Gazanbulag
16 - Godakboz
17 - Ajidere
18 - Sariyaldag
19 - Naftalan
20 - Terter
21 - Lemberan
22 - Hindarkh
23 - Aghjabedi
24 - Aghgol
25 - Janubi Aghjabedi
26 - Kebirli
27 - Gemerli
28 - Chebri
29 - Beylagan

Muradkhanly OGBR

30 - Mursel
31 - Garbi Amirarkh
32 - Mususlu
33 - Garabujag
34 - Garajaly
35 - Garghaly
36 - Garabat
37 - Beyimli
38 - Gishlag
39 - Shargi Gishlag
40 - Zardab
41 - Garavelli
42 - Shikhbaghi
43 - Soyudler
44 - Shargi Shikhbaghi
45 - Shahsunnu
46 - Mammadli
47 - Muradkhanly
48 - Jafarli
49 - Hasanli
50 - Aghamammadli
51 - Garaly
52 - Mil
53 - Hajigasimly
54 - Javadkhanly
55 - Shargi Garagashly
56 - Garagashly

Fig. 1. The Middle Kur depression. Location map of structures with estimated C3 category of prospective oil and gas resources

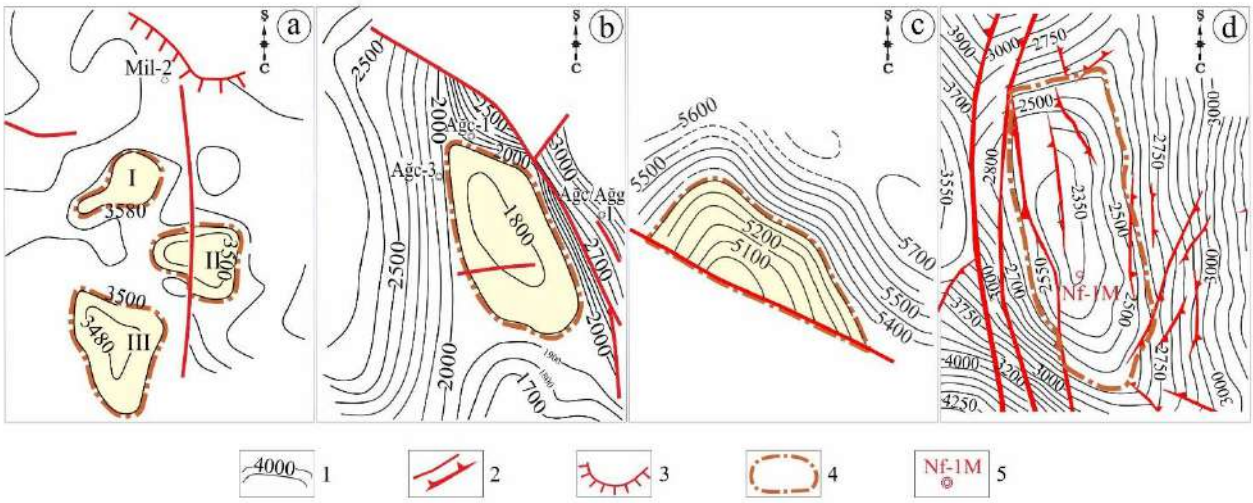

Fig. 2. Structural maps with reserve calculation contours indicating potential hydrocarbon saturation of reservoirs in individual areas of the Middle Kur Depression

Map Legend: 1 - isolines, and 2 - faults interpreted from seismic and well data; 3 - the Eocene pinch-out boundary; 4 - interpreted hydrocarbon saturation contours; 5 - proposed exploratory well location

fig. ⓐ - Structural uplifts (SH-III - on the eroded surface of Middle Eocene): - I-Hajigasimly; II-Shargi Garagashly; III-Garagashly; fig. ⓑ - Aghjabedi uplift (SH-III - on the eroded surface of the Middle Eocene); fig. ⓒ - Eldaroyughu uplift (on the Middle Eocene top); fig. ⓓ - Naftalan field (SH-V - seismic horizon in the uppermost Upper Cretaceous)

There are two deep depressions within Azerbaijan: the South Caspian and Yevlakh-Aghjabedi, which are separated by the Talysh-Vandam zone of positive gravity anomaly. This zone is associated with buried volcanogenic formations, mainly of the Mesozoic age. In the literature, it is also referred to as the "Kurdamir-Saatly Zone" (see Figure 1) and is associated with buried volcanogenic complexes, mainly of the Mesozoic age.

To appropriately assess the oil and gas potential of vast areas of the Middle Kur Depression, it is necessary to conduct more detailed geological, geochemical and geophysical studies both in terms of area and depth of the sedimentary basin. Despite the long history of geological exploration and drilling operations, our knowledge of the structure and cross-section of deep-lying horizons in many areas is insufficient to substantiate the prospects for their oil and gas potential.

Onshore of Azerbaijan given the relatively high level of exploration coverage of the upper level of oil and gas presence, reorientation of exploration work to deep-lying horizons, especially to the lower level of oil and gas presence (to Mesozoic deposits), to buried structures and non-anticline traps is an extremely urgent task (Kerimov et al., 2015).

EVALUATION OF FORECAST AND PROSPECTIVE RESOURCES

The quantitative estimates of predicted and prospective oil and gas resources in the Middle Kur Depression presented in previous studies mainly cover the stratigraphic interval from the Cretaceous to the Pliocene deposits. It is difficult to estimate the hydrocarbon potential of sedimentary facies of the Jurassic deposits due to the lack or limited data on the composition of solid and fluid components of these layers. It is known that in the Gusar-Devechi region and the southeastern subsidence zone of the Greater Caucasus (Khizi Synclinorium, Tengi-Beshbarmag Anticlinorium) these deposits are significantly thick and contain layers enriched in organic matter (OM). The Jurassic strata are considered prospective for the discovery of oil and gas deposits (Alizadeh, 2008).

A number of published works provide quantitative estimates of oil and gas regions of Azerbaijan differing both in geographical coverage and in stratigraphic detail. Naturally, these estimates are difficult to compare making the overall quantitative picture hard to interpret.

The results of quantitative assessment of hydrocarbon resources at a given geographical scale and stratigraphic limits are known from publications by various authors. Thus, according to Kerimov et al., (1999) the initial total hydrocarbon resources amount to 91 billion tons of geological and 34 billion tons of recoverable volumes (hereinafter in brackets, recoverable resources) in the sedimentary strata of the Kur-South Caspian Mega Depression. Under the term "The Kur-South Caspian Mega Depression" the authors unite the vast territory of the South Caspian, including the West Turkmen Depression in the east, the Azerbaijani marine area in the west, the Iranian sector in the south, as well as the Lower, Middle and Upper Kur basins, and even the

southern part of the Terek-Caspian Depression. The predicted resources of the Pliocene 18 (7.4), Paleogene-Miocene 7.0 (1.9) and Mesozoic 16.0 (6.2) complexes amount to a total of 41 (15.5) billion tons.

According to Guliyev I.S. et al. (2003), a schematic description of the predicted resources is presented in the form of color-coded zones within the Caspian basin and adjacent land. The main focus here lies in two schematic maps illustrating the distribution of potential hydrocarbon resources in the Oligocene-Miocene and Cretaceous-Eocene deposits. In the first map, within the Middle Kur Depression, the density of potential hydrocarbon resources is represented by a color scale of 20–50–75–100 thousand tons/km² of oil equivalent (toe) with the majority of the area coded as "20 thousand tons/km²". In the second scheme (the Cretaceous-Eocene), the coloring reflects the coding range of "5-100 thousand tons", where the overwhelming area is occupied by two color codes of 25 and 50 thousand tons/km^2.

Without detailing the data for individual regions of Azerbaijan, in total, potential hydrocarbon resources of the Oligocene-Miocene are represented by 3.54 billion toe (based on an area of 98.1 thousand km^2). Similar tabular data are also presented for the Cretaceous-Eocene. In total, potential hydrocarbon resources for this interval are represented by 2.15 billion toe (74.5 thousand km^2). The assessment of potential hydrocarbon resources for the Jurassic complex in Azerbaijan is characterised by a moderate value of 0.41 billion toe (38.1 thousand km^2). It should be noted that the authors' calculations for the Cretaceous-Eocene and Jurassic are limited to the upper part of the sedimentary cover, i.e., deposits lying no deeper than 7 km.

According to Aliyev H-M.A. and co-authors (2007) estimates are given the initial total geological hydrocarbon resources (in conventional units or in oil equivalent) for the Mesozoic, which in total amount to 1.25 billion toe. According to the geological fund materials we used to clarify this value, it represents estimates of reserves and resources in the onshore regions of Azerbaijan. In particular, the Muradkhanly, Ganja, Kur-Iori interfluve OGBRs and the Ajinohur prospective region located within the area of our study combined account for one third of the initial total resources (ITR) of the onshore Azerbaijan. As can be seen from Table 1, the ITR values are essentially formed from the predicted D1+D2 hydrocarbon categories.

So far, the Middle Kur Depression has undergone extensive and relatively high-density field geophysical surveys. The deep structure of the depression's sedimentary cover has been clarified to a significant extent due to seismic surveys carried out over the past decades. By means of seismic sounding using the common depth point method, numerous structural uplifts were identified and delineated with areas ranging from a few to several tens of square kilometers. Thus, the existence of many previously identified structures was confirmed, although some were found to be considerably smaller in area than earlier structural interpretations had suggested. In a number of cases, positive features formerly regarded as closed proved to be structural noses or lacked confirmation entirely.

The areal characteristics of the identified structures with such calculation parameters as thickness of the expected reservoirs, their fluid storage capacity properties made it possible to calculate the prospective resources of the C3 category taking into account the predicted phase state of hydrocarbon accumulations.

Table 2 summarises the main calculation parameters compiled from the analysis of reference areas, which are essentially known fields. The values of prospective hydrocarbon resources of category C3 are calculated on the basis of parameters, which include the area of the structure along the deepest closed contours, effective hydrocarbon-saturated thickness, open porosity, oil saturation, oil density and gas factor. The calculation formula also includes a correction for oil shrinkage. It is necessary to immediately make a reservation regarding open porosity. Along with pore space, it also reflects fracturing, a petrophysical parameter that has a significant impact on the filtration and capacity characteristics of rocks.

Table 1

Initial total hydrocarbon resources of the Mesozoic complex by OGBRs*
with indication of predicted resources D1+D2

On Mesozoic strata	Oil and gas bearing region			
	Muradkhanly	Ganja	The Kur-Iori interfluve	Ajinohur prospective region
ITR**	215	128	52	20
D1+D2	187	120	45	20

** OGBR – oil and gas bearing region*
*** ITR – initial total resources*

Table 2

Reference parameters used for the estimation of C3 category of oil and dissolved gas resources

OGBR	Reference area	Reference stratigraphic position	Net thickness (m)	Effective porosity (%)	Oil saturation (%)	Oil density (g/cm³)	Gas-oil ratio (GOR) (m^3/t)	Structural area (min–max); km^2
Kur-Iori	Tarsdaller	Middle Eocene	17.0	13.0	80.0	0.870	109.0	2.5-34.0
Kur-Iori	Muradkhanly	Upper Cretaceous	10.2	14.3	54.2	0.877	31.2	0.7-8.1
Ganja	Tarsdaller	Middle Eocene	17.0	13	80.0	0.870	109.0	2.2-12.5
Ganja	Muradkhanly	Middle Eocene	9.4	12	55.6	0.882	31.4	1.0-41.1
Ganja	Muradkhanly	Upper Cretaceous	10.2	14.3	54.2	0.877	31.2	5.5-15.0
Muradkhanly	Zardab-Shikhbaghi	Maykop formation	5.2	18	60	0.873	10	6.8
Muradkhanly	Jafarli	Middle Eocene	20.0	9.8	57.4	0.872	24	1.0-6.5
Muradkhanly	Muradkhanly	Middle Eocene	9.4	12	55.6	0.882	31.4	2.1-4.3
Muradkhanly	Muradkhanly	Upper Cretaceous	10.2	14.3	54.2	0.877	31.2	0.3-30.3

Resource estimates of category C3 were presented for a number of promising structures of the Middle Kur Depression. Thus, of this amount, the share of the Kur-Iori Interfluve OGR accounted for 8 structures. For the Ganja OGBR, 16 structures were covered by estimates, and 33 structures were quantitatively characterised for the Muradkhanly OGBR.

Table 3 shows the distribution of prospective resources by stratigraphic complexes. In this table, the data are divided between three oil and gas complexes: The Mesozoic, Eocene, and the Oligocene-Lower Miocene Maykop Fm. According to the presented estimates, the sedimentary section of the Muradkhanly oil and gas bearing region is characterised by the largest hydrocarbon resources of the C2 category (111/26 million tons). In individual consideration, the Eocene complex within the Ganja OGBR contains the largest volume of hydrocarbons (68/12 million tons) compared to all other elements of the table.

Table 3

Distribution of C3 category of prospective resources by stratigraphic complexes

HC resources C3 ► / **OGBR ▼**	**oil (thou.t)**	**dissolved gas (mln m³)**	**stratigraphic complex**					
	geological	geological	**Mesozoic**		**Eocene**		**Maykop**	
	recoverable	*recoverable*	oil	dissolved gas	oil	dissolved gas	oil	dissolved gas
Kur-Iori	59 937	5 465	13 727	428	46 210	5 037		
	16 883	*1 497*	*4 407*	*137*	*12 477*	*1 360*		
Ganja	84 639	5 383	16 201	505	68 438	4 877		
	17 023	*1 270*	*5 200*	*162*	*11 822*	*1 108*		
Muradkhanly	111 022	3 175	52 455	1 637	55 890	1 512	2 677	27
	26 399	*794*	*16 838*	*525*	*9 160*	*264*	*402*	*4*
Total	**255 598**	**14 023**	**82 383**	**2 570**	**170 538**	**11 426**	**2 677**	**27**
	60 305	***3 561***	***26 445***	***825***	***33 458***	***2 732***	***402***	***4***

Table 4 presents the distribution by depth intervals. Here, a distinct difference in the depth distribution of oil resources between the studied regions is observed. In the Ganja region, the peak of C3 oil resources corresponds to a depth interval of 1-2 km. In the Muradkhanly oil and gas bearing region, it is deeper – in the range of 2-3 km. In the region of Kur and Iori Interfluve, the peak occurs within deeply buried sedimentary layers, at depths exceeding 5 km. This can be explained by the fact that, in the Eldaroyughu area, which hosts the largest C3 resources, the seismogeological surface of the Middle Eocene occurs at depths exceeding 5 km.

Figure 3 presents the distribution of prospective resources by sedimentary cover depth for each OGBR individually as well as for their overall total. According to the obtained estimates, the largest volumes of hydrocarbon resources are concentrated at depths of 3–4 km (see Fig. 3b). Stratigraphically, the greatest volumes of resources are associated with the Eocene complex (see Fig. 3d).

The ratio between prospective (C3) and predicted (D1, D2) resources is of considerable interest (Figure 4). Predicted resource categories are considered the least reliable, due to the fact that they reflect the part of the hydrocarbon potential that is based on very approximate estimations. Nevertheless, the quantitative picture would be incomplete without them.

The hydrocarbon resource estimates presented in this study underscore the need to consider the deeper levels of oil and gas potential in the Middle Kur Depression, especially buried structures and non-anticlinal traps related to the Mesozoic formations. These areas require increased attention to enable the development of more scientifically robust assessments of oil and gas potential.

With advances in equipment and production technology, the development of unconventional hydrocarbon resources in the Middle Kur Depression has come to the forefront. The paleotectonic basis and the geological and geochemical conditions for the exploration of shale oil and shale gas in the Yevlakh–Agjabedi Depression are discussed in the publication by Huseynov et al., 2015.

The authors noted a number of factors that favor the search for shale hydrocarbons in the Maykop deposits of this depression. The subsidence of the Oligocene–Miocene strata in the depocentral area of the depression below 3.5 km promoted catagenetic transformation, a process necessary for hydrocarbon formation within shale formations. The quantity and type of organic matter suggest a capacity for the generation of gaseous hydrocarbons. The presence of alternating clayey layers and impermeable siltstone partings is regarded as advantageous from the standpoint of development potential. Preliminary encouraging results highlight the necessity to continue research aimed at identifying and delineating the most prospective areas for shale hydrocarbons.

Table 4

Distribution of C3 category of prospective resources by depth intervals of the sedimentary cover

HC resources C3 ► / **OGBR ▼**	**oil (thou.t) / k.t**	**dissolved gas (mln m³)**	**depth, km**											
	geological	geological	**0 - 1**		**1 - 2**		**2 - 3**		**3 - 4**		**4 - 5**		**5 +**	
	recoverable	*recoverable*	oil	dissol-ved gas	oil	dissol-ved gas	oil	dissol-ved gas	oil	dissol-ved gas	oil	dissol-ved gas	oil	dissol-ved gas
Kur-Iori	59 937	5 465					4 170	341	9 296	843	9 638	301	36 833	3 981
	16 883	*1 497*					*1 200*	*94*	*2 622*	*231*	*3 094*	*97*	*9 967*	*1 076*
Ganja	84 639	5 383	21 718	2 263	39 766	2 396	14 828	463	4 706	147	3 620	114		
	17 023	*1 270*	*5 595*	*603*	*5 741*	*490*	*4 279*	*134*	*1 155*	*36*	*253*	*8*		
Muradkhanly	111 022	3 175							80 213	2 374	21 246	571	9 563	230
	26 399	*794*							*21 941*	*669*	*3 579*	*103*	*880*	*21*
Total	**255 598**	**14 023**	**21 718**	**2 263**	**39 766**	**2 396**	**18 998**	**804**	**94 215**	**3 364**	**34 503**	**986**	**46 397**	**4 210**
	60 305	***3 561***	***5 595***	***603***	***5 741***	***490***	***5 479***	***228***	***25 717***	***936***	***6 926***	***208***	***10 847***	***1 097***

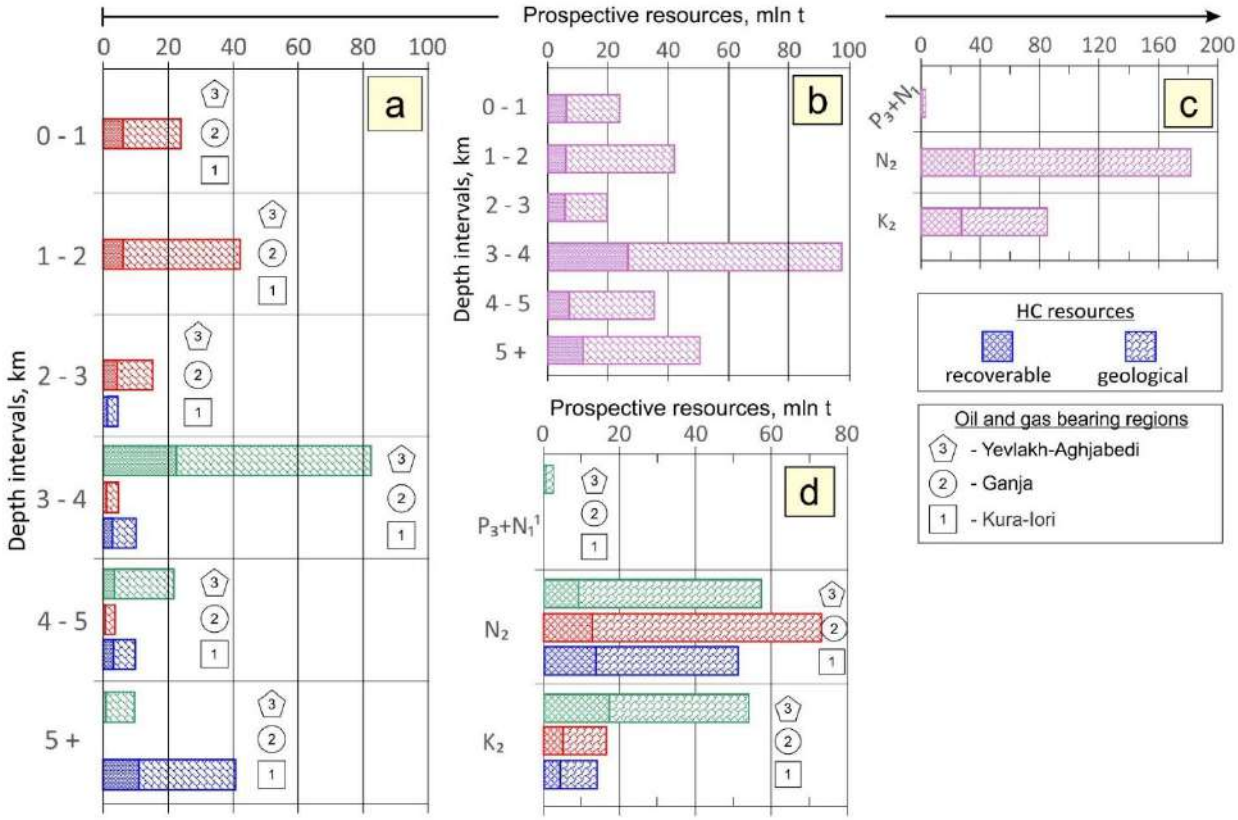

Fig. 3. Distribution of estimated C3 category of prospective resources in OGBRs: (a) by depth intervals; (b) total for the three OGBRs; (c) by stratigraphic units; (d) total for the three OGBRs

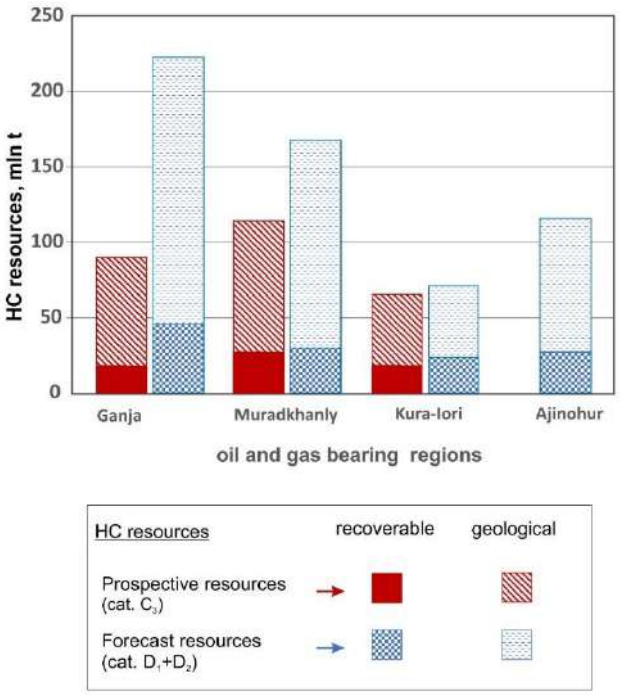

Fig. 4. Distribution of C3 and D1+D2 category of resources in the hydrocarbon-bearing regions of the Middle Kur Depression

The least studied deposits in the Middle Kur Depression are the Lower Cretaceous and Jurassic strata, which, fall outside the scope of this presentation due to the limited geological and geophysical explorations. Insufficient geochemical data to evaluate the hydrocarbon generation potential combined with the unknown extent and distribution of these deposits constitutes an additional constraint on resource assessment.

CONCLUSION

Prospective resource estimates (C3 category) were presented for a total of 57 prospective structures of the Middle Kur Depression.

Prospective resources are distributed between three major petroliferous stratigraphic complexes: the Mesozoic, Eocene and Maykop. The sedimentary strata in the Muradkhanly oil and gas bearing region is estimated to be the largest C3 category hydrocarbon resource container (with 111 / 26 million tons of geological / extractible HCs). When considered separately, the Eocene complex within the Ganja region contains the highest hydrocarbon volumes (68/12 million tons) compared to all other stratigraphic units of the studied regions.

In the distribution of oil resources by depth intervals, a clear difference is revealed between the hydrocarbon bearing regions under consideration. In the Ganja region, the C3 oil resource peak corresponds to a depth interval of 1-2 km. In the Muradkhanly region, it is deeper – in the range of 2-3 km.

In the Kur and Iori interfluve the peak even shifts to deeper sedimentary horizons (below 5 km).

In the distribution of prospective resources by depth of sedimentary pile, the highest volumes are confined to depths of 3-4 km. In the stratigraphic allocation the largest resources fall within the Eocene complex.

The mentioned estimates for hydrocarbon resources emphasise to some extent the need to pay attention to the lower stage of oil and gas presence in the Middle Kur Depression, particularly to the buried structures and non-anticlinal traps associated with the Mesozoic deposits.

REFERENCES

Akhundov ShKh, Khuduzade AI, Tagiyev MF, Mammadov EE (2022) Lithological and stratigraphic characterization of the Upper Cretaceous and Eocene sediments in the Middle Kura Depression, Azerbaijan. Mineral resources of Ukraine 1:17–23. https://doi.org/10.31996/mru.2022.1.17-23 (in Russian)

Akhundov ShKh, Tagiyev MF, Khuduzade AI, Aliyev AN (2021) Hydrocarbon generative properties and maturity of Cretaceous and Eocene sediments in the Middle Kura Depression, Azerbaijan. In: SPE Annual Caspian Technical Conference, Baku, Azerbaijan, Oct.5-7, 2021 (SPE-207041-MS)

Ali-zadeh AkA (ed) (2008) Geology of Azerbaijan. vol VII: Oil and gas. Nafta-Press, Baku, p 672 (in Russian)

Aliyev H-MA, Yusifov KhM, Suleymanov AM, Mustafayeva TM (2007) Geological justification of predicted hydrocarbon resources of Mesozoic deposits in onshore Azerbaijan. SOCAR, Institute of Scientific Research, Scientific Proceedings 08:3–10 (in Azerbaijani)

Feyzullayev AA (2025) Hydrocarbon systems of sedimentary basins: Theoretical foundations and scientific and practical aspects. Nafta-Press, Baku, p 448 (in Russian)

Feyzullayev AA, Huseynov DA, Lerche I (2016) Oil geochemistry of the Middle Kura Basin, Azerbaijan. Journal of Scientific and Engineering Research 3(6): 479–487

Guliyev IS, Levin LE, Fedorov DL (2003) Hydrocarbon potential of the Caspian region (systematic analysis). Nafta-Press, Baku, p 127 (in Russian)

Guliyev KG, Guliyeva BA (2012) Perspective of study on Oligocene-Miocene deposits of oil and gas fields. Azerbaijan oil industry 6:7–12 (in Russian)

Huseynov AN, Shirinov FA (1985) Petroleum geological zoning of the Azerbaijan SSR. Map scale 1:500,000 (Scientific editor: Mamedov AV) (in Russian)

Kerimov KM, Haciyev FM, Hasanov IS (1999) Hydrocarbon resources of the Kura-South Caspian megadepression. Azerbaijan oil industry 7:1–11 (in Russian)

Kerimov VYu, Guliyev IS, Huseynov DA et al (2015) Prediction of petroleum potential in regions with complex geological structure. Nedra, Moscow, p 404 (in Russian)

Khain VYe, Ali-zadeh AkA (eds) (2005) Geology of Azerbaijan, vol IV Tectonics. Nafta-Press. Baku, p 506 (in Russian)

Khuduzade A, Akhundov Sh et al (2025) Oil and gas prospects of the Middle Kura Basin. Azerbaijan geologist 28:75–87

Khuduzade AI, Akhundov ShKh, Tagiyev MF, Guliyev II (2023) Modeling of the tectonic setting and prediction of trap types in the petroleum-bearing area of the Kura-Iori Interfluve (Western Azerbaijan). In: Proceedings of the scientific-practical conference "Heydar Aliyev and the oil strategy of Azerbaijan: Achievements in petroleum geology and geotechnologies". May 23-26, Baku, p 92–97 (in Russian)

Khuduzade AI, Tagiyev MF, Askerov IN (2020) Estimation of undiscovered hydrocarbon resources: traditional methods and up-to-date development tendencies. Azerbaijan oil industry, 1:11–18 (in Azerbaijani)

Klosterman MJ, Abrams MA, Aleskerov EA et al (1997) Hydrocarbon system of the Evlakh-Agdzhabedi Depression. Azerbaijan geologist 1:90-120

Kocharli ShS, Ismayilova GG, Feyzullayev AA (2019) Prognosis evaluation of oil-gas bearing content in Ajinohur region of Azerbaijan based on geological-geochemical data. Azerbaijan oil industry 3:4–10 (in Russian)

Mamedov AV (1977) Geological evolution and paleogeography of the Middle Kura Depression and their relationship to hydrocarbon potential. Elm, Baku, p 212 (in Russian)

Methodological guidelines for the quantitative assessment of prospective oil, gas, and condensate resources (1983) All-Russian Scientific Research Geological Oil Institute (VNIGNI), Moscow, p 215 (in Russian)

Nemčok M, Feyzullayev AA, Kadirov FA et al (2011) Neotectonics of the Caucasus and Kura valley, Azerbaijan. Global Engineers and Technologists Review 1:1–14

ОЦЕНКА РЕСУРСОВ УГЛЕВОДОРОДОВ СРЕДНЕКУРИНСКОЙ ВПАДИНЫ НА ОСНОВЕ НОВЫХ ГЕОЛОГО-ГЕОХИМИЧЕСКИХ ДАННЫХ

Тагиев М.Ф.[1]*, Худузаде А.И.[2], Ахундов Ш.Х.[1], Ахундова Х.Р.[1]
[1]НИПИ «Нефтегаз» SOCAR, Азербайджан
AZ1122, Баку, просп. Г.Зардаби, 88а
[2] ПО «АзНефть» SOCAR, Азербайджан
AZ1000, Баку, просп. Нефтчиляр, 73
**Автор, отвечающий за переписку: mushfiq.taghiyev@socar.az*

Резюме. На сегодняшний день глубинное строение осадочной толщи Среднекуринской впадины в значительной степени детализировано сейсмическими исследованиями. Путем сейсмического зондирования выявлены и оконтурены многочисленные структурные поднятия, площади которых варьируют в пределах от нескольких до первых десятков квадратных километров. Хотя существование многих ранее выявленных структур подтверждено, при этом некоторые из них оказались значительно скромнее по площади, чем было представлено в результате предыдущих структурных интерпретаций. В ряде случаев считавшиеся ранее замкнутыми положительные элементы оказались структурными выступами или вовсе не нашли своего подтверждения. Площадные характеристики выявленных структур вкупе с такими подсчетными параметрами, как мощности предполагаемых резервуаров, их емкостные свойства и с учетом фазового состояния углеводородов в известных скоплениях легли в основу расчетов ресурсов. Таким образом, представилась возможность оценки перспективных ресурсов категории С3 в потенциально нефтесодержащих горизонтах структурных поднятий, не охваченных бурением. В данной работе представлен прогноз перспективных ресурсов нефти и газа палеогеновых и меловых отложений Среднекуринской впадины, имеющих доказанную промышленную нефтегазоносность. Оценки ресурсов категории С3 были представлены по ряду перспективных структур Гянджинского и Мурадханлинского нефтегазоносных районов и междуречья Куры и Иори. В общей сложности оценками были охвачены 57 структур. В распределении перспективных ресурсов по глубинным интервалам выявляется четкое различие между рассматриваемыми районами. Наиболее высокие объемы углеводородных ресурсов приурочены к глубинам 3-4 км, тогда как в стратиграфическом распределении наибольшие ресурсы приходятся на долю эоценового комплекса.

Ключевые слова: *Среднекуринская впадина, нефтегазоносность, перспективные ресурсы нефти и газа, категория С3*

YENI GEOLOJI-GEOKİMYƏVİ MƏLUMATLAR ƏSASINDA ORTA KÜR ÇÖKƏKLİYİNİN KARBOHİDROGEN RESURSLARININ QİYMƏTLƏNDİRİLMƏSİ

Tağıyev M.F.[1]*, Xuduzadə Ə.İ.[2], Axundov Ş.X.[1], Axundova X.R.[1]
[1] SOCAR, "Neftqazelmitədqiqatlayihə" İnstitutu, Azərbaycan
AZ1122, Bakı, H.Zərdabi küç., 88a
[2] SOCAR, "AzNeft" İB, Azərbaycan
AZ1000, Bakı, Neftçilər prosp., 73
**Yazışmalara məsul: mushfiq.taghiyev@socar.az*

Xülasə. Bu günə qədər Orta Kür çökəkliyinin çöküntü qatının dərinlik quruluşu seysmik tədqiqatlar vasitəsilə əhəmiyyətli dərəcədə dəqiqləşdirilmişdir. Seysmik zondlama vasitəsilə çoxsaylı struktur qalxımlar aşkar edilmiş və onların qapanma konturları müəyyən edilmişdir. Bu qalxımların sahəsi bir neçə kvadrat kilometrdən onlarla kvadrat kilometrə qədər dəyişir. Əvvəllər məlum olan strukturların çox hissəsinin mövcudluğu təsdiqlənsə də, onların bir qisminin əvvəlki struktur interpretasiyaların nəticələri ilə müqayisədə əhəmiyyətli dərəcədə kiçik sahəyə malik olduğu müəyyən edilmişdir. Bəzi hallarda əvvəllər qapalı sayılan müsbət struktur elementlər yeni interpretasiyada struktur çıxıntılar kimi şərh edilmiş və ya ümumiyyətlə öz təsdiqini tapmamışdır. Aşkar edilmiş strukturların sahəvi xüsusiyyətləri, ehtimal olunan rezervuarların qalınlığı, onların flüid tutum xassələri və proqnozlaşdırılan yığımların karbohidrogen faza halı nəzərə alınmaqla, C3 kateqoriyalı perspektiv resursların hesablanması həyata keçirilmişdir. Beləliklə, indiyədək qazma ilə əhatə edilməmiş struktur qalxımların perspektiv horizontları üçün C3 kateqoriyalı karbohidrogen resursların qiymətləndirilmə imkanı əldə edilmişdir. Məqalədə Orta Kür çökəkliyində neftqazlılığı təsbit edilmiş Paleogen və Təbaşir çöküntü intervalları üçün perspektiv neft və qaz resurslarının proqnozu təqdim olunur. Kür-Qabırrı çaylararası, Gəncə və Muradxanlı neftli-qazlı rayonlarının bir sıra perspektivli strukturları üçün C3 kateqoriyalı resursların qiymətləndirilməsi ümumilikdə 57 sahəni əhatə etmişdir. Baxılan rayonları müqayisə etdikdə perspektiv resursların müxtəlif dərinlik intervalları üzrə paylanma mənzərəsində aydın fərqlilik aşkar şəkildə görünməkdədir. Neft-qaz resurslarının ən böyük həcmləri 3-4 km dərinliklərə aid olduğu halda, stratiqrafik paylanma baxımından ən böyük resurs miqdarı Eosen kompleksinin payına düşür.

Açar sözlər: *Orta Kür çökəkliyi, neftqazlılıq, neft və qazın perspektiv resursları, C3 kateqoriyası*

ANAS Transactions Earth Sciences 1 / 2026

http://www.journalesgia.com

АНАЛИЗ ФИЗИКО-ХИМИЧЕСКИХ ХАРАКТЕРИСТИК ПОЛИМЕРОВ ДЛЯ ПОВЫШЕНИЯ НЕФТЕОТДАЧИ НА ПРИМЕРЕ ЭМБИНСКИХ МЕСТОРОЖДЕНИЙ

Досказиева Г.Ш.[1], Бисенгалиев М.Д.[1]*, Абдешова Г.Г.[1], Тулегенова О.Ш.[1], Пиривердиев И.А.[2]

[1]Атырауский университет нефти и газа им. С.Утебаева, Республика Казахстан
060027, г. Атырау, ул. М.Баймуханова, 45а
[2]Министерство науки и образования Республики Азербайджан,
Институт нефти и газа, Азербайджан
AZ1000, Баку, ул. Ф.Амирова, 9
**Автор, отвечающий за переписку: maks_bisengali@mail.ru*

ANALYSIS OF PHYSICOCHEMICAL CHARACTERISTICS OF POLYMERS FOR ENHANCED OIL RECOVERY (THE EMBA FIELDS AS CASE STUDY)

Doskaziyeva G.Sh.[1], Bisengaliyev M.D.[1]*, Abdeshova G.G.[1], Tulegenova O.Sh.[1], Piriverdiyev I.A.[2]
[1]Atyrau University of Oil and Gas named after S.Utebayev, Republic of Kazakhstan
45a, M.Baimukhanov str., Atyrau city, 060027
[2]Ministry of Science and Education of the Republic of Azerbaijan, Institute of Oil and Gas, Azerbaijan
9, F.Amirov str., Baku, AZ1000
**Corresponding author: maks_bisengali@mail.ru*

Keywords: *oil field, polymer, viscosity, permeability, reservoir pressure maintenance, displacement coefficient*

Summary. The efficiency of water flooding systems in oil reservoirs using advanced stimulation technologies largely depends on the quality of site selection. Each site requires an individual approach based primarily on methodologies that define areas of effective technology application, which in turn are determined by the geological and physical characteristics of the productive formations, optimal technological parameters of well operations, technical capabilities, and economic feasibility. To address this challenge, the development of new reagents that can significantly increase the oil recovery factor (ORF) at already developed fields is highly relevant. This paper presents detailed results of laboratory research on the selection of polymers. Preparation of selected polymers for laboratory experiments was conducted using both synthetic water models and formation water samples collected from the field. Special attention was paid to the chemical composition of the formation water, as water viscosity is highly dependent on mineralisation. To study the criteria for polymer flooding and assess its effectiveness, Field "X" (a conditionally designated name) was selected. Additionally, the main properties of polymer compositions for the conditions of Fields "X" and "Y" were studied. Based on laboratory studies, a technology was developed and pilot-industrial tests were conducted in real wells of Fields "X" and "Y." Among the polymers studied, Flopaam 5115VHM was found to be the most suitable for Field "X" in terms of solubility and viscosity, while FP5205 VHM and FC 6725 were identified as optimal for Field "Y."

Введение

Как известно, одним из высокоэффективных методов физико-химического воздействия на продуктивный пласт является полимерное заводнение. Вопросам полимерного заводнения посвящены многочисленные труды ученых. Несмотря на большое количество накопленных к настоящему времени исследований, все же вопросы, связанные с применением полимерных систем, являются актуальными, требуя проведения экспериментальных исследований реологических характеристик различных полимеров с учетом геолого-физических характеристик рассматриваемого месторождения. В связи с этим в представленной статье приведены подробные результаты лабораторных исследований по подбору полимеров. Подготовка выбранных полимеров для лабораторных исследований прово-

дилась как на моделях синтезированной воды, так и на образцах пластовой воды, доставленных с месторождения.

Особое внимание уделялось химическому составу пластовой воды, так как вязкость воды значительно зависит от минерализации. Для наиболее обоснованной постановки исследований необходимо было провести анализ исследований, выполненных в этом направлении в различных научных и проектных организациях.

Анализ современного состояния изученности технологии применения различных полимерных систем

Технология полимерного заводнения успешно применяется ТОО «Алстрон» на месторождении «Y» с 2014 года. Проект по полимерному заводнению был начат на основании проекта «Разработка проекта полимерного заводнения и проведение лабораторных исследований для подбора полимера», составленного ТОО НИИ «КаспийМунайГаз». Опытно-промышленные испытания были начаты 22.11.2014 года. В сентябре 2017 года было осуществлено расширение проекта с охватом всего III блока II неокомского горизонта. Применение технологии позволило получить более 60 тысяч тонн дополнительно добытой нефти (Report of the Open Joint-Stock Company “Giprovostokneft”, 2006; Report of Caspian Energy Research LLP, 2010; Report of Caspian Energy Research LLP, 2009; Report of Rİ "Kaspiymunaygas" LLP, 2017; Report of Rİ Kaspiymunaygas LLP, 2016; Caspian Energy Research LLP, 2009).

Применение полимеров с целью повышения эффективности разработки осуществлялось в различных регионах, в частности, на многих объектах США, Канады, Венесуэлы, Аргентины, России, Азербайджана, Казахстана (Manyrin, Shvetsov, 2002; Grigorashchenko et al., 1978; State Standard 153.0-75 – State Standard 21153.7-75, 1975; State Standard 21534-76, 1976; State Standard 26450.0-85, 1985; Gazizov, 2002). Как показывает анализ, полимеры обычно применяются на месторождениях с обводненностью 95%, при этом обеспечивается прирост КИН до 10% (Gallyamov, Rakhimkulov, 1978; Delamaide E. et al., 2014; Surguchev, 1985; Chang et al., 2006; Wang et al., 2008; Surguchev et al., 1991; Saboorian-Jooybari et al., 2015; Abasov et al., 2009).

Основным методом искусственного воздействия на нефтяные пласты является заводнение, и одним из способов повышения его эффективности считается применение физико-химических способов воздействия на пласт путем добавок к закачиваемой воде различных компонентов, улучшающих ее нефтевытесняющие свойства. Данному вопросу посвящены многочисленные исследования. Среди них следует отметить публикации последних лет (Delamaide E. et al., 2014; Chang et al., 2006; Saboorian-Jooybari et al., 2015; Abasov et al., 2009; Moldabayeva et al., 2023a; Moldabayeva et al., 2023b). Результатом внедрения данной технологии, как отмечается в этих работах, является:

- перераспределение фильтрационных потоков по площади и разрезу обрабатываемого участка залежи;
- сдерживание прорыва вод из нагнетательных в добывающие скважины;
- подключение в разработку трудноизвлекаемых запасов из зон с пониженной проницаемостью.

Исследованиями (Abasov et al., 2009; Moldabayeva et al., 2023a; Moldabayeva et al., 2023b) установлено, что на реологические характеристики осадкогелеобразующих составов оказывают влияние как компоненты, входящие в них, так и степень минерализации пластовой воды. В пресной воде в связи с отсутствием ионов кальция и магния полимеры обладают хорошей растворимостью и способностью увеличения вязкости растворов. С увеличением концентрации вытесняющего агента вязкость растворов возрастает. Следует отметить, что физико-химические свойства и реологические особенности осадкогелеобразующих составов (ОГОС) зависят от концентраций полимера и щелочи, температуры и минерализации воды, причем при малых концентрациях полимера состав проявляет ньютоновский характер (Moldabayeva et al., 2023a; Moldabayeva et al., 2023b; Zhdanov, 2001).

Таким образом, подводя итог анализу современного состояния применения полимерных материалов при разработке месторождений, можно прийти к следующим выводам, которые позволят обоснованно направить исследования.

Следует отметить, что недостаточно проработана методология создания основы системы, позволяющей проводить комплекс теоретических, экспериментальных исследований и промысловых наблюдений для наиболее глубокого изучения условий и результатов водопроявлений; отмеченное обстоятельство существенно затрудняет процесс принятия адекватных решений по выбору технологии ограничения водопритоков.

Обзор публикаций, накопленных к настоящему времени и посвященных вопросам применения ОГОС, подтвердил значимость и важность отмеченных исследований, направленных на принятие решений при реализации методов повышения нефтеотдачи. Для принятия наиболее

правильных и обоснованных технологических решений при мероприятиях, связанных с применением полимерных композиций, необходимы: анализ геолого-физических условий и особенностей рассматриваемого месторождения и факторов, оказывающих влияние на выбор эффективной технологии, в частности, водоизоляционных работ; планирование и проведение экспериментальных исследований по изучению эффекта изоляции полимерными растворами.

Решение отмеченных задач, причастных к выбору наилучших композиций и технологий их применения, требует анализа и построения моделей, адекватно описывающих объективные связи между исследуемыми параметрами и позволяющих в дальнейшем успешно осуществлять принятие технологических решений. В этой связи получение, анализ информации и принятие решений в отмеченных условиях представляют интерес, что в свою очередь требует проведения исследований по изучению закономерностей изменения вязкостных характеристик полимерных растворов в зависимости от концентрации полимерных композиций.

Условия применения полимерного заводнения на некоторых месторождениях

Как известно, основными критериями для выбора потенциальных участков для полимерного заводнения являются:

- удовлетворительное техническое состояние действующих скважин (в первую очередь нагнетательных);
- правильная оценка начальных и текущих геологических запасов нефти;
- энергетическое состояние на уровне начального или близкого к нему;
- сформированный девятиточечный элемент с небольшим расстоянием между нагнетательной и добывающими скважинами (+200 метров);
- хорошая гидродинамическая связь между нагнетательной и добывающими скважинами;
- расположение участков в сводовой части нефтеносной залежи.

С учетом перечисленных критериев полимерное заводнение было предусмотрено на месторождениях, условно именованных как «X» (M-II горизонт) и «Y» (II неокомский горизонт). Основные геолого-физические характеристики эксплуатационных объектов по месторождениям представлены в таблице 1.

Материалы и методы

Для системы поддержания пластового давления (ППД) и приготовления полимеров для закачки на рассматриваемых месторождениях используют попутно добываемую воду.

Для проведения анализа с резервуарного парка были отобраны пробы и изучены в лаборатории исследования нефти, газа и воды, результаты приведены в таблице 2.

Подбор применяемого полимера основывался на 3-х основных параметрах:

1. Температура пласта, необходимая для выбора полимера, должна оставаться стабильной в течение процесса вытеснения нефти в пласте;

2. Минерализация пластовой воды, применяемой для закачки, необходима с целью оценки степени гидролиза различных полимеров для увеличения вязкости (Abirov et al., 2022).

Таблица 1

Исходная геолого-физическая характеристика выделенных объектов для закачки полимера

Параметры	«X», M-II	«Y», Неоком II
Средняя глубина залегания, м	258.7	942
Тип коллектора	терригенный	терригенный
Пористость по ГИС, д.ед.	0.36	0.303
Средняя нефтенасыщенность по ГИС, д.ед.	0.669	0.638
Проницаемость по керну, мкм2	0.748	0.526
Начальная пластовая температура, ^{0}C	19.8	39
Начальное пластовое давление, МПа	1.82	9.18
Давление насыщения нефти газом, МПа	0.98	5.4
Вязкость нефти в пластовых условиях, мПа*с	130	15.3
Плотность нефти в пластовых условиях, г/см^3	0.875	0.811
Плотность нефти в поверхностных условиях, г/см^3	0.908	0.895
Вязкость пластовой воды, мПа*с	1.3	1.6
Плотность пластовой воды, г/см^3	1.12	1.092
Общая минерализация пластовой воды, г/л	135.6	141.5

Учитывая все три параметра по выделенным объектам для закачки полимера, с помощью таблицы 3 был сформирован основной состав кандидатов-полимеров (State Standard 21 153.0-75 – State Standard 21153.7-75, 1975; State Standard 21534-76, 1976; State Standard 26450.0-85, 1985).

Лабораторные работы по подбору полимеров проводились на синтезированной модели воды. Подготовка выбранных полимеров для лабораторных исследований велась как на моделях синтезированной пластовой воды, так и на образцах пластовой воды, доставленной с месторождения.

Изготовление модели пластовой воды осуществлялось на основе химического состава пластовой воды, с использованием видов компонентов солей (таблица 4).

Таблица 2

Результаты анализа воды для применения закачки месторождений «X» и «Y»

Показатели	Ед. изм.	«X», M-II	«Y», Неоком II
Количество проб		1	1
Дата поступления воды в лабораторию		11.03.14г	24.02.14г
Дата анализа		12.03.14г	
Гидрокарбонат-ион HCO_3^-	мг/л	256.00	232.00
Хлорид –ион Cl^-	мг/л	83437.00	83437.00
Сульфат-ион SO_4^{2-}	мг/л	Отс	Отс
(Натрий+калий) ион $Na^+ + K^+$	мг/л	46856.00	47996.00
Кальций-ион Ca^{2+}	мг/л	2906.00	2806.00
Магний-ион Mg^{2+}	мг/л	2128.00	1581.00
Общая минерализация	мг/л	135583.00	136052.00
Йод J^-	мг/л	0.02	0.53
Бром Br^-	мг/л	14.50	3.52
Жесткость общая	мг-экв/л	320.00	270.00
Сухой остаток	мг/л	-	136553.00
Нефтепродукты	мг/л	36.00	1.2
Механические примеси	мг/л	Отс	Отс
Сероводород H_2S	мг/л	Отс	Отс
Плотность при 20^0C	г/см^3	1.0911	1.0920
Соленость	^{0}Be	12.3	12.4
pH	ед. pH	6.72	6.20

Таблица 3

Руководство по выбору полимера

Форма	**Тип полимера**	**Мономер**	**Наименование полимера**	**Параметры**
Порошок	Сополимер	Акриламид – Акрилат натрия	Flopaam 3630S	T<80°C Средняя жесткость
	Сополимер После гидролиза	Акриламид – Акрилат натрия	Flopaam 6030S	T<75°C Низкая жесткость
	Сополимер	Акриламид – АТБС	Flopaam AN125SH	T<95°C Любой уровень минерализации
	Терполимеры	Акриламид - Акрилат натрия – АТБС	Flopaam 5205SH Flopaam 5115SH	T<90°C Любой уровень минерализации
	Ассоциирован-ные полимеры	Акриламид – Акрилат натрия – гидрофобный мономер	Superpusher C319	Относительно низкая проницаемость породы Средняя жесткость
	Терполимеры	Акриламид - АТБС - НВП	Flopaam SAV225	T<140°C Любой уровень минерализации
Жидкая эмульсия нефть/ вода	Сополимеры	Акриламид - Акрилат натрия	Flopaam EM533	T<80°C Средняя жесткость

Таблица 4

Необходимое количество солей для изготовления модели пластовой воды

	Наименование солей	«X», M-II	«Y», Неоком II
		г/л	
1	Бикарбонат натрия ($NaHCO_3$)	0.352	0.319
2	Карбонат натрия (Na_2CO_3)	-	-
3	Бромид натрия (NaBr)	0.019	0.005
4	Сульфат натрия (Na_2SO_4)	-	-
5	Хлористый магний ($MgCl_2*6H_2O$)	17.8	13.224
6	Хлорид кальция ($CaCl_2$)	8.047	7.77
7	Хлорид натрия (NaCl)	118.857	121.786

Особое внимание уделяется химическому составу пластовой воды, так как вязкость воды является зависимой от минерализации. Подготовка модели пластовой воды происходила исходя из массы.

Наиболее подходящий для месторождения полимер выбирался по следующим параметрам (Abirov et al., 2022):

- Хорошая растворимость в пластовой воде;
- Самая высокая вязкость при заданной концентрации;
- Хорошая стабильность;
- Экономические параметры.

Для отбора по вышеперечисленным параметрам нужного полимера из числа кандидатов необходимо было провести испытания с каждым из них. После достижения хорошей растворимости второй задачей является получение необходимой вязкости полимера. Следует отметить, что полимерное заводнение представляет собой закачку воды, загущенной синтетическими полимерами с целью повышения ее вязкости. Данная обработка воды приводит к изменению реологических характеристик, вязкости, обуславливая ее увеличение при равных скоростях закачки, а следовательно, и снижение подвижности воды. При этом одним из важных показателей является коэффициент мобильности M, представляющий собой отношение подвижности вытесняющей жидкости (т.е. воды) к подвижности вытесняемой жидкости (нефти) (Al-Shakry et al., 2018):

$$M = \frac{\lambda_0}{\lambda_\omega} = \frac{\mu_0/k_0}{\mu_\omega/k_\omega} = \frac{\mu_0 * k_\omega}{\mu_\omega * k_0}, \qquad (1)$$

где λ, μ и k – соответственно мобильность, вязкость и эффективная проницаемость относительно воды и нефти.

Для объекта закачки полимера на месторождении «X» выделены 2 вида полимера по 2 модификациям:

1. Flopaam 5205SH и Flopaam 5205VHM: терполимеры акриламида, акриловая кислота и АТБС;
2. Flopaam 5115SH и 5115VHM: терполимеры акриламида, акриловая кислота и АТБС с более высоким содержанием.

Для «Y» был выбран ряд полимеров:

1. Flopaam 3630S: сополимер акриламида и акриловая кислота;
2. Flopaam 6030S: сополимер акриламида и акриловая кислота, после гидролиза;
3. Flopaam 5115VHM, Flopaam 5205SH, Flopaam 5205VHM: терполимеры акриламида, акриловая кислота и АТБС;
4. Superpusher C1205: ассоциированный полимер (содержащий как гидрофобные, так и гидрофильные составляющие);
5. FLOCOMB 6725: продукт пост-гидролиза с характерным солестойким мономером;
6. Flopaam AN110VHM: сополимер акриламида и сульфированный мономер.

Результаты исследований обрабатывались методами математической статистики.

Результаты исследований

Результаты практической реализации получены на двух месторождениях, названия которых по известным причинам не приводим. Так, на месторождениях «X» и «Y», где вязкость нефти примерно 130 сП и 13,8 сП соответственно, величина коэффициента подвижности не является благоприятной. Из этого следует, что увеличение вязкости воды позволит улучшить коэффициент охвата пласта заводнением.

На синтезированной пластовой воде были приготовлены стандартные растворы с концентрацией 10000 ppm (долей на миллион). Затем в зависимости от пластовой температуры («X» M-II – 19^0C, «Y» Неоком II – 39^0C) были проведены исследования по оценке вязкости как функции от концентрации полимера. Величина вязкости измерялась на вискозиметре Brookfield со скоростью вращения шпинделя UL 6 об/мин (соответствует скорости сдвига в 7.34 с-1). После 2-х часового растворения независимо от используемого полимера не было замечено образование комков, фильтрация с целью проверки

степени гидратации также дала положительный результат (Рис. 1). По результатам исследований строились зависимости вязкости полимерного раствора от концентрации полимера. Результаты подвергнуты статистической обработке с оценкой числа необходимых повторных опытов и построением эмпирических частных зависимостей, приведенных в таблице 5.

Построенная зависимость вязкости от концентрации представлена на рисунках 2 и 3.

Из исследованных полимеров для месторождения «X» наиболее подходящим по высоким показаниям растворимости и вязкости оказался полимер Flopaam 5115VHM. Этот полимер позволяет получить самую высокую вязкость при концентрации 2000 ppm, которая могла бы стать хорошим целевым значением для данного параметра.

В качестве подходящих вариантов для одного из месторождений («Y») были отобраны полимеры Flopaam 5205VHM и FLOCOMB 6725. Необходимая концентрация активного полимера составит примерно 1500 ppm, что соответствует вязкости 13 сП для Flopaam 5205VHM и 16.5 сП для FLOCOMB 6725 (Zhdanov, 2001; Kukin, Solyakov, 1982).

Рис. 1. Остатки полимера после фильтрации

FLOCOMB 6725 – высокомолекулярный полимер, и целевое значение вязкости может быть достигнуто при более низких концентрациях, как видно из рисунка 3.

Таблица 5

Вязкость полимерных составов, концентрации полимеров и взаимосвязь между ними при различных температурах

C, %	FC6725	FP3630S	FP5205VHM	FP6030S	FP5205SH	SP C1205	AN110VHM	FP5115VHM
t = 39 °C								
0.05	2.5	2.5	4	3	3	3	3,5	4
0.1	10	5	5	5	7	12	7	8
0.15	17	8	12	11	13	16	14	14
0.2	26	15	20	18	19	23	22	22
0.25	48	26	31	29	28	39	37	36
0.3	72	42	50	48	39	61	53	52
v =	$571.5C^{1,81}$	$206.42C^{1,55}$	$219.65C^{1,45}$	$241.36C^{1,55}$	$199.29C^{1,42}$	$349.68C^{1,57}$	$285.32C^{1,53}$	$243.11C^{1,42}$
t = 19 °C								
C, %	**FP 5115 SH**		**FP 5115 VHM**		**FP 5205 SH**		**FP 5205 VHM**	
0.05	4		4		4		4	
0.1	7		9		7		8	
0.15	12		16		12		14	
0.2	20		28		20		24	
0.3	45		58		47		53	
0.4	77		108		88		111	
0.5	127		165		137		162	
v =	$292.78C^{1,54}$		$425.71C^{1,66}$		$329.09C^{1,59}$		$444.77C^{1,65}$	

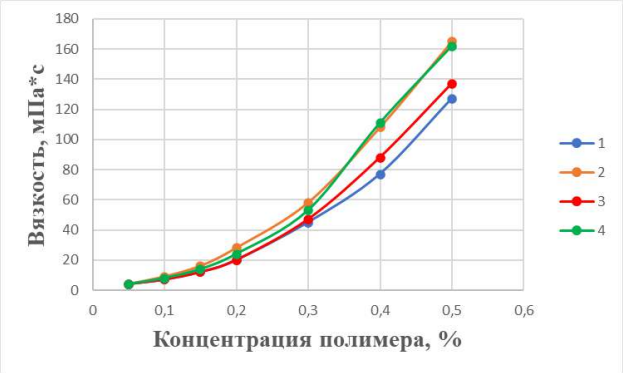

Рис. 2. Вязкость различных полимеров как функция от концентрации в пластовых водах месторождения «X» при температуре 19°C:
1 - FP 5115 SH; 2 - FP 5115 VHM;
3 - FP 5205 SH; 4 - FP 5205 VHM

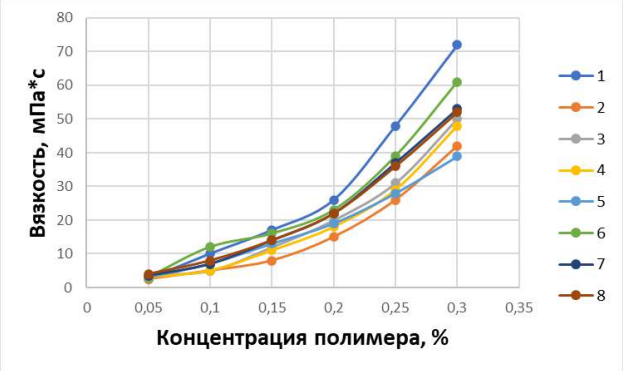

Рис. 3. Вязкость различных полимеров как функция от концентрации в пластовых водах месторождения «Y» при температуре 39°C:
1 - FC6725; 2 - FP3630S; 3 - FP5205VHM; 4 - FP6030S;
5 - FP5205SH; 6 - SP C1205; 7 - AN110VHM; 8 - FP5115VHM

Анализ и обсуждение результатов

Окончательный выбор полимеров для месторождений «X» и «Y» основывался на химической и термической стабильности молекулярной характеристики. Все выбранные полимеры по характеристике соответствуют условиям данных месторождений. В таблице 6 приведены основные характеристики выбранных полимеров для дальнейшего их применения при закачке.

Для оценки эффективности закачки полимера были проведены прогнозные расчеты показателей разработки эмпирическими зависимостями на участках скважин №№ 1242-1244 и №№ 1225-1227-1229 месторождения «X» (Report of the Open Joint-Stock Company "Giprovostokneft", 2006; Report of Rİ "Kaspiymunaygas" LLP, 2017; Report of Rİ Kaspiymunaygas LLP, 2016).

Для каждого участка рассчитаны по 2 варианта разработки. Начало полимерного заводнения было запланировано с 01.04.2019 г. Все варианты разработки были спрогнозированы до 31.03.2024 г.

Первый вариант базовый – разработка месторождения без полимерного заводнения на опытном участке с учетом сложившегося на данный момент количества действующего фонда участка с закачкой воды в нагнетательные скважины.

Второй вариант с полимерным заводнением разработки включает в себя проведение мероприятий по полимерному воздействию на опытном участке с учетом сложившегося на данный момент количества действующего фонда участка с закачкой полимера в нагнетательные скважины.

Для оценки эффективности в качестве базового варианта используется эмпирическая модель разработки, выбранная из совокупности характеристик вытеснения, построенная до проведения мероприятия (за период, выбранный в качестве базы сравнения). Дополнительная добыча нефти оценивается как разность между фактическим объемом добытой нефти (или прогнозным объемом добытой нефти при полимерном заводнении) и количеством нефти, которое могло бы быть добыто при базовом режиме разработки.

Таблица 6

Характеристики полимеров X и Y

Полимер	FP5115 VHM	FP5205 VHM	FC6725
Партия	RG 2617/1-3	X 4372	FGR 2159-7
Сверхнизкая вязкость	6.3	6.15	7.16
Содержание твердых веществ	91.4%	89.2%	89.28%
Степень гидролиза	20-30%	20-30%	20-30%
Молекулярный вес	15-17*10^6 Да	14-16*10^6 Да	19-21*10^6 Да
Содержание нерастворимых веществ	0.01%	0.02%	0.01%
Время растворения	<2ч	<2ч	<2ч
Содержание остаточного мономера	<0.1%	<0.1%	<0.1%

Общие положения для прогноза вариантов разработки:

Для прогнозирования данных используется имеющийся 4-х летний опыт применения полимерного заводнения в Мангистауской области на месторождении «Z», а именно динамика обводненности участка скважин №№ 2041-2049 «Запад» до заполнения 9,5% порового объема. Прогнозный суточный объем закачки воды при базовом варианте разработки принимается как среднее значение суточной закачки в период аппроксимации (в базовый период). При увеличении закачки воды вероятны прорывы к добывающим скважинам. В случае полимерного заводнения такие прорывы маловероятны.

Прогнозный суточный объем закачки полимерного раствора увеличен относительно базового варианта: по участку №№ 1242-1244 в сумме на величину 37 м^3/сут; по участку №№ 1225-1227-1229 в сумме на величину 56 м^3/сут. Прогнозная жидкость при базовом варианте разработки принимается как среднее значение в период аппроксимации (базовый период).

Прогнозная жидкость при варианте разработки с полимерным заводнением увеличена относительно базового варианта на величину увеличенной закачки. При этом в первые 4 месяца закачки предусмотрено плавное увеличение жидкости. Начало подсчета технологического эффекта – с апреля 2019 года, т.е. с начала закачки полимера на опытном участке. Для приготовления полимерного раствора необходимо использовать артезианскую слабоминерализованную воду. Необходимая концентрация полимера составит 2000 г/м^3, обеспечивая вязкость 44 сП. С целью увеличения эффективности технологии предусматривается изменение концентрации полимерного раствора с 2000 до 3000 г/м^3, обеспечивая вязкость 95 сП. Длительность закачки высоковязкой оторочки ежегодно составит 1 квартал.

Прогноз обводненности при полимерном заводнении на участке скважин №№ 1242-1244 выполнен исходя из динамики обводненности участка «Запад» месторождения «Z» до заполнения 9,5% порового объема. Фактическая обводненность участка «Запад» месторождения «Z» описана логарифмическим уравнением, далее рассчитано процентное изменение обводненности относительно предыдущего месяца. От полученной зависимости рассчитана прогнозная обводненность участка скважин №№ 1242-1244, которая опирается на заполнение порового пространства участка «Запад». Далее обводненность участка скважин №№ 1242-1244 описана зависимостями, приведенными ниже с целью дальнейшего прогнозирования зависимости обводненности от заполнения порового пространства участка скважин №№ 1242-1244. Кривые зависимости обводненности от степени заполнения порового пространства при полимерном заводнении на участке скважин №№ 1242-1244 представлены на рисунках 4 и 5.

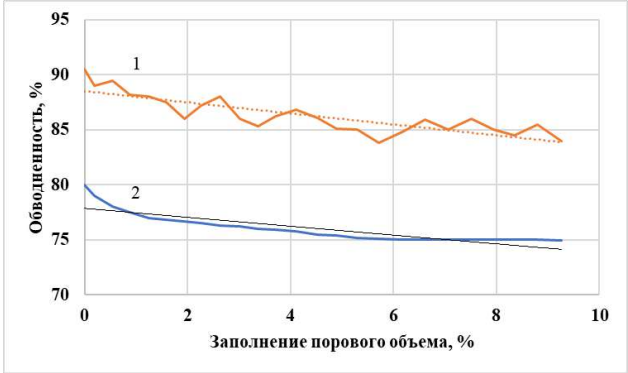

Рис. 4. Зависимости обводненности от степени заполнения порового пространства при полимерном заводнении на участке скважин №№ 1242 (1) и 1244 (2)

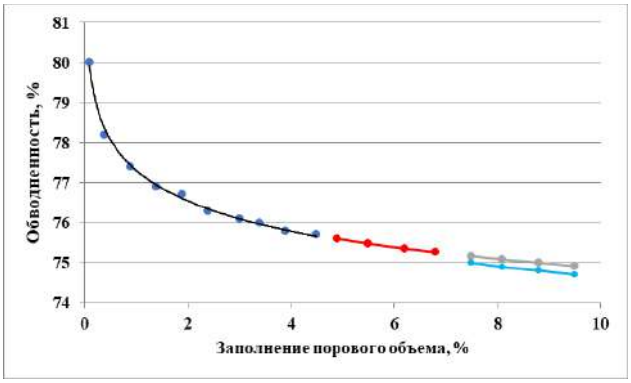

Рис. 5. Зависимость заполнения порового объёма от обводненности при полимерном заводнении на участке скважин №№ 1242-1244

В результате было получено уравнение:

$$y=77{,}311V^{-0{,}014},\ R^2 = 0{,}9973.$$

Условия прогноза при полимерном заводнении следующие:

Полимерный раствор закачивался в 2 действующие нагнетательные скважины №№ 1242 и 1244 с 01.0.4.2019 г. с суточным объемом закачки 50 и 30 м^3/сут соответственно. Данный период условно рассматривается как будущее с позиции предыдущих лет.

Заполнение порового объема при существующих объемах закачки должно составить 4,9% к 31.03.2024 г. Снижение обводненности достигнет 75,5% к 31.03.2024 г. Предполагалось снижение обводненности до 11,3% относительно базовой обводненности. Прогнозная жидкость составляет 3378,91 т/мес + увеличение на суточную добычу 37 т/сут.

На основании вышеизложенных условий прогноза построены графики добычи жидкости, изменения обводненности и добычи нефти по базовому варианту и с полимерным заводнением с закачкой полимера в 2 скважины в зависимости от заполнения порового пространства участка (рисунки 6-7).

Итоговые результаты:

Прогнозная накопленная дополнительная добыча нефти за период 01.04.2019-31.03.2024 гг. должна составить 29,959 тыс. тонн.

КИН на 31.03.2024 г. должен составить:

при полимерном заводнении – 8,3 %;

базовый – 7,05 %;

прирост КИН –1,25%.

Последующий период показал достоверность прогнозов на период, условно выбранный в качестве будущего, т.е. с 01.04.2019 г. до 31.03.2024 г.

Выводы

В результате статистического анализа показана возможность прогнозной оценки вариантов и периода реализации технологии полимерного заводнения, результаты которых позволяют обосновать наиболее эффективные технологические варианты продолжения закачки полимерного раствора на скважинах.

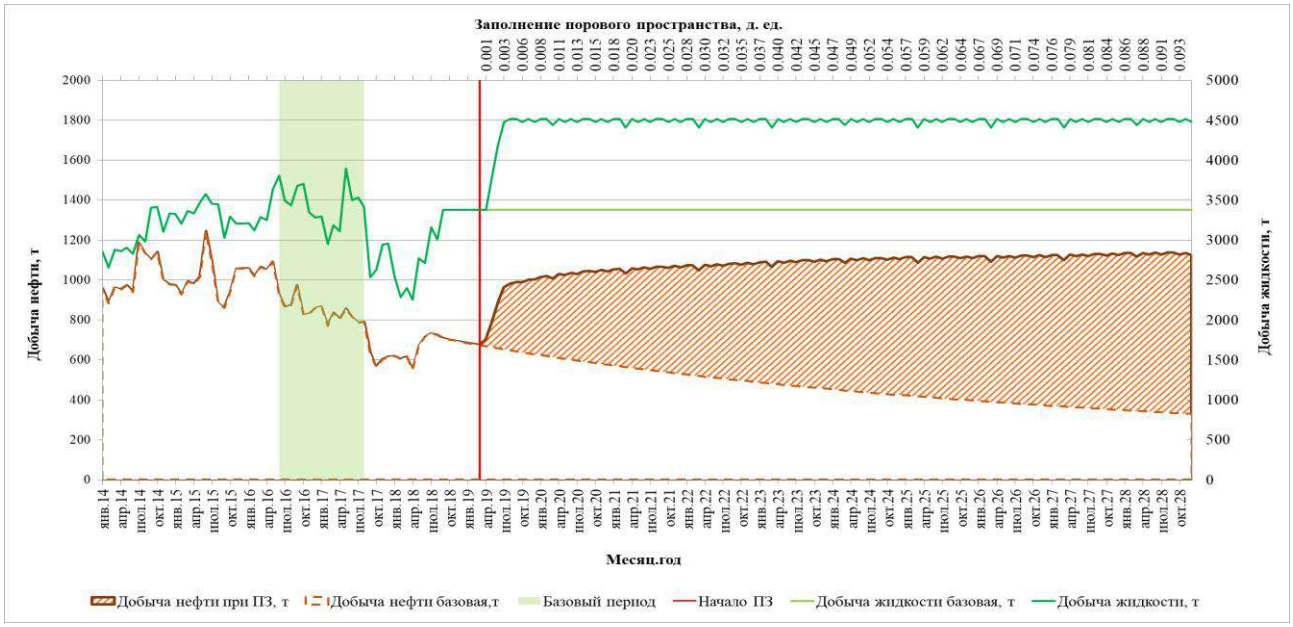

Рис. 6. Прогноз добычи жидкости и добычи нефти с базовым вариантом и с полимерным заводнением на участке скважин №№ 1242-1244

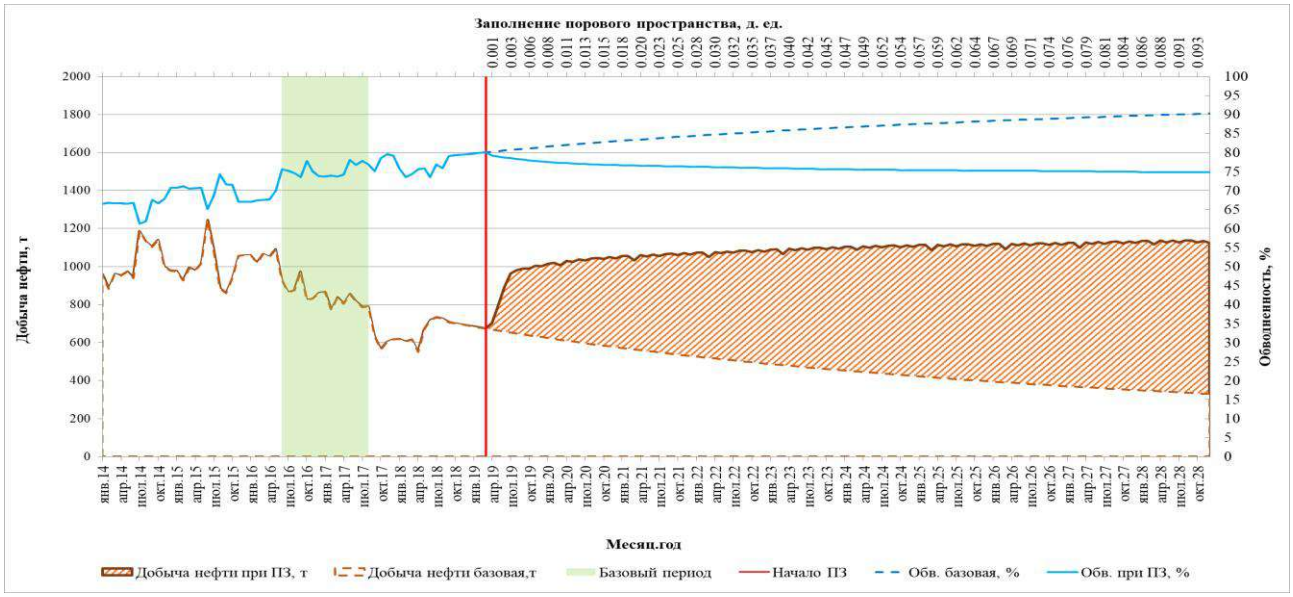

Рис. 7. Динамика изменения обводненности и добычи нефти с базовым вариантом и с полимерным заводнением на участке скважин №№ 1242-1244

Одной из основных задач данных экспериментов является оценка коэффициента вытеснения и, как показывают результаты, в зависимости от коллекторских свойств пород коэффициенты вытеснения при применении полимеров значительно увеличиваются. Результаты реализации мероприятий по вытеснению нефти водой и выбранным полимером на моделях образцов керна и их оценка для применения в дальнейшем на выбранных участках месторождения оправдывают применение полимерного заводнения на рассматриваемом месторождении.

REFERENCES

Abasov MT, Strekov AS, Efendiev GM (2009) Improving the efficiency of water inflow control in oil wells. Nafta-Press, Baku, p 256 (in Russian)

Abirov JJ, Abirov R, Sayuk B et al (2022) Research of the impact of switching to low-salinity water during polymer water flooding Journal of the Oil and Gas Industry of Kazakhstan 4(4):68–77. https://doi.org/10.54859/kjogi108594

Al-Shakry B, Skauge T, Shiran BS, Skauge A (2018) Impact of mechanical degradation on polymer injectivity in porous media. Polymers 10(7):742. https://doi.org/10.3390/polym10070742

Caspian Energy Research LLP “Estimation of oil and soluble gas-in-oil reserves of the Eastern Wing of the Zhanatalap field (Central Arch) as of 01.09.2008”, Atyrau, 2009 (in Russian)

Chang HL, Zhang ZQ, Wang QM et al (2006) Advances in polymer flooding and alkaline/surfactant/polymer processes as developed and applied in the People’s Republic of China. JPT 58(2):84–89. https://doi.org/10.2118/89175-JPT

Delamaide E, Bazin B, Rousseau D, Degré G (2014) Chemical EOR for heavy oil: the Canadian Experience. Paper SPE 169715 presented at the SPE EOR Conference at Oil and Gas West Asia held in Muscat, Oman, 31 March–2 April

Gallyamov MN, Rakhimkulov RS (1978) Improving the operational efficiency of oil wells during the late stage of field development. Nedra, Moscow, p 207 (in Russian)

Gazizov AA (2002) Increase in oil output of heterogeneous layers at the last development stage. Nedra-Businesscentre Ltd, Moscow, p 639 (in Russian)

Grigorashchenko GI, Zaitsev YV, Kukin VV et al (1978) The use of polymers in oil production. Nedra, Moscow, p 213 (in Russian)

Kukin VV, Solyakov YuV (1982) Application of water-soluble polymers for enhancing oil recovery from reservoirs. VNIIOENG, Moscow, p 44

Manyrin VN, Shvetsov IA (2002) Physico-chemical methods for enhancing oil recovery during water flooding. Samara, Rosing.Publ, p 392 (in Russian)

Moldabayeva GZ, Efendiyev GM, Kozlovskiy AL et al (2023a) Modeling and adoption of technological solutions in order to enhance the effectiveness of measures to limit water inflows into oil wells under conditions of uncertainty. ChemEngineering 7(5):89. https://doi.org/10.3390/chemengineering7050089

Moldabayeva GZ, Efendiyev GM, Kozlovskiy AL et al (2023b) Study of the rheological characteristics of sediment-gelling compositions for limiting water inflows. Applied Sciences (Switzerland) 13(18), 10473. https://doi.org/10.3390/app131810473

Report of Caspian Energy Research LLP “Recalculation of oil and gas reserves of the Y field”. Atyrau, 2009 (in Russian)

Report of Caspian Energy Research LLP “Y Field Development Project.” Atyrau, 2010 (in Russian)

Report of Rİ "Kaspiymunaygas" LLP under Contract No. 241-113-58/DGR dated 24.02.2017 "Analysis of the Development of Field X" Atyrau, 2017, p 371 (in Russian)

Report of Rİ Kaspiymunaygas LLP "Analysis of Development of Field X", Atyrau, 2016, p 265 (in Russian)

Report of the Open Joint-Stock Company “Giprovostokneft” under Contract No. 2848/49-17 dated 20 September 2005: “Author’s supervision of the implementation of the technical scheme for the development of the X field”. Samara, 2006 (in Russian)

Saboorian-Jooybari H, Dejam M, Chen Z (2015) Half-century of heavy oil polymer flooding from laboratory core floods to pilot tests and field applications. Paper SPE-174402-MS Canada Heavy Oil Technical Conference, 9-11 June 2015, Calgary, Alberta, Canada. https://doi.org/10.2118/174402-MS

State Standard 21 153.0-75 – State Standard 21153.7-75. Physical testing methods. Sampling and general requirements for physical testing methods (in Russian)

State Standard 21534-76. Petroleum. Method for determining the chloride salt content (in Russian)

State Standard 26450.0-85. Methods for determining reservoir properties. General requirements for the sampling and preparation of samples for the determination of reservoir properties (in Russian)

Surguchev ML (1985) Secondary and tertiary methods for increasing oil recovery from reservoirs. Nedra, Moscow, p 308 (in Russian)

Surguchev ML, Gorbunov AT, Zabrodin DP et al (1991) Methods for the recovery of residual oil. Nedra, Moscow, p 347 (in Russian)

Wang D, Han P, Shao Z et al (2008) Sweep improvement options for the Daqing oil field. SPE Reservoir Eval Eng 11(1):18-26, 25 February. https://doi.org/10.2118/99441-PA

Zhdanov SA (2001) The application of methods to enhance oil recovery: challenges and prospects. Neftyanoye Khozyaystvo 4:11–12 (in Russian)

АНАЛИЗ ФИЗИКО-ХИМИЧЕСКИХ ХАРАКТЕРИСТИК ПОЛИМЕРОВ ДЛЯ ПОВЫШЕНИЯ НЕФТЕОТДАЧИ НА ПРИМЕРЕ ЭМБИНСКИХ МЕСТОРОЖДЕНИЙ

Досказиева Г.Ш.[1], Бисенгалиев М.Д.[1]*, Абдешова Г.Г.[1], Тулегенова О.Ш.[1], Пиривердиев И.А.[2]
[1]Атырауский университет нефти и газа им. С.Утебаева, Республика Казахстан
060027, г. Атырау, ул. М.Баймуханова, 45а
[2]Министерство науки и образования Республики Азербайджан, Институт нефти и газа, Азербайджан
AZ1000, Баку, ул. Ф.Амирова, 9
**Автор, отвечающий за переписку: maks_bisengali@mail.ru*

Резюме. При выборе участков для проведения работ по внедрению систем заводнения пластов, как известно, необходимо к каждому из них подходить индивидуально, руководствуясь при этом соответствующей методикой, которая позволяет определять области эффективного применения технологий, с учетом геолого-физических характеристик продуктивных пластов, технологических параметров работы скважин, а также технических возможностей и экономической целесообразности. Для решения данной проблемы актуальными являются задачи разработки новых реагентов, позволяющих значительно увеличить коэффициент извлечения нефти (КИН) на уже разрабатываемых месторождениях. В статье приведены подробные результаты лабораторных исследований по подбору полимеров. Подготовка выбранных полимеров для лабораторных исследований проводилась как на моделях синтезированной воды, так и на образцах пластовой воды, доставленных с месторождения. При этом особое внимание уделялось химическому составу пластовой воды, так как вязкость воды значительно зависит от минерализации. Для изучения критериев полимерного заводнения и оценки эффективности его применения было выбрано месторождение «X» (наименование условно присвоенное). Также были изучены основные свойства полимерной композиции для условий месторождений «X» и «Y». На основании лабораторных исследований была разработана технология и проведены опытно-промышленные испытания на реальных скважинах месторождения «X» и «Y». Из исследованных полимеров для месторождения «X» наиболее подходящим по показаниям растворимости и вязкости оказался полимер Flopaam 5115VHM, а для месторождения «Y» – полимеры FP5205 VHM и FC 6725. Последующий период показал достоверность прогнозов на период, условно выбранный в качестве будущего, т.е. с 01.04.2019 г. до 31.03.2024 г.

Ключевые слова: *месторождение, полимер, вязкость, проницаемость, поддержание пластового давления, коэффициент вытеснения*

EMBA YATAQLARI TİMSALINDA NEFT VERİMİNİN ARTIRILMASI ÜÇÜN İSTİFADƏ OLUNAN POLİMERLƏRİN FİZİKİ-KİMYƏVİ XÜSUSİYYƏTLƏRİNİN TƏHLİLİ

Doskaziyeva G.Ş.[1], Bisenqaliyev M.D.[1]*, Abdeşova G.G.[1], Tulegenova O.Ş.[1], Piriverdiyev İ.A.[2]
[1]S. Ötebayev adına Atırau Neft və Qaz Universiteti, Qazaxıstan Respublikası
060027, Atırau şəhəri, M.Baymuxanov küçəsi, 45a
[2]Azərbaycan Respublikası Elm və Təhsil Nazirliyinin Neft və Qaz İnstitutu, Azərbaycan
AZ1000, Bakı, F.Əmirov küç., 9
**Yazışmalara məsul: maks_bisengali@mail.ru*

Xülasə. Lay sulaşdırma sistemlərinin tətbiqi üçün sahələrin seçilməsi zamanı, məlum olduğu kimi, hər bir sahəyə fərdi yanaşmaq, bu texnologiyaların effektiv tətbiqi üçün sahələri müəyyən etməyə imkan verən müvafiq metodologiyaya əsasən, hasilat laylarının geoloji və fiziki xüsusiyyətlərini, quyuların iş parametrlərini, eləcə də texniki imkanları və iqtisadi məqsədəuyğunluğu nəzərə almaq vacibdir. Bu məsələni həll etmək üçün mövcud yataqlarda neftvermə əmsallarını (NÇ) əhəmiyyətli dərəcədə artıra bilən yeni reagentlərin hazırlanması vacibdir. Bu məqalədə polimerlərin seçilməsi üzrə laboratoriya tədqiqatlarının ətraflı nəticələri təqdim olunur. Laboratoriya tədqiqatları üçün seçilmiş polimerlər həm sintez edilmiş su modelləri, həm də yataqdan gətirilən hasilat suyu nümunələri istifadə edilərək hazırlanmışdır. Suyun özlülüyü duzluluqdan əhəmiyyətli dərəcədə asılı olduğundan, hasil suyunun kimyəvi tərkibinə xüsusi diqqət yetirilmişdir. Polimer daşqınlarının meyarlarını öyrənmək və onun effektivliyini qiymətləndirmək üçün "X" (yatağın şərti adı) sahəsi seçilmişdir. "X" və "Y" yataqlarının şərtləri üçün polimer tərkibinin əsas xüsusiyyətləri də öyrənilmişdir. Laboratoriya tədqiqatlarına əsasən, "X" və "Y" yataqlarındakı real quyularda bir texnologiya hazırlanmış və pilot sınaqlar aparılmışdır. Tədqiq olunan polimerlərdən Flopaam 5115VHM həllolma və özlülük baxımından "X" sahəsi üçün ən uyğun, FP5205VHM və FC 6725 isə "Y" sahəsi üçün ən uyğun olduğu sübut edilmişdir. Növbəti dövr üçün (01.04.2019 - 31.03.2024) aparılmış "ekstrapolyasiya" hesablamaları proqnozların mötəbər olduğunu təsdiqlənmişdir.

Açar sözlər: *sahə, polimer, özlülük, keçiricilik, lay təzyiqinin saxlanılması, yerdəyişmə səmərəliliyi*

ANAS Transactions Earth Sciences 1 / 2026

http://www.journalesgia.com

HYDROCARBON EXPLORATION AND RESOURCE BASE DEVELOPMENT IN THE REPUBLIC OF UZBEKISTAN: HISTORICAL TRENDS AND FUTURE PERSPECTIVE

Bogdanov A.N.*, Karshiyev O.A., Khmirov P.V.

Institute of Geology and Exploration of Oil and Gas Deposits, Republic of Uzbekistan
64, Olimlar Street, Mirzo Ulugbek District, Tashkent, 100164
**Corresponding author: bogdalex7@yandex.ru*

Keywords: *oil, gas, hydrocarbons, geological exploration, resources, reserves*

Summary. The paper presents the results of a comprehensive analysis of oil and gas prospecting and exploration activities in the Republic of Uzbekistan from the late 19th century to 2025. The study aims to identify the main patterns in the development of the geological exploration sector, assess the efficiency of hydrocarbon resource base replenishment, and determine the prospects for further reserve growth. The research is based on official statistical data, archival materials and results of geological exploration activities conducted during different periods. The dynamics of key production and geological indicators were analysed, including exploration drilling volumes, preparation of structures for deep drilling, oil and gas reserve growth, and the efficiency of exploration activities at various stages of industry development. The study identifies periods of intensive subsurface development associated with the discovery and commercial deve-lopment of major oil and gas fields, as well as stages of declining exploration activity accompanied by reductions in drilling volumes and reserve growth. Particular attention is paid to the analysis of conversion coefficients of forecast resources into commercial reserves, which show considerable variability over different time periods. The results demonstrate that actual reserve growth in several cases significantly exceeded initial forecast estimates, indicating the need to improve methodological approaches to resource assessment and update the forecast resource base. The study confirms the high potential for further development of Uzbekistan's oil and gas sector through intensified exploration activities and the implementation of modern resource modeling and assessment technologies.

Introduction

A significant part of the territory of the Republic of Uzbekistan (more than 60%) is promising for oil and gas. The history of oil and gas industry of the country dates back more than 100 years. It originated in the Fergana Valley in the second half of the 19th century, initially with the development of oil sources using artisanal methods, and then with the establishment of the first oil field in Turkestan, Chimion (Bogdanov, Khmyrov, 2025). The annual growth in oil production necessitated the construction of refining facilities. Therefore, in 1906, the Vannovsky oil refinery was put into operation, later renamed the Altyaryk oil refinery, which is currently a branch of the Fergana oil refinery (Bogdanov et.al., 2024).

The development of the oil refining industry in the Republic of Uzbekistan was largely ensured by the activities of the geological exploration service, which, through the discovery of new hydrocarbon deposits and the expansion of the mineral resource base, formed the fuel and energy foundation for sustainable economic growth.

Thus, during the first 50 years of the 20th century, seven oil and gas fields were discovered in the Fergana region, three of which were medium-sized in terms of hydrocarbon reserves and four were small. It is noteworthy that all of these fields, with the exception of one (Chongara-Galcha), are still in operation today with Chimion-Yarkutan-Chaur having been in operation for over 120 years.

Chronologically, the next region was the Surkhandarya in which industrial oil and gas potential of the Republic was established, where in 1934, a powerful oil fountain with a flow rate of 400 tons per day struck from the deposits of the Bukhara Paleogene layers at the Haudag field (Bogdanov et.al., 2024). By 1950, three more fields had been discovered in the Surkhandarya region, all of them small in terms of hydrocarbon reserves, but oil production continues there to this day (Bogdanov, Khmyrov, 2025).

These 11 fields located in the Fergana and Surkhandarya regions were the only ones producing hydrocarbons in the republic until 1953, when the discovery of the Tashkuduk and Setalantepe fields

proved the industrial productivity of the Bukhara-Khiva region, which has been the flagship of oil and gas industry of Uzbekistan for over 70 years (Bogdanov et al., 2023; Bogdanov, Khmirov, 2024).

With the discovery of the Adamtash field in 1962 and the Shahpakhty field in 1963, two more oil and gas regions were identified: South-West Gissar and Ustyurt, respectively (Bogdanov et.al., 2024).

The involvement in the geological exploration process, primarily of the Bukhara-Khiva, as well as the Ustyurt and South-West Gissar regions, made it possible to identify a large number of hydrocarbon deposits, mainly gas accumulations. This made it possible to consider the territory of the Republic of Uzbekistan for the presence of deposits with reserves of mainly free gas. Currently, natural gas ranks third in terms of its share of fossil fuels in the global balance of primary energy resources, and for many years the world has been discussing the possibility that natural gas will play a decisive role in building a more sustainable energy future (World Energy Council, 2016). The subsoil of the Republic contains natural resources, including hydrocarbon raw materials, the conversion of which into land-based assets — human and physical capital — is seen as a strategic direction that ensures sustainable employment for the population and stimulates economic growth (Venables, 2016; Tatar et.al., 2024).

Overall, the discovery of a significant number of hydrocarbon deposits has contributed to the systematic and sustainable development of the republic's economy for many decades (van Krevel, Peters, 2024; Henstridge, Roe, 2018).

Materials and methods

The study is based on a comprehensive analysis of the history of geological explorations aimed at identifying oil and gas deposits in the Republic of Uzbekistan. Due to the lack of reliable data available to the authors on the types, volumes, and results of geological exploration activities conducted prior to 1962, the analytical coverage is limited to the period from 1962 to 2024. Data on the volumes of geophysical explorations using the MOGT-2D method are taken into account since 1970.

The database is based on materials from state statistical reports, including the State Balances of Mineral Resources of the Republic of Uzbekistan (forms 06-Gr, 07-Gr), annual reports of geological exploration organisations, reports on the state of the fund of structures promising for oil and gas exploration (form 03-Gr), as well as data on the volumes of liquid and gaseous hydrocarbon extraction (form 3).

The comparison made it possible to determine the contribution of each of five oil and gas regions of the country, as well as to analyse the state, dynamics, and growth of industrial-grade hydrocarbon reserves, annual and cumulative oil and gas production.

Results of geological exploration works

As noted above, the Fergana region was a pioneer in the discovery of oil and gas deposits among oil and gas-bearing territories of Uzbekistan. This region has the widest stratigraphic range of hydrocarbon deposits, from the Paleozoic rock complex to the Neogene inclusive. Within the Fergana region, mainly oil accumulations have been identified, i.e., the region belongs to the oil and gas category. As a result of geological exploration only three (Northern Hankyz, Chakar, and Yangi Avval) of the 34 hydrocarbon deposits identified in the region have no oil deposits. On January 1, 2025 if we convert the initial reserves of industrial categories into tons of fuel equivalent, the share of oil, free gas, and condensate looks like this: oil accounts for 81.8%, free gas for 17.6%, and recoverable condensate for 0.6% (Fig. 1).

As we can see, oil reserves are of paramount importance. During the entire period of geological explorations in the Fergana region, 189 hydrocarbon deposits have been identified in 34 fields, including 125 oil fields, 24 gas condensate fields, 21 gas fields, 18 oil and gas fields, and 1 oil and gas condensate field (Fig. 2).

The discovery of large oil deposits in the Fergana region against the backdrop of a lack of discoveries in the rest of Uzbekistan in the early stages (before 1934), led to the extraction of oil in the first place. In 1962, annual oil production in the Fergana region amounted to 1.522 million tons, which accounted for 88.3% of the annual oil production in the Republic of Uzbekistan. Currently, the volume of annual oil production in the region has significantly decreased due to the heavy depletion of deposits (some deposits have been in operation for over 100 years) and in 2024 amounted to 121 thousand tons, or 17% of the annual oil production in the republic. Developing production strategies for the most efficient exploitation of oil deposits requires optimizing processes that reflect the nature of operational decisions and the associated geological uncertainties. For the Fergana region, as for the republic as a whole, the oil recovery factor is quite low (0.1-0.3), which is a consequence of the use of oil reservoir flooding techniques and the lack of application of modern secondary and tertiary methods of reservoir stimulation. In this context, there is a potential opportunity to increase production from even depleted hydrocarbon deposits in the republic provided that innovative exploitation methods are used (Barros et al., 2020).

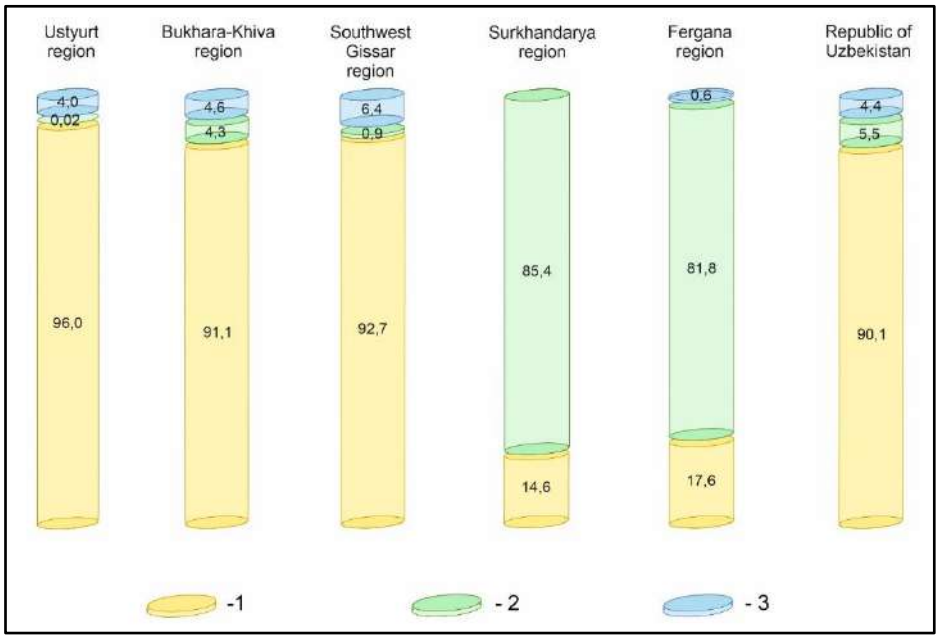

Fig. 1. Structure of initial total resources. Legend: 1 – gas, 2 – oil, 3 – condensate

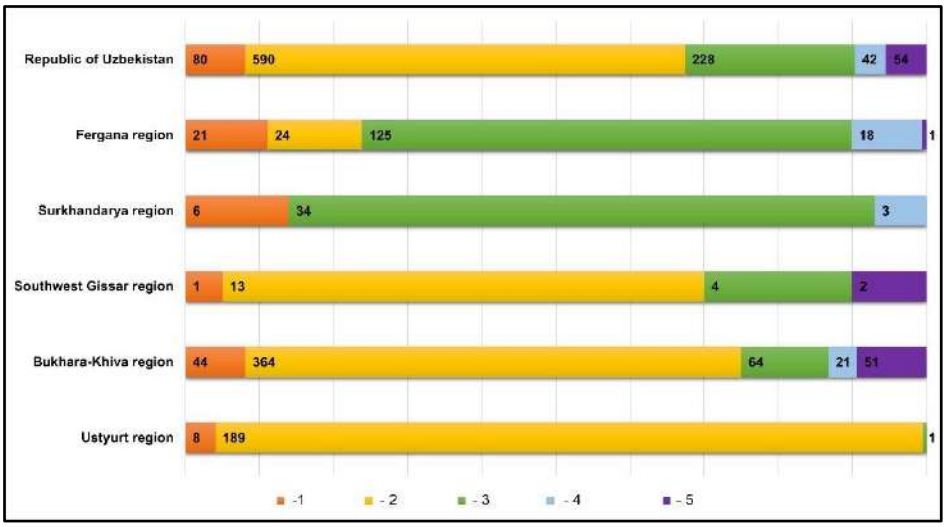

Fig. 2. Distribution of deposits by oil and gas bearing regions of the Republic of Uzbekistan. Legend: 1 – gas fields, 2 – gas condensate fields, 3 – oil fields, 4 – oil gas fields, 5 – oil and gas condensate fields

The analysis and summary of the source materials show that until the end of the 1930s, oil deposits were mainly found in the Paleogene sediments, then the stratigraphic range of productivity expanded due to the Neogene deposits, from the mid-1950s due to the Cretaceous deposits, and from the mid-1960s due to the Jurassic deposits. In addition, gas deposits were discovered in the Paleozoic sediments at two fields (Garbi Polvontosh and Southern Alamyishik), from which gas was extracted for a short time, but the deposits were not geometrised and reserves were not calculated.

Currently, despite high depletion rates, oil fields of the Fergana region rank second (26.2%) in the Republic after the Bukhara-Khiva region in terms of current reserves of commercial oil. In terms of current reserves of free gas, the region ranks last, in fifth place.

Further prospects for increasing the hydrocarbon resource base in the Fergana region are primarily associated with the exploration of traditional Paleogene-Neogene deposits and underlying the Cretaceous and Jurassic deposits, in the latter of which mainly gas deposits are expected to be discovered. Certain prospects are also associated with the refinement of the geological structure of previously discovered hydrocarbon deposits based on the results of exploitation, in which the recovery of extractable reserves exceeded 100% (layers I and KKS of the Andijan field; layers I, III, VIII of the Sharikhan-Khojaabad field; layer IV of the Vorukh

field, etc.). In general, it can be stated that the process of searching of oil and gas deposits within the Fergana region looks promising in the future, but its geological and economic efficiency is questionable due to the high degree of exploration of the territory and the complexity of its geological structure.

As of January 1, 2025, the initial total hydrocarbon resources of the Fergana region amounted to 835.6 million tons of oil equivalent, of which 4.4% were current reserves of industrial categories (ABC_1), accumulated production for the entire period of operation – 9.1%, preliminary estimated reserves (C_2) – 14.5%, prospective resources (C3) – 21.5%, and forecast resources (D1+D2) – 50.5% (Bogdanov, Khmyrov, 2025).

In 1934, based on the results of geological explorations, the Surkhandarya region was transferred from the oil and gas prospective category to the oil and gas bearing category following the discovery of the Haudag oil field. The stratigraphic range of oil and gas deposits covers rocks from the Jurassic to the Paleogene age inclusive. At the same time, the main stratigraphic complex of rocks containing the overwhelming majority of deposits (86.7%) are the Paleogene deposits. In addition, two fields (Lyalmiqar and Kuyi Haudag) have deposits in the Upper Cretaceous sediments, and one field (Mustaqillikning 25 Yilligi) has deposits in the Lower Cretaceous and the Middle-Upper Jurassic rocks.

Only two sites of 15 hydrocarbon deposits identified within the studied region as a result of geological explorations – Mustakillikning 25 Yilligi and Kuii Haudag – have been found to contain oil deposits and only gas deposits in the Cretaceous and the Jurassic sediments. At the same time, the Kuyi Haudag field, according to its geological and structural characteristics, is in fact a lower productive horizon of the Haudag field, which allows being considered not as an independent oil and gas structure, but as a part of a previously discovered field. Thus, it can be stated that there is only one new object where no oil deposits have been recorded – Mustakillikning 25 Yilligi. It should be noted that in the current practice of recording the results of geological exploration in the republic, the focus remains not only on the increase in recoverable hydrocarbon reserves, but also on the quantitative indicators of the discovered fields. In the absence of uniform criteria for differentiating between independent deposits and productive horizons within a single oil and gas bearing object, this approach can lead to a statistical increase in the number of new deposits.

Within the Surkhandarya oil and gas region, oil deposits have been the main focus of development, which allows being classified as a gas-oil-bearing territory with a predominance of oil-type fluids. As of January 1, 2025, the structure of initial total hydrocarbon reserves is characterised by a significant predominance of liquid hydrocarbons: oil accounts for 85.4% of total resources, while free gas accounts for only 14.6% (Fig. 1). Condensate has not been identified in the region, which reflects the specific thermobaric conditions and fluid composition characteristic of the sedimentary cover of this section of the South Tajik oil and gas province.

Thus, the oil component forms the basis of the resource potential of the region. During geological explorations in the region, 43 hydrocarbon deposits were identified associated with 15 fields of various sizes. 34 of them are oil fields, 6 are gas fields, and 3 are oil and gas fields (Fig. 2). This ratio indicates the pronounced specialisation of the region in oil production with limited gas reserves, reflecting the characteristic features of the formation and spatial distribution of hydrocarbon accumulations in the southern part of the Republic of Uzbekistan.

In 1962, annual oil production in the Surkhandarya region amounted to 201,600 tons, which accounted for 11.7% of the annual oil production in the Republic of Uzbekistan. Currently, the volume of annual oil production in the region has decreased due to the depletion of fields (some fields have been in operation for 90 years) and in 2024 amounted to 71,000 tons, or 10% of the annual oil production in Republic.

Currently, based on current reserves of commercial oil, the fields in the Surkhandarya region rank third (3.5%) in the republic. The region also ranks third in terms of current reserves of free gas (6.0%).

Further prospects for increasing the hydrocarbon resource base in the Surkhandarya region are linked along with the Paleogene deposits, primarily to the exploration of deep Cretaceous and Jurassic deposits, in the latter of which mainly gas deposits are expected to be discovered. In general, the search for oil and gas deposits in the Surkhandarya region will directly depend on the technical capabilities of drilling equipment capable of drilling to depths of more than 6-8 km in order to study the Jurassic carbonate deposits under salt, which are associated with the main prospects for hydrocarbon growth in the Surkhandarya region (more than 80% of the region's forecast resources (D1+D2)) and the republic (more than 11% of the republic's forecast resources) (Shuster, 2022).

As of January 1, 2025, the total initial hydrocarbon resources of the Surkhandarya region are estimated at 1,762.2 million tons of fuel equivalent. The structure of resource distribution by category shows the dominance of the forecast component, which indicates an insufficient level of geological exploration and a limited degree of industrial development of the territory. Thus, current reserves of industrial categories (ABC_1) account for only 7.4% of total

resources, while cumulative production for the entire period of operation accounts for 1.1%. Preliminarily estimated reserves of category C_2 account for 4.0%, prospective resources (C3) — 10.9%, while the bulk is accounted for by projected resources of categories D1+D2, which make up 76.6% of the total volume (Bogdanov, Khmyrov, 2025).

This ratio of categories indicates the high potential for further expansion of the resource base through the identification and preparation of new hydrocarbon traps, as well as the need to intensify exploration and prospecting activities in order to transfer projected resources to higher categories of accounting.

The next region to receive oil and gas bearing status was Bukhara-Khiva, where the first exploratory reconnaissance work dates back to the 1920s, and with the discovery of the Tashkuduk and Setalantepe fields in 1953, the identification of oil and gas fields in this territory began.

The stratigraphic range of oil and gas deposits covers rocks from the Lower Jurassic to the Upper Cretaceous age inclusive. The main stratigraphic complex of rocks containing the vast majority of deposits (90.3%) is the carbonate formation of the Jurassic age (Bogdanov, Khmirov, 2024). In addition, four fields (Gazli, Tashkuuk, Akdzhar, and Kaltakyr) also have deposits in the Upper Cretaceous sediments, 32 fields have deposits in the Lower Cretaceous sediments, and 28 fields have deposits in the Middle Jurassic rocks.

In 216 hydrocarbon deposits identified within the Bukhara-Khiva region as a result of geological explorations, oil deposits were found in 95 deposits and gas deposits were found in 159 deposits.

Within the Bukhara-Khiva oil and gas region, gas deposits have been the main focus of development, which allows being classified as an oil and gas region with a pronounced predominance of gas-type fluids. On January 1, 2025, the structure of initial total hydrocarbon reserves is characterised by the dominance of free gas, which accounts for 91.1% of total resources. The share of recoverable oil is 4.3%, and condensate is 4.6% (Fig. 1). Thus, gas components form the bulk of the region's resource potential, determining its strategic specialisation in natural gas production.

Over the entire period of geological exploration in the region, 544 hydrocarbon deposits have been identified, located within 216 fields of various sizes. Among them, gas condensate deposits predominate — 364 deposits, which is more than two-thirds of the total number. In addition, 44 gas, 21 oil and gas, 51 oil and gas condensate, and 64 oil deposits have been identified (Fig. 2) (Bogdanov, Khmirov, 2024). This ratio of deposit types reflects the complex structure of the region's fluid system, in which gas condensate and gas formations have become widespread, forming the basis of the modern industrial potential of the Bukhara-Khiva oil and gas province.

Analysis of the spatial distribution of deposits shows that gas and gas condensate fields are concentrated mainly in the Mesozoic and Cenozoic sediments controlled by large anticline structures and regional fault zones. The predominance of gas in the resource structure is due to a combination of factors: the considerable depth of productive horizons, high thermobaric gradient, and the specific facies composition of the sedimentary cover, which is conducive to the generation and preservation of gas systems. Together, these features form a stable trend of gas specialisation in the region, which is consistent with its location in the southwestern part of the Amudarya oil and gas province and the overall evolution of its oil and gas-forming systems.

In 1962, annual free gas production in the Bukhara-Khiva region amounted to 9.6 billion cubic meters, or 96.9% of the annual gas production in the Republic of Uzbekistan. Oil and condensate production in the Bukhara-Khiva region had not yet begun in 1962. The first oil production in the region was recorded in 1963 at the Karaulbazar-Sarytash field (3,000 tons) (Bogdanov, Khmirov, 2024).

Here it is necessary to explain this situation. The fact is that oil and gas reserves in the region were discovered relatively recently (1953), and despite the fact that the first unique gas field in the Soviet Union, Gazli (1956) with reserves of more than 500 billion m^3 (Bogdanov et al., 2024), the fields of the region were still in the early stages of development and production volumes were low. In addition, during this period, the discovered oil and gas fields in the region were located only in the Bukhara step (with the exception of the Uchkyr field, discovered in 1960 and put into operation in 1968), where hydrocarbon deposits were associated with structural traps.

However, with the start of exploration of the Chargos stage deposits, the detailed study of core material from the Urtabulak field wells allowed a number of researchers concluding that the productive horizons of the carbonate Jurassic of this field are reef-based and, possibly, that the productive horizons of other fields in the region are also reef-based. As a result of the studies, significant variations in the thickness of the carbonate formation were established, associated with the presence of reef-type traps. At that time, this was of great importance for the oil and gas geology of Uzbekistan, as it opened up a new direction of work in the search for reef massifs with high concentrations of hydrocarbon reserves per unit volume. Subsequent discoveries of fields with hydrocarbon deposits in reef traps (Zevardy, Alan, Southern Pamuk, Kokdumalak, etc.) made it possible not only to significant-

ly increase the hydrocarbon resource base, but also to significantly increase hydrocarbon production, primarily free gas, thereby making the Bukhara-Khiva region a leader in terms of hydrocarbon reserve growth and production (Punanova, 2022).

Currently (2024), the annual production of free gas in the region amounted to 32.6 billion cubic meters, or 74.2% of the annual gas production of the Republic. This is not the highest development indicator for the region over the entire period of operation, as in 2010 gas production reached 53.0 billion m^3, but due to the high depletion of unique and large hydrocarbon deposits, this indicator is gradually declining. A similar situation is observed with oil and condensate production volumes.

In 2024, oil and condensate production volumes in the region will be 495,000 tons (69.5% of the republic's annual production) and 517,000 tons (52.9% of the republic's annual production), respectively. In 1998, these figures were 4.508 million tons and 4.402 million tons, respectively, or a total of 8.910 million tons of liquid hydrocarbons (oil + condensate). In 1998, this accounted for 96.4% of the total annual republican production. These figures in 1998 were mainly influenced by the Kokdumalak oil and gas condensate field, which was discovered in 1985 and put into production in 1989. To date, the depletion of this field has led to a significant decline in oil and condensate production.

Currently, in terms of current reserves of hydrocarbon raw materials (free gas, recoverable oil, and condensate) of industrial categories, the fields of the Bukhara-Khiva region rank first (65.9%, 69.1%, and 74.0%, respectively) in the republic.

As of January 1, 2025, the total initial hydrocarbon resources of the Bukhara-Khiva region are estimated at 8,933.3 million tons of oil equivalent. The distribution of resources by reserve category shows a fairly balanced ratio between the developed and projected parts of the resource base. Thus, current reserves of industrial categories (ABC_1) account for 17.4%, which reflects the high level of exploration and involvement of resources in industrial development. The share of cumulative production for the entire period of operation is 34.5%, which indicates intensive and continuous industrial development of the region.

At the same time, preliminary estimated reserves (C_2) account for 2.9% of total resources, and prospective resources (C_3) account for 7.5%, confirming the potential for expanding the mineral resource base through further exploration of identified structures. The largest share, 37.7%, is accounted for by projected resources (D_1+D_2), reflecting the region's significant prospects for discovering new deposits, primarily in poorly explored areas with deep productive horizons.

Thus, the current ratio of reserve categories characterises the Bukhara-Khiva region as a highly developed oil and gas bearing territory that still has potential for development, where further resource growth can be achieved by intensifying exploration and prospecting in deep and poorly studied stratigraphic complexes.

The next oil and gas region in chronological order was South-West Gissar, where the Adamtash gas condensate field was discovered in 1962.

The stratigraphic range of oil and gas deposits covers rocks of the Middle-Upper Jurassic age (carbonate formation).

Within the South-West Gissar oil and gas region, many years of geological explorations have revealed 19 hydrocarbon deposits, of which 16 contain free gas and 5 contain oil accumulations. Thus, the region belongs to the category of oil and gas bearing territories with a pronounced predominance of gas in the structure of resources.

As of January 1, 2025, the structure of the initial total hydrocarbon reserves is characterised by the dominance of free gas, which accounts for 92.7%. The share of recoverable oil is only 0.9%, and gas condensate – 6.4% (Fig. 1). This ratio of fluid components indicates gas condensate specialisation of the region, where the bulk of hydrocarbons is concentrated in gas and gas condensate deposits of the Mesozoic complex.

During geological explorations within the region, 20 hydrocarbon deposits were identified, associated with 19 fields. Among them, gas condensate deposits predominate – 13 deposits, with an additional 1 gas, 2 oil and gas condensate, and 4 oil deposits (Fig. 2). This distribution of deposit types reflects the structural and facies heterogeneity of the section, where gas and gas condensate formations are mainly confined to tectonically complex anticline uplifts and zones of tectonic disturbances, which form favorable traps for gas accumulation.

The predominant gas orientation of the hydrocarbon system in the South-West Gissar region is due to the deep occurrence of source rocks, the high level of catagenesis of organic matter, and the predominantly thermogenic type of fluid generation. Together, these factors determine the high degree of maturity of the oil and gas source rocks and the formation of regional-scale gas condensate systems, ensuring its key role in the modern gas production structure of the Republic of Uzbekistan.

The first oil production in the region dates back to 1991 (Okul), which amounted to 7,000 tons or 0.5% of the republic's annual oil production. In 2001, free gas production began in the region (Southern Tandyrcha) – 533 million cubic meters, or 0.4% of the republic's annual gas production. The launch of the Southern Tandyrcha field was prompt-

ed by the need to supply the Shurtan gas chemical complex with hydrocarbon raw materials and was associated with the beginning of a decline in production at the Shurtan field due to its gradual depletion.

At the end of 2024, the South-West Gissar region demonstrated stable production activity with a clear predominance of gas. The annual volume of free gas production amounted to 6.125 billion m³, which is equivalent to 13.9% of the total production of this type of raw material in the Republic of Uzbekistan. At the same time, oil production is estimated at 25 thousand tons (3.5%), and gas condensate production at 358 thousand tons (36.6%) of the republic's total figures.

Currently, in terms of current reserves of free gas and extracted oil of industrial categories, the fields of the South-West Gissar region rank fourth (4.5% and 1.0%, respectively), and in terms of current reserves of extracted condensate, they rank third (4.4%) in the Republic.

Further prospects for increasing the hydrocarbon resource base in the South-West Gissar region are associated with Jurassic carbonate deposits.

As of January 1, 2025, the total initial hydrocarbon resources of the South-West Gissar region are estimated at 810.3 million tons of oil equivalent. A structural analysis of their distribution by category shows that the region is characterised by a moderate degree of geological exploration with significant potential for further reserve growth. Current reserves of industrial categories (ABC_1) account for only 12.7%, which indicates limited involvement of explored structures in active development. At the same time, the share of accumulated production is 16.7%, reflecting a relatively high level of industrial use of open deposits.

The share of preliminary estimated (C_2) and prospective resources (C_3) remains relatively low – 2.7% and 3.4%, respectively. This indicates an insufficient level of detail in the geological data on a number of local structures, which opens up opportunities for in-depth study of the section and refinement of resource parameters. The most significant part of the region's potential is formed by the projected resources of categories D_1+D_2, which account for 64.5%. Their predominance indicates the presence of significant but poorly studied areas that are promising for the discovery of new hydrocarbon deposits.

Thus, the South-West Gissar region can be characterised as a territory with a developed industrial base for gas and oil production, while a significant share of projected resources determines the need to intensify geological exploration and appraisal activities. In the long term, this will ensure the reproduction of the mineral resource base and strengthen the role of the region in the country's hydrocarbon potential.

The last region to receive oil and gas bearing status was Ustyurt, within which the first gas field, Shakhpakhta, was discovered in 1963.

The stratigraphic range of oil and gas deposits covers rocks from the Paleozoic to the Upper Jurassic age inclusive. At the same time, the main stratigraphic complex of rocks containing the overwhelming majority of deposits (71.4%) is the Middle Jurassic deposits. In addition, nine fields also have deposits in the Upper Jurassic sediments, 17 fields have deposits in the Lower Jurassic sediments, and two fields have deposits in the Paleozoic rocks.

As a result of many years of geological explorations in the Ustyurt oil and gas region, 28 hydrocarbon deposits have been identified, all of which contain gas reserves, with only one containing oil reserves (the West Aral field). Thus, in terms of fluid type, the region is classified as oil and gas bearing, but its resource base is clearly gas-specialised.

As of January 1, 2025, the structure of the initial total hydrocarbon reserves shows a significant predominance of free gas, which accounts for 95.99% of the total volume. Meanwhile, the share of recoverable oil is only 0.02%, and gas condensate is 3.99% (Fig. 1). This imbalance indicates the sustained dominance of gas, which determines the region's strategic role in shaping the gas production potential of the Republic of Uzbekistan.

198 hydrocarbon deposits have been identified within the region, located in 28 fields up to now. Among them, 189 deposits are gas condensate, 8 are gas, and only one is oil (Fig. 2).

The productivity of the Ustyurt region is largely determined by the specifics of its tectonic and stratigraphic structure—the presence of a thick sedimentary cover with a developed the Mesozoic-Paleozoic complex and deep structural traps associated with regional platform-type dislocations. Together, these factors have ensured a high level of maturity of oil and gas source rocks and the formation of significant gas condensate systems, which determine the industrial significance of the region in the modern structure of the country's fuel and energy balance.

The first production of free gas in the Ustyurt region took place in 1971 at the Shakhpakhta field, which amounted to 404 million m^3, or 1.2% of the annual gas production in the Republic of Uzbekistan. Oil production in the Ustyurt region has never been carried out and is still not being carried out. The first production of condensate in the region, amounting to 2,000 tons, was recorded in 1995 at the Urga field.

It should be noted that between 1963 and 1999, only eight hydrocarbon deposits were discovered in the Ustyurt region as a result of geological exploration work. The turning point came in 1998, when, in accordance with the Protocol of Instructions of the

President of the Republic of Uzbekistan, I.A.Karimov dated February 11, 1998, on intensifying oil and gas explorations on the Ustyurt Plateau and in the Aral Sea basin, extremely important decisions were developed and adopted on a radical change in geophysical and drilling explorations in the region. The implementation of these measures ensured a sharp expansion in the volume of geological explorations, resulting in the discovery of 20 new gas condensate fields to date (Berdakh, East Berdakh, Shagyrlyk, Surgil, North Aral, Uchsay, Shege, Aral, Dali, Northern Berdakh, etc.). Subsequently, a number of fields were combined into a single entity based on the results of hydrocarbon reserve calculations: Surgil and Northern Aral into Surgil; Berdakh and Northern Berdakh into Berdak-Shimoliy Berdak; Eastern Berdakh and Uchsay into Sharkiy Berdak.

The significant shallowing of the Aral Sea over the past decades has opened up opportunities for geological exploration in the area that was previously the Aral Sea basin (Fig. 3).

As a result of the discovery of new deposits, the hydrocarbon resource base has been significantly expanded, as individual deposits have been reclassified as large in terms of hydrocarbon reserves: Surgil, Sharkiy Berdak, Berdak-Shimoliy Berdak.

Currently, only four fields with unique hydrocarbon reserves (> 300 million tons of oil equivalent) have been discovered within the Republic of Uzbekistan (Gazli, Shurtan, Dengizkul-Khuzak-Shady-Northern Dengizkul-Khodjasayat, Zevardy), which are located in the Bukhara-Khiva region and have been the foundation of production, primarily gas, in the republic for many decades. No other regions with unique hydrocarbon reserves have been identified yet.

However, there is currently a real possibility of identifying a unique hydrocarbon deposit within the Ustyurt region. The fact is that between 1999 and 2021, seven deposits were discovered in the southern part of the former Aral Sea basin, some of which (Surgil, Berdak-Shimoli Berdak) are currently under development, one field (Arslan) is ready for industrial development, and four (Inam, Kyzyl-Shaly, Kuyi Surgil, and Western Kuyi Surgil) are under exploration. According to final and operational estimates of hydrocarbon reserves carried out in various years, the productivity contours of these fields for various productive formations are located within a single gas-bearing contour, i.e., they are in fact a single field (Fig. 4).

Already today, by combining these fields and, accordingly, hydrocarbon reserves into a single entity, it is possible to obtain a field with initial reserves of industrial-grade hydrocarbons of approximately 346 million tons of oil equivalent, which means that this combined field can already be classified as unique in terms of hydrocarbon reserves. In addition, as noted above, four fields are under exploration and an increase in hydrocarbon reserves is seen in the future. Furthermore, these seven fields have preliminary estimated reserves of 74.6 million tons of oil equivalent in the C_2 category. In the Republic of Uzbekistan, the average conversion factor for preliminary estimated C_2 reserves to industrial ABC_1 reserves is more than one. However, exercising a degree of caution and assuming this factor to be 0.9, an increase in hydrocarbon reserves of 67.2 million tons of oil equivalent can be expected. The prospects of this approach are quite attractive, and given the development of a unified project, we can hope for high operational efficiency.

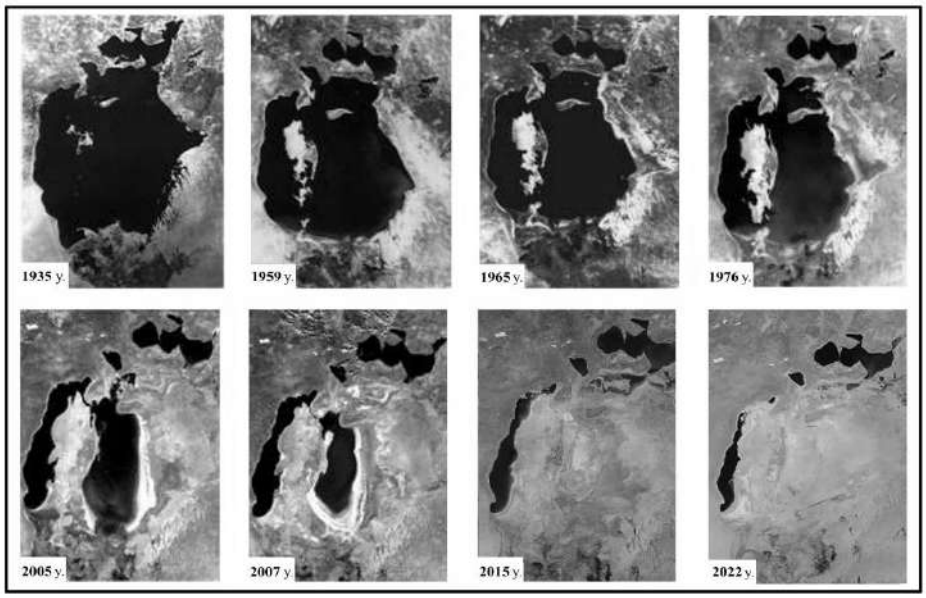

Fig. 3. Dynamics of the decline in the level of the Aral Sea

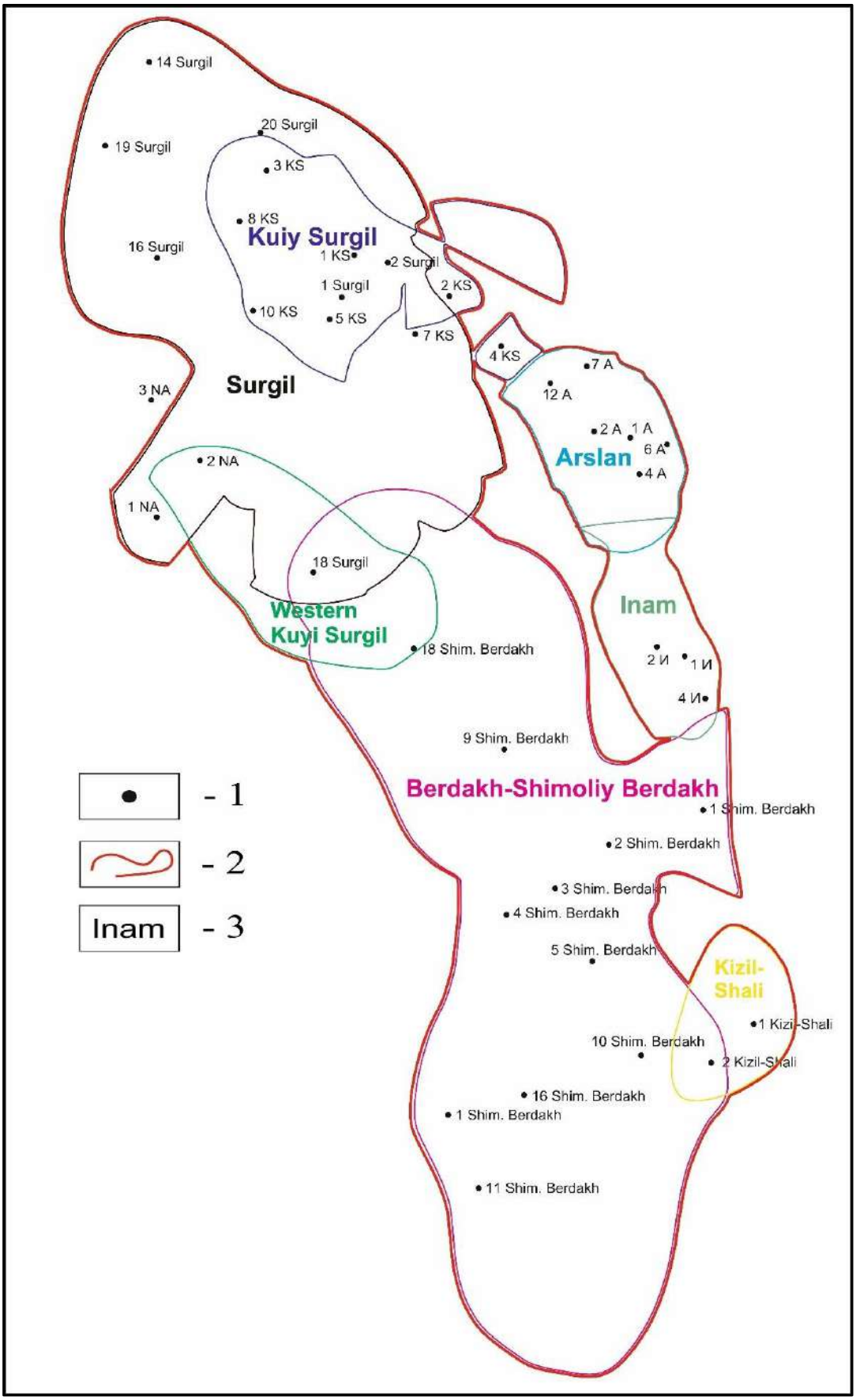

Fig. 4. Approved productivity contours of fields in the Ustyurt region, united by a common gas-water contact. Legend: 1 – exploration and appraisal wells (KS – Kuyi Surgil, NA – Nothern Aral, A – Arslan, И – Inam), 2 – approved productivity contours by fields, 3 – name of deposits

As of 2024, the annual production of free gas within the Ustyurt region amounted to 5.2 billion m³, which is equivalent to 11.7% of the total annual production in the Republic of Uzbekistan. Gas condensate production for the same period reached 100,000 tons, or 10.2% of the republican level. These proportions indicate the significant contribution of the Ustyurt region to the national gas production balance, despite the relatively low degree of involvement of reserves in industrial development.

Today, in terms of current reserves of industrial-grade hydrocarbon raw materials (free gas and recoverable condensate), the fields in the Ustyurt region rank second (23.2% and 21.0%, respectively) in the republic. In terms of current recoverable oil reserves, the region ranks fifth (0.1%).

Further prospects for increasing the hydrocarbon raw material base in the Ustyurt region are primarily associated with the Jurassic deposits, as well as the Paleozoic formations.

As of January 1, 2025, the total initial hydrocarbon resources of the Ustyurt region are estimated at 3,007.8 million tons of oil equivalent. Analysis of the distribution of resources by reserve category indicates an uneven degree of geological exploration and industrial development. Current reserves of industrial categories (ABC_1) account for only 10.8%, which indicates limited involvement of identified structures in exploitation. At the same time, cumulative production for the entire development period is 3.2%, reflecting the relatively short history of industrial development in the region compared to more mature oil and gas provinces in the country.

Preliminary estimated reserves (C_2) account for 3.3%, and prospective resources (C_3) — 19.4%, which confirms the existence of significant potential for reserve growth through refinement of the structure of prospective areas and further exploration. The most significant share — 63.2% is made up of projected resources (D_1+D_2), concentrated mainly in poorly studied areas in the northern and central parts of the region, where the development of deep-lying Paleozoic and Mesozoic complexes creates the conditions for the formation of new hydrocarbon deposits.

Thus, the structure of the resource base of the Ustyurt region is characterised by a high proportion of prospective categories with a relatively low level of industrial development, reflecting the early stage of the geological-industrial cycle. With targeted development of exploration and prospecting, especially in the deep horizons of the Paleozoic basement, the region has the potential for significant growth in gas and condensate reserves, which could compensate for the decline in production in the more developed provinces of Uzbekistan.

Discussion of the results of geological explorations

Overall, in the 125 years since the first field was discovered in the Fergana region, a great deal of work has been done, including various regional and exploratory geophysical surveys and deep drilling, which has led to the discovery of 312 oil and gas fields.

The stratigraphic range of oil and gas deposits is quite wide, as hydrocarbon deposits are located in sediments from the Paleozoic to the Neogene age inclusive. The majority of deposits are located in carbonate sediments of the Middle-Upper Jurassic age (68.9%).

Analysis of the results of many years of geological explorations shows that 312 hydrocarbon deposits have been identified to date within the oil and gas bearing territories of the Republic of Uzbekistan, represented by various types of fluids and structural-lithological conditions of occurrence. Gas plays a dominant role: gas deposits have been identified at 258 fields, while oil deposits have been identified at 145 sites.

As of January 1, 2025, free gas resources predominate in the structure of the initial total hydrocarbon reserves of the Republic of Uzbekistan, accounting for 90.1%, while oil and gas condensate account for 5.5% and 4.4%, respectively (Fig. 1). This ratio reflects a steady trend towards a shift in the resource base towards gas specialisation, which is characteristic of large sedimentary basins in the Central Asia.

To date, 994 hydrocarbon deposits have been identified in the republic, confined to 312 fields, of which gas condensate facilities account for 59.4%, oil facilities for 22.9%, gas facilities for 8.0%, oil and gas condensate fields account for 5.4%, and oil and gas fields account for 4.3% (Fig. 2). This structural organisation of reserves indicates a complex relationship between fluid systems and traps of different ages, caused by both the evolution of the sedimentary cover and the heterogeneity of the thermobaric conditions of hydrocarbon generation.

In 2024, the total volume of hydrocarbon production in the Republic of Uzbekistan amounted to 43.9 billion m³ of natural gas, 712 thousand tons of oil, and 1,271 thousand tons of gas condensate. At the same time, the share of gas in the overall production balance reaches almost 94%, which underscores the gas-producing vector of development of the national fuel and energy industry.

A long-term (1962–2024) analysis of hydrocarbon reserves growth shows that this indicator depends on the volume of parametric, exploratory, and prospecting drilling (Fig. 5). However, as can be seen from the graph, the increase in deep drilling volumes in recent years has not had a significant impact on hydrocarbon reserve growth indicators. This situation is due to the fact that, as in previous

years, the main oil and gas-bearing region in terms of reserve growth and hydrocarbon production is the Bukhara-Khiva region, which has been extensively explored. As a result, increasingly smaller traps are being drilled, which, in the event of a discovery, will result in insignificant hydrocarbon reserves. The effectiveness of exploration and prospecting is also affected by the need to search for deeper horizons. Systematic explorations carried out between 1962 and 2024 has made it possible to identify characteristic patterns in changes in the annual growth of hydrocarbon reserves, which, following a downward trend, indicate a gradual but steady decline in the growth of hydrocarbon reserves (Sokolov, 2023).

Figure 6 shows the dynamics of hydrocarbon production in the Republic of Uzbekistan for the period of 1962-2024. This figure shows that hydrocarbon production in the Republic of Uzbekistan peaked between 1996 and 2020 (Delannoy et al., 2021). It also clearly shows that the basis of annual hydrocarbon production is unique and large oil and gas fields. The share of large and unique hydrocarbon deposits in total annual production varies from 37% (1963) to 95% (1992). In 2024, it was 72.2%. Given that as of 2024 there were 312 oil and gas fields in the republic, it turns out that 31 fields (4 unique and 27 large) or 9.9% of the total number account for 72.2% of the republic's annual hydrocarbon production (Nuriyev, McFerren, 2025). Analysis of the data in Figure 6 suggests that the downward trend in hydrocarbon production will continue in the future (Laherrere et al., 2022).

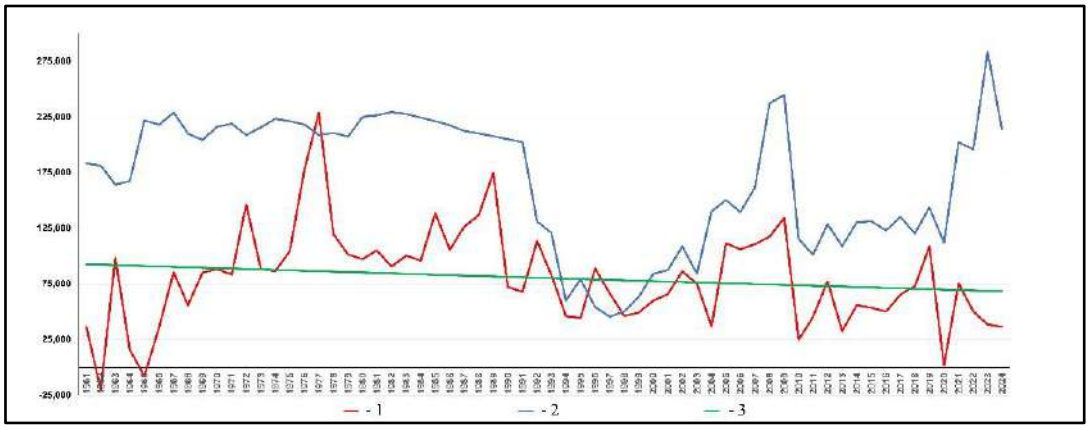

Fig. 5. Comparison of deep drilling indicators and hydrocarbon reserves growth. Legend: 1 – increase in oil reserves (million tons of oil equivalent), 2 – volumes of exploration and parametric drilling (thousand meters), 3 – trend line (million tons of oil equivalent)

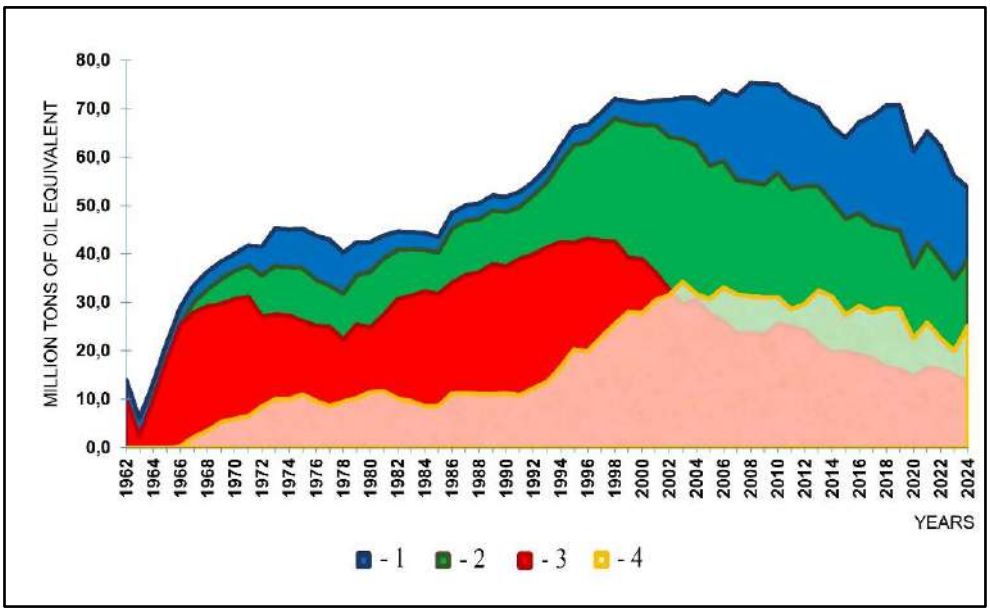

Fig. 6. Share of large and unique deposits in the production of the Republic of Uzbekistan. Legend: 1 – hydrocarbon production in the Republic of Uzbekistan, 2 – production of hydrocarbons from unique and large deposits, 3 – production of hydrocarbons from four unique deposits, 4 – hydrocarbon production from large deposit**s**

If we consider only the share of unique hydrocarbon reserves, this indicator ranges from 22.8% (2019) to 87.2% (1966). In 2024, it was 25.4%, meaning that four unique fields, or 1.3% of the total number, account for more than a quarter of the republic's annual hydrocarbon production.

Figure 7 shows a graph of cumulative production from all oil and gas fields in the Republic of Uzbekistan for the period 1962-2024. This graph shows that more than half (50.3%) of the total cumulative hydrocarbon production in the republic comes from fields that are unique in terms of hydrocarbon reserves. This indicates that existing hydrocarbon reserves are unevenly involved in active production. A study of the distribution of cumulative production and current reserves of different groups of fields by reserve size shows significant heterogeneity in the distribution of these indicators (Sokolov, Shubina, 2023).

As of January 1, 2025, the total initial resources of hydrocarbon raw materials in the Republic of Uzbekistan are estimated at 18,141.1 million tons of fuel equivalent. This figure also includes the projected resources of categories D_1+D_2, determined for the Khorezm and Middle Syr Darya oil and gas prospective regions, where the total estimate is 1,041.4 million tons of fuel equivalent, and more detailed geological exploration data is not yet available.

An analysis of the resource base structure shows that the distribution of reserves by category varies significantly: current industrial reserves (ABC_1) account for 12.9%, which reflects the level of exploration and industrial development of deposits; cumulative production for the entire period of operation accounts for 19.1%, indicating the degree of involvement of resources in economic turnover. Preliminary estimated reserves (C_2) account for 3.5%, while prospective resources (C_3) account for 11.0%. The most significant part – projected resources of categories D_1+D_2, reaching 53.5% of the total volume — characterises the significant potential for further reserve growth with the intensification of exploration and prospecting activities.

This ratio of reserve categories shows that despite the high level of geological exploration of main oil and gas regions of the country, the potential for growth in hydrocarbon resources remains significant, especially in poorly studied areas with predominantly projected estimates.

The relevance of conducting geological exploration aimed at increasing oil and gas reserves in the Republic of Uzbekistan remains an indisputable and strategically important task. In this context, the volume of hydrocarbon resources, estimated at 9,706.5 million tons of oil equivalent, is traditionally considered as the initial resource base for planning and implementing exploration drilling with the aim of transferring hydrocarbon resources into the category of commercial reserves. However, quantitatively significant estimated resources do not in themselves guarantee the economic and technical feasibility of conducting the relevant exploration activities. When determining resource potential benchmarks, key questions inevitably arise: how much drilling is needed to confirm and transfer estimated resources to the category of proven reserves? What is the time frame for implementing such a volume of work? What is the expected efficiency of the geological explorations being carried out? The answers to these questions are critically important, as they allow us to assess the feasibility of drilling programs and determine the prospects for the commercial development of prospective resources (Sokolov, 2023).

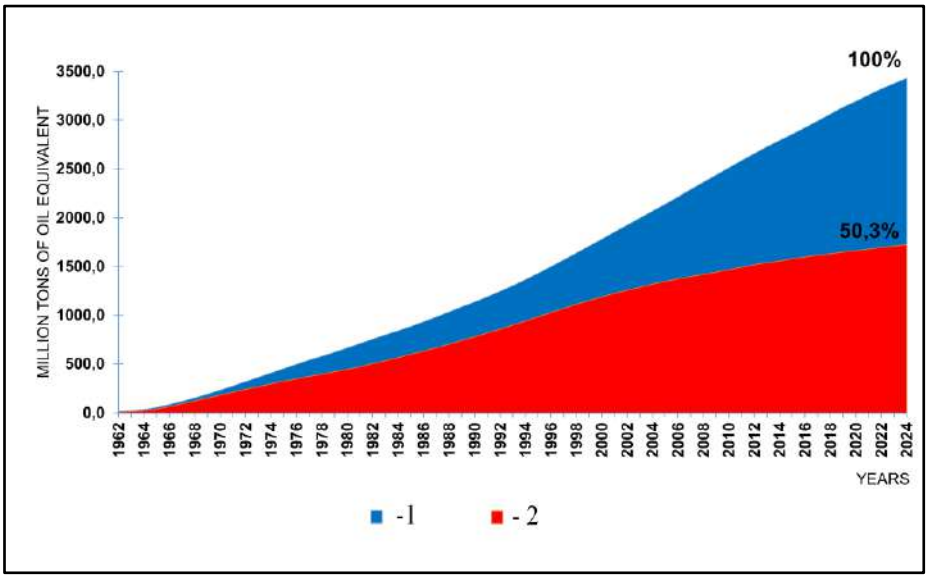

Fig. 7. The impact of unique deposits on cumulative production in the Republic of Uzbekistan. Legend: 1 – Accumulated hydrocarbon production in the Republic of Uzbekistan, 2 – Accumulated hydrocarbon production from four unique deposits

Based on the analysis of the conversion rates of forecast resources into industrial category reserves, it can be reasonably asserted that previous estimates of forecast hydrocarbon resources in categories D_1+D_2 (using the Bukhara-Khiva region as an example) are clearly underestimated. This is confirmed by actual data on the growth of industrial reserves of categories ABC_1 over the past decades, which indicate a high confirmation rate of forecast resources.

Thus, the increase in reserves for 1980-2022 significantly exceeded the estimated increase due to the total forecast resources previously included in the estimates. The coefficients for converting forecast resources into reserves, calculated based on actual data, range from 0.51 to 0.64, and in certain periods (e.g., 1999-2020), they reach values above 1, which indicates a very high coefficient of confirmation of forecast resources, especially against the backdrop of a lower coefficient of conversion of prospective resources into industrial reserves (0.4).

These data indicate that the previously adopted methodology for assessing forecast resources probably underestimated the actual potential of the region's subsoil, failing to take into account a number of deep-lying objects, as well as poorly studied areas with significant geological potential.

Thus, this analysis demonstrates that within the Republic of Uzbekistan (using the Bukhara-Khiva region as an example), the volume of hydrocarbon forecast resources may be significantly higher than previously stated figures and requires a corresponding upward adjustment.

Conclusion

As of January 1, 2025, 312 oil and gas fields have been identified in the Republic of Uzbekistan as a result of geological exploration work. These can be classified as follows:

– by oil and gas geological zoning – Ustyurt region (28 deposits), Bukhara-Khiva region (216), South-West Gissar (19), Surkhandarya (15), Fergana (34) (Bogdanov, Khmirov, 2023);

– by fluid type – gas (10), gas condensate (159), oil and gas condensate (59), oil and gas (29), and oil (55) (Bogdanov, Khmirov, 2023);

– by degree of development – under development (114), prepared for industrial development (93), explored (96) and mothballed (9) (Bogdanov, Khmirov, 2023);

– by size of hydrocarbon reserves – unique (4), large (27), medium (34), and small (247) (Bogdanov, Khmirov, 2023).

The main source of hydrocarbon reserves growth throughout the history of geological explorations in the Republic of Uzbekistan has been four unique hydrocarbon deposits (Gazli, Dengizkul-Khozak-Shady-Northern Dengizkul-Khojasayat, Shurtan, Zevardy), which account for 36% of the initial reserves of hydrocarbons of industrial categories (ABC_1) or an average of 9% of the republic's initial hydrocarbon reserves per unique deposit (Bogdanov et al., 2024). For comparison, the 247 small hydrocarbon deposits account for a total of 11.4% of the initial reserves of industrial categories (ABC_1). The 27 large hydrocarbon deposits account for 43.6% of the republic's initial reserves of industrial categories. Together, unique and large deposits account for 79.6% of the total balance of initial hydrocarbon reserves.

An analysis of hydrocarbon production in the republic's main gas-producing regions – Bukhara-Khiva and Ustyurt – shows that despite the high depletion of industrial reserves in the Bukhara-Khiva region, it continues to be the leader in terms of annual production volumes compared to the Ustyurt region, despite the relatively low depletion of the latter's hydrocarbon reserves.

This is primarily due to the type of traps containing gas deposits. In the Bukhara-Khiva region, where the main gas volumes are associated with reef-type traps, the highest annual production reached 10-14% of current reserves, while in the Ustyurt region, where there are large quantities of hydrocarbon deposits concentrated in relatively low-capacity terrigenous reservoirs, the maximum annual production volume is within the range of 2-4% of current hydrocarbon reserves. Thus, the Bukhara-Khiva region continues to be the main center of gas production in Uzbekistan.

Hydrocarbon production figures, both cumulative and annual (2024) indicate that throughout the entire period of oil and gas field operation in the Republic of Uzbekistan, unique and large fields have been the basis for hydrocarbon production, accounting for 50.3% and 38.9% of cumulative hydrocarbon production, respectively, which together total 89.2%. Medium and small fields in terms of hydrocarbon reserves account for 5.1% and 5.7%, respectively. Approximately the same trend is observed today. Despite the high depletion of all four unique hydrocarbon deposits in terms of reserves, as well as some large ones, these two groups of deposits still account for the bulk of annual hydrocarbon production: 25.3% and 46.6%, respectively, which together account for 71.9% of the republic's total annual production. This is a very high figure. Medium and small hydrocarbon deposits account for 12% and 16.1%, respectively.

Analysing this situation, it can be predicted that, provided no new unique (primarily) or large deposits are discovered, there will be a further decline in hydrocarbon production volumes. Since traditional hydrocarbons are running out, one solution is to explore unconventional hydrocarbons, which are the main candidate for future hydrocarbon production (Muther et al., 2022).

There is cause for concern regarding the number of explored deposits, which has reached 96, or 30.8% of the total number of deposits in the republic. In 2000, the share of explored deposits in the republic was 20.3%. The reason lies in the fact that in recent decades, most of the newly discovered deposits have begun to be exploited at an accelerated rate, sometimes at industrial rates, in order to compensate for the decline in production, which does not allow proper completion of exploration, reliable assessment of hydrocarbon reserves, and the development of an up-to-date industrial development project aimed at ensuring the reliability of the exploited facility and increasing the efficiency of hydrocarbon field development (Suleymanov et al., 2022). As a result, not only the geological exploration process suffer, when fields are not completed by exploration and the fund of explored fields is artificially increased, in which the latter "hang" for decades, but also in the long term, damage is done to the operational process, when intensive hydrocarbon production reduces the potential for further development.

In conclusion, it can be stated that the oil and gas industry provides the republic's economy with energy resources, and despite some problems, the overall outlook for the continued effective conduct of oil and gas exploration activities appears quite optimistic (Masnadi, Brandt, 2017). The presence of significant volumes of projected resources (18,141.1 million tons of oil equivalent), with the prospect of their possible increase, gives hope for the discovery of new oil and gas fields, including those with large reserves of hydrocarbons (Bogdanov, Khmirov, 2025).

REFERENCES

Barros EGD, Van den Hof PMJ, Jansen JD (2020) Informed production optimization in hydrocarbon reservoirs. Optimization and Engineering 21:25–48. https://doi.org/10.1007/s11081-019-09432-7

Bogdanov AN, Karshiev OA, Khmirov PV (2023) The role of the Bukhara-Khiva region in the state of the hydrocarbon potential of the Republic of Uzbekistan. ANAS Transactions, Earth Sciences, Special Issue:168–172. https://doi.org/10.33677/ggianasconf20230300041 (in Russian)

Bogdanov AN, Khmirov PV (2023) Raw hydrocarbons base of the Republic of Uzbekistan – growth and production structure. Socar Proceedings 2:1–5. http://dx.doi.org/10.5510/OGP2023SI200887 (in Russian)

Bogdanov AN, Khmirov PV (2024) Results of geological exploration for oil and gas and hydrocarbon resource base development in Bukhara-Khivinsky region. Russian Oil And Gas Geology 1:45–57. https://doi.org/10.47148/0016-7894-2024-1-45-57 (in Russian)

Bogdanov AN, Khmyrov PV (2025) Petroleum potential of the Republic of Uzbekistan and its development prospects. Russian Oil and Gas Geology 2:113–123. https://doi.org/10.47148/0016-7894-2025-2-113-123 (in Russian)

Bogdanov AN, Qarshiyev OA, Gaffarov MA, Khmirov PV, Rabbimkulov SA (2024) Evolution of oil and gas prospecting in the Bukhara-Khiva Region. Socar Proceedings 4:12–19. http://dx.doi.org/10.5510/OGP20240401012

Delannoy L, Longaretti P-Y, Murphy DJ et al (2021) Peak oil and the low-carbon energy transition: a net-energy perspective. Applied Energy 304(117843). https://doi.org/10.1016/j.apenergy.2021.117843

Henstridge M, Roe A (2018) The macroeconomic management of natural resources. In: Extractive industries: the management of resources as a driver of sustainable development 8:161–178. https://doi.org/10.1093/oso/9780198817369.003.0008

Laherrere J, Hall CAS, Bentley R (2022) How much oil remains for the world to produce? Comparing assessment methods, and separating fact from fiction. Current Research in Environmental Sustainability 4(100174). https://doi.org/10.1016/j.crsust.2022.100174

Masnadi MS, Brandt AR (2017) Energetic productivity dynamics of global super-giant oilfields. Energy & Environmental Science 6(10):1493–1504. https://doi.org/10.1039/C7EE01031A

Muther T, Qureshi HA, Syed FI et al (2022) Unconventional hydrocarbon resources: geological statistics, petrophysical characterization, and field development strategies. J Petrol Explor Prod Technol 12(31):1463–1488. https://doi.org/10.1007/s13202-021-01404-x

Nuriyev RE, McFerren CJ (2025) The current state of the gas industry and the emerging green energy sector in Azerbaijan. SOCAR Proceedings 2:159–170. http://dx.doi.org/10.5510/OGP20250201077

Punanova SA (2022) Megareservoirs of hydrocarbons are accumulation of giant by oil and gas deposits. Socar Proceedings 2:39–51. http://dx.doi.org/10.5510/OGP2022SI200724 (in Russian)

Shuster VL (2022) Features of formation and placement of large and giant oil and gas deposits in megareservaries of sedimentary basins. Socar Proceedings 2:30–38. http://dx.doi.org/10.5510/OGP2022SI200723

Sokolov AV (2023) Retrospective analysis of prospecting and exploration efficiency at the Glavtyumengeologia in 1960–1990 in the Shirotny Ob region as the basis for planning prospecting and exploration drilling. Georesursy-Georesources 25(1):36-44. https://doi.org/10.18599/grs.2023.1.4 (in Russian)

Sokolov AV, Shubina AV (2023) Analysis of the reserves-to-production ratio for various stratigraphic complexes of Western Siberia. Georesursy-Georesources 25(1):45–50. https://doi.org/10.18599/grs.2023.1.5 (in Russian)

Suleymanov GG, Ismayilova HG, Qasumov ER (2022) Main direction for improving the use of oil and qas fields. Socar Proceedings 3:61–65. http://dx.doi.org/10.5510/OGP20220300709 (in Russian)

Tatar M, Harati J, Farokhi S et al (2024) Good governance and natural resource management in oil and gas resource-rich countries: A machine learning approach. Resources Policy 89(104583). https://doi.org/10.1016/j.resourpol.2023.104583

van Krevel Ch, Peters M (2024) How natural resource rents, exports, and government resource revenues determine Genuine Savings: Causal evidence from oil, gas, and coal. World Development, 181(106657). https://doi.org/10.1016/j.worlddev.2024.106657

Venables AJ (2016) Using natural resources for development: Why has it proven so difficult? Journal of Economic Perspectives, 30(1):161–184. https://doi.org/10.1257/jep.30.1.161

World Energy Council (2016) World Energy Resources: Unconventional gas, a global phenomenon. London: World Energy Council. ISBN 978-0-946121-45-8. Retrieved from http://www.worldenergy.org

РАЗВИТИЕ РЕСУРСНОЙ БАЗЫ УГЛЕВОДОРОДОВ И НЕФТЕГАЗОРАЗВЕДОЧНЫХ РАБОТ В РЕСПУБЛИКЕ УЗБЕКИСТАН: ИСТОРИЧЕСКИЕ ТЕНДЕНЦИИ И ПЕРСПЕКТИВЫ РАЗВИТИЯ

Богданов А.Н.*, Каршиев О.А., Хмыров П.В.
Институт геологии и разведки нефтяных и газовых месторождений, Республика Узбекистан
100164, Ташкент, Мирзо-Улугбекский район, ул. Олимлар, 64
**Автор, отвечающий за переписку: bogdalex7@yandex.ru*

Резюме. В статье представлены результаты комплексного анализа развития нефтегазопоисковых и разведочных работ на территории Республики Узбекистан в период от конца XIX века до 2025 года. Исследование направлено на выявление закономерностей развития геологоразведочной отрасли, оценку эффективности восполнения минерально-сырьевой базы углеводородов и определение перспектив дальнейшего прироста запасов нефти и газа. В качестве исходных материалов использованы официальные статистические данные, фондовые и архивные источники, результаты геологоразведочных работ, а также сведения о динамике добычи и освоения месторождений. Проведён анализ основных производственных и геологических показателей, включая объёмы поисково-разведочного бурения, показатели подготовки структур к глубокому бурению, прирост запасов нефти и газа, а также эффективность геологоразведочных работ на различных этапах развития отрасли. Выделены периоды наиболее интенсивного освоения недр, связанные с открытием и вводом в промышленную разработку крупных нефтяных и газовых месторождений, и этапы снижения геологоразведочной активности, сопровождавшиеся сокращением объёмов бурения и прироста запасов углеводородов. Особое внимание уделено анализу коэффициентов перевода прогнозных ресурсов в промышленные запасы, характеризующихся значительной изменчивостью в различные временные периоды. Установлено, что фактический прирост запасов в ряде случаев существенно превышал первоначальные прогнозные оценки, что свидетельствует о необходимости совершенствования методических подходов к оценке ресурсной базы и актуализации прогнозных ресурсов. Полученные результаты подтверждают высокие перспективы дальнейшего развития нефтегазового комплекса Узбекистана при условии активизации геологоразведочных работ, внедрения современных технологий моделирования и повышения эффективности оценки ресурсов.

Ключевые слова: *нефть, газ, углеводороды, геологоразведка, ресурсы, запасы*

ÖZBƏKİSTAN RESPUBLİKASINDA KARBOHİDROGEN EHTİYATLARININ KƏŞFİYYATI VƏ XAMMAL-RESURS BAZASININ İNKİŞAFI: TARİXİ İNKİŞAF MEYLLƏRİ VƏ GƏLƏCƏK PERSPEKTİVLƏR

Boqdanov A.N.*, Karşiyev O.A., Xmırov P.V.
Neft və Qaz yataqlarının Geologiyası və Kəşfiyyatı İnstitutu, Özbəkistan Respublikası
100164, Daşkənd, Mirzo-Uluqbek rayonu, Olimlar küç., 64
**Yazışmalara məsul: bogdalex7@yandex.ru*

Xülasə. Məqalə IX-cu əsrin sonlarından 2025-ci ilə qədər Özbəkistan Respublikasında neft və qaz axtarışı və kəşfiyyat fəaliyyətlərinin inkişafının əhatəli təhlilinin nəticələrini təqdim edir. Tədqiqatın məqsədi geoloji kəşfiyyat sektorunun inkişafındakı tendensiyaları müəyyən etmək, karbohidrogen mineral resurs bazasının bərpasının effektivliyini qiymətləndirmək və neft və qaz ehtiyatlarının daha da artması perspektivlərini müəyyən etməkdir. Rəsmi statistik məlumatlar, istinad və arxiv mənbələri, geoloji kəşfiyyat işlərinin nəticələri, eləcə də istehsal və sahə inkişafının dinamikası haqqında məlumatlar mənbə materialları kimi istifadə olunub. Əsas istehsal və geoloji göstəricilərin – kəşfiyyat qazma həcmi, dərin qazma üçün sahənin hazırlanması göstəriciləri, neft və qaz ehtiyatlarının artımı və sənayenin inkişafının müxtəlif mərhələlərində geoloji kəşfiyyat işlərinin effektivliyinin – təhlili aparılıb. Böyük neft və qaz yataqlarının kəşf edilməsi və istismara verilməsi ilə əlaqədar mineral ehtiyatların ən intensiv istismar dövrləri, eləcə də qazma həcmində və karbohidrogen ehtiyatlarının artımında azalma ilə müşayiət olunan kəşfiyyat fəaliyyətinin azalma mərhələləri müəyyən edilib. Təxmin edilən ehtiyatların kommersiya ehtiyatlarına çevrilmə nisbətlərinin təhlilinə xüsusi diqqət yetirilir; bu nisbətlər müxtəlif dövrlərdə əhəmiyyətli dəyişiklik göstərir. Məlum olub ki, bir sıra hallarda ehtiyatların faktiki artımı ilkin proqnozları əhəmiyyətli dərəcədə üstələyib, bu isə resurs bazasını qiymətləndirmək üçün metodoloji yanaşmaları təkmilləşdirməyə və resurs proqnozlarını yeniləməyə ehtiyac olduğunu göstərir. Əldə olunan nəticələr geoloji kəşfiyyat işləri gücləndirildikdə, müasir modelləşdirmə texnologiyaları tətbiq edildikdə və resursların qiymətləndirilməsinin səmərəliliyi artırıldıqda Özbəkistanın neft və qaz sektorunun daha da inkişafı üçün güclü perspektivlərin mövcudluğunu təsdiqləyir.

Açar sözlər: *neft, qaz, karbohidrogenlər, geoloji kəşfiyyat, resurslar, ehtiyatlar*

ANAS Transactions Earth Sciences 1 / 2026

http://www.journalesgia.com

TO THE STUDY OF FOSSIL BONE REMAINS OF TORTOISES (TESTUDINES, TESTUDINIDAE) FROM THE BINAGADI BITUMEN DEPOSIT (AZERBAIJAN)

Novruzov N.E.[1]*, Eybatov T.M.[2], Taptygova K.A.[1]

[1]Ministry of Science and Education of the Republic of Azerbaijan, Institute of Zoology, Azerbaijan
1128, Passage, block 504, Baku, AZ1073
[2]Ministry of Science and Education of the Republic of Azerbaijan,
Museum of Natural History, Azerbaijan
3(17), Lermontov, Baku, AZ1006
**Corresponding author: niznovzoo@mail.ru*

Keywords: *bitumen deposit, fossil remains, tortoises, morphology, bones, microstructure*

Summary. The objects of the study were fossilised bone remains of tortoises extracted from the soil during excavations in the Binagadi bitumen deposit and suburban summer cottages of Absheron. The material was collected and processed during the period from 2020 to 2023 during expeditionary and laboratory researches. The study of the material revealed a large number of bone fragments. The generic and species affiliation of the discovered bone fragments of tortoises was established. The study of the skeletal remains of tortoises found in the Binagadi bitumen deposit in the Late Pleistocene layer (the Late Dryas) and its comparison with the bones of tortoises found in the Holocene layer (the Middle Subatlantic period) on Absheron allowed assuming that the climate at the end of the Pleistocene was cooler and more humid than in the Holocene. This was indicated by some changes in the morphology of the bony shell of tortoises: a decrease in the indices of the ratio of shell length to its width and height, as well as the width of the shell to its height; changes in the size proportions of some bone plates of the carapace and plastron. All these changes presumably reflect some intensification of the adaptation processes associated with significant climate changes in Azerbaijan in general and in its eastern part particularly during the specified geological period (more than 0.012 million years ago).

Introduction

Bitumen deposits with ancient remains of flora and fauna are confined to areas where oil comes to the Earth's surface and are most often of Quaternary age. In deposits of this type, organic remains accumulate over a long period of time and have a fairly diverse species composition, with the remains preserved to a satisfactory level for study. Natural bitumen deposits in Azerbaijan are concentrated mainly in the Absheron, Shemakha-Gobustan, Nizhne-Kura, Gabala and Guba regions. Several bitumen deposits are known on the Absheron Peninsula: Gyrmaki, Binagady, Khirdalan, Babazanan and Pirallahi Island (Artem). Only two of them - Gyrmaki and Binagady have been studied for paleofauna (Halilov, 2003; Alizadeh, 2024).

The Binagadi bitumen deposit is a unique and the largest Upper Pleistocene cemetery of flora and fauna of global significance. More than 300 species of animals and plants have been identified here (43 species of mammals, 110 species of birds, two species of reptiles, one species of amphibians, 107 species of insects, one species of mollusk, and 22 species of plants). Only the Californian deposit Rancho La Brea in the USA is comparable to it.

The Binagadi bitumen deposit was discovered in 1938 by geologist A.S.Mastan-zade, who, having discovered animal bones in bitumen, handed over the unique paleontological finds to V.V.Bogachev, who was able to appreciate the scientific significance of these finds (Jafarov, 1966). Since then, employees of the Natural History Museum named after G.Zardabi (Natural History Museum), and since 2020, the staff of the paleozoology laboratory of the Institute of Zoology of Azerbaijan have been excavating and studying the fossil remains of flora and fauna there. The location of the remains of flora and fauna coincided with the site of the most ancient oil and bitumen production on the Absheron Peninsula, where wells from which oil products were previously extracted manually have survived to this day.

The study of the Binagadi remains of animals and plants is very important for the reconstruction of the fauna of the Quaternary period of Eurasia and the history of the formation of the modern fauna of Absheron (Eybatov et al., 2015). Macrostructural markers played a leading role in determining the Binagadi osteological material, which have proven their priority significance for determining the taxonomic status of many groups of animals (Burchak-Abramovich, 1966).

The Binagadi burial site of the Quaternary fauna and flora is located on the Absheron Peninsula in the village of Binagadi. On the site of the Binagadi burial site 150-40 thousand years ago there was an ancient freshwater or slightly salty lake, around which there were natural oil spills that were destructive to animals. Oil spills also penetrated into the lake itself, increasing the area of the territory posing a danger to representatives of the local fauna. As a result of many years of work by the employees of the G.Zardabi Natural History Museum: V.V.Bogachev (1938;1939), P.V.Serebrovsky (1945;1948), N.I.Burchak-Abramovich (1949-1962), R.D.Jafarov (1954-1966), D.V.Gadzhiev (1968-1978), T.M.Eybatov (2022), N.E.Novruzov, K.A.Taptygova, T.M.Eybatov (2024) et al. identified many species of insects, birds and mammals by collecting and studying the fossil remains of the Binagadi fauna.

Since 2012, the third stage of research and excavations in the territory of the Binagadi site of fossil Quaternary fauna and flora began. During these works, old and new layers rich in samples of fossil fauna and flora were studied, in the study of which, since 2020, employees of the Paleozoology Laboratory of the Institute of Zoology of Azerbaijan have taken part together with the employees of the Natural History Museum. Currently, all collected fossil plant, entomological and osteological material is stored in the Natural History Museum of Baku.

Material and methods

The fossil bone material of tortoises was collected from 2020 to 2023 on the Absheron Peninsula in the southeastern part of the Binagadi settlement (40.06°N; 47.45°E), where the Binagadi burial site of Quaternary fauna and flora is located. During excavations, the soil mixed with bitumen containing bone and plant remains was removed layer by layer in large blocks and packed into large plastic containers. Subsequently, in the laboratory, the blocks were carefully divided into small parts, sorted and their composition was studied visually and using magnifying devices (magnifying glasses; MBI-6 and Nikon SMZ 1270 binoculars). The found objects were photographed in different projections with a scale ruler superimposed and sorted according to taxonomic classification and morphological nomenclature. When identifying the Binagadi fossil bone remains, the main consideration was given to the structural features of the macro- and microstructure of the bones, taking into account the geochronological scale, paleoclimatic and paleoecological conditions of the Upper Pleistocene (Velichko, 2009). According to the stratigraphic scale, the studied horizons corresponded to the Late Pleistocene (50-70 thousand years ago).

During the primary office processing for sorting and identifying the material, the osteological collections of the Natural History Museum and the Institute of Zoology were used as comparative (reference) samples. Additional literature was also used: anatomical atlases, identifiers and guides to comparative animal anatomy (Gurtovoy et al., 1978; Carroll, 1992; Romer, Parsons, 1992; Kartashev et al., 2004; Dzerzhinsky, 2005; Titov et al., 2011; Zagumenov, 2021). Various methods have been proposed for preparing bone tissue sections (Eidlin, 1971; Smirina, 1989; Castanet, Smirina, 1990; Smirina, 1994; Klevezal, 2007). However, in our case, they did not fully ensure the production of thin sections (up to 0.02-0.04 mm), especially from bones stored in the soil for a long time, the surface layers and compacts of which, having undergone mineralisation processes during their stay in the soil, are easily destroyed and their value may ultimately be lost. At the same time, the degree of mineralisation of bone tissue in the soil is one of the important features determining the time of death of an animal [Rubezhansky, Nedilko, 1972). In addition, the methods proposed by the authors are quite complex in terms of technique and require a significant investment of time. We used a simplified method for preparing thin sections, which allows avoiding the above-mentioned disadvantages and preserve the mineralised compacta layer on the bones for measuring its thickness using the eyepiece micrometer of the microscope. The essence of the method for preparing of thin transverse sections of long tubular bones was as follows. From the middle of the diaphyses of long tubular bones, cuts were made with a dental disk cutter and by further grinding on grindstones with different degrees of graininess (M20–M5 μm) transverse sections were prepared suitable for examination under a microscope in transmitted light. Then the thin sections (15–30 μm) were decalcified in a 3% nitric acid solution for 20 minutes, washed with running water and examined under a binocular microscope at 40–60x magnification. The thin sections were stored in glass penicillin vials in pure glycerin. The described method is characterised by the speed of preparative of the preparat, allows obtaining very thin sections, and is especially suitable for bones extracted from the ground. We used it in the study of a large number of bones of varying degrees of preservation.

The material for the comparative study of the skeletons of tortoises from the Binagadi Pleistocene bitumen deposits with the skeletons of modern tortoises were the bone remains of land tortoises obtained in the Holocene layer (at a depth of up to 1.5 m) when digging wells in old suburban summer cottages of the Absheron Peninsula (Shuvalan, Dubendy, Govsan, Turkyan). All linear measurements of the shells and separate bones were carried out with mechanical and digital calipers with an accuracy of 0.1 mm. Measurements of the microstructural elements of bone sections were carried out with an accuracy of 0.01 mm using the eyepiece micrometer of the MBI-6 microscope. To fully describe the incomplete skeletons of tortoises, a reconstruction of the shells was carried out using the typological extrapolation method (Meyen et al., 1988), i.e., completing the missing parts using analog (standard) images taken from zootomic atlases and processed in the graphic editors Paint and Corel Draw. Statistical processing of the primary digital data was carried out in Microsoft Excel and in the PAST 4.03 programs (Hammer et al., 2001).

Results and discussion

***Description of the fossil material*.** Two incomplete skeletons of tortoises and separate bones of these animals were found in bituminous deposits at a depth of about 2.5 m (Fig. 1). These finds were of particular value, since they are extremely rare. The postcranial skeletons of tortoises included bones of the carapace and plastron (cervical, pygal, costal, neural, marginal, suprapygal, epiplastron, entoplastron, hyoplastron, hypoplastron, xiphiplastron), as well as the caracoid, pelvic bones, part of the cervical and caudal vertebrae, long tubular bones of the appendicular skeleton (humerus, radius, ulna and clavicle, femur, tibia) (Fig. 2).

All bones were in satisfactory condition. The presence of ossified epiphyses at the distal ends of long bones indicated that these skeletal specimens belonged to adults.

The material for the comparative study was the bone remains of land tortoises, obtained in the Holocene layer during the digging of wells in old summer cottages on the Absheron Peninsula. The number of claws on the limbs of tortoises extracted from a depth of up to 1.5 m at old summer cottages on the Absheron Peninsula was five on the front limbs and four on the back limbs. This feature clearly indicated that the discovered skeletons belonged to the genus *Testudo*, presumably to the species *Testudo graeca* Linnaeus, 1758 (Fig. 3).

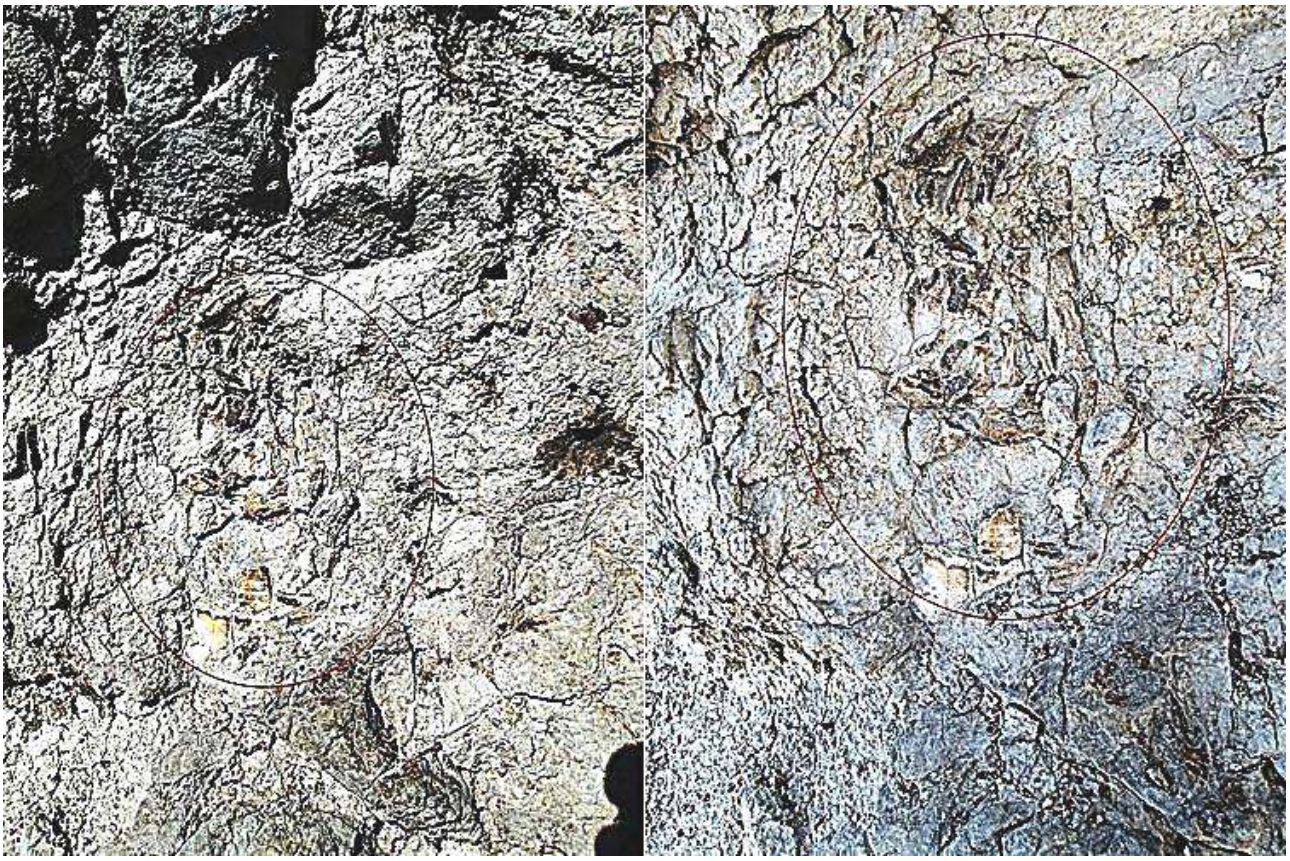

Fig. 1. Location of tortoise bone fragments in bitumen layers in a section of the formation at a depth of 2.5 m (Binagady, 2020)

Fig. 2. Bone material of tortoises recovered during excavations at the Binagadi bitumen deposit

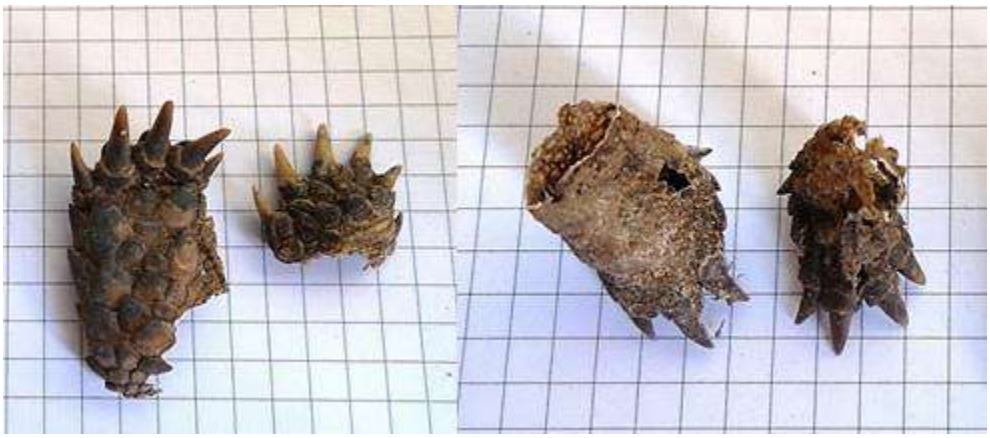

Fig. 3. Fragments of the front five-fingered and back four-fingered limbs of the tortoise *Testudo graeca* extracted from a depth of up to 1.5 m in the summer cottages of the Absheron Peninsula (paws with claws)

Due to the complex and confusing taxonomy of this group, we did not carry out subspecific identification of tortoise bones. Usually, it is carried out based on a set of key morphological features (Vasilyev et al., 2014). However, different geographic populations of *Testudo graeca* are characterised by morphological heterogeneity in a number of diagnostic features, which complicates the unambiguous recognition of subspecies. Therefore, mitochondrial genome markers were used by different researchers for the taxonomy of this group. Different authors distinguish from 4 to 20 subspecies within this taxon (Ananyeva et al., 1998; Fritz et al., 1996; Pieh, Perälä, 2002). Currently, it is customary to consider all populations of this species as a difficult polytypic *T. graeca* complex, consisting of 11 morphological species and six subspecies (Fritz et al., 2007).

Taxonomic position of tortoises of the genus Testudo in the Caucasus. Until the mid-1980s, it was believed that only one subspecies of the spur-thighed tortoise *T. graeca ibera* Pallas, 1814 inhabits the Caucasus (Bannikov et al., 1977). It was later discovered that it is polymorphic and, based on the morphological differences of individual populations, three new subspecies with isolated ranges were described: *T. g. nikolskii* Chkhikvadze et Tuniev, 1986 (the western Caucasus); *T. g. armeniaca* Chkhikvadze, 1991 (Armenia: Araks River valley to the Zangezur Gate) and *T. g. pallasi* Chkhikvadze et Bakradze, 2002 (foothills of Dagestan) (Parham et al., 2006). Later, based on the variability of the mtDNA cytb gene and ISSR markers, it was concluded that the taxon *T. g. pallasi* Chkhikvadze et Bakradze, 2002 is a junior synonym of the subspecies *T. g. armeniaca* Chkhikvadze, 1991. It is believed that the habitat of this subspecies covers the central part of the western coast of the Caspian Sea, the eastern and central parts of the Caucasus region, including the Araks River valley in Armenia and Turkey (Fritz et al., 2007). It has been shown that allopatric populations of tortoises belonging to the subspecies *T. g. armeniaca* live on

the territory of Dagestan (Russia), Azerbaijan, Armenia and part of Turkey, and *T. g. ibera*, living in Transcaucasia, represent two separate evolutionary lineages. One of them unites tortoises *T. g. ibera* from Georgia and the Mediterranean (ibera sensu lato), as well as the West Caucasian tortoises *T. g. nikolskii*, and the other – the tortoises *T. g. ibera* from Azerbaijan, *T. g. armeniaca* and *T. g. pallasi*. According to paleontological data, *T. g. nikolskii* and *T. g. pallasi* descended from a single ancestor and could have diverged in the late Pliocene or early Pleistocene (Chkhikvadze, Tuniev, 1986).

Reliable remains of Pliocene land tortoises belonging to the *Testudo graeca* complex are known from a number of locations in the North Caucasus. Fossil remains of *T. g. ibera* tortoises are known in Western Georgia from the Paleolithic and Neolithic, i.e. this tortoise was widespread in Western Transcaucasia much later, at the end of the Holocene (Chkhikvadze, 2010). A special place among the *Testudo graeca* species complex is occupied by *T. g. zarudnyi* tortoises, which are found in a few refugia of the ancient Mediterranean on the Iranian Plateau. They probably survived there since the end of the Miocene or the beginning of the Pliocene, i.e. they are the most ancient forms of land tortoises in the region and belong to the relics of the Eastern Mediterranean (Pereshkolnik, Leontyeva, 2014). In addition, another extinct subspecies *Testudo graeca binagadensis* Khozatsky, 1978 existed in the Pleistocene of Apsheron (Alekperov, Khozatsky, 1977). The form *T. g. binagadensis*, described by L.I.Khozatsky as a special subspecies of the Mediterranean tortoise, differs from the typical modern one in a number of details of the structure of the shell and postcranial skeleton. The most important feature of the Binagadi subspecies is the relatively greater thickness of all bones, which is revealed both while comparing the same parts of the shell of this form with the modern one, and the proportions of the bones of their postcranial skeleton. This is especially noticeable on such bones as the humerus, femur and other tubular bones of the appendicular skeleton. The structural features of the Binagadi land tortoise allow, according to L.I.Khozatsky, to suggest that "it, hiding in shallow burrows, inhabited more or less open biotopes and adhered to shrub and sparse woody vegetation." It should be noted that the descendants of the Binagadi tortoises in eastern Transcaucasia now live in an environment somewhat similar to that which existed during the late Pleistocene (Alekperov, 1978).

Taxonomy of tortoises based on the bones of the postcranial skeleton. The taxonomic position of the tortoises which remains were found in the Binagadi bitumen deposit is presented below:

Class: Reptilia
Order: Testudines
Suborder: Cryptodira
Superfamily: Testudinoidea
Family: Testudinidae Gray, 1825
Genus: *Testudo* Linnaeus, 1758
Testudo graeca Linnaeus, 1758
Testudo graeca ssp. indet.

The tortoises which remains of incomplete skeletons and separate bones were found in the Binagadi bitumen deposit should presumably be considered subspecies of *Testudo graeca*: *Testudo graeca ibera* Pallas, 1814 (lives to this day) or the extinct *Testudo graeca binagadensis* Khozatsky, 1978 (which lived in the Middle and Upper Pleistocene of the Absheron Peninsula) (Alekperov, Khozatsky, 1977) until their molecular (DNA) studies are conducted.

Material: incomplete postcranial skeletons of two specimens of land tortoise, including carapace and plastron bones, two or three posterior cervical vertebrae, forelimb bones (two humeri), hindlimb bones, and anterior caudal vertebrae. It was decided to temporarily retain the third specimen from the bitumen layers of the horizon at the excavation site until further stratigraphic studies could be conducted.

The shells (carapaces and plastrons) were reconstructed using the available fragments was carried out using the typological extrapolation method (Material and Methods) (Fig. 4).

Comparative study of osteological material of tortoises. At the first stage of the work on the study of faunal remains of the Binagadi Pleistocene bitumen deposits, as a result of excavations, bitumen material was removed from a new bone-bearing horizon located at a depth of 1.5-2.5 m, which was a dense accumulation of plant fragments and bones of various animals enclosed in bitumen. According to the stratigraphic scale, the removed material corresponded to the Upper Pleistocene. A detailed study of the material revealed fragments of the skeleton, specimens of the humerus, radius, femur, tibia and other tubular and flat bones belonging to various animals: birds, small mammals, as well as fragments of the shell and long tubular and flat bones of tortoises. In addition to a visual study of the shape of the shell bones and tubular bones of tortoises, a reconstruction of the shells was carried out (Material and Methods), and the main morphometric parameters were measured: 1) maximum bone length; 2) width of the proximal epiphysis; 3) thickness of the articular head; 4) minimum width of the diaphysis; 5) maximum width of the diaphysis; 6) width of the distal epiphysis; 7) anteroposterior diameter of the proximal articular complex; 8) anteroposterior size of the distal articular complex.

At the second stage of the work, a comparative study of the osteological material of tortoises obtained during the digging of wells in the old summer cot-

tages of the Absheron Peninsula was carried out. The material of the comparative study of fossil and modern osteological materials were all the bones of land tortoises of the Binagadi Pleistocene bituminous deposits discovered by us at the first stage of excavations, their reconstructed shells (Fig. 4); bones of the internal skeleton, as well as whole shells of modern land tortoises found during the second stage of excavations in the Holocene layer on the Absheron Peninsula (Shuvalan, Dubendy, Govsan, Turkan) (Fig. 5).

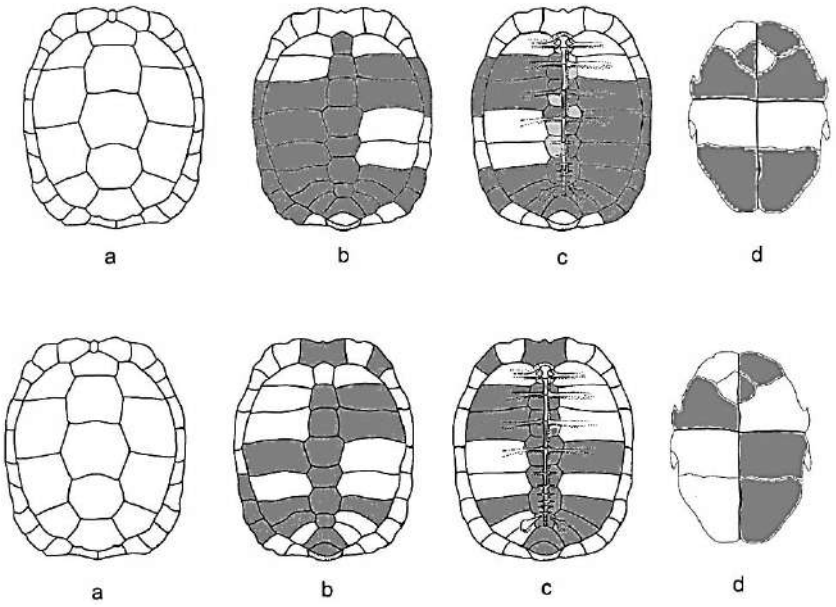

Fig. 4. Schematic figures of reconstructed tortoise shells found in bitumen deposits: a – general view of the nominal bony-horny carapace (dorsal surface); b – bony carapace (dorsal surface); c – bony carapace (ventral surface); d – bony plastron (ventral surface). The present skeletal fragments are highlighted in dark gray in the drawings

Fig. 5. Fragments of the internal skeleton and whole shells of tortoises extracted from the Holocene layer of Absheron on old summer cottages (up to 1.5 m)

The compared osteological material was represented by the humerus, radius, femur, tibia long tubular bones and flat bones of the carapace and plastron (Tables 3-8). The fossil bones were visually and morphologically almost indistinguishable from the bones of modern representatives of the species, except that the metric indicators of the fossil tortoises for separate bones differed slightly from the bone sizes of modern individuals (Tables 4, 6, 8). The compared osteological material was extracted from a depth of up to 1.5 m.

The humerus, radius, femur, tibia, as well as the bones of the carapace and plastron (98 in total) were examined. The following morphometric parameters were used:

1) long bones: maximum bone length; width of the proximal epiphysis; thickness of the articular head; minimum width of the diaphysis; maximum width of the diaphysis; width of the distal epiphysis; anteroposterior diameter of the proximal joint complex; anteroposterior size of the distal joint complex;

2) carapace: bone plates of the vertebral row, including the supracaudal and caudal parts (measurements – length along the midline and greatest width); all costal plates (measurements – proximal width, distal width, maximum length); all marginal plates (measured in the same way as the costal plates);

3) plastron: length and greatest width of all plates along the midline.

In addition, the general dimensions of whole and reconstructed shells were used: length of the carapace (L. car.), greatest width of the carapace (Lt. car.), height of the shell (Al. t), length of the plastron (L. pl.) and its greatest width (S. pl.) (Table 1).

The age of fossil tortoises from the late Pleistocene and Holocene layers was estimated using two methods: an empirically developed formula (L.car(mm)/12) (Novruzov, 2016) and thin sections from the middle of the diaphysis of long tubular bones (Table 2). The number of annual layers found in the thin sections was supplemented by 2-3 layers that underwent resorption during the growth of the animal.

Table 1

Metric parameters of reconstructed late Pleistocene (No. 1, 2) and whole Holocene (No. 3-7) bony shells of tortoises of the genus *Testudo* (mm)

Character/Indice	№ 1	№ 2	№ 3	№ 4	№ 5	№ 6	№ 7
L. car.	123.5	108.0	93.0	96.4	86.4	71.6	73.7
Lt. car.	102.9	85.6	77.3	75.8	73.2	62.7	59.2
Al.t	63.3	59.0	47.5	49.6	47.9	39.9	40.3
L. pl.	110.5	93.7	78.1	85.8	76.4	66.6	63.6
S. pl.	90.5	81.5	69.8	70.5	66.3	57.5	57.0
L. car. / Lt. car.	1.20	1.26	1.20	1.27	1.18	1.14	1.24
L. car. / Al.t	1.95	1.83	1.95	1.94	1.80	1.79	1.82
Lt. car. /Al.t	1.62	1.45	1.62	1.52	1.52	1.57	1.46

Table 2

Data on the age of tortoises obtained empirically (by formula) and from bone sections

№	L. car.(мм)	Age (years)		
		By formula	By thin sections	Average
1	123.5	10.29	6(+3)	9.6
2	108.0	9.00	5(+3)	8.5
3	93.0	7.75	4(+3)	7.3
4	96.4	8.03	4(+3)	7.5
5	86.4	7.20	4(+2)	6.6
6	71.6	5.96	3(+2)	5.4
7	73.7	6.14	3(+2)	5.5

The correlation analysis of morphometric parameters of bone elements of the carapace and plastron and the overall dimensions of the reconstructed shell of land tortoises of the genus *Testudo* found during excavations at the Absheron summer cottages and in the Binagadi bitumens was carried out. Comparison of the correlation coefficients showed that the area of the greatest correlation of bone elements of the shell falls on the middle (dome-shaped) part, where the vertebral (I-IV) and costal (I-V) plates come into contact. At the junction of the first spine and the first marginal plate to the cervical plate, the area of the carapace is characterised by a reliable correlation. Some parameters of the plates are also significantly related: supracaudal, caudal and the last marginal. The largest correlation zone between the studied parameters in the plastron falls on the area of the epiplastral and endoplastral plates.

Table 3

Morphometric indices of long tubular bones of fossil tortoises (No. 1, 2)

№	Material	Dimensions, mm							
		1	2	3	4	5	6	7	8
1	Humerus	32.4	13.1	5.1	4.1	7.8	8.6	11.6	8.5
	Radius	20.4	6.6	5.1	4.2	3.4	5.1	7.2	6.8
	Femur	28.3	9.7	5.8	3.2	5.5	7.9	9.6	7.2
	Tibia	21.1	6.8	5.0	4.3	6.7	4.9	7.1	4.6
2	Humerus	28.5	11.3	6.6	3.9	6.1	8.9	10.9	8.1
	Radius	22.2	7.9	5.1	2.3	4.3	5.8	7.9	5.8
	Femur	23.2	6.7	5.0	2.6	3.6	6.9	8.3	6.1
	Tibia	18.0	5.3	4.1	2.0	3.5	3.7	5.1	3.4

Table 4

Morphometric indices of long tubular bones of the modern tortoise

Material	Dimensions, mm							
	1	2	3	4	5	6	7	8
Humerus	29.1	12.0	4.6	2.3	5.3	6.1	9.0	7.1
Radius	20.8	4.1	2.2	1.4	2.4	2.1	4.0	2.2
Femur	26.1	14.6	4.1	0.23	1.09	7.1	9.5	3.6
Tibia	20.8	5.0	3.8	1.7	3.1	3.4	4.1	3.3

Note (for tables 3, 4): 1 – maximum bone length; 2 – width of proximal epiphysis; 3 – thickness of articular head; 4 – minimum width of diaphysis; 5 – maximum width of diaphysis; 6 – width of distal epiphysis; 7 – anteroposterior diameter of proximal articular complex; 8 – anteroposterior size of distal articular complex.

Table 5

Morphometric indices of carapace bones of fossil tortoises (No. 1, 2)

№	Material	Dimensions, mm			
		1	2	3	4
1	Marginale	15.7	18.2	21.0	22.5
	Neurale	18.7	13.3	19.4	19.1
	Costale	41.2	20.3	44.4	44.2
	Nuchale	31.1	24.3	27.7	27.3
	Pygale	19.4	15.3	21.7	22.3
2	Marginale	18.8	16.3	22.9	21.6
	Neurale	12.1	20.0	19.1	19.6
	Costale	45.1	44.1	46.9	47.1
	Nuchale	24.8	30.1	27.1	27.3
	Pygale	15.1	18.9	21.6	22.1

Table 6

Morphometric indices of carapace bones of modern tortoise

Material	Dimensions, mm			
	1	2	3	4
Marginale	15.1	12.6	15.4	17.7
Neurale	18.7	10.8	18.2	18.6
Costale	33.2	13.4	34.2	36.1
Nuchale	22.0	22.4	20.1	20.2
Pygale	20.6	13.5	22.7	23.1

Table 7

Morphometric indices of plastron bones of fossil tortoises (No. 1, 2)

№	Material	Dimensions, mm			
		1	2	3	4
1	Epiplastron	20.8	20.5	18.2	19.7
	Entoplastron	23.4	23.0	22.2	23.1
	Hyoplastron	36.5	45.6	50.1	47.2
	Hypoplastron	31.5	44.4	52.3	52.8
	Xiphiplastron	33.6	29.8	39.6	36.1
2	Epiplastron	21.0	20.1	15.6	20.2
	Entoplastron	23.1	23.3	22.7	23.0
	Hyoplastron	50.9	36.5	49.6	46.6
	Hypoplastron	45.1	30.8	51.7	52.8
	Xiphiplastron	29.3	34.1	39.4	36.4

Table 8

Morphometric indices of the plastron bones of the modern tortoise

Material	Dimensions, mm			
	1	2	3	4
Epiplastron	19.8	21.0	15.1	23.2
Entoplastron	22.2	23.1	23.1	21.7
Hyoplastron	36.1	45.2	49.8	46.1
Hypoplastron	31.9	44.6	51.8	46.2
Xiphiplastron	33.9	29.7	39.1	36.6

Note (for tables 5–8): 1 – transverse length of bone; 2 – transverse width of bone; 3 – transverse diagonal of bone to the left; 4 – transverse diagonal of bone to the right

Correlation and regression analysis of the measurements of the tortoise bones (Tables 9-11) showed a strong positive correlation between the long tubular bones (r = 0.925-0.998) with the bones of the carapace (r = 0.612-0.996) and the bones of the plastron (r = 0.606-0.998). The exceptions were the nuchale (r = - 0.097) and (r = 0.203) on the carapace and the entoplastron (r = - 0.062) and hyoplastron (r = - 0.245) on the plastron (Tables 10-11).

Microstructure of long tubular bones of tortoises in transverse sections. Thin-sectioned bone crossections (0.03 mm) suitable for examination under a microscope in transmitted light were made after taking the main measurements from the middle of the diaphysis of the long tubular bones. In total, three series of thin sections were made: thin sections from one bone from several sections of the diaphysis and the proximal and distal epiphyses of tortoises; thin sections from the middle of the diaphysis of different bones.

A study of the microstructure of the long tubular bones of tortoises found in the Binagadi bituminous deposits showed that the periosteum is significantly damaged or virtually absent in most bones (Fig. 6). The bones have a clearly defined growth cycle, demonstrating all stages of postembryonic ontogenesis. The narrow dark layers visible in the sections can be considered as winter layers (the period of growth cessation), and the wide transparent layers as spring-summer, i.e., a continuous growth cycle. Closer to the opening of the medullary canal, the process of resorption of bone tissue previously replaced by endosteum occurs, which leads to complete or partial disappearance of the first layers. The layers are better expressed in the diaphyseal part of the long tubular bones.

Table 9

Results of correlation and regression analysis of morphometric parameters of long tubular bones of fossils (No. 1, 2) and modern tortoises

№	Material	*r*	*t*	*p*	*m*
1	Humerus	0.996	28.05	0.0001	10.3%
	Radius	0.983	13.27	0.0001	28.7%
	Femur	0.942	6.85	0.001	127.0%
	Tibia	0.989	16.05	0.0001	22.1%
2	Humerus	0.993	20.60	0.0005	10.6%
	Radius	0.984	13.31	0.0004	40.6%
	Femur	0.925	5.96	0.001	135.1%
	Tibia	0.998	35.87	0.00001	8.7%

Note: r – Pearson correlation coefficient; t – Student's t-test; p – significance of difference; m – average approximation error (%)

Table 10

Results of correlation and regression analysis of morphometric parameters of carapace bones of fossil (No. 1, 2) and modern tortoises

№	Material	*r*	*t*	*p*	*m*
1	Marginale	0.612	1.09	0.471	9.0%
	Neurale	0.988	9.22	0.0687	2.2%
	Costale	0.996	15.17	0.0403	2.1%
	Nuchale	-0.097	0.138	0.9126	4.9%
	Pygale	0.988	8.94	0.0708	2.6%
2	Marginale	0.776	1.74	0.3318	6.6%
	Neurale	-0.439	0.691	0.6149	18.5%
	Costale	0.836	2.15	0.2766	18.4%
	Nuchale	0.203	0.294	0.8181	4.8%
	Pygale	0.350	0.528	0.6908	18.6%

Table 11

Results of correlation and regression analysis of morphometric parameters of plastron bones of fossil (No. 1, 2) and modern tortoises

№	Material	*r*	*t*	*p*	*m*
1	Epiplastron	0.672	1.28	0.42145	9.1%
	Entoplastron	-0.630	1.14	0.45650	1.6%
	Hyoplastron	0.998	22.54	0.02821	0.6%
	Hypoplastron	0.947	4.18	0.14924	4.6%
	Xiphiplastron	0.994	13.33	0.04763	1.0%
2	Epiplastron	0.851	2.29	0.26149	5.9%
	Entoplastron	-0.062	0.08	0.94387	2.5%
	Hyoplastron	-0.245	0.35	0.78173	9.8%
	Hypoplastron	0.234	0.34	0.79070	15.2%
	Xiphiplastron	0.606	1.07	0.47597	7.3%

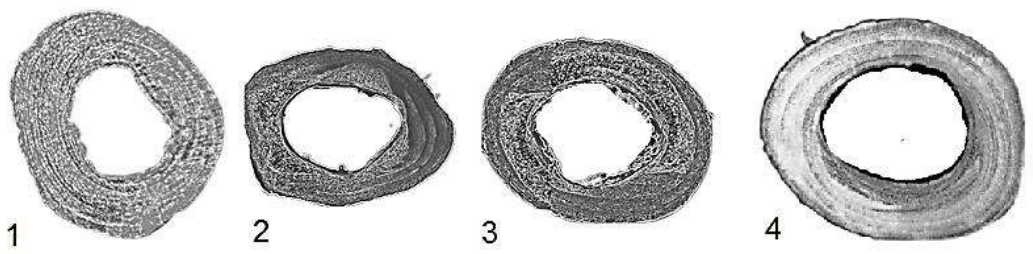

Fig. 6. Microstructure of long tubular bones of tortoises from Binagadi bitumens: 1 – femur; 2 – tibia; 3, 4 – humerus (×64)

Microstructural elements were also noted in the thin sections of long tubular bones: vascular and Haversian canals, osteons, lacunae, insertions of coarse fibrous bone tissue in the middle and endosteal zones. The thin sections of the bones of the skeletons of identified tortoises (Pleistocene horizon) were compared with the thin sections made from the bones of identified tortoises (Holocene horizon) by the number of microstructural elements. To count the microstructural elements (lacunae, osteons, Haversian and vascular canals), we used the method of Golubovich (1991) with some modification. In the space of the bone thin section, using the eyepiece of a microscope with an inserted lens with a grid (grid square = 10,000 sq. μm) at 64x magnification, the microstructural elements were counted (Table 12).

Correlation and regression analysis of the number of microstructural elements in the bone sections of the compared tortoises showed a strong positive correlation only for the metatarsus (r = 0.987), a moderate negative correlation for the fibula (r = −0.562), and a weak correlation for the radius and femur (r = 0.200 and 0.261, respectively). The number of adhesion lines in the sections made from one bone and from all the studied long tubular bones taken from one skeletal sample was the same. A study of a series of sections made from the middle of the diaphysis of the long tubular bones of turtles showed that the process of endosteal bone tissue resorption, which caused the complete or partial disappearance of the first two or three layers in the growth zone, makes it difficult to determine the exact stage of reptile ontogenesis. Comparative study of the microstructure of long tubular bones of tortoises discovered during the second stage of excavations in the Binagadi bituminous deposits and tortoises found in the Holocene layer showed: 1) all bones have a clearly expressed growth cycle; 2) narrow dark layers visible in thin sections should be considered winter layers (growth cessation period); 3) wide light (transparent) layers should be considered spring-summer continuous growth cycle; 4) the number of gluing lines in thin sections of all studied long tubular bones taken from one sample is the same; 5) a clear pattern of resorption of endosteal bone tissue and complete or partial destruction of the first two or three layers of the growth zone is observed. The process of resorption of bone tissue previously replaced by endosteum leading to complete or partial disappearance of the first layers in both cases makes it difficult to determine the exact stage of ontogenesis of these reptiles. Consequently, in each specific case of determining the duration of ontogenesis, 2-3 layers that underwent resorption during the growth of the animal should be added to the number of annual layers found in the sections.

Conclusion

The study of bitumen material extracted from the Binagadi burial site of the Quaternary fauna and flora allowed identifing two incomplete skeletons and separate bones of land tortoises of the genus *Testudo*. The study of the bone skeleton of tortoises found in the Binagadi burial site in the Late Pleistocene layer (Late Dryas) in comparison with the bones of tortoises found on Absheron in the Holocene layer (Middle Subatlantic period) leads to the assumption that the climate at the end of the Pleistocene was cooler and more humid than in the Holocene. This is indicated by some changes in the morphology of the bony shell of the Mediterranean tortoise: a decrease in the indices of the ratio of the length of the shell to its width and height (L.car/L.t.car.; L.car/Al.t.); the width of the shell to its height (L.t.car/Al.t.); changes in the size proportions of some bone plates of the carapace and plastron.

Table 12

Number of microstructural elements in thin sections of different bones of identified and already identified tortoises (per 10,000 sq. μm)

Microstructural element	Name of the bone													
	Humerus		Ulna		Radius		Femur		Fibula		Tibia		Metatarsus	
	I	II	I	II	I	II	I	II	I	II	I	II	I	II
Osteon	–	–	–	–	+	+	+	+	+	+++	–	–	++	++
Haversian Canal	+	+	+	+	+	+	+	++	+	++	+	+	++	+++
Vascular canal	+	–	+	+	+	+	+	+	+	+	+	–	+	+
Lacuna	+	+	+	–	+	+	+	+	+	+	–	–	+	+

Note: I – material being identified; II – already identified material. Number of microstructural elements: (+++) – 20-30; (++) – 10-20; (+) – less than 10; (−) – absent

All these changes, confirmed by correlation-regression analysis, presumably reflect some intensification of adaptation processes associated with significant climate changes in Azerbaijan in general and in its eastern part in particular during the specified geological period. They are expressed in a greater need of the species for protective and thermoregulatory-compensatory burrowing in the ground during periods of night pause, winter hibernation and summer aestivation, ensuring its successful survival in the resulting arid climatic conditions. In the microstructure of tortoise bones removed from bituminous layers, resorption processes are more pronounced and affect 3-4 adhesion lines and the endosteum region, whereas in the comparative material of Holocene tortoises, resorption affects 1-2, less often 3 adhesion lines, without affecting the endosteum. The ontogenetic age of the fossil remains of tortoises was determined to be within 10-12 years.

REFERENCES

Alekperov AM (1978) Amphibians and reptiles of Azerbaijan. Elm, Baku p 272 (in Russian)

Alekperov AM, Khazatsky LI (1977) Structural features of the Greek tortoise's shell. Scientific Notes of Azerbaijan State University, Biology Series 4:43–49 (in Russian)

Alizadeh AkA (2024) Current status of paleontological-stratigraphic studies in Azerbaijan. ANAS Transactions, Earth Sciences 1:9–27. https://doi.org/10.33677/ggianas20240100106

Ananyeva NB, Borkin LYa, Darevskij IS et al (1998) Amphibians and reptiles. Encyclopaedia of Russian Nature. ABF, Moscow, p 576 (in Russian)

Bannikov AG, Darevsky SI, Ishchenko VG et al (1977) A Guide to the amphibians and reptiles of the USSR. Prosveshchenie, Moscow, p 416 (in Russian)

Bogachev VV (1938) Discovery of post-Tertiary mammalian fauna in the vicinity of Baku. Priroda 7/8:150 (in Russian)

Bogachev VV (1939) Latest news on the discovery of fossil-bearing layers in the vicinity of Baku. Priroda 1:83 (in Russian)

Burchak-Abramovich NI (1966) A study of the Pleistocene fauna of the Caucasus (Fossil Birds). Proceedings of the Academy of Sciences of the Azerbaijan SSR, Earth Sciences Series 6:38–42

Caroll R (1992) Vertebrate palaeontology and evolution. Tom 1. Mir, Moscow, p 280 (in Russian)

Castanet J, Smirina EM (1990) Introduction to the skeletochronological method in amphibians and reptiles. Annales des Sciences Naturelles, Zoologie 11(4):191–196 (in French)

Chkhikvadze VM (2010) Annotated catalog of Paleogene, Neogene and recent turtles of Northern Eurasia. Georgian National Museum, Bulletin of the Natural Sciences and Prehistory Section 2: 95–111 (in Russian)

Chkhikvadze VM, Tuniev BS (1986) On the systematic position of the modern terrestrial tortoise of the Western Caucasus. Bulletin of the Academy of Sciences of the Georgian SSR 124(3):617–620 (in Russian)

Jafarov RD (1966) The Binagadi fossil vertebrate fauna. Proceedings of the Academy of Sciences of the Azerbaijan SSR, Earth Sciences Series 1:50–56 (in Russian)

Dzerzhinsky FY (2005) Comparative anatomy of vertebrates. Aspect-Press, Moscow, p 320 (in Russian)

Eybatov TM, Zeyniev OA, Mustafaev IM et al (2015) New findings of *Anser erythropus L.* in Pleistocene Binagadi limestone deposits in Azerbaijan. Proceedings of the Azerbaijan National Academy of Sciences, The Sciences of Earth 1-2:43–47 (in Russian)

Eybatov TM, Gadzhiev DV (2022) Fossil and modern pinnipeds of Azerbaijan. ANAS Transactions, Earth Sciences 1:106-118; https://doi.org/10.33677/ggianas20220100077

Eydlin AL (1971) On certain new possibilities for forensic medical differentiation of human and animal bones. Abstract of a PhD thesis in Medical Sciences. Moscow, p15 (in Russian)

Fritz U, Keller C, Budde M (1996) A new subspecies of the European pond turtle from south-western Spain, Emys orbicularis hispanica subsp. nov. Salamandra 32(3):129–152 (in German)

Fritz U, Hundsdörfer AK, Široký P et al (2007) Phenotypic plasticity leads to incongruence between morphology-based taxonomy and genetic differentiation in western Palaearctic tortoises (Testudo graeca complex; Testudines, Testudinidae). Amphibia-Reptilia 28: 97–121. https://doi.org/10.1163/156853807779799135

Golubovich LL (1991) Current possibilities for forensic identification of individuals using bones exposed to high temperatures. Abstract of a PhD thesis in Medical Sciences, p 48 (in Russian)

Gurtovoy NN, Matveev BS, Dzerzhinsky FY (1978) Practical zoology of vertebrates (Amphibians, Reptiles). Vysshaya Shkola, Moscow, p 406 (in Russian)

Halilov NYu (2003) A journey to the Kirmakinskaya Valley. Newspaper: Vyshka 15, 18 April (in Russian)

Hammer Ø, Harper DAT, Ryan PD (2001) PAST: Paleontological statistics software package for education and data analysis. Palaeontologia Electronica 4(1):1–9

Kartashev NN, Sokolov VE, Shilov IA (2004) Practical course in vertebrate zoology. Aspekt press, Moscow, p 384 (in Russian)

Klevezal GA (2007) Principles and methods of age determination of mammals. KMK Scientific Publications Association, Moscow, p 283 (in Russian)

Mejen SV, Makridin VP, Stepanov DL (1988) Modern palaeontology. A reference guide. Volume 1. Methods, approaches, issues, and practical applications. Nedra, Moscow, p 540 (in Russian)

Novruzov NE (2016) Biological and morphoecological characteristics of tortoises (Reptilia, Testudines) in the arid regions of eastern Azerbaijan. Abstract of a PhD thesis in Biology, p 20 (in Russian)

Novruzov NE, Taptygova KA, Eybatov TM (2024) New records of arthropod fragments (Arachnida, Insecta) from Late Pleistocene bitumen deposits of the Absheron (Azerbaijan). ANAS Transactions, Earth Sciences 1:145-157. https://doi.org/10.33677/ggianas20240100116 (in Russian)

Parham JF, Feldman CR, Boore JL (2006) The complete mitochondrial genome of the enigmatic bigheaded turtle (Platysternon): description of unusual genomic features and the reconciliation of phylogenetic hypotheses based on mitochondrial and nuclear DNA. BMC Evolutionary Biology 6(11). https://doi.org/10.1186/1471-2148-6-11

Pereskholnik SL, Leonteva OA (2014) Testudo zarudnyi: an ancient relict species in the eastern part of the Testudo graeca complex's range. Second All-Russian Conference 'Contemporary Problems of Biological Evolution'. Moscow (11–14 March) (in Russian)

Pieh A, Perälä J (2002) Variation amongTestudo graeca Linnaeus, 1758 in eastern North Africa, with a description of a new taxon from Cyrenaica (North-East Libya). Herpetozoa, 15(1/2):3–28 (in German)

Romer A, Parsons T (1992) Anatomy of the vertebrates. Mir, Moscow, p 358 (in Russian)

Rubezhansky AF, Nedilko ES (1972) A new method for the objective assessment of the degree of mineralization of exhumed bone tissue. In: "Physical and technical methods in forensic medicine." Moscow—Stavropol, No 128, p 127 (in Russian)

Serebrovsky PV (1945) Birds of the Binagadi bats. Proceedings of the Natural History Museum of the Academy of Sciences of the Azerbaijan SSR, 1:27–85 (in Russian)

Serebrovsky PV (1948) Birds of the Binagadi brea deposits. Proceedings of the Natural History Museum of the Academy of Sciences of the Azerbaijan SSR, I-II:21–75 (in Russian)

Smirina EM (1989) Methodology for determining the age of amphibians and reptiles based on bone layers. A Guide to the Study of Amphibians and Reptiles. Kyiv, p 144–153 (in Russian)

Smirina EM (1994) Age determination and longevity in amphibians. Gerontology 40(2-4):133–146

Titov SV, Smirnov DG, Kurmaeva NM (2011) A Guide to the anatomy of vertebrates. Part 1. The skeleton. Penza, VG Belinsky Penza State Pedagogical University Press, p 78 (in Russian)

Vasilyev VA, Korsunenko AV, Pereshkolnik SL, Mazanaeva LF et al (2014) Differentiation of tortoises of the genera Testudo and Agrionemys (Testudinidae) based on the polymorphism of nuclear and mitochondrial markers. Genetika 50(10):1200–1215 (in Russian)

Velichko AA (2009) Paleoclimates and paleolandscapes of the northern hemisphere's non-tropical regions: Late Pleistocene–Holocene: Atlas and Monograph. GEOS, Moscow, p 120 (in Russian)

Zagumenov MN (2021) The construction of skeletons in vertebrates. Publishing Center of Udmurt University. Izhevsk, p 54 (in Russian)

К ИЗУЧЕНИЮ ИСКОПАЕМЫХ КОСТНЫХ ОСТАНКОВ ЧЕРЕПАХ (TESTUDINES, TESTUDINIDAE) ИЗ БИНАГАДИНСКОГО БИТУМНОГО МЕСТОРОЖДЕНИЯ (АЗЕРБАЙДЖАН)

Новрузов Н.Э.[1]*, Эйбатов Т.М.[2], Таптыгова К.А.[1]

[1]Министерство науки и образования Республики Азербайджан, Институт зоологии, Азербайджан AZ1073, Баку, проезд 1128, квартал 504

[2]Министерство науки и образования Республики Азербайджан, Естественноисторический музей, Азербайджан AZ1006, Баку, ул. Лермонтова, 3(17)

**Автор, отвечающий за переписку: niznovzoo@mail.ru*

Резюме. Объекты исследования – ископаемые костные останки черепах, извлеченные из грунта в процессе раскопок в Бинагадинском битумном месторождении и старых дачных участках Абшерона. Материал собран и обработан за период с 2020 по 2023 гг. в процессе экспедиционных и лабораторных исследований. Собранный остеологический материал хранится в Естественноисторическом музее города Баку и в лаборатории палеозоологии Института зоологии Азербайджана. Изучение материала позволило выявить большое количество костных фрагментов. Установлена родовая и видовая принадлежность обнаруженных костных фрагментов черепах. Изучение костных останков скелетов черепах найденных в Бинагадинском битумном месторождении в позднеплейстоценовом слое (поздний дриас) и сравнение его с костями черепах найденных на Абшероне в голоценовом слое (средний субатлантический период) позволило сделать предположение, что климат в конце плейстоцена был более прохладным и влажным, чем в голоцене. На это указывали некоторые изменения в морфологии костного панциря черепах: уменьшение индексов соотношения длины панциря к его ширине и высоте, а также ширины панциря к его высоте; изменения размерных пропорций некоторых костных пластинок карапакса и пластрона. Все эти изменения, предположительно, отражают некоторое усиление адаптационных процессов, связанных со значительными изменениями климата в Азербайджане вообще и в его восточной части в частности за указанный геологический период (более 0.012 млн. лет назад). Совокупность идентифицированных останков бинагадинского тафоценоза весьма важна для реконструкции фауны четвертичного периода Евразии и истории формирования современной фауны Абшерона. Обнаруженные микро- и макроструктурные маркеры Бинагадинского остеологического материала могут иметь приоритетную значимость для установления таксономического статуса будущих ископаемых находок. Цикличность роста костной ткани в микроструктуре длинных трубчатых костей черепах позднеплейстоценового слоя позволяет корректировать данные о климатических условиях четвертичного периода.

Ключевые слова*: битумное месторождение, ископаемые останки, черепахи, морфология, кости, микроструктура*

AZƏRBAYCANIN BİNƏQƏDİ QIR YATAĞINDA TAPILAN TISBAĞALARIN (TESTUDİNES, TESTUDINIDAE) FOSİL SÜMÜK QALIQLARININ ÖYRƏNİLMƏSİNƏ DAYİR

Novruzov N.Ə.[1]*, Eybatov T.M.[2], Taptıqova K.A.[1]
[1]Azərbaycan Respublikasının Elm və Təhsil Nazirliyi, Zoologiya İnstitutu, Azərbaycan
AZ1073, Bakı şəh., 1128, məhəllə 504
[2]Azərbaycan Respublikasının Elm və Təhsil Nazirliyi, Azərbaycan Təbiət Tarixi Muzeyi, Azərbaycan
E-AZ1006, Bakı şəh. , Lermontov küç., 3(17)
**Yazışmalara cavabdeh olan müəllif: niznovzoo@mail.ru*

Xülasə. Tədqiqat obyektləri Binəqədi qır yatağında və Abşeron baqlarında su quyularının qazıntı zamanı torpaqdan çıxarılan tısbağaların sümük qalıqlarıdır. Material 2020-2023-cü illərdə toplanmışdır. Toplanmış osteoloji material Bakı şəhərinin Təbiət Tarixi Muzeyində və Azərbaycan Zoologiya İnstitutunun paleozoologiya laboratoriyasında saxlanılır. Tədqiqat nəticəsində çoxlu sayda sümük fraqmentləri aşkar edilmişdir. Tısbağaların aşkar edilmiş sümük parçalarının cinsi və növ mənsubiyyəti müəyyən edilmişdir. Binəqədi bitum yatağında gec Pleistosen qatında (gec drias) tapılan tısbağaların skeletlərinin sümük qalıqlarının öyrənilməsi və Abşeronda Holosen qatında (orta subatlantik dövr) tapılan tısbağaların sümükləri ilə müqayisə edilməsi pleistosenin sonundakı iqlimin holosenə nisbətən daha sərin və rütubətli olduğunu irəli sürdü. Bunu tısbağaların sümük qabığının morfologiyasındakı bəzi dəyişikliklər göstərdi: qabığın uzunluğunun eninə və hündürlüyünə, həmçinin qabığın genişliyinin hündürlüyünə nisbətinin indekslərində azalma; bəzi karapaks və plastron sümük lövhələrinin ölçü nisbətlərində dəyişikliklər. Bütün bu dəyişikliklər, ehtimal ki, ümumilikdə Azərbaycanda və onun şərq hissəsində, xüsusən də göstərilən geoloji dövrdə (0.012 milyon ildən əvvəl) iqlimdəki əhəmiyyətli dəyişikliklərlə əlaqəli uyğunlaşma proseslərinin bir qədər güclənməsini əks etdirir. Tısbağa skeletləri haqqında əldə edilən morfoloji məlumatlar Testudo cinsinin mürəkkəb politipik kompleksinin fərqləndirilməsində müqayisəli morfoloji tədqiqatlarda, filogenetik və taksonomik növ fərqlərində istifadə edilə bilər. Binəqədi tafosenozunun müəyyən edilmiş qalıqlarının məcmusu Avrasiyanın dördüncü dövrünün faunasının yenidən qurulması və Abşeronun müasir faunasının yaranma tarixi üçün çox vacibdir. Binəqədi osteoloji materialının aşkar edilmiş mikro və makrostruktur markerləri gələcək fosil tapıntılarının taksonomik statusunun yaradılması üçün prioritet ola bilər. Gec Pleistosen təbəqəsinin tısbağalarının uzun borulu sümüklərinin mikrostrukturunda sümük toxumasının dövri böyüməsi dördüncü dövrün iqlim şəraiti haqqında məlumatları tənzimləməyə imkan verir.

Açar sözlər*: bitum yatağı, fosil qalıqları, tısbağalar, morfologiya, sümüklər, mikrostrukturu*

ANAS Transactions Earth Sciences 1 / 2026

http://www.journalesgia.com

MÜNDƏRİCAT

Qorbunov A.A., Lavrenova Y.A., Kərimov V.Y., Mustayev R.N., Bunyatov A.A. – Seysmik interpretasiya sahəsində innovativ texnologiyaların tətbiqi 3-9

Bayramov A.A., Yetirmişli Q.C., Babayev Q.R., Hacıyev N.E., Abusəlimov N.G., Əliyev M.M. – Seysmik proseslərin təsviri üçün güclü yer hərəkəti parametrlərinin modelləşdirilməsi və süni intellekt alqoritmləri 10-16

Nurvidyanto M.I., Harmoko U., Gernovo R., Fernando G.A. – İndoneziyanın Demak sahil zonası nümunəsində üfüqi şaquli spektral əlaqələr (HVSR) metodundan istifadə edərək allüvial çöküntülərin sulu qatının potensialının təyini 17-26

Xabarova O.V., Eppelbaum L.V. – Qobustanda kəhrizlərin yüksək dəqiqlikli uzaqdan zondlama məlumatları əsasında müəyyənləşdirilməsi 27-33

Qədirov F.Ə., Salamov Ə.M., Səfərov R.T., Nəcəfov O.F., Səmədli P.M., Məmmədov S.Q., Zamanova A.H. – Elektrik müqaviməti müşahidələri və Şıxzahırlı palçıq vulkanında kiçik dərinliklərdə mövcud olan strukturların tədqiqi (Azərbaycan) 34-44

Sudirman, Maulana A., Ömər H. – Indoneziyada Cənubi Sulavesinin Palopo əyalətində Babak və Siquntu çaylarında çoxfazalı intruziv süxurların petrologiyası, dəyişdirilməsi və minerallaşması 45-56

Mindiaşvili G., Bluaşvili D., Lipartiya T., İobidze G., Makadze M., Cəfəridze N., Benaşvili K., Xetsuriani G., Bluaşvili V. – Bektakari-Bnelihevi kompleksinin maqmatogen-hidrotermal təkamülü və filiz potensialı, Bolnisi filiz rayonu, Kiçik Qafqaz 57-65

Əliyev Ç.S., Kazımova L.A. – Abşeron yarımadasının texnogen dəyişilmiş zonalarında ağır metalların miqrasiya xüsusiyyətləri 66-76

Tağıyev M.F., Xuduzadə Ə.İ., Axundov Ş.X., Axundova X.R. – Yeni geoloji-geokimyəvi məlumatlar əsasında Orta Kür çökəkliyinin karbohidrogen resurslarının qiymətləndirilməsi 77-87

Doskaziyeva G.Ş., Bisenqaliyev M.D., Abdeşova G.G., Tulegenova O.Ş., Piriverdiyev İ.A. – Emba yataqları timsalında neft veriminin artırılması üçün istifadə olunan polimerlərin fiziki-kimyəvi xüsusiyyətlərinin təhlili 88-98

Boqdanov A.N., Karşiyev O.A., Xmırov P.V. – Özbəkistan Respublikasında karbohidrogen ehtiyatlarının kəşfiyyatı və xammal-resurs bazasının inkişafı: tarixi inkişaf meylləri və gələcək perspektivlər 99-113

Novruzov N.Ə., Eybatov T.M., Taptıqova K.A. – Azərbaycanın Binəqədi qır yatağında tapılan tısbağaların (testudines, testudinidae) fosil sümük qalıqlarının öyrənilməsinə dair 114-127

CONTENTS

Gorbunov A.A., Lavrenova E.A., Kerimov V.Yu., Mustaev R.N., Bunyatov A.A. – Implementation of disruptive technologies in seismic interpretation 3-9

Bayramov A.A., Yetirmishli G.J., Babayev G.R., Hajiyev N.E., Abusalimov N.G., Aliyev M.M. – Modeling of strong ground motion parameters and artificial intelligence algorithms for describing seismic processes 10-16

Nurwidyanto M.I., Harmoko U., Gernowo R., Fernando G.A. – Aquifer potential in alluvium litology using the Horizontal-To-Vertical Spectral Ratio (HVSR) method, case study: Coastal Demak, Indonesia 17-26

Khabarova O.V., Eppelbaum L.V. – High-resolution remote sensing unmasks qanats in Gobustan 27-33

Kadirov F.A., Salamov A.M., Safarov R.T., Najafov O.F., Samadli P.M., Mammadov S.G., Zamanova A.H. – Electrical resistivity survey and near-surface structure exploration of the Shikhzahirli mud volcano (Azerbaijan)..... 34-44

Sudirman, Maulana A., Umar H. – Petrology, alteration and mineralisation of multiphase intrusion rocks in the Babak River and Siguntu River, Palopo, South Sulawesi, Indonesia 45-56

Mindiashvili G., Bluashvili D., Lipartia T., Iobidze G., Makadze M., Jafaridze N., Benashvili K., Khetsuriani G., Bluashvili V. – Magmatic-hydrothermal evolution and ore potential of the Bektakari-Bnelikhevi khot, Bolnisi ore district, the Lesser Caucasus 57-65

Aliyev Ch.S., Kazimova L.A. – Features of heavy metal migration in technogenic zones of the Absheron Peninsula..... 66-76

Tagiyev M.F., Khuduzade A.I., Akhundov Sh.Kh., Akhundova Kh.R. – Updated hydrocarbon resource assessment of the Middle Kur Depression, Azerbaijan 77-87

Doskaziyeva G.Sh., Bisengaliyev M.D., Abdeshova G.G., Tulegenova O.Sh., Piriverdiyev I.A. – Analysis of physicochemical characteristics of polymers for enhanced oil recovery (the Emba fields as case study)..... 88-98

Bogdanov A.N., Karshiyev O.A., Khmirov P.V. – Hydrocarbon exploration and resource base development in the Republic of Uzbekistan: historical trends and future perspective..... 99-113

Novruzov N.E., Eybatov T.M., Taptygova K.A. – To the study of fossıl bone remaıns of tortoıses (Testudınes, Testudınıdae) from the Bınagadı bıtumen deposıt (Azerbaıjan)..... 114-127

ОГЛАВЛЕНИЕ

Горбунов А.А., Лавренова Е.А., Керимов В.Ю., Мустаев Р.Н., Буньятов А.А. – Внедрение инновационных технологий в сейсмической интерпретации 3-9

Байрамов А.А., Етирмишли Г.Д., Бабаев Г.Р., Гаджиев Н.Э., Абусалимов Н.Г., Алиев М.М. – Моделирование параметров сильных колебаний грунта и алгоритмы искусственного интеллекта для описания сейсмических процессов 10-16

Нурвидьянто М.И., Хармоко У., Герново Р., Фернандо Г.А. – Определение потенциала водоносного слоя аллювиальных отложений с использованием метода горизонтального и вертикального спектральных отношений (HVSR) на примере прибрежной зоны Демака, Индонезия 17-26

Хабарова О.В., Эппельбаум Л.В. – Обнаружение кяризов в Гобустане по данным дистанционного зондирования высокого разрешения 27-33

Кадиров Ф.А., Саламов А.М., Сафаров Р.Т., Наджафов О.Ф., Самедли П.М., Мамедов С.Г., Заманова А.Г. – Исследования методом электрического сопротивления и изучение приповерхностной структуры грязевого вулкана Шыхзахырли (Азербайджан) 34-44

Судирман, Маулана А., Умар Х. – Петрология, изменения и минерализация многофазных интрузивных пород в районах рек Бабак и Сигунту, Палопо, Южный Сулавеси, Индонезия.....45-56

Миндиашвили Г., Блуашвили Д., Липартия Т., Иобидзе Г., Макадзе М., Джафаридзе Н., Бенашвили К., Хецуриани Г., Блуашвили В. – Магматогенно-гидротермальная эволюция и рудный потенциал комплекса Бектакари-Бнелихеви, Болнисский рудный район, Малый Кавказ 57-65

Алиев Ч.С., Казымова Л.А. Особенности миграции тяжёлых металлов в техногенных зонах Абшеронского полуострова 66-7

Тагиев М.Ф., Худузаде А.И., Ахундов Ш.Х., Ахундова Х.Р. – Оценка ресурсов углеводородов Среднекуринской впадины на основе новых геолого-геохимических данных 77-87

Досказиева Г.Ш., Бисенгалиев М.Д., Абдешова Г.Г., Тулегенова О.Ш., Пиривердиев И.А. – Анализ физико-химических характеристик полимеров для повышения нефтеотдачи на примере Эмбинских месторождений..... 88-98

Богданов А.Н., Каршиев О.А., Хмыров П.В. – Развитие ресурсной базы углеводородов и нефтегазоразведочных работ в Республике Узбекистан: исторические тенденции и перспективы развития..... 99-113

Новрузов Н.Э., Эйбатов Т.М., Таптыгова К.А. – К изучению ископаемых костных останков черепах (Testudines, Testudinidae) из Бинагадинского битумного месторождения (Азербайджан) 114-127